

Role of ROP GTPases and Nod Factor Signaling in Medicago Root Nodule Infection

Rossana Mirabella

Promoter: Prof. Dr. A. H. J. Bisseling
Hoogleraar in de Moleculaire Biologie
Wageningen Universiteit

Co-promoter: Dr. ir. R. Geurts
Laboratorium voor Moleculaire Biologie
Wageningen Universiteit

Samenstelling promotiecommissie:

Dr. A. Jahraus, Beta-Cell N.V., Brussel, België
Prof. Dr. C. Mariani, Katholieke Universiteit Nijmegen
Prof. Dr. M.A. Haring, Universiteit van Amsterdam
Prof. Dr. A. M. C. Emons, Wageningen Universiteit

Het werk beschreven in dit proefschrift is uitgevoerd binnen de onderzoeksschool voor Experimentele Planten Wetenschappen.

Role of ROP GTPases and Nod Factor Signaling in Medicago Root Nodule Infection

Rossana Mirabella

Proefschrift

ter verkrijging van de graad van doctor
op gezag van de rector magnificus
van Wageningen Universiteit
Prof. Dr. ir. L. Speelman
in het openbaar te verdedigen
op dinsdag 29 juni 2004
des namiddags te vier uur in de Aula

Role of ROP GTPases and Nod Factor Signaling in Medicago Root Nodule Infection
Mirabella, Rossana

Thesis Wageningen University, The Netherlands
With references – with summary in Dutch and Italian

ISBN 90-8504-048-5

Contents

| | | |
|------------------|---|-----|
| | Outline | 7 |
| Chapter 1 | LCO Signaling in the Interaction between Rhizobia and Legumes | 9 |
| Chapter 2 | Use of the “Fluorescent Timer” DsRED-E5 as Reporter to Monitor Dynamics of Gene Activity in Plants | 31 |
| Chapter 3 | Regulation of Actin Gene Expression during <i>Medicago truncatula</i> Root Hair Development | 49 |
| Chapter 4 | Tight Regulation of ROP GTPases Expression is Required to Maintain Symbiosomes in <i>Medicago truncatula</i> Root Nodules | 73 |
| Chapter 5 | NODULATION RECEPTOR KINASE Controls the Switch from Infection Thread Growth to Release of Bacteria in Nodule Cells | 99 |
| Chapter 6 | The Expression Pattern of Nod Factor Signaling Genes Reveals a role For Nod Factor Signaling in Nodule Infection | 115 |
| Chapter 7 | Concluding Remarks | 131 |
| | Samenvatting | 141 |
| | Riassunto | 143 |
| | Curriculum Vitae | 147 |
| | List of publications | 148 |
| | Appendix | 149 |
| | Acknowledgements | 160 |

Outline

Legume plants form root nodules by interacting with the soil bacterium *Rhizobium*. In these nodules the bacteria reduce atmospheric nitrogen into ammonium that can be used by the plant. The formation of nitrogen fixing nodules requires that the bacteria enter the plant. The infection of plant cells takes place at two different sites: the root epidermis and the nodule. The bacterial signal molecule that induces root responses in the host is the so called Nod factor. This molecule is also required to induce the infection process. At the root epidermis the bacteria enter the root hairs by a newly formed tubular structure called infection thread. Infection threads traverse the root hairs and grow towards the cortical cells that have divided to form a nodule primordium. In these bacteria are released. Upon release, the bacteria become surrounded by a host derived membrane, the symbiosome membrane, and together are called symbiosome. Upon infection, the nodule primordium develops into a nodule. *Medicago truncatula* forms indeterminate nodules, in which a persistent meristem, located at the nodule apex, continuously divides adding new cells to the nodule tissues. As a consequence, the nodule central tissue can be divided into several zones representing successive developmental stages, from the apex (distal region) to the root attachment point (proximal region). The cell layers adjacent to the meristem form the infection zone, also indicated as zone II, in which the newly formed cells are infected. The infection of the nodule cells can be divided in four subsequent steps: (1) infection thread growth, (2) bacterial release into the host cells, (3) symbiosome proliferation/differentiation and (4) symbiosome maintenance. The first two steps of the infection take place in the most distal cell layers of zone II, after which the symbiosomes divide and differentiate into the nitrogen fixing forms.

The aim of the research described in this thesis was to study the mechanism regulating this infection process. We focused on the role of Nod factor signaling and small GTPases.

Nod factors induce several responses at the root epidermis. In **chapter 1** we gave an overview of these responses and of the components of the Nod factor signaling as they were known when we started this research.

Several evidences show that the actin cytoskeleton is involved in the infection process both in the epidermis and in the nodule cells. To create a basis for studies on the role of actin in the infection process we first analyzed the expression of the actin genes during root hair development in *Medicago* (**chapter 3**). For this purpose we used promoter fusions with the fluorescent marker DsRED-E5. In **chapter 2** we showed that this marker can be used to obtain detailed information on the dynamics of gene regulation. We showed that the expression of the actin genes is regulated during root hair development and discuss that one actin gene, *MtACT1*, is the most obvious candidate to play a role during the infection process.

In **chapter 4** we analyzed the role of the ROP GTPases in the infection process in the nodule. By *in situ* hybridization, we showed that in *Medicago* wild-type nodules *ROP* genes

are expressed in the apical region of the nodule, including the meristem and the distal cell layers of zone II, whereas in nodules elicited by a Fix^- *Rhizobium* strain *ROPs* are expressed at the same level in all the infected cells. These Fix^- nodules are characterized by early senescence and symbiosome degradation. Therefore, we hypothesized that symbiosome degradation in these nodules was due to the sustained expression of *ROP* genes in all the infected cells. This was proven to be correct by nodules in which *ROP* expression was induced in the proximal cell layers of zone II. In this way we showed that ectopic expression of *ROP* in these cell layers is sufficient to induce nodule senescence and symbiosome degradation. This indicates that down regulation of *ROP* expression in the proximal cell layers of zone II is required to avoid symbiosome degradation and therefore for symbiosome maintenance.

In **chapter 5** and **chapter 6** we analyzed the role of Nod factor signaling in the infection process in the nodule. Recently, several *Medicago* genes involved in Nod factor perception and transduction have been cloned. Among these is a leucine rich repeat receptor kinase (*NORK*). By *in situ* hybridization, we showed that all the Nod factor signaling, including *NORK*, are highly expressed in the first cell layers of zone II, in which infection thread growth and bacterial release occurs, suggesting a role for Nod factor signaling in these processes. This was further studied in roots in which *NORK* was silenced by RNA interference. In nodules in which a residual level of *NORK* was present the release of bacteria in the nodule cells was impaired, indicating that Nod factor signaling is specifically involved in this process.

In **chapter 7** we discuss the possible mechanisms by which Nod factor signaling can regulate the infection process as well as the role of *ROP* GTPases and actin in the nodule infection.

CHAPTER 1

LCO Signaling in the Interaction between Rhizobia and Legumes

Rossana Mirabella, Henk Franssen and Ton Bisseling

Introduction

Bacteria belonging to the genera *Rhizobium*, *Bradyrhizobium*, *Azorhizobium*, *Mesorhizobium* and *Synorhizobium*, collectively referred to as rhizobia, are able to invade the roots of their legume host plant. There they trigger the formation of a new organ, the root nodule in which nitrogen fixation occurs (1-6). In a nutshell, the formation of root nodules starts with the exchange of signals between the root and the bacteria, which is followed by the colonization of the root surface. Subsequently, the root hairs deform and curl and the bacteria invade the plant by newly formed infection threads (Fig. 1). These threads grow towards the basis of the root hair and then they traverse cortical cells. Concomitantly, cortical cells are mitotically activated, by which a nodule primordium is formed. Infection threads grow towards the primordium and there bacteria, surrounded by a plant membrane, are released into the cytoplasm of the host cell. Subsequently, the primordium develops into a nodule and the bacteria start to reduce nitrogen into ammonia that can be utilized by the plant. During each step of nodule formation nodule specific plant genes, the so-called nodulin genes, are activated. For example, *ENOD12* is activated in the epidermis and *ENOD40* in the root pericycle and both nodulin genes are also expressed in the nodule primordium.

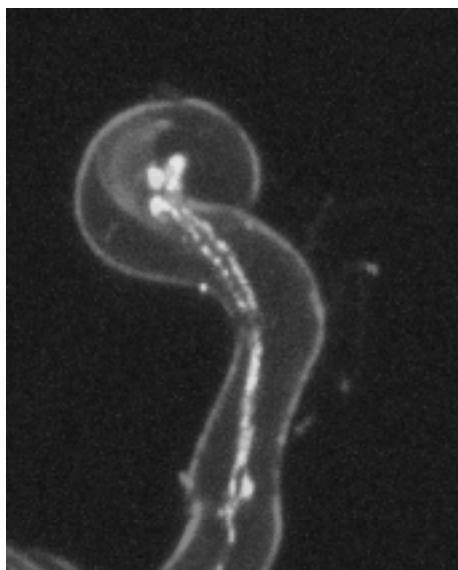


Figure 1. *Medicago truncatula* root hair that has formed a shepherd's crook in which rhizobia (GFP expressing) have accumulated. An infection thread is initiated in the curling and it grows to the basis of the cell. Individual bacterium can be seen in the thread.

During nodule development, the host and the rhizobia probably exchange several signals, however, two classes of signal molecules play a crucial role in the initiation of this symbiotic interaction (Fig. 2). The first are compounds excreted by the roots of the host, in general flavonoids; they induce the transcription of bacterial nodulation genes (*nod* genes). One of these *nod* genes, *nodD*, is constitutively active and upon recognition of a certain flavonoid becomes a transcriptional activator of the other *nod* genes. The proteins encoded by these genes are involved in the biosynthesis or secretion of the second class of signal molecules, specific lipo-chitooligosaccharides (LCOs), or so-called Nod factors (7, 8), which are perceived by the plant.

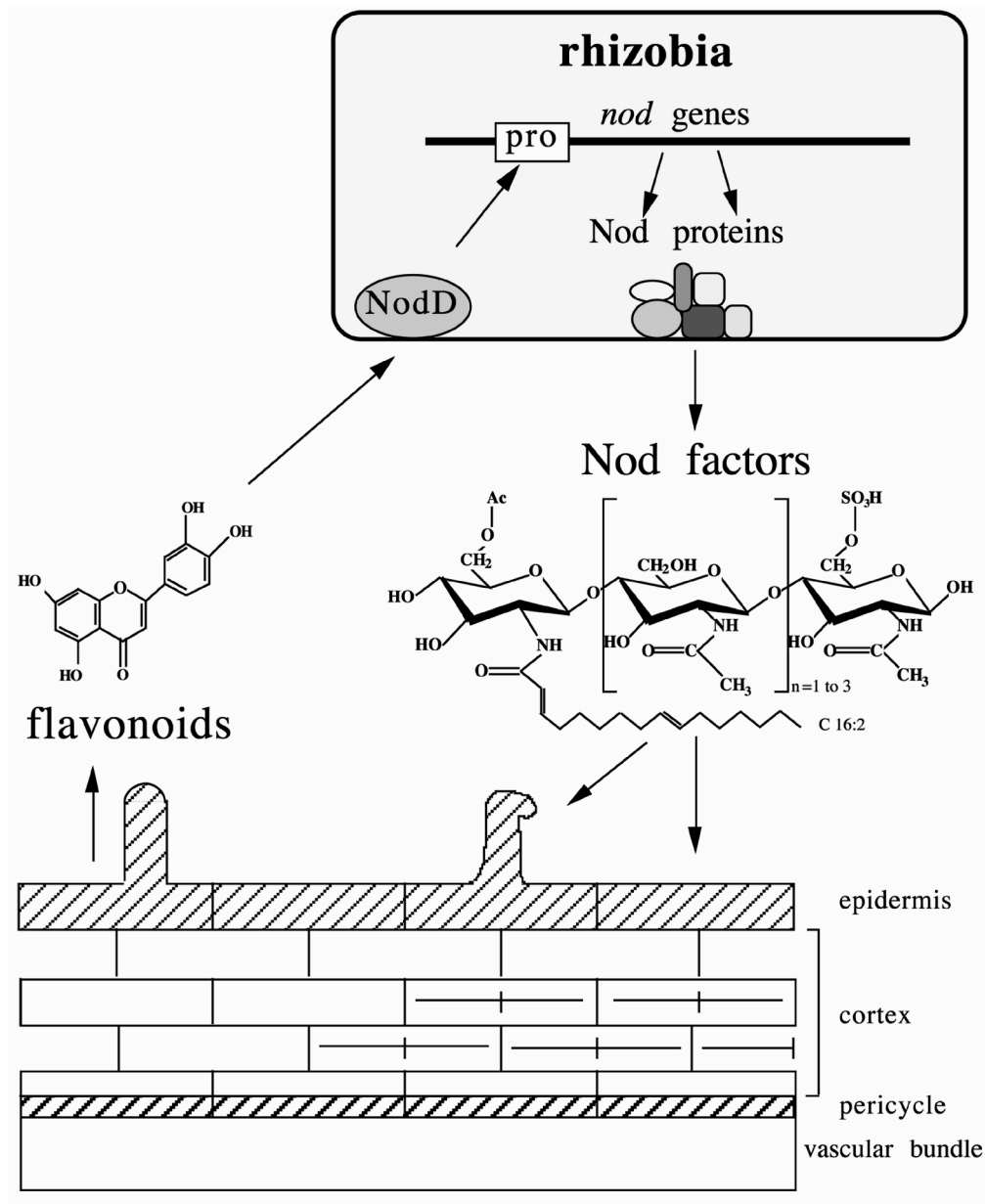


Figure 2. Early events in the interaction between legumes and rhizobia (modified from 36). NodD, constitutively formed, is activated by specific flavonoids (an activator of *S. meliloti* NodD is luteolin) excreted by the plant and becomes a transcriptional activator of the other nod genes. The Nod proteins are involved in the biosynthesis and the secretion of Nod factor. In this figure the major *S. meliloti* Nod factor is depicted. Nod factors induce various responses in three root tissues, like root hair deformation and curling (epidermis), nodulin gene expression (pericycle) and cell division (cortex).

In Fig. 2 the structure of a major *S. meliloti* Nod factor is shown. The structure of Nod factors produced by most rhizobia has now been elucidated (9-12) showing that they have a generic LCO structure. In general, they consist of a β -1,4-linked N-acetyl-D-glucosamine backbone with 4 or 5 residues, although some Nod factors have a backbone of 3 or 6 sugar units. The non-reducing terminal sugar moiety is substituted at the C2 position with a fatty acid, that in general has a length of 16 or 18 carbons. Depending on the rhizobial species additional substitutions are present on the terminal sugar residues. The major *S. meliloti* Nod factor (Fig. 2) contains a sulfonyl group at its reducing sugar residue. This substitution is essential for the biological activity on *Medicago truncatula* roots. Other rhizobia produce molecules with different substitutions at this position. For example, *M. loti* Nod factors can have an acetylated-fucose group. Whereas *M. loti* strains make in general molecules without a substitution, but in case they have a *nodX* gene they produce Nod factors with an acetyl substitution at the reducing terminal sugar residue. For the interaction with certain pea lines this acetyl group is essential for infection thread growth (see paragraph 2.2). The major *S. meliloti* Nod factor (Fig. 2) has an acetyl substitution at its non-reducing terminal sugar; this substitution is important for the induction of the infection process, but is not essential for most other responses (see paragraph 2.2). Other rhizobial species can have different substitutions at this position (11, 12). The acyl chain of the major *S. meliloti* Nod factor has α , β unsaturated bonds. Nod factors with such α , β unsaturated acyl chains are especially made by rhizobia that interact with legumes belonging to the galeoid phylum (including *Medicago*, *Pea* and *Vicia*; 13). These specific acyl groups are especially important in the induction of the infection process (see paragraph 2.2).

Nod factors are involved in the induction of various responses in the root, like deformation and curling of root hairs, infection thread formation, mitotic activation of cortical cells and induction of gene expression in the epidermis, cortex (nodule primordia) and pericycle. However, whether the cortical and pericycle cells perceive Nod factors or whether the Nod factor responses are induced by secondary signals, e.g. generated in the epidermis is unclear. For these reasons in this chapter we will focus on the mechanism of Nod factor perception and signaling active in the root epidermis. In the first part the morphological changes induced in the root hairs are summarized. Then, the biochemical and genetic studies concerning perception and transduction are reviewed and finally it is discussed how future research could provide insight in the mechanisms by which the Nod factor signal can induce the morphological changes in root hairs.

1. Morphological changes induced in root hairs

1.1 Root hair growth

The root epidermis is the plant tissue that is in direct contact with Nod factor secreting rhizobia, when they colonize the root. It also forms a cell layer that the rhizobia have to traverse to reach the nodule primordia, formed in the cortex. In most legumes the bacteria induce the formation of a sophisticated infection structures, the infection thread (Fig. 1). This

is a tube-like structure the formation of which is strictly controlled by the host plant and it exemplifies how rhizobia recruit and modify the cell biological machinery of the host to create an apparently novel structure. In order to appreciate the morphological responses induced by rhizobial Nod factors we first provide some background information about root hair growth.

Root hairs elongate by tip growth a process in common with pollen tubes, and fungal hyphae (14, 15). A common feature of tip growing cells is the presence of a high Ca^{++} gradient at the apex. The deposition of cell wall and membrane material by Golgi vesicles is confined to the tip and this determines the localized growth. To maintain the delivery of vesicles at this site of the cell, growing root hairs have a polar organization of the cytoplasm, with an apical region at the tip containing a large number of Golgi vesicles; this region is devoid of large organelles and therefore is sometimes called "empty zone" (16-20).

The actin cytoskeleton has been shown to be essential for the maintenance of the polar cytoarchitecture in growing root hairs and in other tip growing plant cells like pollen tubes (14, 21-23).

The organization of the actin cytoskeleton in legume root hairs has been studied in most detail in *Vicia sativa* (21). Growing root hairs have thick axial actin bundles along the length of the hair. In the sub-apical region of the hair the bundles flare out into thinner bundles. These sub-apical fine bundles have a net-axial orientation and are called FB-actin (Fine Bundles; 21). The apex of growing root hairs appears to be devoid of actin (21). In root hairs that are terminating growth FB-actin has almost disappeared and the region devoid of actin at the tip is not present; in full grown root hairs the FB-actin is not present and the thick actin bundles loop through the tip (21). Cytochalasin D, which affects actin polymerization, causes a disappearance of the FB-actin and of the vesicle-rich region and as a result root hairs stop growing. This suggests that the FB-actin is essential for vesicle delivery at the tip and therefore tip growth of root hairs (21).

The role of the microtubular cytoskeleton during root hair development is less clear but in contrast with the actin it is not essential for tip growth, as is the case in other tip growing plant cells like pollen tubes (24-27). In root hairs, microtubules are predominantly located in the cortical cytoplasm next to the plasma membrane with a longitudinal or helical orientation (28-32), and with a random orientation in the root hair tip. In addition, bundles of endoplasmatic microtubules connecting the nucleus to the root hair tip are present in *Vicia hirsuta* (33) and growing *Medicago truncatula* root hairs (34, 35) whereas in full grown root hairs they are no longer present (Sieber and Emons, pers. comm.). Therefore, the endoplasmatic microtubules may function in nuclear positioning and movement. Recent work by Bibikova (24) suggests that the CMT (Cortical Microtubules) could determine the direction of root hair growth. When *Arabidopsis* was grown in the presence of drugs stabilizing or depolymerizing (taxol and oryzalin, respectively) the CMT, a loss of directionality in root hair growth was observed, causing a waving of the root hairs as they elongated. However, the rate of growth was not affected. Thus CMT are not required for tip growth but are involved in controlling the direction of growth (24).

Since the actin and microtubular skeleton are important for root hair tip growth and for the direction of growth, respectively, it is very probable that both skeletons play an important role in the rhizobial Nod factor induced morphological responses.

1.2 Root hair deformation

Purified Nod factors are sufficient to induce root hair deformation at a concentration as low as 10^{-12} M (9, 10). In *Vicia* especially the root hairs that are terminating growth deform (36) whereas in *Medicago truncatula* as well as in *Lotus japonicus* also younger growing root hairs do deform (35; van der Krogt and Bisseling, pers. comm.). Within a susceptible zone the vast majority of root hairs respond to Nod factor application with a swelling of the root hair tip, followed by a new outgrowth from the swelling. In some species, e.g. *M. truncatula*, the growth direction of this new outgrowth is markedly different from the original growth direction of the responding hair by which the deformation has the appearance of a branch. The swelling is the result of isotropic growth, whereas the outgrowth/branch is the result of a reinitiation of polar growth (21, 36, 37). In fact the outgrowth has all the typical features of tip growing cells: e.g. calcium gradient at the tip (37), polar cytoarchitecture (21), actin organization typical of growing root hairs (21).

Since deformation/branching is caused by a modification of the tip growth process it is probable that Nod factor induce changes in the configuration of the actin skeleton. The first reports on the effect of Nod factors on the actin cytoskeleton are from Allen (38) and Allen and Bennet (39). They reported a fragmentation of the actin cytoskeleton in *M. sativa* root hairs within 15 min. after Nod factor application. Later, Cárdenas (40) showed a similar fragmentation in *Phaseolus vulgaris* root hairs (40). In *V. sativa* root hairs no actin fragmentation was observed after Nod factor application (21, 41, 42). De Ruijter (41) reported an increase of the number of fine actin bundles in the sub-apical region of most root hairs within 3-15 min. after Nod factor application. This increase occurs in root hairs at all stages of development also in those hairs that do not deform. At a later stage when the outgrowth is formed the architecture of the actin cytoskeleton is the same as in growing root hairs and the formation of the outgrowth can be inhibited by cytochalasin D (21), showing that the actin skeleton is essential for root hair deformation.

Although the observed changes in the actin configuration markedly vary in the different studies it has become clear that the actin skeleton is one of the first targets of the Nod factor signaling in root hairs. Nod factors induce these rearrangements in the actin configuration within minutes, but the molecular mechanisms controlling these changes are unknown.

1.3 Root hair curling and infection

Unlike root hair deformation and branching, root hair curling only occurs in a relatively small number of hairs upon inoculation with rhizobia. Nod factors are essential for the induction of curling but in most legume species curling is only induced when the bacteria are present (43).

During curling a so-called shepherd's crook, is formed (Fig. 1) which is the result of a redirection of root hair tip growth by more than 360°(19).

Curling is probably caused by a gradual and constant reorientation of tip growth (44, 45). During curling the bacteria become entrapped within the curl and there the plant cell wall is modified in a very local manner (46-48). At this site the plasma membrane invaginates and the host deposits new material around the site of infection. In this way a tube-like structure, the infection thread, is formed by which the bacteria enter the root.

Studies on cytoskeletal changes during curling and infection have been focused on the microtubular skeleton. Since microtubules play an important role in controlling the direction of root hair growth it seems probable that this part of the cytoskeleton will play a pivotal role in the curling process. The microtubular cytoskeleton in root hairs markedly rearranges during curling, initiation of infection and infection thread growth. Electron microscopic studies showed that microtubules are present at the site of infection thread initiation (19, 47, 49). Recently, Timmers (34) studied in more detail the rearrangements in *Medicago* root hairs during infection thread formation by immunocytochemistry. At the start of infection the nucleus migrates to the root hair tip and the microtubules concentrate in the region between the nucleus and the hair tip. When curling is initiated these endoplasmatic microtubules move to the area within the curl where the infection will initiate. This results in an asymmetric organization of the skeleton. When thread formation is initiated (24-48 hours post inoculation) the microtubules are predominantly located within the curl at the site of infection thread initiation and they do no longer connect the nucleus with the root hair tip. Subsequently, the infection thread grows into the root hair and it is always preceded by the nucleus. At this stage the infection thread tip is surrounded by a dense network of microtubules, that is connected with the nucleus; the complete body of the thread is covered with a longitudinal array of microtubules (34, 50). The described rearrangements in the microtubules cytoskeleton are in agreement with the idea that microtubules play a key role in controlling the direction of root hair growth. However, the molecular mechanism by which Nod factors induce these changes still remains to be discovered.

2. Nod factor perception

Some of the changes induced by Nod factors in the plant cytoskeleton occur very rapidly. Therefore, it is very likely that the cytoskeleton is the target of the Nod factor activated signaling. For this reason we will describe the mechanism involved in the perception and transduction of the Nod factor signaling.

When roots are treated with purified Nod factors (or inoculated with rhizobia) responses are induced in the majority of the epidermal cells within a susceptible zone. This is most apparent when the activation of early nodulin promoters is visualized by a reporter gene. For example *ENOD12-GUS* (β -Glucuronidase; see paragraph 3.1) is activated in all epidermal cells, with or without a hair, in direct contact with Nod factors, in the zone where root hairs are formed and grow (51). The induction of responses in root epidermal cells appears to requires a

direct contact with Nod factors (51) and some of the responses occur within seconds (52, 53). Therefore, it seems probable that these cells respond in a cell autonomous manner and it is probable that all epidermal cells (within a susceptible zone) have a LCO perception mechanism. Whether in addition to intact LCOs also cleavage products could have a signaling function can not be excluded. Legumes produce several enzymes that can degrade Nod factors (6, 11). However, it has not been demonstrated that Nod factor cleavage products can induce epidermal responses. In contrast, it is possible that certain cleavage products might play a role in the induction of some responses in the inner layers of the roots. For example chitin fragments are sufficient to induce cortical cell divisions (54).

In the following paragraphs the knowledge about the sub-cellular location of the perception process as well as the candidate molecules that could have a function in LCO perception are reviewed.

2.1 Site of Nod factor perception

The amphiphilic nature of Nod factors with their hydrophobic lipid tail and more hydrophilic sugar backbone suggests that Nod factors have a high affinity for membranes. Indeed, *in vitro* studies show that Nod factors rapidly insert into membranes, but are unable to flip-flop between membrane leaflets (55). This indicates that Nod factors are perceived by a receptor located in the plasma membrane. However, the behavior of fluorescent Nod factors on roots show that perception might also occur at the cell wall and even it can not be completely excluded that Nod factors are perceived in the cytoplasm. Using fluorescence correlation microscopy it was shown that biologically active Nod factors, that were tagged with a fluorescent group, do accumulate in the cell wall of epidermal cells at a concentration 50 fold higher than in the medium that was applied to the roots (56). Further, it was shown that Nod factors are present at low quantities in the plasma membrane and even a low level of fluorescence was detected in the cytoplasm. Also another study indicates that Nod factor could be internalized (57), but it remains to be demonstrated that intact Nod factors are present in the cytoplasm.

The fluorescence correlation microscopy studies furthermore revealed that Nod factors become highly immobilized in the cell wall. This accumulation of Nod factors in the cell wall as well as its immobilization does also occur in a non-legume (55). Nevertheless these properties might be of importance in curling of root hairs. To obtain a proper shepherd's crook it is probable that a certain dominant micro colony of rhizobia induces a gradual and constant reorientation of tip growth by which a 360° turn is created. It seems probable that the bacteria within such colony have to provide information about their position to the hair. It is hypothesized that the bacteria, within a micro colony, locally secrete Nod factor, which becomes more or less immobilized in the plant cell wall at the site of the colony and this could provide the positional information to the hair (45, 55).

2.2 Multiple receptors

Studies with purified Nod factors and mutant rhizobia provided insight in the Nod factor structure requirements for various epidermal responses. Such studies have especially been done in *Medicago*, *Pea* and *Vicia*. These showed that responses like root hair deformation, *ENOD12* activation and ion fluxes (see paragraph 3.1), have similar Nod factor structural requirements. In *Medicago* these responses highly depend on the presence of the sulfate group at the reducing terminal sugar residue. Whereas in *Pea* and *Vicia* at this position no substitution (for the H atom) is required. Substitutions at the non-reducing terminal sugar are not essential for these responses and also there are no specific demands concerning the structure of the lipid moiety except that it has to be longer than 10 carbon atoms (55). In contrast, for the initiation and growth of the infection thread in the epidermis the structure of the fatty acyl group and the presence of the O-acetyl group at the non-reducing end are important. Rhizobial mutants that produce Nod factors that do not carry the appropriate unsaturated fatty acid and the O-acetyl group at the non-reducing terminal sugar (*nodEL* mutant) have almost completely lost the ability to initiate the infection process (58-60). These data support the hypothesis that two receptors are operational in the epidermal cells (60): an "entry" receptor involved in the rhizobia infection with high stringency for the Nod factor structure and a "signaling" receptor involved in the other epidermal responses with a lower stringency.

Also the characterization of the *SYM2* allele of Afghanistan pea showed that infection highly depends on the Nod factor structure. This *SYM2* allele is responsible for the inability of European *M. loti* strains to nodulate Afghanistan pea. When pea plants containing the Afghanistan *SYM2* allele are inoculated with European *R. leguminosarum biovar viciae*, the bacteria induce all responses except the infection process which is affected; the number of infections is markedly reduced and the few infection threads that are formed in the root hairs are aborted (61). However, certain *M. loti* strains carrying *nodX* can form nodules on pea lines containing the *SYM2* allele (62). *NodX* is an acetyl transferase responsible for the addition of an O-acetyl group at the reducing sugar residue (63), where *S. meliloti* Nod factors have sulfuryl group. Therefore, the O-acetyl group is essential for the infection of (Afghanistan) *sym2* peas but not for the induction of all the other responses. Therefore, *SYM2* is probably involved in the recognition of the *NodX* modified Nod factors and it may act as an "entry" receptor.

2.3 Nod factor binding proteins

By a biochemical approach two Nod factor binding sites, NFBS1 and NFBS2, have been identified in *Medicago* (64, 65). NFBS1 has an affinity of 86 nM for *S. meliloti* Nod factors. However, it does not discriminate between factors with or without the sulfate substitution, although the sulfate group is essential for most of the *S. meliloti* Nod factor induced response during *Medicago* nodulation. Furthermore, a similar binding site has been identified in a non-legume. NFBS1 has been identified in a 1000g fraction of *Medicago* roots and therefore might be located in the cell wall (64). This in combination with its lack of specificity

and its occurrence in non-legumes make it a good candidate to be involved in the cell wall binding of Nod factors (55; see paragraph 2.1).

NFSB2 has been identified in *Medicago* cell suspension and might be located in the plasma membrane (65). It has a higher affinity (4nM) for Nod factors than NFSB1, but like this binding site it also does not discriminate between sulfated and non-sulfated Nod factors.

Due to the lack of specificity it is unlikely that these NFSBs by themselves can function as Nod factor signaling or entry receptor. However, both NFSBs only efficiently bind chitin fragments with a covalently attached acyl, showing a very different specificity from that of chitin fragment receptors so far reported (66). Therefore, these sites might be part of a Nod factor binding complex, in combination with other components that confer specificity to the complex.

Lectins have been shown to be a determinant of host specificity (67). White clover plant expressing a pea lectin have an extended host range since they can form nodules with the microsymbiont of pea, *M. loti*. Similarly, *Lotus corniculatus* plants, that are normally nodulated by *M. loti*, obtained the ability to interact with *B. japonicum*, that form nodules on soybean, when they express a soybean lectin (68). Although these studies show that lectins play a role in the nodulation process it was never demonstrated that they could bind Nod factors. In contrast, a lectin from the roots of *Dolichos biflorus* was shown to bind Nod factors albeit with a rather low affinity. This lectin is a member of the eukaryotic ATPase superfamily, with an apyrase specificity that is activated upon Nod factor binding. Moreover it is an extracellular protein located at the tip of the root hairs and an antibody against the protein block nodulation (69, 70). Although these studies strongly suggest that this lectin most likely has a role in nodulation, its precise role in Nod factor signaling remains to be demonstrated.

3. Nod factor signaling

3.1 Biochemical approach

Nod factors induce rapid changes in ion concentrations in the root epidermis (71). The earliest response to Nod factors is a calcium influx, induced within seconds after Nod factor addition (53). This Ca^{++} influx is followed by a Cl^- efflux and together they cause the observed plasma membrane depolarization, which is induced about 1 min. after Nod factor addition (53, 72-74). Upon depolarization of the membrane, a K^+ efflux is induced by which the membrane can repolarize (53).

The Ca^{++} influx is sufficient to cause a membrane depolarization since the Ca^{++} ionophore A23187 was able to induce Ca^{++} and Cl^- fluxes leading to the membrane depolymerization. Moreover, the Ca^{++} influx appears also to be essential for Nod factor induced membrane depolarization since nifedipine, a Ca^{++} channel antagonist, as well as EGTA, that chelates Ca^{++} ions, inhibited this response in Nod factor treated plants (53, 75).

The Ca^{++} influx causes an increase of the cytoplasmic Ca^{++} concentration (75-78) but whether this increase is only due to the Ca^{++} influx or also to Ca^{++} release from internal stores is not clear. Furthermore, about 6-10 min. after Nod factor application Ca^{++} spiking has

been observed in the perinuclear region of root hairs of *Medicago*, *Vicia*, *Pisum* and *Lotus* (78-81).

Further insight in the Nod factor signaling came from pharmacological approaches where it was aimed to mimic or block certain Nod factor responses with drugs interfering with a specific signaling step. An assay based on the transcriptional activation of an early nodulin gene (e.g. *ENOD12*) was shown to be very useful. *Medicago* plants expressing a fusion between the *M. truncatula ENOD12* promoter (*MtENOD12*) and the reporter gene *GUS* were used for these studies. The *ENOD12* promoter is induced in the root epidermal cells 2-3 hours after Nod factor application (51, 82, 83). It was tested whether trimeric G-proteins could be involved in Nod factor signaling by studying the effect of mastoparan. Mastoparan is a cationic tetradecapeptide that acts as an activator of G-proteins in animal system (84). Strikingly, mastoparan induced the expression of *MtENOD12::GUS* in the root epidermis in a similar spatial and temporal way as Nod factors. Further, the pertussis toxin, an inhibitor of G-protein activity, blocked the Nod factor induced *MtENOD12::GUS* expression (51).

Further evidence for the involvement of a G-protein coupled receptor in Nod factor signaling came from studies by den Hartog and coworkers (85). They showed that mastoparan was able to induce deformation of *V. sativa* root hairs. Since trimeric G-proteins are known to activate phospholipid signaling in animal cells, it was hypothesized that phospholipids were involved in Nod factor signaling and biochemical studies showed that this is indeed the case. *Vicia* plants were grown in the presence of radioactive phosphate, to label phospholipids and it was shown that Nod factors as well as mastoparan induced an increase of the concentration of phosphatidic acid (PA) and diacylglycerol pyrophosphate (DGPP). Changes in the concentration of other phospholipids, like phosphatidylinositol-4,5-bisphosphate (PIP_2) were not observed. The concentration of PA and DGPP increases in a dose- and time-dependent manner, reaching a maximum 10-15 min. after Nod factor/mastoparan application (85). PA is a potential signal molecule in plants (86-92) and it is converted to DGPP by PA kinase. The increase of PA concentration was shown to be caused by the activation of two plant enzymes namely, phospholipase C (PLC) and phospholipase D (PLD). PLD activity leads to PA formation directly by hydrolysis of structural phospholipids as phosphatidylcholine. In contrast, PLC hydrolyzes PIP_2 into inositol 1,4,5-trisphosphate (IP_3) and diacylglycerol (DAG). DAG is then quickly phosphorylated to PA. By blocking the activation of PLC (neomycin) or PLD (primary alcohols) it was demonstrated that the activation of both phospholipases is essential to induce root hair deformation. PLC activation was also shown to be essential for *ENOD12* induction (51). PLC activation most probably leads to P_3 formation, but the methods used by den Hartog (85) were probably not sensitive enough to detect this increase. Whether IP_3 and/or PA are involved in the induction of *ENOD12* is not known.

3.2 Genetic dissection of the Nod factor signaling

The comparison of the *Rhizobium*-legume interaction and the mycorrhiza-plant association has been of direct importance for the genetic dissection of Nod factor signaling in legume

nodulation. Before these genetic studies are reviewed some background information is provided on the endomycorrhizal symbiosis.

About two decades ago a genetic analysis showed that nodulation and mycorrhizae formation in pea share some common steps (93). This was a surprising discovery since at first glance these two endosymbiotic interactions seem to have little in common. Such genetic analyses have now been done in several legumes and provided insight in the relationship of these two endosymbiotic interactions. The vast majority of higher plants are able to form an endosymbiotic association with fungi belonging to the order of Glomales, which results in the formation of arbuscular mycorrhiza (AM; 94-97). These fungi enter the inner cortical cells of the root where they differentiate into highly branched structure, the so-called arbuscles. Thus the induced morphological responses in the root appear to be very different from those induced by rhizobia. Furthermore, the two interactions are extremes in terms of host specificity: whereas the rhizobial nodulation is highly specific and restricted to legumes (with one exception, namely *Parasponia*), in AM formation there is very little host specificity. Despite these differences, genetic studies showed that several common steps are involved in establishing these symbioses. Furthermore, some nodulin genes are induced during both the interactions e.g. *ENOD12* (96).

Several plant mutants defective in nodulation (*Nod*⁻) have been isolated in legumes like pea (98-100), *M. truncatula* (101-104), *L. japonicus* (105-108) and *M. sativa* (79). In all these host species it was shown that some mutants are blocked in nodulation as well as AM formation. The mutants of pea and *M. truncatula* have been studied in greatest detail with respect to Nod factor responses and their ability to form AM. Therefore the data obtained with these host species will be summarized. It has been tested whether rhizobia (or purified Nod factors) could induce Ca⁺⁺ spiking, activation of early nodulin gene expressions e.g. *ENOD11/12*, root hair deformation/branching and infection thread formation, respectively, in pea and *M. truncatula* mutants. Recently, in *M. truncatula* five loci, *DMI-1*, *DMI-2*, *DMI-3*, *HCL* and *NSP-1* were analyzed. Mutants in these loci are *Nod*⁻ and are blocked at a very early stage of the symbiotic interaction (35, 58). These mutants could be divided in a few groups. The mutants in the loci *DMI-1*, *DMI-2* and *DMI-3* showed root hair tip swelling upon Nod factor treatment, but were blocked in branching (Fig. 3).

Moreover, the early nodulin genes *MtENOD11*, root hair curling, infection as well as cortical cell divisions could not be induced.

Unlike the *dmi* mutants, the root hairs of *hcl* and *nsp-1* mutants were able to branch but curling and initiation of infection thread formation were blocked (35, 58). These data suggest that HCL and NSP act downstream of the *DMI* genes in the Nod factor induced signaling pathway (Fig. 3). The *dmi* mutants could be further classified by examining their Ca⁺⁺ response to Nod factor: *dmi-1* and *dmi-2* mutants were blocked for Ca⁺⁺ spiking, whereas *dmi-3* mutants showed Ca⁺⁺ spiking indistinguishable from wild-type plants (81). This indicates that the *DMI-1* and *DMI-2* genes act upstream of *DMI-3* in the Nod factor signaling pathway (81; Fig. 3).

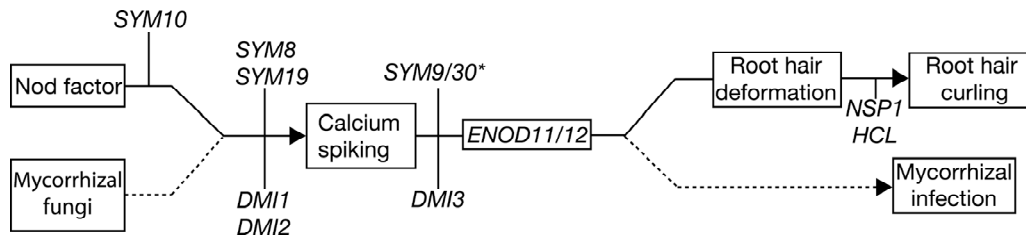


Figure 3. Genetic dissection of Nod factor and mycorrhizal signaling in the root epidermis (modified from 80). Mutations in *SYM8*, *SYM19*, *DMI1* and *DMI2* loci block all the Nod factor induced responses in the epidermis as well as mycorrhizal infection; mutations in *SYM9* and *DMI3* inhibits *ENOD12* induction, root hair deformation and curling and mycorrhizal infection but not Ca^{++} spiking; since mutation in *SYM10* blocks Ca^{++} spiking but not mycorrhizal infection *SYM10* acts upstream of the common steps to rhizobia and mycorrhizal infection; on the other site mutations in *NSP-1* and *HCL* block root hair curling but not deformation, Ca^{++} spiking or mycorrhizal infection. The induction of Ca^{++} spiking during mycorrhizal infection has not been tested. *, preliminary data (80) suggest that *SYM9* and *SYM30* belong to the same complementation group.

Also several pea mutants have been identified that are affected in early steps of the symbiotic interaction (these all are all named *sym* mutants; 98-100, 109). Like the Medicago *dmi-1* and *dmi-2* mutants, *sym8*, *sym10* and *sym19* mutants were blocked in Nod factor induced Ca^{++} spiking, *ENOD12* induction and root hair deformation, whereas *SYM9* like the Medicago *DMI-3* is positioned in between Ca^{++} spiking and *ENOD12* induction (80, 110; Figure 3).

When these pea and Medicago mutants were analyzed for their ability to form AM all the *dmi* mutants as well as the pea *sym8*, *sym19* and *sym9* mutants were also unable to interact with endomycorrhizal fungi (Myc⁻), whereas the Medicago *hcl* and *nsp-1* mutants were not affected (Myc⁺). This observation indicates that the *DMI* and the orthologs pea *SYM* genes control common steps in the signal transduction cascade induced by rhizobial and mycorrhiza signals leading (among others) to *ENOD12* activation. The signaling pathway obviously branches upstream of *ENOD11/12* induction, since the *hcl* and *nsp-1* mutants are Myc⁺ (Figure 3). The pea *SYM10* gene has a unique property. It is obviously involved in a very early stage of the interaction since: Ca^{++} spiking is blocked in the *sym10* mutant and, in contrast with the other genes required for Ca^{++} spiking, it is not essential for AM formation. Since the ultimate morphological responses induced by mycorrhizal fungi and rhizobia are different it seems probable that the mycorrhizal signal molecule differs in some way from the rhizobial Nod factors. This assumption would imply that the perception of Nod factors and maybe early steps of signaling are not shared by the two interactions. Therefore *SYM10* could be a Nod factor receptor or could be involved in a very early stage of the Nod factor signaling.

The cloning of the above-described genes will ultimately provide insight in the molecular mechanisms controlling signaling events in both interactions. Since several genes are also involved in AM formation it is probable that these genes are wide spread in the plant kingdom and are not restricted to legumes. Such genes will therefore be also important tools to study the phylogenetic origin of nodulation.

4. Concluding remarks

In the second part of this review we have summarized the biochemical and genetic studies on the mechanisms of Nod factor perception (paragraphs 2.1-2.3) and transduction (paragraphs 3.1-3.2) in root hairs. It is obvious that these studies have revealed many candidate pieces of the Nod factor perception/signaling jigsaw, but in most cases their relevance and precise role needs to be carefully evaluated.

4.1 Cloning of legume genes involved in Nod factor perception or transduction

It is clear that the genetically identified genes are essential for certain steps in the Nod factor induced signaling and cloning of these genes will be of pivotal importance to advance our knowledge on Nod factor perception and transduction.

Up till recently, legume mutants had especially been made in agronomically important crop plant, like pea, soybean and clover. Unfortunately, these legumes have large and/or complex genomes which have impeded a map-based cloning with the result that none of these genes has been cloned. To overcome these problems two legume model systems have now been developed *Medicago truncatula* and *Lotus japonicus* (111, 112). Both model legumes are diploid, have a rather small genome (4-5 times bigger than *Arabidopsis*) and worldwide genome projects on these legumes have and will provide the tools to clone and analyze the genes of interest. However, it still might be important to clone certain genes of non-model legumes especially when these genes play a key role in the process and have not been identified by genetic approaches in the model legumes. An example is the pea *SYM10* gene that is a good candidate for the Nod factor receptor (80). Fortunately pea is highly microsyntenic with *M. truncatula* and therefore it is very probable that *M. truncatula* can be used as an intergenomic cloning vehicle for the cloning of pea genes of interest (113).

Many mutants in *L. japonicus* and *M. truncatula* have been identified, that are specifically affected in the infection by rhizobia. Moreover, Nod factor signaling in *M. truncatula* has now been genetically dissected (paragraph 3.2). The achievements of the genome projects on these model legumes will now make it possible to clone the identified loci. Recently, indeed the first *L. japonicus* gene required for infection has been cloned. This is the *NIN* gene, which encodes a putative transcription factor (106). It is to be expected that most *M. truncatula* genes indicated in Fig. 3 will be cloned within a couple of years and this will provide tools to test hypothesis as depicted in Fig. 3. It is probable that this proposed signaling cascade is far more complex and this is illustrated by the preliminary data of the group of Kiss (see 114). They showed that a *M. sativa* gene with a similar function as *DMI-1* or *DMI-2*, and which is probably an ortholog of one of these genes, encodes a putative receptor kinase containing an extracellular leucine-rich repeat domain. However, the scheme depicted in Fig. 3 suggests that this gene is active downstream of Nod factor perception. Therefore a further analysis of this gene might falsify the proposed hypothesis or alternatively, this gene could have a very intriguing function in the signaling cascade.

4.2 Integration of biochemical and genetic studies

The cell biological, biochemical and genetic studies on Nod factor signaling each provided insight in Nod factor perception mechanisms. Fortunately, most studies are now focused on the model legumes and many of the data described in this review were obtained with *Medicago* species. This will facilitate the integration of data obtained with the various approaches.

The analysis of Ca^{++} spiking in the various *Medicago* and pea mutants is a first step towards an integration of the biochemical and genetic approaches. This study made it possible to classify the identified legume mutants but it also provided a strong indication that Ca^{++} spiking is a relevant step in Nod factor signaling. Further biochemical and electrophysiological studies on the available mutants will be essential to integrate the signaling pathways obtained with the two different approaches. Moreover, this can also reveal the relevance of certain proposed steps of the signaling cascade signaling process. For example the set of *Medicago* mutants will make it possible to assess whether indeed trimeric G-proteins play a role in signaling. This is especially important since not all subunits of trimeric G-proteins have been identified in plants (115). Further, trimeric G-proteins are almost exclusively activated by serpentine receptors (116), which are also scarce in plants.

4.3 From signal to form

The cell biological analysis of root hair curling and infection thread formation indicate that these processes are regulated by mechanisms that are derived of those controlling “normal” root hair growth. Furthermore, it is clear that both the actin and microtubule skeleton play a key role in these processes. The configuration of the actin skeleton rapidly (within 3-15 min.) changes after Nod factor addition. This shows that this part of the skeleton is one of the first targets of Nod factor signaling and therefore, it will be important to correlate the elements involved in Nod factor signaling, e.g. ion fluxes, G-protein activation and phosphoinositides, with the actin cytoskeleton rearrangements. Although the mechanism by which Nod factors induce these changes in the actin cytoskeleton is not known, it is likely to involve the activation of several Actin Binding Proteins (ABPs). These proteins, including monomer-sequestering, end capping, cross-linking, severing and side-binding proteins, regulate the rate of actin polymerizing and the configuration of the skeleton (F-actin; 117, 118). A few ABPs have been identified in plants and some of these can be regulated by phosphoinositides (e.g. ADF/cofilin and profilin) or by Ca^{++} (ADF/cofilin and villin; 119, 120). Since both intracellular Ca^{++} and phosphoinositide concentrations rapidly change after Nod factor addition it is possible that ABP like ADF and profilin are involved in the Nod factor induced changes of the configuration of the actin cytoskeleton.

Both root hair deformation and curling have in common that tip growth is put under control of Nod factor secreting rhizobia, and moreover, during root hair curling, also the direction of tip growth is strictly controlled. Curling is accompanied by marked changes in the configuration of the microtubule skeleton. Since it has been shown that this part of the cytoskeleton is especially involved in controlling the direction of growth it seems probable that the

microtubules are a key player in the curling process. It will be a major challenge to unravel the mechanism controlling curling (and the initiation of infection) since bacteria secreting Nod factor are essential and purified Nod factors are not sufficient to induce these processes. Furthermore, these processes are only induced in a minority of the root hairs by which (classical) biochemical studies are almost impossible. Fortunately, cell biological approaches are being developed by which important components of signal transduction cascades can be monitored in living cells. Examples are chameleon construct by which free Ca^{++} concentrations can be monitored in living cells (121) or PP_2 binding domain (pleckstrin domain) that allow to follow its localization in living cells (122). This, in combination with the fact that both actin and microtubule skeleton can be visualized *in vivo* with GFP (Green Fluorescent Protein; 123-125) based fusions, will make it possible to study fascinating processes like curling and infection thread initiation. Such a cell biological approach should be integrated with molecular genetic studies aiming to clone genes that are specifically involved in curling and infection, like *HCL*, *NSP* and *SYM2*. In years to come, the symbioses between the achievements of the genetic analysis and the effort put in establishing the cell biological tools, will add relevant insights in our knowledge on the Nod factor signaling.

References

1. Cohn, J., Day, B., and Stacey, G. (1998). Legume nodule organogenesis. *Trends Plant Sci*: **3**, 105.
2. Bladergroen, M. R., and Spaik, H. P. (1998). Genes and signal molecules involved in the rhizobia-leguminosae symbiosis. *Curr. Opin. Plant Biol*: **1**, 353.
3. Hadri, A.-E., Spaik, H. P., Bisseling, T., and Brewin, N. J. (1998). Diversity of Root Nodulation and Rhizobial Infection Processes. In *Rhizobiaceae*. Spaik, H.P., Kondorosi, A. and Hooykaas, P.J.J. (ed.), Kluwer Academic publisher, Dordrecht, **1**, 347.
4. Long, S. R. (1996). *Rhizobium* symbiosis: Nod factors in perspective. *Plant Cell*: **8**, 1885.
5. Mylona, P., Pawlowski, K., and Bisseling, T. (1995). Symbiotic Nitrogen Fixation. *Plant Cell*: **7**, 869.
6. Schultze, M., and Kondorosi, A. (1998). Regulation of symbiotic root nodule development. *Annu. Rev. Genet*: **32**, 33.
7. Schlaman, H. R. M., Phillips, D. A., and Kondorosi, E. (1998). Genetic Organization and Transcriptional Regulation of Rhizobial Nodulation Genes. In *Rhizobiaceae*. Spaik, H. P., Kondorosi, A. and Hooykaas, P. J. J. (ed.), Kluwer Academic publisher, Dordrecht, **1**, 361.
8. Downie, J. A. (1998). Functions of rhizobial nodulation genes. In *Rhizobiaceae*. Spaik, H. P., Kondorosi, A. and Hooykaas, P. J. J. (ed.), Kluwer Academic publisher, Dordrecht, **1**, 387.
9. Lerouge, P., Roche, P., Faucher, C., Maillet, F., Truchet, G., Prome, J. C., and Dénarié, J. (1990). Symbiotic host-specificity of *Rhizobium meliloti* is determined by a sulphated and acylated glucosamine oligosaccharide signal. *Nature*, **344**: 781.
10. Spaik, H. P., Sheeley, D. M., van Brussel, A. A., Glushka, J., York, W. S., Tak, T., Geiger, O., Kennedy, E. P., Reinhold, V. N., and Lugtenberg, B. J. (1991). A novel highly unsaturated fatty acid moiety of lipo-oligosaccharide signals determines host specificity of *Rhizobium*. *Nature*, **354**: 125.
11. Perret, X., Staehelin, C., and Broughton, W. J. (2000). Molecular basis of symbiotic promiscuity. *Microbiol. Mol. Biol. Rev*: **64**, 180.
12. Dénarié, J., Debelle, F., and Prome, J. C. (1996). *Rhizobium* lipo-chito-oligosaccharide nodulation factors: signaling molecules mediating recognition and morphogenesis. *Annu. Rev. Biochem*: **65**, 503.
13. Yang, G. P., Debelle, F., Savagnac, A., Ferro, M., Schiltz, O., Maillet, F., Prome, D., Treilhou, M., Vialas, C., Lindstrom, K., Dénarié, J., and Prome, J.C. (1999). Structure of the *Mesorhizobium huakuii* and *Rhizobium galegae* Nod factors: a cluster of phylogenetically related legumes are nodulated by rhizobia producing Nod factors with alpha, beta-unsaturated N-acyl substitutions. *Mol. Microbiol*: **34**, 227.
14. Cai, G., Moscatelli, A. and Cresti, M. (1997). Cytoskeleton organization and pollen tube growth. *Trends Plant Sci*: **2**, 86.

15. **Kropf, D. L.** (1997). Induction of polarity in fucoid zygotes. *Plant Cell*: **9**, 1011.
16. **Sieber, B., and Emons, A. M. C.** (2000). Cytoarchitecture and pattern of cytoplasmic streaming in root hair of *Medicago truncatula* during development and deformation by nodulation factor. *Protoplasma*: **214**, 118.
17. **Miller, D. D., de Ruijter, N. C. A., and Emons A. M. C.** (1997). From signal to form: aspects of the cytoskeleton-plasma membrane-cell wall continuum in root hair tips. *J. Exp. Botany*: **48**: 1881.
18. **Miller, D. D., Leferink-ten Klooster, H. B., and Emons, A. M. C.** (2000). Lipochito-Oligosaccharide Nodulation Factors Stimulate Cytoplasmic Polarity with Longitudinal Endoplasmatic Reticulun and Vesicles at the Tip in Vetch Root Hairs. *Molecular Plant Microbe-Interact*: **13**: 1385.
19. **Ridge, R. W.** (1992). A model of legume root hair growth and *Rhizobium* infection. *Symbiosis*, **14**: 359.
20. **Galway, M. E.** (2000). Root Hair Ultrastructure and Tip Growth. In *Root Hair: Cell and Molecular Biology*. Ridge, R. W. and Emons, A. M. C. (ed.), Springer: **1**, 1.
21. **Miller, D. D., de Ruijter, N. C. A., Bisseling, T., and Emons, A. M. C.** (1999). The role of actin in root hair morphogenesis: studies with lipochito-oligosaccharide as a growth stimulator and cytochalasin as an actin perturbing drug. *Plant J*: **17**, 141.
22. **Esseling, J., de Ruijter, N. C. A., and Emons, A. M. C.** (2000). The Root Hair Actin Cytoskeleton as Backbone, Highway. Morphogenic Instrument and Target for Signaling. In *Root Hair: Cell and Molecular Biology*. Ridge, R. W. and Emons, A. M. C. (ed.), Springer: **1**, 29.
23. **Kropf, D. L., Bisgrove, S. R., and Hable, W. E.** (1998). Cytoskeletal control of polar growth in plant cells. *Curr. Opin. Cell Biol*: **10**, 117.
24. **Bibikova, T. N., Blancaflor, E. B., and Gilroy, S.** (1999). Microtubules regulate tip growth and orientation in root hairs of *Arabidopsis thaliana*. *Plant J*: **17**, 657.
25. **Emons, A. M. C., Wolters-Arts, J.A., Traas, J., and Derksen, J.** (1990). The effects of colchicine on microtubules and microfibrils in root hairs. *Acta Bot. Neerl*: **39**, 19.
26. **Sievers, A., and Schnepf, E.** (1981). Morphogenesis and polarity in tubular cells with tip growth. In *Cytomorphogenesis in Plants*. Kiermayer, O. (ed.), Springer-Verlag, New-York: 265.
27. **That, T. C., Rossier, C., Barja, F., Turian, G., and Roos, U. P.** (1988). Induction of multiple germ tubes in *Neurospora crassa* by antitubulin agents. *Eur. J. Cell Biol*: **46**, 68.
28. **Traas, J. A., Braat, P., Emons, A. M., Meekes, H., and Derksen, J.** (1985). Microtubules in root hairs. *J. Cell Sci*: **76**, 303.
29. **Lloyd, C. W., and Wells, B.** (1985). Microtubules are at the tips of root hairs and form helical patterns corresponding to inner wall fibrils. *J. Cell Sci*: **75**, 225.
30. **Emons, A. M. C.** (1989). Helicoidal microfibril deposition in a tip growing cell and microtubule alignment during tip morphogenesis: a dry cleaving and freeze-substitution study. *Canadian J. of Botany*: **67**, 2401.
31. **Ketelaar, T., and Emons, A. M. C.** (2000). The Role of Microtubules in Root Hair Growth and Cellulose Microfibril Deposition. In *Root Hair: Cell and Molecular Biology*. Ridge, R.W. and Emons, A.M.C. (ed.), Springer: **1**, 17.
32. **Ridge, R. W.** (1996). Root hairs: cell biology and development. In *Plant roots: the hidden half*. Waisel, Y., Eshel, A., Kafkafi, U. (ed), Marcel Dekker Inc., New York: **1**, 127
33. **Lloyd, C. W., Pearce, K. J., Rawlins, D. J, Ridge, R. W., and Shaw, P. J.** (1987). Endoplasmatic microtubules connect the advancing nucleus to the tip of legume root hairs, but F-actin is involved in basipetal migration. *Cell Motility and Cytoskeleton*: **8**, 27.
34. **Timmers, A. C., Auriac, M. C., and Truchet, G.** (1999). Refined analysis of early symbiotic steps of the *Rhizobium*-*Medicago* interaction in relationship with microtubular cytoskeleton rearrangements. *Development*: **126**, 3617.
35. **Catoira, R., Galera, C., de Billy, F., Penmetsa, R. V., Journet, E. P., Maillet, F., Rosenberg, C., Cook, D., Gough, C., and Dénarié, J.** (2000). Four genes of *Medicago truncatula* controlling components of a nod factor transduction pathway. *Plant Cell*: **12**, 1647.
36. **Heidstra, R., Geurts, R., Franssen, H., Spaink, H., van Kammen, A., and Bisseling, T.** (1994). Root hair deformation activity of nodulation factors and their fate on *Vicia Sativa*. *Plant Physiol*: **105**, 787.
37. **de Ruijter, N. C. A., Rook, M. B., Bisseling, T., and Emons, A. M. C.** (1998). Lipochito-oligosaccharides re-initiate root hair tip growth in *Vicia sativa* with high calcium and spectrin-like antigen at the tip. *Plant J*: **13**, 341.
38. **Allen, N. S., Bennett, M. N., Cox, D. N., Shipley, A., Ehrhardt, D. W., and Long, S. R.** (1994). Effect of Nod factors on alfalfa root hair Ca^{++} and H^+ currents and on cytoskeletal behavior. In *Advances in Molecular Genetics of Plant-Microbe interactions*. Daniels, M. J., Downie, J. A., Osbourn, A. E. (ed.), Kluwer Academic Publishers, Dordrecht, The Netherlands: **1**, 107-113.
39. **Allen, N. S., and Bennett, M. N.** (1996). Electro-optical imaging F-actin and endoplasmatic reticulum in living and fixed plant cells. *Scanning Microsc. Suppl*: **10**, 177.
40. **Cárdenas, L., Vidali, L., Dominguez, J., Perez, H., Sanchez, F., Hepler, P. K. and Quinto, C.** (1998). Rearrangement of Actin Microfilaments in Plant Root Hairs Responding to *Rhizobium etli* Nodulation Signals. *Plant Physiol*: **116**, 871.
41. **de Ruijter, N. C. A., Bisseling, T. and Emons, A. M. C.** (1999). *Rhizobium* Nod factors induce an increase in sub-apical fine bundles of actin filaments in *Vicia sativa* root hairs within minutes. *Molecular Plant-Microbe interact*: **12**, 829.

42. **Emons, A. M. C., and deRuijter, N. C. A.** (2000). Actin: a target of signal transduction in root hairs. In *Actin: A Dynamic Framework of Multiple Plant Cell Functions*. Staiger, C.J. (ed.), Kluwer Academic Publisher, The Netherlands: **1**, 373.
43. **Relic, B., Talmont, F., Kopcinska, J., Golinowski, W., Prome, J. C., and Broughton, W. J.** (1993). Biological activity of *Rhizobium* sp. NGR234 Nod-factors on *Macroptilium atropurpureum*. *Molecular Plant-Microbe Interact*: **6**, 764.
44. **van Batenburg, F. H. D., Jonker, R., and Kijne, J. W.** (1986). *Rhizobium* induces marked root hair curling by redirection of tip growth: a computer simulation. *Physiol. Plant*: **66**, 476.
45. **Emons, A. M. C., Mulder, B.** (2000). Nodulation Factor Trigger an Increase of Fine Bundles of Subapical Actin Filaments in *Vicia* Root Hair: Implication for Root Hair Curling around Bacteria. In *Biology of Plant-Microbe Interactions*. P. J. G. M. De Wit, T. Bisseling and W. J. Stiekema, (ed.), Published by the International Society of Molecular Plant-Microbe Interaction, St. Paul, Minnesota, USA: **2**, 272.
46. **van Spronsen, P. C., Bakhuizen, R., van Brussel, A. A., and Kijne, J. W.** (1994). Cell wall degradation during infection thread formation by the root nodule bacterium *Rhizobium leguminosarum* is a two-step process. *Eur. J. Cell Biol*: **64**, 88.
47. **Ridge, R. W., Rolfe, B. G.** (1985). *Rhizobium* sp. Degradation of legume root hair cell wall at the site of infection thread origin. *Appl. Environ. Microbiol*: **50**, 717.
48. **Bauer, W. D.** (1981). Infection of legumes by rhizobia. *Annu. Rev. Plant Physiol*: **32**, 407.
49. **Bakhuizen, R.** (1988). The plant cytoskeleton in the *Rhizobium*-legume symbiosis. PhD thesis. Leiden University, The Netherlands.
50. **Timmers, A. C. J.** (2000). Infection of Root Hairs by Rhizobia: Infection Thread Development with Emphasis on the Microtubular Cytoskeleton. In *Root Hair: Cell and Molecular Biology*. Ridge, R. W. and Emons, A. M. C. (ed.), Springer: **1**, 223.
51. **Pingret, J. L., Journet, E. P., and Barker, D. G.** (1998). *Rhizobium* Nod factor signaling. Evidence for a G protein-mediated transduction mechanism. *Plant Cell*: **10**, 659.
52. **Felle, H. H., Kondorosi, E., and Schultze, M.** (1996). Rapid alkalinization in alfalfa root hairs in response to rhizobial lipochitooligosaccharide signals. *Plant J*: **13**, 455.
53. **Felle, H. H., Kondorosi, E., Kondorosi, A. and Schultze, M.** (1998). The role of ione fluxes in Nod factor signaling in *Medicago sativa*. *Plant J*: **13**, 455.
54. **Schlaman, H. R., Gisel, A. A., Quaadvlieg, N. E., Bloemberg, G. V., Lugtenberg, B. J., Kijne, J. W., Potrykus, I., Spaik, H. P., and Sautter, C.** (1997). Chitin oligosaccharides can induce cortical cell division in roots of *Vicia sativa* when delivered by ballistic microtargeting. *Development*, **124**: 4887.
55. **Goedhart, J., Rohrig, H., Hink, M. A., van Hoek, A., Visser, A. J., Bisseling, T., and Gadella, T. W., Jr.** (1999). Nod factors integrate spontaneously in biomembranes and transfer rapidly between membranes and to root hairs, but transbilayer flip-flop does not occur. *Biochemistry*: **38**: 10898.
56. **Goedhart, J., Hink, M. A., Visser, A. J., Bisseling, T., and Gadella, T. W., Jr.** (2000). *In vivo* fluorescence correlation microscopy (FCM) reveals accumulation and immobilization of Nod factors in root hair cell walls. *Plant J*: **21**, 109.
57. **Philip-Hollingsworth, S., Dazzo, F. B., and Hollingsworth, R. I.** (1997). Structural requirements of *Rhizobium* chitolipooligosaccharides for uptake and bioactivity in legume roots as revealed by synthetic analogs and fluorescent probes. *J. Lipid Res.*, **38**: 1229.
58. **Catoira, R., Timmers, A. C. J., Maillet, F., Galera, C., Varma Penmetsa, R., Cook, D., Dénarié, J., and Gough, C.** (2001). The *HCL* gene of *Medicago truncatula* controls *Rhizobium*-induced root hair curling. *Development*:
59. **Walker, S. A., and Downie, J. A.** (2000). Entry of *Rhizobium leguminosarum* bv.viciae into root hairs requires minimal Nod factor specificity, but subsequent infection thread growth requires *nodO* or *nodE*. *Molecular Plant-Microbe Interact*: **13**, 754.
60. **Ardourel, M., Demont, N., Debelle, F., Maillet, F., de Billy, F., Prome, J. C., Dénarié, J., and Truchet, G.** (1994). *Rhizobium meliloti* lipooligosaccharide nodulation factors: different structural requirements for bacterial entry into target root hair cells and induction of plant symbiotic developmental responses. *Plant Cell*: **6**, 1357.
61. **Geurts, R., Heidstra, R., Hadri, A-E., Downie, A., Franssen, H., van Kammen, A., and Bisseling, T.** (1997). *SYM2* of *Pisum sativum* is involved in a Nod factor perception mechanism that controls the infection process in the epidermis. *Plant Physiol*: **115**, 351.
62. **Davis, E. O., Evans, I. J., and Johnston, A. W.** (1988). Identification of *nodX*, a gene that allows *Rhizobium leguminosarum* biovar viciae strain TOM to nodulate Afghanistan peas. *Mol Gen Genet*: **212**, 531.
63. **Firmin, J. L., Wilson, K. E., Carlson, R. W., Davies, A. E., and Downie, J. A.** (1993). Resistance to nodulation of cv. Afghanistan peas is overcome by *nodX*, which mediates an O-acetylation of the *Rhizobium leguminosarum* lipo-oligosaccharide nodulation factor. *Mol. Microbiol*: **10**, 351.
64. **Bono, J. J., Rioud, J., Nicolaou, K. C., Bockovich, N. J., Estevez, V. A., Cullimore, J. V., and Ranjeva, R.** (1995). Characterization of a binding site for chemically synthesized lipo-oligosaccharidic NodRm factors in particulate fractions prepared from roots. *Plant J*: **7**, 253.
65. **Gressent, F., Drouillard, S., Mantegazza, N., Samain, E., Geremia, R. A., Canut, H., Niebel, A., Driguez, H., Ranjeva, R., Cullimore, J., and Bono, J. J.** (1999). Ligand specificity of a high-affinity binding site for lipo-chitooligosaccharidic nod factors in medicago cell suspension cultures. *Proc. Natl. Acad. Sci U S A*: **96**, 4704.

66. **Stacey, G., and Shibuya, N.** (1997). Chitin recognition in rice and legumes. *Plant Soil*: **194**, 161.
67. **Diaz, C. L., Spaink, H. P., and Kijne, J. W.** (2000). Heterologous rhizobial lipochitin oligosaccharides and chitin oligomers induce cortical cell divisions in red clover roots, transformed with the pea lectin gene. *Molecular Plant Microbe-Interact*: **13**, 268-76.
68. **van Rhijn, P., Goldberg, R. B., and Hirsch, A. M.** (1998). *Lotus corniculatus* nodulation specificity is changed by the presence of a soybean lectin gene. *Plant Cell*: **10**, 1233.
69. **Thomas, C., Sun, Y., Naus, K., Lloyd, A., and Roux, S.** (1999). Apyrase functions in plant phosphate nutrition and mobilizes phosphate from extracellular ATP. *Plant Physiol.*, **119**, 543.
70. **Day, R. B., McAlvin, C. B., Loh, J. T., Denny, R. L., Wood, T. C., Young, N. D., and Stacey, G.** (2000). Differential expression of two soybean apyrases, one of which is an early nodulin. *Mol. Plant-Microbe Interact*: **13**, 1053.
71. **Cárdenas, L., Holdaway-Clarke, T. L., Sanchez, F., Quinto, C., Feijó, J. A., Kunkel, J. G., and Hepler, P. K.** (2000). Ion Changes in Legume Root Hairs Responding to Nod Factors. *Plant Physiol*: **123**, 443.
72. **Ehrhardt, D. W., Atkinson, E. M., and Long, S. R.** (1992). Depolarization of alfalfa root hair membrane potential by *Rhizobium meliloti* Nod factors. *Science*: **256**, 998.
73. **Kurkdjian, A. C.** (1995). Role of the differentiation of root epidermal cells in Nod factor from *Rhizobium meliloti*-induced depolarization of *Medicago sativa*. *Plant Physiol*: **107**, 783.
74. **Felle, H. H., Kondorosi, E., Kondorosi, A. and Schultze, M.** (1995). Nod signal-induced plasma membrane potential changes in alfalfa root hairs are differently sensitive to structural modifications of the lipo-chitooligosaccharide. *Plant J*: **7**, 939.
75. **Felle, H. H., Kondorosi, E., Kondorosi, A., and Schultze, M.** (1999). Nod factors modulate the concentration of cytosolic free calcium differently in growing and non-growing root hairs of *Medicago sativa* L. *Planta*: **209**, 207.
76. **Gehring, C. A., Irving, H. R., Kabbara, A. A., Parish R. W., Boukli, N. M. and Broughton, W. J.** (1997). Rapid, plateau-like increases in intracellular free calcium are associated with Nod-factor-induced root hair deformation. *Molecular Plant-Microbe Interact*: **7**, 791.
77. **Felle, H. H., Kondorosi, E., Kondorosi, A., and Schultze, M.** (1999). Elevation of the cytosolic free $[Ca^{2+}]$ is indispensable for the transduction of the Nod factor signal in alfalfa. *Plant Physiol*: **121**, 273.
78. **Cárdenas, L., Feijo, J. A., Kunkel, J. G., Sanchez, F., Holdaway-Clarke, T., Hepler, P. K., and Quinto, C.** (1999). *Rhizobium* Nod factors induce increases in intracellular free calcium and extracellular calcium influxes in bean root hairs. *Plant J*: **19**, 347.
79. **Ehrhardt, D. W., Wais, R., and Long, S. R.** (1996). Calcium spiking in plant root hairs responding to *Rhizobium* nodulation signals. *Cell*: **85**, 673.
80. **Walker, S. A., Viprey, V., and Downie, J. A.** (2000). Dissection of nodulation signaling using pea mutants defective for calcium spiking induced by nod factors and chitin oligomers. *Proc. Natl. Acad. Sci. U S A*: **97**, 13413.
81. **Wais, R. J., Galera, C., Oldroyd, G., Catoira, R., Penmetza, R. V., Cook, D., Gough, C., Dénarié, J., and Long, S. R.** (2000). Genetic analysis of calcium spiking responses in nodulation mutants of *Medicago truncatula*. *Proc. Natl. Acad. Sci. U S A*: **97**, 13407.
82. **Pichon, M., Journet, E. P., Dedieu, A., de Billy, F., Truchet, G., and Barker, D. G.** (1992). *Rhizobium meliloti* elicits transient expression of the early nodulin gene *ENOD12* in the differentiating root epidermis of transgenic alfalfa. *Plant Cell*: **4**, 1199.
83. **Chabaud, M., Larssonneau, C., Marmouget, C., and Huguet, T.** (1996). Transformation of barrel medic (*Medicago truncatula* Gaertn.) by *Agrobacterium tumefaciens* and regeneration via somatic embryogenesis of transgenic plants with the *MtENOD12* nodulin promoter fused to the *GUS* reporter gene. *Plant Cell Rep*: **15**, 305.
84. **Ross, E. M., and Higashijima, T.** (1994). Regulation of G-protein activation by mastoparans and other cationic peptides. *Methods Enzymol*: **237**, 26.
85. **den Hartog, M., Musgrave, A., and Munnik, T.** (2001). Nod factor-induced phosphatidic acid and diacylglycerol pyrophosphate formation: a role for phospholipase C and D in root-hair deformation. *Plant J*: **25**, 1.
86. **Munnik, T., Arisz, S. A., De Vrije, T., and Musgrave, A.** (1995). G-protein activation stimulates phospholipase D signaling in plants. *Plant Cell*: **7**, 2197.
87. **Munnik, T., Van Himbergen, J. A. J., Ter Riet, B., Braun, F. J., Irvine, R. F., Van den Hende, H., and Musgrave, A.** (1998). Detailed analysis of the turnover of polyphosphoinositides and phosphatidic acid upon activation of phospholipase C and D in *Clamydomonas* cells treated with non-permeabilizing concentrations of mastoparan. *Planta*: **207**, 133.
88. **Munnik, T., Meijer, H. J., Ter Riet, B., Hirt, H., Frank, W., Bartels, D., and Musgrave, A.** (2000). Hyperosmotic stress stimulates phospholipase D activity and elevates the levels of phosphatidic acid and diacylglycerol pyrophosphate. *Plant J*: **22**, 147.
89. **Ritchie, S., and Gilroy, S.** (1998). Absciscic acid signal transduction in the barley aleurone is mediated by phospholipase D activity. *Proc. Natl. Acad. Sci. U S A*: **95**, 2697.
90. **Ritchie, S., and Gilroy, S.** (2000). Absciscic acid stimulation of phospholipase D in the barley aleurone is G-protein-mediated and localized to the plasma membrane. *Plant Physiol*: **124**, 693.
91. **Jacob, T., Ritchie, S., Assmann, S. M., and Gilroy, S.** (1999). Absciscic acid signal transduction in guard cells is mediated by phospholipase D activity. *Proc. Natl. Acad. Sci. U S A*: **96**, 12192.

92. **Munnik, T., Irvine, R. F., and Musgrave, A.** (1998). Phospholipid signalling in plants. *Biochim. Biophys. Acta*, **1389**, 222.
93. **Duc, G., Trouvelot, A., Gianinazzi-Pearson, V., and Gianinazzi, S.** (1989). First report of non-mycorrhizal plant mutants (Myc⁻) obtained in pea (*Pisum sativum*) and Fababean (*Vicia Faba* L.). *Plant Sci*: **60**, 215.
94. **Harrison, M. J.** (1997). The arbuscular mycorrhizal symbiosis: an underground association. *Trends in Plant Sci*: **2**, 54.
95. **Harrison, M. J.** (1998). Development of the arbuscular mycorrhizal symbiosis. *Curr. Opin. Plant Biol*: **1**, 360.
96. **Albrecht, C., Geurts, R., Lapeyrie, F., and Bisseling, T.** (1998). Endomycorrhizae and Rhizobial Nod factors both require *SYM8* to induce the expression of the early nodulin genes *PsENOD5* and *PsENOD12A*. *The Plant J*: **15**, 605.
97. **Albrecht, C., Geurts, R., and Bisseling, T.** (1999). Legume nodulation and mycorrhizae formation; two extremes in host specificity meet. *Embo J*: **18**, 281.
98. **Kneen, B. E., Weeden, N. F., and LaRue, T. A.** (1994). Non nodulating mutants of *Pisum sativum* (L.) cv. Sparkle. *J. Heredity*: **85**, 129.
99. **Sagan, M., Huguet, T., and Duc, G.** (1994). Phenotypic characterization and classification of nodulation mutants of pea (*Pisum sativum*). *Plant Sci*: **100**, 59.
100. **Duc, G., and Messenger, A.** (1989). Mutagenesis of pea (*Pisum sativum* L) and the isolation of mutants for nodulation and nitrogen fixation. *Plant Sci.*, **60**, 207.
101. **Sagan, M., Morandi, D., Tarengi, E., and Duc, G.** (1995). Selection of nodulation and mycorrhizal mutants in the model plant *Medicago truncatula* (Gaertn) after g-ray mutagenesis. *Plant Sci*: **111**, 63.
102. **Sagan, M., de Larambergue, H., and Morandi, D.** (1998). Genetic analysis of symbiosis mutants in *Medicago truncatula*. In *Biological Nitrogen Fixation for the 21st Century*. Elmerich, C., Kondorosi, A., Newton, W. E. (ed.), Kluwer Academic Publisher, Dordrecht, The Netherlands: **1**, 317.
103. **Penmetsa, R. V., and Cook, D. R.** (1997). A Legume Ethylene-Insensitive Mutant Hyperinfected by Its Rhizobial Symbiont. *Science*: **275**, 527.
104. **Penmetsa, R. V., and Cook, D. R.** (2000). Production and Characterization of Diverse Developmental Mutants of *Medicago truncatula*. *Plant Physiology*: **123**, 1387.
105. **Schauser, L., Handberg, K., Sandal, N., Stiller, J., Thykjaer, T., Pajuelo, E., Nielsen, A., and Stougaard, J.** (1998). Symbiotic mutants deficient in nodule establishment identified after T-DNA transformation of *Lotus japonicus*. *Mol. Gen. Genet*: **259**, 414.
106. **Schauser, L., Roussis, A., Stiller, J., and Stougaard, J.** (1999). A plant regulator controlling development of symbiotic root nodules. *Nature*: **402**, 191.
107. **Wopereis, J., Pajuelo, E., Dazzo, F. B., Jiang, Q., Gresshoff, P. M., De Bruijn, F. J., Stougaard, J., and Szczyglowski, K.** (2000). Short root mutant of *Lotus japonicus* with a dramatically altered symbiotic phenotype. *Plant J*: **23**, 97.
108. **Szczyglowski, K., Shaw, R. S., Wopereis, J., Copeland, S., Hamburger, D., Kasiborski, B., Dazzo, F.B., and de Bruijn, F. J.** (1998). Nodule Organogenesis and Symbiotic Mutants of the Model Legume *Lotus Japonicus*. *Molecular Plant-Microbe Interact*: **11**, 684.
109. **Markwei, C. M., and La Rue, T. A.** (1992). Phenotypic characterization of *SYM8* and *SYM9*, two genes conditioning non nodulation in *Pisum sativum* "sparkle". *Can. J. Microbiol*: **38**, 548.
110. **Schneider, A., Walker, S. A., Poyser, S., Sagan, M., Ellis, T. H., and Downie, J. A.** (1999). Genetic mapping and functional analysis of a nodulation-defective mutant (*SYM19*) of pea (*Pisum sativum* L.). *Mol. Gen. Genet*: **262**, 1.
111. **Cook, D. R.** (1999). *Medicago truncatula*--a model in the making! *Curr. Opin. Plant Biol*: **2**, 301.
112. **Jiang, Q., and Gresshoff, P. M.** (1997). Classical and molecular genetics of the model legume *Lotus japonicus*. *Molecular Plant-Microbe Interact*: **10**, 59.
113. **Gualtieri, G., Kulikova, O., Limpens, E., Kim, D-J., Bisseling, T., and Geurts, R.** (2002). Microsynteny between Pea and *Medicago truncatula* in the *SYM-2* region. *Plant Mol Biol* **12**: 157-167.
114. **Cullimore, J. V., Ranjeva, R., and Bono, J.-J.** (2001). Perception of lipo-chitooligosaccharidic Nod factor in legumes. *Trends Plant Sci*: **6**, 24.
115. **Millner, P. A., and Causier, B. E.** (1995). G-protein coupled receptors in plant cells. *J. Exp. Bot*: **47**, 983.
116. **Dohlman, H. G., Thorner, J., Caron, M. G., and Lefkowitz, R. J.** (1991). Model systems for the study of seven-transmembrane-segment receptors. *Annu. Rev. Biochem*: **60**, 653.
117. **Schmidt, A., and Hall, M. N.** (1998). Signaling to the actin cytoskeleton. *Annu. Rev. Cell Dev. Biol*: **14**, 305.
118. **Ayscough, K. R.** (1998). *In vivo* functions of actin-binding proteins. *Curr. Opin. Cell Biol*: **10**, 102.
119. **Staiger, C. J., Gibbon, B. C., Kovar, D. R., and Zonia, L. E.** (1997). Profilin and actin-depolymerizing factor: modulators of actin organization in plants. *Trends Plant Sci.*: **2**, 275.
120. **Vidali, L., Yokota, E., Cheung, A. Y., Schimmen, T., and Hepler, P. K.** (1999). 135 kDa actin-bundling protein from *Lilium longiflorum* the plant homologue of villin. *Protoplasma*: **209**, 283.
121. **Allen, G. J., Kwak, J. M., Chu, S. P., Llopis, J., Tsien, R. Y., Harper, J. F., and Schroeder, J. I.** (1999). Cameleon calcium indicator reports cytoplasmic calcium dynamics in Arabidopsis guard cells. *Plant J*: **19**, 735.

- 122. **Kost, B., Lemichez, E., Spielhofer, P., Hong, Y., Tolias, K., Carpenter, C., and Chua, N. H.** (1999). Rac homologues and compartmentalized phosphatidylinositol 4, 5- biphosphate act in a common pathway to regulate polar pollen tube growth. *J. Cell Biol*: **145**, 317.
- 123. **Ludin, B., and Matus, A.** (1998). GFP illuminates the cytoskeleton. *Trends Cell Biol*: **8**, 72.
- 124. **Kost, B., Spielhofer, P., and Chua, N. H.** (1998). A GFP-mouse talin fusion protein labels plant actin filaments *in vivo* and visualizes the actin cytoskeleton in growing pollen tubes. *Plant J*: **16**, 393.
- 125. **Marc, J., Granger, C. L., Brincat, J., Fisher, D. D., Kao, T., McCubbin, A. G., and Cyr, R. J.** (1998). A GFP-MAP4 reporter gene for visualizing cortical microtubule rearrangements in living epidermal cells. *Plant Cell*: **10**, 1927.

CHAPTER 2

Use of the “Fluorescent Timer” DsRED-E5 as Reporter to Monitor Dynamics of Gene Activity in Plants

Abstract

Fluorescent proteins, such as green fluorescent protein (GFP) and red fluorescent protein (DsRED) have become frequently used reporters in plant biology. However, their potential to monitor dynamic gene regulation is limited by their high stability. The recently made DsRED-E5 variant overcame this problem. DsRED-E5 changes its emission spectrum over time from green to red, in a concentration independent manner. Therefore, the green to red fluorescence ratio indicates the age of the protein and can be used as fluorescent timer to monitor dynamics of gene expression. Here, we analyzed the potential of DsRED-E5 as reporter in plant cells. We showed that in *Vigna unguiculata* mesophyll protoplasts DsRED-E5 changes its fluorescence in a similar way as in animal cells. Moreover the timing of this shift is suitable to study developmental processes in plants. To test whether DsRed-E5 can be used to monitor gene regulation in plant organs, we placed DsRED-E5 under the control of promoters that are either up/down regulated (*MtACT4* and *LeEXT1* promoters) or constitutively expressed (*MtACT2* promoter) during root hair development in *Medicago truncatula*. Analysis of the fluorescence ratios clearly provided more accurate insight in the timing of promoter activity.

Rossana Mirabella, Carolien Franken, Gerard N.M. van der Krogt, Ton Bisseling and René Geurts

Introduction

Reporter genes are useful tools to study gene expression in transformed organisms. The most widely used reporters in plants are *uidA* (*GUS*; Jefferson et al., 1987), luciferase (*LUC*; Ow et al., 1986) and genes encoding fluorescent proteins including GFP, YFP, CFP and DsRED (Chalfie et al., 1994; Chalfie, 1995; Cubitt et al., 1995; Matz et al., 1999). Compared to *GUS* and *LUC* that require addition of specific substrates to monitor reporter activity, fluorescent proteins, due to their intrinsic fluorescence, allow non-invasive detection in living cells without the addition of substrates. This enables, for example, real time visualization of gene expression or analysis of transformants in the first generation.

Derivatives of the *Aequorea victoria* Green Fluorescent Protein (GFP; e.g. eGFP, RS-smGFP; Cormack et al., 1996; Davis and Vierstra, 1998) are the most commonly used fluorescent reporters. They are attractive because of their high quantum yield (0.60 and 0.67, respectively, for eGFP and RS-smGFP; Tsien, 1998) and stability (estimated half life of ~1 day; Verkhusha et al., 2003). In addition to GFP, a Red Fluorescent Protein (DsRED), has been isolated from a coral of the genus *Discosoma* (Matz et al., 1999). DsRED has an excitation and emission maximum shifted to the red when compared to GFP, (excitation/emission maximum of GFPs 488-495 nm/507-510 nm versus 558 nm/583 nm for DsRED). Moreover DsRED and GFP fluorescence can be easily discriminated using appropriate filter settings, allowing simultaneous multi color imaging of different genes (Jach et al., 2001).

Although GFP and DsRED are very useful reporter genes in living cells, their high stability (half life of GFP ~ 1 day and of DsRED1 ~4.6 days; Verkhusha et al., 2003) makes them less useful for monitoring dynamic processes such as transient changes in gene expression. Recently the DsRED-E5 variant was isolated, that might be used to circumvent this problem (Terskikh et al., 2000). Both DsRED and DsRED-E5 form a green fluorescent intermediate before maturing to the red fluorescent configuration (Baird et al., 2000; Terskikh et al., 2000). Compared to DsRED, the DsRED-E5 green fluorescent configuration has a higher intensity and, therefore, can be easily detected. As a consequence, DsRED-E5 fluorescence shifts from green to red during maturation of the protein, with yellow and orange intermediate fluorescence, due to the presence of both green and red fluorophores. The maturation from green to red fluorescence occurs, *in vitro*, in about 18 hours and is rather unaffected by pH, ionic strength or protein concentration. These properties indicate that the ratio of green to red fluorescence can be used to determine the age of DsRED-E5 protein, which could facilitate the visualization of dynamics in gene regulation (Terskikh et al., 2000).

Here we studied the potential of DsRED-E5 as reporter gene in plants. We used a transient expression system, *Vigna unguiculata* mesophyll protoplasts, to determine its fluorescent properties (e.g. color conversion over time) in plant cells. Further, we investigated whether DsRED-E5 can visualize dynamics of promoter activity in plants. We chose *Medicago*

truncatula root hairs, as experimental system, since root hairs, protruding from the root epidermis, are accessible for microscopic analysis. We placed DsRED-E5 under the control of promoters that are either up/down regulated or constitutively expressed during root hair development. These studies showed that DsRED-E5 can be used as fluorescent timer to monitor dynamics of gene regulation in plants.

Results and Discussion

Characterization of DsRED-E5 Fluorescence in Vigna unguiculata Mesophyll Protoplasts

In order to characterize the fluorescent properties of DsRED-E5 in plant cells, we cloned the DsRED-E5 coding region in the vector pMon999e35S, carrying the constitutive CaMV 35S promoter. The resulting *35S::DsRED-E5* transgene was transiently expressed in *Vigna unguiculata* (Cowpea) mesophyll protoplasts. After transfection, protoplasts were analyzed for green and red fluorescence over time by Confocal Laser Scanning Microscopy (CLSM; see materials and methods and below for more details).

Protoplasts carrying the *35S::DsRED-E5* construct became fluorescent 9-10 h after transfection (Fig. 1A). At this time-point only green fluorescence was detectable (Fig. 1A). Red fluorescence appeared, in these protoplasts, 14-15 h after transfection (Fig. 1B) and increased in intensity over time (Fig. 1C and D). These data show that also in plant cells DsRED-E5 shifts its fluorescence from green to red over time and, therefore, can be used to follow regulation of promoter activity. Moreover, the green fluorescent form appears markedly earlier (~5 h) than the red fluorescent form, suggesting that DsRED-E5 is suitable to study dynamic processes in plants. To obtain a better idea of the timing of DsRED-E5 fluorescence maturation in plants, we determined the ratio between the green and the red fluorescence intensities in the DsRED-E5 expressing protoplasts at different time points after transfection.

This ratio will be defined as G/R. The optimal wavelengths to excite the green and the red form of dsRED-E5 are 488 nm and 558 nm, respectively. Alternatively, a single excitation wavelength can be used to excite both forms due to the overlap of their excitation spectra. The use of two different wavelengths to excite dsRED-E5 (488 nm and 543 nm) has major disadvantages. A pronounced photobleaching of DsRED-E5 was observed, especially at the high laser power required to excite DsRED-E5 in root hairs. This photobleaching would affect the fluorescence intensity measured after excitation with the second laser, by which the data would be unreliable. Further, the use of two lasers to excite DsRED-E5 could lead to variations in the fluorescence intensities due to laser instability over time. The use of a single excitation wavelength for both emitting forms will overcome these problems. Therefore we decided to use a single argon laser (488 nm) to excite both the green and the red emitting form of DsRED-E5, although, at this wavelength, the absorbance of the red form of DrRED-E5 is ~ 40% of the absorbance at 558 nm. However, the reduced red

fluorescence intensity, due to the non optimal excitation of the red emitting form of DsRED-E5 will not invalidate our data, since G/R will be affected similarly in all stages.

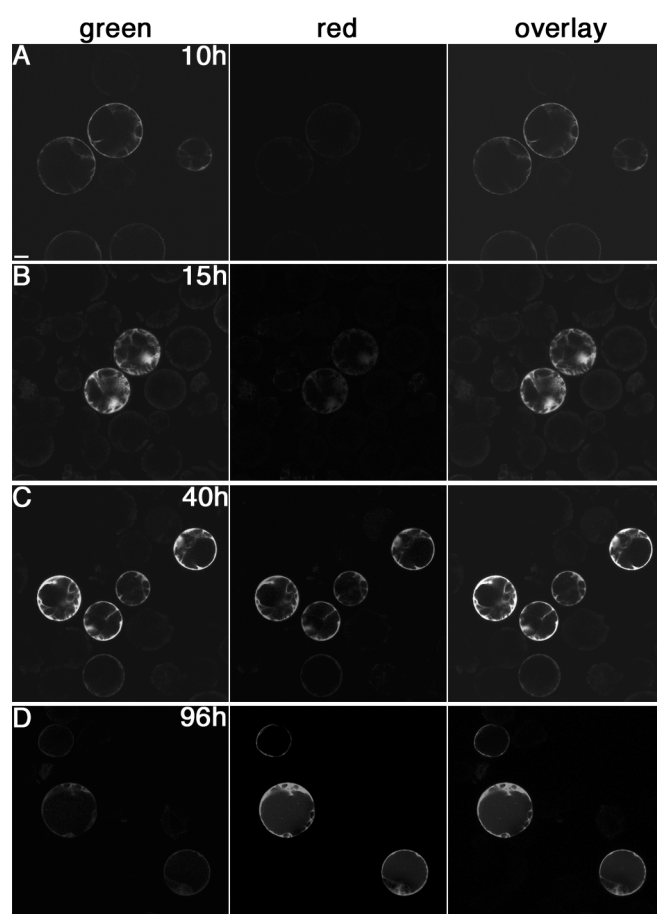


Figure 1. Confocal fluorescence images of Cowpea protoplasts transiently expressing DsRED-E5 under the control of the CaMV 35S promoter, 10 h (A), 15 h (B), 40 h (C) and 96 h (D) after transfection. Bar = 10 μ m. (Color figure, see appendix).

The green emitting form of DsRED-E5 has a broad emission spectrum that extends from 475 to 625 nm and is similar to that of GFP (Tsien, 1998; Terskikh et al., 2000). Using the 488 nm laser to excite DsRED-E5, this broad spectrum causes a bleed-through in the red channel (emission: band pass 565-595 nm) by the green fluorescent form. To quantify this, we measured the fluorescence intensity in the red channel of protoplasts expressing GFP. As expected from the emission spectrum, a signal was detected in the red channel, which was significantly higher than the back-ground level (auto-fluorescence) of non-transfected protoplasts. After subtracting the background level, the fluorescence detected in the red channel was 15% of the fluorescence intensity measured in the green channel. Moreover, by analyzing several protoplasts ($n = 20$) we observed that this relative value was independent of the absolute fluorescence intensity (data not shown). Based on these data we concluded that the intensity of the red channel had to be reduced by 15% of the intensity detected in the green channel. In contrast, the red fluorescent form does not cause any bleed-through in the green channel.

To determine G/R in the DsRED-E5 expressing protoplasts, ~ 20 protoplasts for each time point were analyzed by CLSM. Within a transfection experiment, protoplasts show a high

heterogeneity of signal intensity. To determine G/R protoplasts were randomly selected and therefore they express DsRED-E5 at different level. The green and red fluorescences were corrected for the back-ground signal observed in non-transfected protoplasts as well as for the above described bleed-through in the red channel. About 10 hours after transfection G/R was between 15 and 10 (12 ± 2.3 (standard deviation); $n = 20$; Fig. 1A) and subsequently decreased in time reaching a value of $1(1 \pm 0.6$; $n = 22$) at ~ 40 h after transfection (Fig. 1C). From this time point on G/R was lower than 1 and reached the lowest value of $0.17 (0.17 \pm 0.02$; $n = 20)$ 95-105 h after transfection (Fig. 1D). The differences in G/R over time corresponded to clear differences in the hue color of the protoplasts (Fig. 1, overlay). The protoplasts in fact shifted from a bright green fluorescence, observed in the first hours after transfection, when mainly the green emitting form of DsRED-E5 was present, to a yellow-orange fluorescence, when both emitting forms were present with comparable intensities, and finally to a red fluorescence, when the red emitting form was predominantly present (Fig. 1, overlay). Moreover, at a specific time point, G/R was similar in the different protoplasts, although fluorescence intensities varied. For instance, the values of the G/R measured in protoplasts 25 and 90 h after transfection were of 2.73 ± 0.40 ($n = 105$) and 0.20 ± 0.02 ($n = 62$), respectively. The low standard deviation values show that the rate of green to red conversion is independent of DsRED-E5 concentration and therefore from the level of gene expression within a cell (Terskikh et al., 2000). This means that, when DsRED-E5 is continuously expressed, a steady-state value of the G/R will be reached that is independent of the promoter strength. Perturbations in the steady-state G/R value can be used to detect changes in promoter activity, for example during development or after application of a stimulus. A G/R higher than the steady-state value will indicate a recent induction of the promoter activity whereas a lower value of the G/R will mean that the promoter activity has ceased.

Characterization of DsRED-E5 Maturation in Vigna unguiculata Mesophyll Protoplasts

Next we determined the time required for the green form of DsRED-E5 to mature into the red form. From the experiment described above, it appeared that the rate of this maturation is in the order of 1-2 days. A more precise estimation could not be determined in this experiment since, under our experimental condition, the rate of protein synthesis changes over time (Rottier, 1980). As a consequence the steady-state G/R was never reached in protoplasts. To determine the rate of DsRED-E5 maturation more accurately, we used an experimental set-up in which the green form of DsRED-E5 was first accumulated and subsequently protein synthesis was blocked by applying cycloheximide (CHX). CHX was applied 10 h after transfection, when G/R had the highest value (> 10). Subsequently, G/R was followed in time.

After CHX application, the fluorescence intensity remained constant in the treated protoplasts whereas it increased in the untreated sample (data not shown), indicating that

the CHX treatment was effective. Moreover, G/R decreased rapidly and more or less in a linear manner within the first 14 h after CHX treatment, from the initial value of 11.6 ± 2.36 ($n = 23$) to 2.37 ± 0.20 ($n = 19$) at 14 h (Fig. 2C). After this time point a residual level of green fluorescent form remained in the protoplasts and G/R decreased slower (Fig. 2C), reaching a value of 0.93 ± 0.05 ($n = 23$; Fig. 2A and 2C) and the lowest value of $\sim 0.2 \pm 0.05$ ($n = 21$), respectively, ~ 24 and 55-60 h after CHX application (Fig. 2B and 2C). These data show that, once DsRED-E5 synthesis stops, G/R decreased 10 fold in ~ 24 h, whereas under the same experimental condition, the intensity of GFP fluorescence remained about constant (data not shown). Therefore, DsRED-E5 is more suitable than other reporter genes to study regulation of gene activity during plant developmental processes.

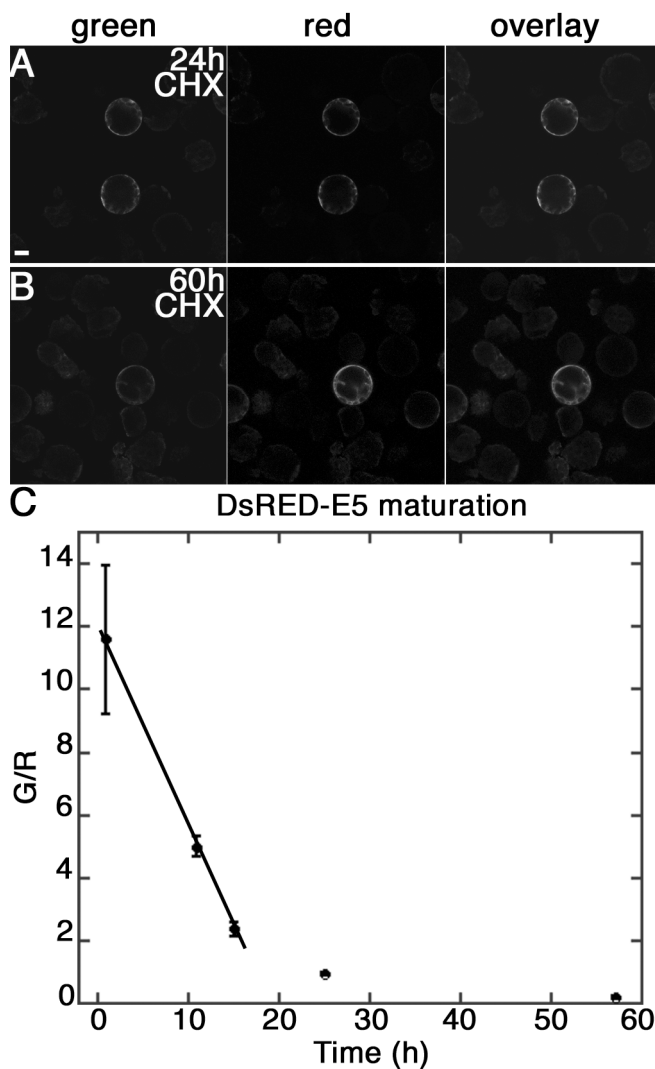


Figure 2. Confocal fluorescence images of Cowpea protoplasts transiently expressing DsRED-E5 under CaMV 35S promoter 24 h (A) and 60 h (B) after 25 µg/ml CHX application. Bar = 10 µm. (C) Maturation rate of DsRED-E5 in Cowpea protoplasts. G/R is depicted as function of time. Errors bar indicate standard deviation. At least 20 protoplasts were analyzed for each time point. (Color figure, see appendix).

DsRED-E5 as Reporter in Medicago truncatula Roots

To determine whether the fluorescent timer could be used as a reporter for studying promoter regulation in plant organs, we analyzed the potential of DsRED-E5 to reveal changes in promoter activity during a dynamic process such as root hair development. Root hairs were selected since they protrude from the epidermal cells, by which they are accessible for microscopic analysis. Root hair development has been investigated in detail in several plant species including *Medicago truncatula* (Sieberer and Emons, 2000). Due to the indeterminate growth of the root, root hairs of different ages are present along the root axis, with the youngest hairs near the root tip and the oldest near the hypocotyl. Root hair development starts with the formation of a bulge on the epidermal cells. These bulges are formed by isotropic growth and their cytoplasm is located at the periphery whereas the vacuole is present in the bulge center (Sieberer and Emons, 2000); (Fig. 5D). Subsequently, a root hair is formed from the bulge by tip growth. Growing root hairs are characterized by a cytoplasmic dense region, devoid of large organelles, at their tip (Fig. 3C). In mature (non-growing) root hairs this region has disappeared and the cellular volume is completely occupied by a large vacuole with a thin layer of cytoplasm located at the periphery (Fig. 3E; Sieberer and Emons, 2000). At the transition from a growing to a non-growing phase (growth terminating hairs), the cytoplasmic dense region at the hair tip becomes smaller and the vacuole extends toward the hair tip (Fig. 3D). Under our experimental condition the development from a bulge to a mature root hair takes 20-24 h; a time-span in which DsRED-E5 maturation could be used to monitor differences in promoter activity.

To test whether DsRED-E5 can be used as reporter to study regulation of gene activity in root hairs, we used three different promoters of which one is constitutively expressed in all cells of the root, including the epidermis, and the other two are induced during root epidermis development. Of the latter, one is expressed during all stages of root hair development and the other is switched off when root hairs become older. These promoters will be described in more detail below.

As a constitutively expressed promoter, we selected the *M. truncatula ACTIN2* (*MtACT2*) promoter (data not shown). Such a constitutive promoter can be used to determine the steady-state value of the G/R in root hairs. Therefore we placed DsRED-E5 under the control of the *MtACT2* promoter and introduced the *MtACT2::DsRED-E5* fusion into *M. truncatula* roots by *Agrobacterium rhizogenes* mediated root transformation.

Transformed roots were identified scoring for DsRED-E5 fluorescence under a stereo fluorescence microscope. The fluorescence pattern confirmed that the *MtACT2* promoter is constitutively expressed in roots: the signal was visible in the root meristem, in the epidermis and root hairs in all stages of development (Fig. 3 A and B). *MtACT2::DsRED-E5* expressing root hairs were further analyzed by CLSM and G/R in root hairs at different developmental stages was measured. The background signal detected in non-transformed root hairs and the bleed-through of the green signal into the red channel were taken into account, as

previously described for the protoplasts. The different classes of root hairs were discriminated considering both (1) their position along the root and (2) their cytoarchitecture, as described above. The data presented here come from the analysis of 5 roots, independently transformed with the *MtACT2::DsRED-E5* fusion (Table I). In bulges, growing hairs (Fig. 3C), growth terminating (Fig. 3D) and "young mature" hairs (Fig. 3E), in a region of 0.5 mm above the growth terminating hairs, G/R had a value of ~ 2.8 (respectively, 2.84 ± 0.33 ($n = 33$), 2.78 ± 0.18 ($n = 22$) and 2.66 ± 0.25 ($n = 15$); Table I). This value was lower in "old mature" root hairs, closer to the hypocotyl (data not shown), probably due to an overall reduction of protein synthesis in old root hairs. These data show that the value of the G/R is constant in the region between bulges and "young mature" root hairs, indicating that a steady-state G/R level of ~ 2.8 is reached at these stages. Moreover, the values of the G/R were similar in independently transformed roots (Table I), confirming that also in *M. truncatula* root hairs G/R is independent of the expression level of the transgene. Further, G/R value was uniform within one root hair (data not shown).

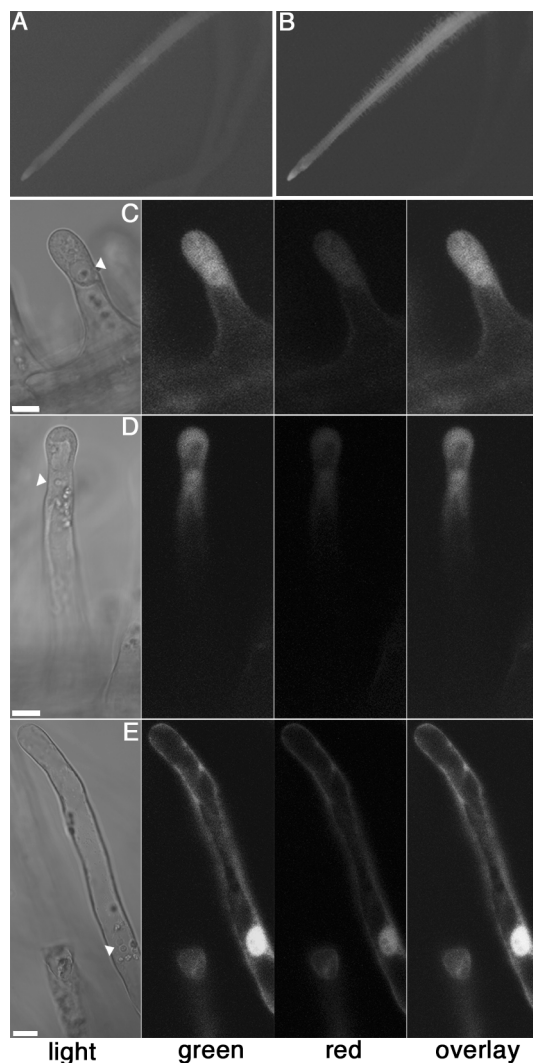


Figure 3. Expression pattern of the *MtACT2* promoter in *M. truncatula* roots transformed with the *MtACT2p::DsRED-E5* fusion. (A) and (B) *MtACT2* promoter expression pattern in roots. Images were collected with the Leica stereo fluorescence microscope using GFP (A) and DsRED (B) filter sets, respectively. (C), (D) and (E) Confocal fluorescence images of growing (C), growth terminating (D) and "young mature" (E) root hairs transformed with the *MtACT2p::DsRED-E5* fusion. Nucleus is indicated by the arrow head. Bars = 10 μ m.

Table I. G/R in the *MtACT2p::DsRED-E5* expressing root hairs

| Root | Bulges\Growing root hairs | Growth terminating root hairs | “Young mature” root hairs |
|--------|------------------------------|----------------------------------|------------------------------|
| Root 1 | 2.93 ± 0.34 (n = 6) | 2.86 ± 0 (n = 5) | 2.86 ± 0.17 (n = 4) |
| Root 2 | 2.86 ± 0 (n = 6) | 2.86 ± 0 (n = 5) | 2.86 ± 0 (n = 2) |
| Root 3 | 2.75 ± 0.22 (n = 10) | 2.66 ± 0.19 (n = 5) | 2.51 ± 0.23 (n = 3) |
| Root 4 | 2.96 ± 0.58 (n = 5) | 2.86 ± 0.17 (n = 4) | 2.75 ± 0.12 (n = 2) |
| Root 5 | 2.76 ± 0.43 (n = 6) | 2.6 ± 0.31 (n = 3) | 2.45 ± 0.23 (n = 4) |
| Total | 2.84 ± 0.33 (n = 33) | 2.78 ± 0.18 (n = 22) | 2.66 ± 0.25 (n = 15) |

Table I. G/R measured in bulges, growing, growth terminating and “young mature” *M. truncatula* root hairs transformed with the *MtACT2p::DsRED-E5* fusion. The data presented were obtained from 5 independently transformed roots. G/R are indicated as mean value ± standard deviation. The number of root hairs (n) analyzed per root for each stage of development is indicated between brackets.

Next we determined whether the induction of promoters in root hairs could be studied using *DsRED-E5* as reporter. For this purpose, we chose the *ACTIN4* (*MtACT4*) gene of *M. truncatula*. In contrast to the *MtACT2* gene, that is constitutively expressed in roots, the *MtACT4* gene is induced during root epidermis development (Mirabella et al., unpublished results). Therefore, we fused *DsRED-E5* to the *MtACT4* promoter. Transformed roots were selected under a stereo fluorescence microscope and analyzed by CLSM. G/R was quantified in root hairs of different ages, in the region of the root encompassing bulges, growing, growth terminating and “young mature” root hairs, in which the steady-state G/R occurred in the *MtACT2::DsRED-E5* expressing root hairs.

Considering that the steady-state value of the G/R in root hairs is ~ 2.8, values higher than 2.8 indicate recent promoter induction, whereas values below 2.8 indicate down-regulation of the promoter activity. In roots transformed with the *MtACT4::DsRED-E5* transgene the fluorescence was first detected in the region where bulges become growing root hairs (Fig. 4A). From these young hairs up to the region of growth terminating root hairs (Fig. 4B) we measured G/R values between 14 and 6, with an average of 9.84 ± 2.26 (n = 20) and 9.56 ± 2.14 (n = 21), in growing and growth terminating root hairs, respectively (Table II). This value, being markedly higher than the steady-state value, indicates that the promoter is induced in these hairs. The fact that the highest G/R measured in the *ACT4::DsRED-E5* growing hairs is very similar to the highest G/R measured in protoplasts (14 versus 15) supports this conclusion. The high variability of the G/R values in these root hairs is probably due to the fact that, under our growth condition, the activation of this actin gene is not strictly synchronized and occurs within a rather broad zone. “Young mature” hairs had a value of the G/R of 2.99 ± 0.54 (n = 11), indicating that G/R has almost reached the steady-state level (Fig. 3C and Table II).

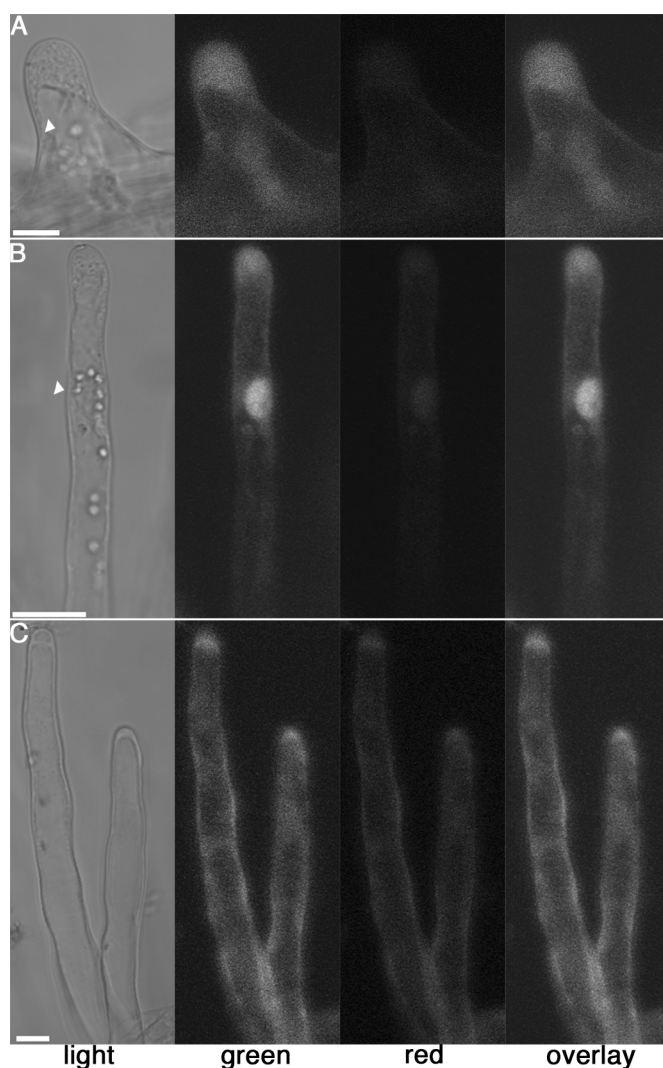


Figure 4. Expression pattern of the *MtACT4* promoter in *M. truncatula* root hairs transformed with the *MtACT4p::DsRED-E5* fusion. Confocal fluorescence images of growing (A), growth terminating (B) and "mature old" (C) root hairs. Nucleus is indicated by the arrow head. Bars = 10 μ m.

Table II. G/R in the *MtACT4p::DsRED-E5* expressing root hairs

| Root | Bulges\Growing root hairs | Growth terminating root hairs | "Young mature" root hairs |
|--------|------------------------------|----------------------------------|------------------------------|
| Root 1 | 8.55 \pm 1.39 (n = 7) | 7.95 \pm 1.5 (n = 6) | nd |
| Root 2 | 11.95 \pm 2.4 (n = 4) | 11.79 \pm 2.48 (n = 5) | 2.87 \pm 0.62 (n = 3) |
| Root 3 | 9.9 \pm 2.19 (n = 9) | 9.42 \pm 1.3 (n = 10) | 3.03 \pm 0.55 (n = 8) |
| Total | 9.84 \pm 2.26 (n = 20) | 9.56 \pm 2.14 (n = 21) | 2.99 \pm 0.54 (n = 11) |

Table II. G/R measured in growing, growth terminating and "young mature" *M. truncatula* root hairs transformed with the *MtACT4p::DsRED-E5* fusion. The data presented were obtained from 3 independently transformed roots. G/R are indicated as mean value \pm standard deviation. The number of root hairs (n) analyzed per root for each stage of development is indicated between brackets. nd = not determined.

These data clearly indicate that DsRED-E5 can be successfully used to detect the induction of the *MtACT4* promoter in root hairs. To determine whether DsRED-E5 is also a useful marker to study repression of gene activity during development we search for a root epidermis promoter that is switched off at an early stage of development. A good candidate is the *EXTENSIN1* gene of tomato (*Lycopersicon esculentum* Mill *LeEXT1* promoter) (Bucher et al., 2002). A *LeEXT1::GUS* transgene has been shown to be active exclusively in root hairs, both in potato and tobacco (Bucher et al., 2002). The same transgene was introduced into *M. truncatula* roots and showed that also in *M. truncatula* the *LeEXT1* promoter is only active in epidermal cells with a hair (Fig. 5A). GUS activity could be detected as soon as a bulge started to emerge (Fig. 5B), was retained in growing root hairs (Fig. 5B) and became weaker in “old mature” hairs (Fig. 5C).

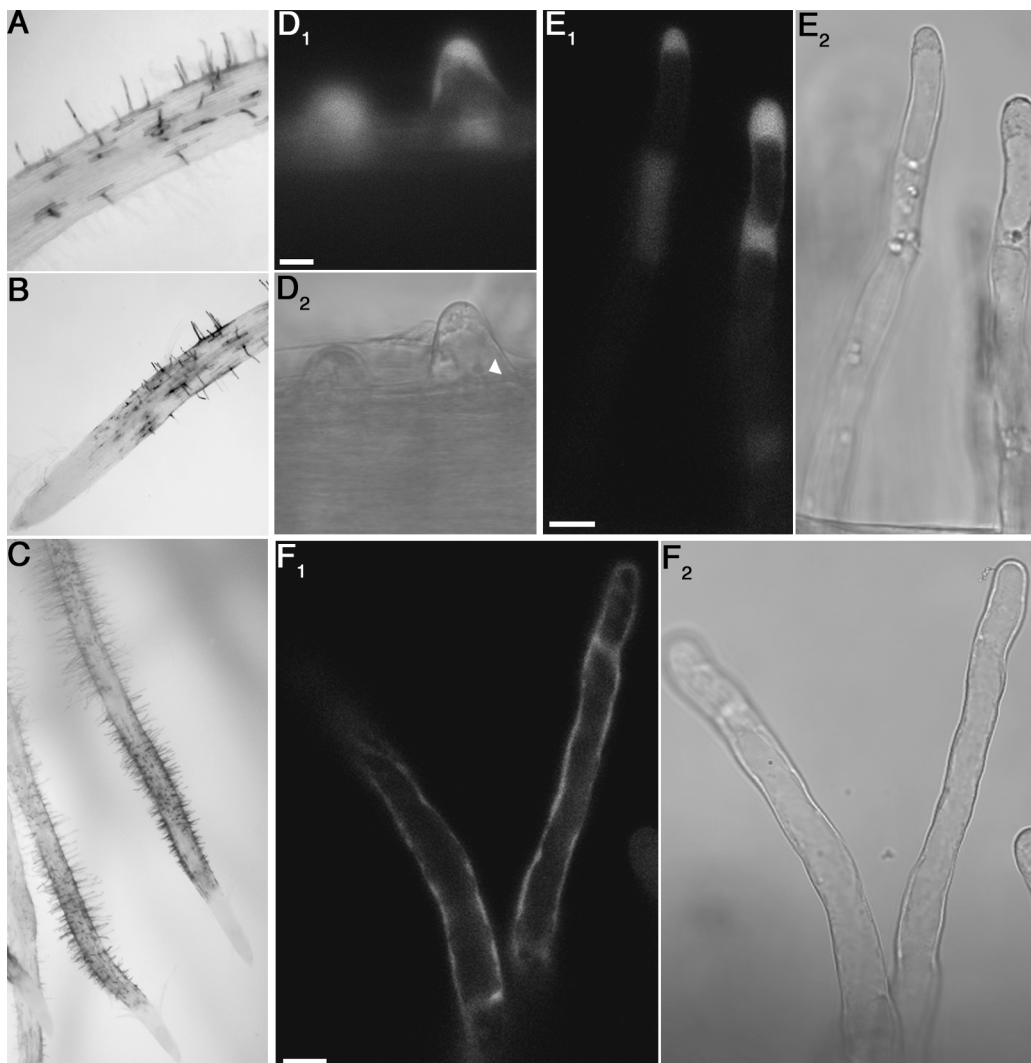


Figure 5. Expression pattern of the *LeEXT1* promoter in *M. truncatula* roots. (A), (B) and (C) Light microscope images of roots transformed with a *LeEXT1p::GUS* fusion. (D_{1-2}), (E_{1-2}) and (F_{1-2}) confocal images of a bulge (D_{1-2}), growth terminating (E_{1-2}) and “young mature” hairs transformed with a *LeEXT1p::GFP* fusion. (D_1 , E_1 and F_1) bright field and (D_2 , E_2 and F_2) fluorescence images. Nucleus is indicated by the arrow head. Bars = 10 μ m.

Therefore, a *LeEXT1::DsRED-E5* fusion was introduced in *M. truncatula* roots. In all the six independent *LeEXT1::DsRED-E5* roots analyzed by CLSM a clear fluorescence was visible only in growing root hairs (Fig. 6A). These growing hairs displayed a G/R of ~ 3 (3.05 ± 0.67 ($n = 41$); Table III), which is close to the steady-state level. At an earlier stage of development (bulges) fluorescence was too low to quantify. Growth terminating (Fig. 6B) and "young mature" hairs (Fig. 6C) had a G/R of ~ 1.5 (1.51 ± 0.22 ($n = 41$)) and ~ 0.6 (0.61 ± 0.09 ($n = 19$)), respectively (Table III). The decrease in G/R value was accompanied by a clear shift in the root hair color, from green in growing hairs to orange-red in "young mature" root hairs (Fig. 6 overlay).

In parallel a *LeEXT1::GFP* (RS-smGFP; Davis and Vierstra, 1998) fusion was also introduced into *M. truncatula* and transformed roots were analyzed by CLSM. The fluorescence could be detected starting from the bulge stage (Fig. 5D) and was present in tip growing, growth terminating and mature root hairs (Fig. 5E and 5F), with a pattern similar to that obtained using GUS as reporter. Moreover the intensity of the GFP fluorescence increased moving from the bulge stage to "young mature" hairs (data not shown).

In "young mature" hairs, expressing *LeEXT1::DsRED-E5*, a value of the G/R lower (~ 0.6) than the steady-state value (~ 2.8) was reached. This indicates that in these hairs the *LeEXT1* promoter activity has been decreased. The down-regulation of the *LeEXT1* promoter already occurs in the growth terminating hairs, as indicated by a G/R value already markedly lower than the steady-state value. In contrast, when the *LeEXT::GFP* fusion was used, no reduction of the fluorescence intensity was detected in root hairs at these developmental stages (Fig. 5). In these roots, as well as in roots transformed with a *LeEXT::GUS* fusion, a decrease of the reporter product could first be observed in the region of the roots with "old mature" hairs, at a distance of about 1.5-2 mm from the growth terminating hairs. The time-span between the growth terminating stage and the stage, where the decrease of GUS or GFP is detected is ~ 24 -30 h. Therefore, compared to GUS or GFP, DsRED-E5 allows a markedly more precise detection of the timing of *LeEXT1* promoter down-regulation. Compared to the *MtACT2* promoter, the *LeEXT1* promoter is active at a lower level. As a consequence we did not detect any fluorescence in bulges and the fluorescence signal could be detected for the first time in growing hairs. In these hairs the value of the G/R had almost reached the steady-state. The observation that, as soon the fluorescence can be detected, in growing hairs, G/R is already at the steady-state indicates that the activation of the *LeEXT1* promoter must have occurred at an earlier stage than growing hairs. This conclusion is in agreement with the expression pattern observed in the *LeEXT1::GUS* or the *LeEXT1::GFP* roots, in which the promoter activity could be detected at earlier stages namely, as soon as the bulges started to emerge from the epidermal cells.



Figure 6. Expression of the *LeEXT1* promoter in *M. truncatula* root hairs transformed with the *LeEXT1p::DsRED-E5* fusion. Confocal fluorescence images of growing (A), growth terminating (B) and “young mature” (C) root hairs. Nucleus is indicated by the arrow head. Bars = 10 μ m. (Color figure, see appendix).

Table III. G/R in the *LeEXT1p::DsRED-E5* expressing root hairs

| Root | Growing root hairs | Growth terminating root hairs | “Young mature” root hairs |
|--------|--------------------------|----------------------------------|------------------------------|
| Root 1 | 2.86 ± 0 (n = 3) | 1.58 ± 0.14 (n = 4) | 0.64 ± 0.02 (n = 4) |
| Root 2 | 2.74 ± 0.24 (n = 3) | 1.43 ± 0.06 (n = 5) | 0.58 ± 0.02 (n = 2) |
| Root 3 | 3.08 ± 0.45 (n = 4) | 1.48 ± 0.23 (n = 9) | 0.58 ± 0.07 (n = 3) |
| Root 4 | 3.21 ± 0.89 (n = 21) | 1.45 ± 0.21 (n = 9) | 0.65 ± 0.05 (n = 6) |
| Root 5 | 2.86 ± 0 (n = 5) | 1.39 ± 0.24 (n = 6) | 0.54 ± 0 (n = 4) |
| Root 6 | 3 ± 0.19 (n = 5) | 1.71 ± 0.05 (n = 8) | nd |
| Total | 3.05 ± 0.67 (n = 41) | 1.51 ± 0.22 (n = 41) | 0.61 ± 0.09 (n = 19) |

Table III. G/R measured in growing, growth terminating and “young mature” *M. truncatula* root hairs transformed with the *LeEXT1p::DsRED-E5* fusion. The data presented were obtained from 6 independently transformed roots. G/R are indicated as mean value \pm standard deviation. The number of root hairs (n) analyzed per root for each stage of development is indicated between brackets. nd = not determined.

In conclusion, these data show that the "fluorescent timer", DsRED-E5, can be used as marker to monitor both promoter activation and down-regulation in plants and by determining its G/R a more accurate timing can be obtained. In principal DsRED-E5 is equally suitable as GFP/GUS to determine when a gene is first induced during development, although due to its low quantum yield it is less sensitive than GFP/GUS. On the other hand, DsRED-E5 is most useful to reveal promoter down-regulation, which is hampered by the high stability of conventional reporter like GFP and GUS. In addition DsRED-E5 can be useful to study increase/decrease of gene activity in cells that already express this gene. For example an external signal might alter the expression level of a certain gene in cells where this gene is already active. In such case, the timing of this alteration can also more accurately be determined by analyzing the G/R value of DsRED-E5.

Materials and Methods

DNA Manipulation and Plasmid Construction

Molecular biology protocols were conducted according to standard procedures (Sambrook and Russel, 2001) and all fragments generated by PCR were sequenced.

To study the expression of DsRED-E5 in protoplasts we used the plant expression vector pMon999e35S (Monsanto). For this purpose the *DsRED-E5* coding region was excised from the vector pTimer (Clontech, Palo Alto, CA) as an *EcoRI-BamHI* fragment and subcloned in the same sites of the pMon999e35S vector.

To isolate the promoters of the *ACTIN2* (*MtACT2*) and *ACTIN4* (*MtACT4*) genes, the *Medicago truncatula* Mth1 bacterial artificial chromosome (BAC) library (Nam et al., 1999) was screened, using, respectively, the *MtACT2* and the *MtACT4* coding region as probes. To isolate the 5' flanking region of *MtACT2* a 2.8 Kb fragment was amplified from the BAC Mth1-01N01, in combination with the following primers: 5' MtACT2p-H CCCAAGCTTGGATGTGGTTTGGTTAATAG (underlined *HindIII* site) and 3' MtACT2p-K GGGGTACCTTGACCATTCAGTTCC (underlined *KpnI* site). To isolate the 5' flanking region of *MtACT4* a 2.9 Kb fragment was amplified using the BAC Mth1-48I22 as template and the following primers: 5' MtACT4p-S ACATGCATGCAATTTAGTATATATTTGGGATGAG (underlined *SphI* site) and 3' MtACT4p-K GGGGTACCTTGACCATGCCGTTCC (underlined *KpnI* site). The amplified fragments (*MtACT2p* and *MtACT4p*) contain the putative promoters, the 5' untranslated regions, the first intron and the coding regions of the first 19 a.a., as used for the analysis of the *Arabidopsis thaliana* actin genes (An et al., 1996). *MtACT2p* and *MtACT4p* were fused in-frame to the DsRED-E5 in the pTimer vector, using, respectively, the *HindIII-KpnI* and the *SphI-KpnI* sites. Next, the *MtACT2::DsRED-E5* and the *MtACT4::DsRED-E5* fusions were excised, respectively, as *HindIII-EcoRI* and *SphI-EcoRI* fragments and sub-cloned in the same sites of the pBinplus vector (van Engelen et al., 1995), containing the NOS terminator (*T-NOS*) between the *EcoRI* and the *PacI* sites.

To obtain the *LeEXTp1::GUS* fusion, a 1.1 Kb fragment of the *Lycopersicon esculentum* *EXTENSIN1* promoter (designed as $\Delta 1.1$ in Bucher et al., 2002) was amplified by PCR, using as template the pBin19-*LeEXTp* (Bucher et al., 2002) in combination with the following primers: 5' EXTp-H CACAAGCTTTAAGTATGAAT (underlined 5' *HindIII* site) and 3' EXTp-XK GCGGTACCTCTAGAAGAAGATTGGATTCTAAGGC (underlined 3' *XbaI* and *KpnI* sites). The amplified fragment was cloned into the *HindIII-XbaI* sites of the pBI101.3 vector (Clontech, Palo Alto, CA). To generate the *LeEXTp1::DsRED-E5* fusion the same *LeEXT1* promoter fragment was cloned in *HindIII-KpnI* sites of the pTimer vector. Finally the *LeEXT1::DsRED-E5* fusion was subcloned in the *HindIII-EcoRI* sites of the pBinplusT-NOS vector. To generate the *LeEXT1::GFP* fusion, the *RS-smGFP* template (EMBL Genebank U70495) was amplified with the following primers: 5' GFP-X GCTCTAGAGCCATGGGCAAAGGAGAAGAACTTT (underlined *XbaI* site) and 3' GFP-B CCGGATCCTTATTTGTATAGTTCATCCATGC (underlined *BamHI* site).

The amplified fragment was then inserted in the *XbaI*-*Bam*HI sites of a pGem4 vector containing the *LeEXT1p* between the *Hind*III-*XbaI* sites. Finally the *LeEXT1::GFP* fusion was digested as an *Hind*III-*Eco*RI fragment and subcloned in the same sites of the pBinplusT-NOS vector.

All the vectors used for plant transformation were transformed into the *Agrobacterium rhizogenes* strain MSU440, containing the helper plasmid pRiA4 (Sonti et al., 1995).

Protoplast Transfection

Vigna Unguiculata L. (Cowpea) protoplasts were prepared and transfected using the polyethylene glycol method as described (van Bokhoven et al., 1993) with 30 µg of plasmid DNA. After transfection protoplasts were incubated under constant environmental conditions (25° C, light, protoplast medium) as described by van Bokhoven et al. (1993). To perform the protein synthesis inhibition test, cycloheximide (Sigma) was added to the protoplast medium at a concentration of 25 µg/ml. For microscope analysis, protoplasts were mounted in 8-chambered cover slides (Nalge, Nunc International, Rochester, U.S.A.).

Plant Material, Growth Condition and Transformation

Medicago truncatula (Jemalong A17) root transformation was performed as previously reported (Stiller et al., 1997), with few modifications. Seeds, sterilized for 10 min with H₂SO₄ followed by 10 min with commercial bleach and extensively washed with sterile water, were germinated on a wet filter paper in a petri dish containing Fåhræus (Fåhræus, 1957) agar medium (0.9% agar; Daishin, Brunswick), supplemented with 0.75 mM Ca(NO₃)₂ and 0.7 mM CaCl₂. Subsequently, seeds were incubated in the dark at 4°C overnight and germinated upside down at 24°C for one more day. After removing the seed coat, seedlings were transferred to new Fåhræus agar plates and sealed for 2/3 with parafilm. The plates were incubated in a growth chamber in a vertical position with 16-h daylight period at 21°C and 70 to 80% relative humidity. Five days later the plantlets, having unfolded cotyledons and the first leaf, were inoculated with *A. rhizogenes*. The bacteria, grown for 2 d on agar plates, were streaked on the top of the hypocotyl area with a sterile curled glass pipette. Subsequently, the root was removed by cutting the hypocotyl region where the *A. rhizogenes* was streaked. In this way the freshly cut surface was inoculated. Plants were cultivated under the same conditions and, after five days, transferred to emergence medium containing: 1x SH-A salt (g liter⁻¹): KNO₃ (2.5), MgSO₄·7H₂O (0.4), NH₄H₂PO₄ (0.3), CaCl₂·2H₂O (0.2), MnSO₄·4H₂O (0.01), H₃BO₃ (5 × 10⁻³), ZnSO₄·7H₂O (1 × 10⁻³), KI (1 × 10⁻³), CuSO₄·5H₂O (2 × 10⁻⁴), NaMoO₄·2H₂O (1 × 10⁻⁴), CoCl₂·6H₂O (1 × 10⁻⁴), FeSO₄·7H₂O (0.015) and Na₂EDTA (0.02); 1x UM-C vitamins (Diaz, 1989; mg liter⁻¹) myoinositol (100), nicotinic acid (5), pyridoxine-HCl (10), thiamine-HCl (10), glycine (2); 1% sucrose, 3mM MES pH 5.8, 0.9% Daishin agar and 300 µg/ml cefotaxime. After 2-3 weeks the newly formed roots could be analyzed. Using this method we obtain a transformation efficiency of ~ 50%.

Transformed roots were selected scoring for green or red fluorescence, using a Leica (Wetzlar, Germany) MZFLIII stereo fluorescence microscope and further analyzed by Confocal Laser Scanning Microscopy (CLSM). For this purpose roots were mounted in liquid emergence medium under a glass coverslip.

Roots carrying the *LeExt1::DsRED-E5* transgene could not be selected using a stereo fluorescence microscope, because of a low fluorescence intensity. Therefore, CLSM had to be used for the selection and only those roots with the highest expression level (~ 5% of the total *LeExt1::DsRED-E5* roots analyzed) could be used to determine the green to red fluorescence ratio (G/R).

Histochemical GUS Analysis

GUS staining was performed according to Jefferson et al., (1987), with few modifications. Plant material was incubated in 0.05% (w/v) X-Gluc (Duchefa) in 0.1M sodium phosphate buffer (pH 7) with 3% sucrose, 5µM potassium-ferrocyanide and 5µM potassium-ferricyanide. Vacuum was applied for 1 h and the samples were incubated at 37°C. For imaging a Nikon (Tokyo, Japan) SMZ-U stereomicroscope and a Nikon optiphot-2 bright field microscope were used. Photographs were made using a Nikon coolpix990 digital camera.

Microscopy and G/R quantification

Fluorescence microscopy was performed using a Zeiss LSM 510 CLSM implemented on an inverted microscope (Axiovert 100). Excitation was provided by the 488 nm Ar laser line, controlled by an acousto optical tuneable filter (AOTF). To separate excitation from emission and to divide the fluorescence emission into the green and red channels, two dichroic beam splitters were used. The HFT 488 dichroic beam splitter was used to reflect excitation and transmit fluorescence emission. A mirror was used to reflect the emitted fluorescence to the NFT 545 secondary beam splitter. Fluorescence reflected by the NFT 545 splitter was filtered through a 505-530 nm band pass filter, resulting in the green channel, whereas fluorescence transmitted by the NFT 545 splitter was filtered through a 565-590 nm band pass filter, resulting in the red channel. A Zeiss plan-neofluar 40× (N.A. 1.3) oil immersion objective lens was used for scanning. For detection of green and red fluorescence equal detection settings were used. For imaging root hairs the pinhole was fully open. To determine G/R, time series images were acquired. To quantify the fluorescence intensities, equally sized regions of interest were drawn in cytoplasmic rich regions of protoplasts/root hairs and the pixel intensities in these regions were determined using the Zeiss LSM 510 software.

Acknowledgements

We thank J. Pouwels and Dr. M. Bucher for providing us the pMon999e35S vector and the *LeEXTENSIN1* promoter, respectively. We are grateful to Dr. M. Hink for the help with CLSM and to J. Vermeer for the helpful discussions.

References

- An Y-Q, Mc Dowell JM, Huang S, Mc Kinney EC and Meagher RB (1996) Strong, constitutive expression of the *Arabidopsis* ACT2/ACT8 actin subclass in vegetative tissues. *Plant Journal* **10**: 107-121
- Baird GS, Zacharias DA and Tsien RY (2000) Biochemistry, mutagenesis, and oligomerization of DsRED, a red fluorescent protein from coral. *PNAS* **97**: 11984-11989
- Bucher M, Brunner S, Zimmermann P, Zardi GI, Amrhein N, Willmitzer L and Riesmeier JW (2002) The expression of an extensin-like protein correlates with cellular tip growth in tomato. *Plant Physiol.* **128**: 911-923
- Chalfie M (1995) Green fluorescent protein. *Photochem Photobiol* **62**: 651-656.
- Chalfie M, Tu Y, Euskirchen G, Ward WW and Prasher DC (1994) Green fluorescent protein as a marker for gene expression. *Science* **263**: 802-805
- Cormack BP, Valdivia RH and Falkow S (1996) FACS-optimized mutants of the green fluorescent protein (GFP). *Gene* **173**: 33-38
- Cubitt AB, Heim R, Adams SR, Boyd AE, Gross LA and Tsien RY (1995) Understanding, improving and using green fluorescent proteins. *Trends Biochem. Sci* **20**: 448-455
- Davis SJ and Vierstra RD (1998) Soluble, highly fluorescent variants of green fluorescent protein (GFP) for use in higher plants. *Plant Mol Biol* **36**: 521-528.
- Fåhræus G (1957) The infection of clover root hairs by nodule bacteria studied by a simple glass slide technique. *Journal of Genetic Microbiology* **16**: 374-381
- Jach G, Binot E, Frings S, Luxa K and Schell J (2001) Use of red fluorescent protein from *Discosoma* sp. (dsRED) as a reporter for plant gene expression. *The Plant Journal* **28**(4): 483-491
- Jefferson AR, Kavanagh TA and Bevan MW (1987) Gus fusions: β -glucuronidase as a sensitive and versatile gene fusion marker in higher plants. *The EMBO Journal* **6**: 3901-3907
- Matz MV, Fradkov AF, Labas YA, Savitsky AP, Zaraisky AG, Markelov ML and Lukyanov SA (1999) Fluorescent proteins from nonbioluminescent *Anthozoa* species. *Nat Biotechnol* **17**: 969-973
- Nam YW, Penmetse RV, Endre G, Uribe P, Kim D and Cook DR (1999) Construction of a bacterial artificial chromosome library of *Medicago truncatula* and identification of clones containing ethylene -response genes. *Theor. Appl. Genet.* **98**: 638-646
- Ow DV, Wood KV, DeLuca M, de Wet JR, Helinski DR and Howell SH (1986) Transient and stable expression of the firefly luciferase gene in plant cells and transgenic plants. *Science* **234**: 856-859
- Rottier P (1980) Viral Protein Synthesis in Cowpea Mosaic Virus Infected Protoplasts. PhD thesis. University of Wageningen, Wageningen

- Sambrook and Russel** (2001) Molecular cloning: a laboratory manual. Cold spring harbor laboratory press, Cold spring harbor, NY
- Sieberer B and Emons AMC** (2000) Cytoarchitecture and pattern of cytoplasmic streaming in root hairs of *Medicago truncatula* during development and deformation by nodulation factors. *Protoplasma* **214**: 118-127
- Sonti RV, Chiurazzi M, Wong D, Davies CS, Harlow GR, Mount DW and Singer ER** (1995) Arabidopsis mutant deficient in T-DNA integration. *Proc Natl Acad Sci U S A* **92**: 11786-11790
- Stiller J, Martirani L, Tuppal S, Chian R, Chiurazzi M and Gresshoff PM** (1997) High frequency transformation and regeneration of transgenic plants in the model legume *Lotus Japonicus*. *Journal Experimental Botany* **48**: 1357-1365
- Tersikh A, Fradkov A, Ermakova G, Zaisky A, Tan P, Kajava AV, Zhao X, Lukyanov S, Matz M, Kim S, Weissman I and Siebert P** (2000) "Fluorescent Timer": Protein That Changes Color with Time. *Science* **290**: 1585-1588
- Tsien RY** (1998) The green fluorescent protein. *Annu. Rev. Biochem.* **67**: 509-544
- van Bokhoven H, Verver J, Wellink J and Kammen A** (1993) Protoplasts transiently expressing the 200K coding sequence of cowpea mosaic virus B-RNA support replication of M-RNA. *J Gen Virol* **74**: 2233-2241
- van Engelen FA, Molthoff JW, Conner AJ, Nap J-P, Pereira A and Stiekema WJ** (1995) pBINPLUS: an improved plant transformation vector based on pBIN19. *Transgenic Research* **4**
- Verkhusha VV, Kuznetsova IM, Stepanenko OV, Zaisky AG, Shavlovsky MM, Turoverov KK and Uversky VN** (2003) High Stability of Discosoma DsRed As Compared to Aequorea EGFP. *Biochemistry* **42**: 7879-7884

CHAPTER 3

Regulation of Actin Gene Expression During *Medicago truncatula* Root Hair Development

Abstract

Growing root hairs possess two different actin configurations: thick actin bundles, that run longitudinally along the hair length and flare out into thinner bundles (FB-actin) at the hair tip. FB-actin is specific for growing root hairs and disappears when root hairs stop growing. The thick actin cables and the FB-actin respond in a different way to stimuli application and are supposed to be functionally different. In plants actins are encoded by multigene families, whose members are differentially regulated during development and in various tissues. Moreover, some of the actin isoforms appear to be functionally non equivalent. In this work we characterized the expression pattern of the actin genes during root hair development in *Medicago truncatula*, to determine whether some of the actin genes were specifically expressed in root hairs or were regulated during root hair development. *M. truncatula* has 6 actin isoforms, of which 4 are highly expressed in root hairs. We analyzed their expression during root hair development by fusing the promoter regions to the fluorescent marker DsRED-E5. This reporter provides accurate information on the timing of gene expression. The fluorescent pattern was analyzed in root hairs at different developmental stages and showed that *MtACT2* and *MtACT3* were constitutively expressed, *MtACT4* expression was induced in root hairs whereas *MtACT1* was down regulated when root hairs stopped growing.

Rossana Mirabella, Carolien Franken, René Geurts and Ton Bisseling

Introduction

In plants, the actin cytoskeleton plays an important role in processes such as cell morphogenesis, positioning of division plane, organelle movement, cytoplasmic streaming, vesicle transport and tip growth of root hairs and pollen tubes (Mascarenhas, 1993; Williamson, 1993; Staehelin and Hepler, 1996; Fowler and Quatrano, 1997; Schmidt and Hall, 1998; Meagher et al., 1999; Nick, 1999; Staiger, 2000). Root hairs are highly specialized cells that elongate by insertion of Golgi vesicles in the plasma membrane at their tip, a process which is named tip growth and requires a functional actin cytoskeleton. Since root hairs are easily accessible for microscopy and take up drugs efficiently, they have been used to study the role of the actin cytoskeleton during tip growth. Another advantage of this system is that root hairs at successive stages of development are aligned along the root axis, with the youngest hairs near the root tip and the oldest near the hypocotyl. The first step in root hair development is the formation of a bulge on the epidermal cells. These bulges are formed by isotropic growth. Subsequently, hairs develop from these bulges by tip growth. Growing root hairs are characterized by a polar cytoarchitecture with a cytoplasmic dense region devoid of large organelles, at their tip and the vacuole is located at the base of the hair (Miller et al., 1999; Sieberer and Emons, 2000). The actin cytoskeleton has been shown to be essential for root hair polar growth in legumes (Miller et al., 1999) and in *Arabidopsis* (Miller et al., 1999; Gilliland et al., 2002; Ringli et al., 2002). Growing root hairs have thick actin bundles that run longitudinally along almost the complete shank of the hair. In the sub-apical region of these growing root hairs the thick bundles flare out into thinner bundles. These sub-apical bundles have a net-axial orientation and are referred to as FB-actin (Fine Bundles; Miller et al., 1999). The FB-actin is only present in growing root hairs, indicating that this actin configuration correlates with root hair tip growth (Miller et al., 1999). In fact, the FB-actin has almost disappeared in hairs that stop growing and is absent in full-grown root hairs, in which the thick actin bundles loop through the tip (Miller et al., 1999). Concomitantly with the changes in the configuration of the actin cytoskeleton, also the root hair cytoarchitecture rearranges during development. In root hairs that stop growing the cytoplasmic dense region at the hair tip becomes smaller and the vacuole extends toward the tip. Finally, in full-grown root hairs the cytoplasmic dense region is no longer present and the cellular volume is almost completely occupied by a large vacuole, and a thin layer of cytoplasm is located at the periphery of the hair (Miller et al., 1999; Sieberer and Emons, 2000).

In angiosperms, actins are encoded by multigene families. For example in *Arabidopsis* the actin gene family contains 8 functional members whereas about 100 members are present in *Petunia* (Hightower and Meagher, 1985; Baird and Meagher, 1990; McElroy et al., 1990; McLean et al., 1990a; McLean et al., 1990b; McDowell et al., 1996a). Based on their sequence and their expression pattern the *Arabidopsis* actin genes can be grouped in two

classes: vegetative and reproductive (McDowell et al., 1996a; Meagher et al., 1999). Members of the latter class are preferentially expressed during pollen development (Huang et al., 1996; An et al., 1996b; Huang et al., 1997; Kandasamy et al., 1999). Of the three vegetative actins, AtACT2 and AtACT8 are expressed in all vegetative tissues and account for about 90% of the actin proteins in mature Arabidopsis tissues (An et al., 1996a), whereas AtACT7 is expressed in young rapidly growing tissues (McDowell et al., 1996b). AtACT2, AtACT8 and AtACT7 are all strongly expressed in root hairs. A mutation that almost completely eliminates the expression of AtACT2 (*act2-1* mutant) impairs root hair elongation, confirming that the actin cytoskeleton is essential for root hair tip growth (Gilliland et al., 2002; Ringli et al., 2002). Although a certain degree of functional redundancy among the actin isovariants is to be expected, several studies report a nonequivalence of these isovariants (Gilliland et al., 2002; Kandasamy et al., 2002). For example, ectopic expression of a reproductive actin (AtACT1) induces severe morphological alteration in the aerial part of Arabidopsis, that are not induced by overexpressing an other isovariant (AtACT2; Gilliland et al., 2002; Kandasamy et al., 2002).

We analyzed the actin gene family of the model legume *Medicago truncatula*. Legumes have the unique ability to establish a symbiosis with *Rhizobium* bacteria. This symbiosis culminates in the formation of root nodules where rhizobia reduce atmospheric nitrogen. The interaction starts with responses that are induced in the epidermis and the root hair actin cytoskeleton configuration rearranges within a few minutes after application of rhizobial signal molecules, called Nod factor (de Ruijter et al., 1999; Miller et al., 1999). Here we aimed to study the expression of the *M. truncatula* actin genes during root hair development as this would provide a base for further studies on the *Rhizobium-M. truncatula* interaction.

We isolated all the actin genes of *M. truncatula* and determined their expression pattern during root hair development. We showed that *M. truncatula* has 6 actin genes of which at least 5 are expressed. The expression of 4 of these genes was studied during root hair development among others by using the fluorescent marker DsRED-E5. This is a DsRED variant, that changes its fluorescence from green to red over time and, therefore, provides accurate information about dynamics in gene regulation (Terskikh et al., 2000; Mirabella et al., 2004). These studies showed that 2 actin genes, *MtACT2* and *MtACT3*, are constitutively expressed in the root epidermis whereas *MtACT4* is induced when root hairs are formed and *MtACT1* expression is down regulated when root hairs stop growing.

Results

Isolation of Medicago truncatula actin cDNAs

To identify actin genes expressed in root hairs we screened a *M. truncatula* cDNA library made from RNA of root hairs and root tips (Covitz et al., 1998), using as probe a 570 bp fragment from a *Pisum sativum* actin clone (Hadri and Bisseling, unpublished data). This

fragment comprises a region of about 400 bp that is highly conserved in all the currently known plant actin genes. Therefore, we expected it to hybridize with cDNA clones of all the *M. truncatula* actin genes. Fifty thousand phages were screened, at low stringency condition (see Materials and Methods), and this resulted in about 350 positive phages. Of these, 52 clones were randomly selected. The sequences of these clones showed that they corresponded to 5 different actin genes and were named *MtACTIN1* (*MtACT1*), *MtACTIN2* (*MtACT2*), *MtACTIN3* (*MtACT3*), *MtACTIN4* (*MtACT4*) and *MtACTIN5* (*MtACT5*; Table I), respectively. *MtACT1* cDNA clones occurred most frequently (61%) within this set of 52 clones, *MtACT2* and *MtACT3* represented, respectively, 15% and 20% of the actin clones, whereas only one clone was isolated for *MtACT4* (2%) and *MtACT5* (2%; Table I).

Table I. Screening of *M. truncatula* root hairs/tips cDNA library

| <i>MtACTIN 1</i> | <i>MtACTIN 2</i> | <i>MtACTIN 3</i> | <i>MtACTIN 4</i> | <i>MtACTIN 5</i> | Total |
|------------------|------------------|------------------|------------------|------------------|-------|
| 61% | 15% | 20% | 2% | 2% | 100% |
| (32) | (8) | (10) | (1) | (1) | (52) |

Table I. Fifty-two actin clones, isolated from the root hair/tip enriched library, were sequenced and, according to the DNA sequences, were grouped in 5 classes. For each actin gene the number of ESTs is indicated as percentage of the total number of actin EST sequenced. The absolute number of ESTs is also indicated between brackets.

Previously, about 900 randomly selected clones from the same cDNA library were sequenced. Five were shown to be actin cDNAs and, of these, four were *MtACT1* and one *MtACT3* (Covitz et al., 1998; Table II). Therefore, this EST analysis is consistent with our data. Full-size cDNA clones of *MtACT1*, *MtACT2* and *MtACT3* and the single *MtACT4* and *MtACT5* clones were sequenced. Each cDNA had an open reading frame coding for a 377 a.a. long protein (Fig. 1), a 3' as well as a 5' untranslated region (UTR) of about 250-150 bp and a long polyA tail. *MtACT1*, *MtACT2* and *MtACT3* cDNA clones with a 3'UTR having a different length were identified, suggesting the presence of multiple polyadenylation sites in these actin genes.

| | | | | | |
|--------|------------|------------|------------|------------|------------|
| MtACT1 | MADAEDIQPL | VCDNGTGMVK | AGFAGDDAPR | AVFPSIVGRP | RHTGVMVGMG |
| MtACT2 | ----- | -V----- | ----- | -----I--- | ----- |
| MtACT3 | ----- | ----- | ----- | ----- | ----- |
| MtACT4 | --ES----- | ----- | ----- | ----- | ----- |
| MtACT5 | ----- | ----- | ----- | ----- | ----- |
| MtACT6 | ----- | ----- | ----- | ----- | ----- |
| | | | | | |
| MtACT1 | QKDAYVGDEA | QSKRGILTLK | YPIEHGIVSN | WDDMEKIWHH | TFYNELRVAP |
| MtACT2 | ----- | ----- | ----- | ----- | ----- |
| MtACT3 | ----- | ----- | ----- | ----- | ----- |
| MtACT4 | ----- | ----- | ----- | ----- | ----- |
| MtACT5 | ----- | ----- | ----- | ----- | ----- |
| MtACT6 | ----- | ----- | ----- | ----- | ----- |
| | | | | | |
| MtACT1 | EEHPVLLTEA | PLNPKANREK | MTQIMFETFN | VPAMYVAIQ | VLSLYASGRT |
| MtACT2 | ----- | ----- | ----- | ----- | ----- |
| MtACT3 | ----- | ----- | ----- | T----- | ----- |
| MtACT4 | ----- | ----- | ----- | T----- | ----- |
| MtACT5 | ----- | ----- | ----- | A----- | ----- |
| MtACT6 | ----- | ----- | ----- | T----- | ----- |
| | | | | | |
| MtACT1 | TGIVLDSDGD | VSHTVPIYEG | YALPHAILRL | DLAGRDLTDS | LMKILTERGY |
| MtACT2 | ----- | ----- | ----- | -----EY | -V----- |
| MtACT3 | ----- | ----- | ----- | -----F | ----- |
| MtACT4 | ----- | ----- | ----- | -----A | ----- |
| MtACT5 | ----- | ----- | ----- | -----A | ----- |
| MtACT6 | ----- | ----- | ----- | -----A | ----- |
| | | | | | |
| MtACT1 | MFTTSAEREI | VRDIKEKLAY | VALDYEQELE | TAKSSSSIEK | NYELPDGQVI |
| MtACT2 | S-S----- | ---V----- | ---F----- | -T---AV-- | ----- |
| MtACT3 | S----- | ---V---S- | I----- | --RT---V-- | S----- |
| MtACT4 | T----- | ---M----- | I----- | ---T--AV-- | T----- |
| MtACT5 | S---T----- | ---V---L-- | I----- | -S-T--AV-- | S----- |
| MtACT6 | S---T----- | ---V---L-- | I---F----- | -S-T--AV-- | S-----I- |
| | | | | | |
| MtACT1 | TIGAERFRCP | EVLFPQSMIG | MEAAGIHETT | YNSIMKCDVD | IRKDLYGNIV |
| MtACT2 | ---S----- | ----- | ---T----- | ----- | ----- |
| MtACT3 | ---D----- | ----- | ----- | ----- | ----- |
| MtACT4 | ----- | ----- | --SP----- | F----- | ----- |
| MtACT5 | ----- | ----- | ---P----- | ----- | ----- |
| MtACT6 | ----- | ----- | ---V----- | ----- | ----- |
| | | | | | |
| MtACT1 | LSGGSTMFPG | IADRSKEIT | ALAPSSMKIK | VVAPPERKYS | VWIGGSILAS |
| MtACT2 | ----- | -----S | ----- | ----- | ----- |
| MtACT3 | ----- | -----S | ----- | ----- | ----- |
| MtACT4 | ----- | ----- | ----- | ----- | ----- |
| MtACT5 | ---T----- | ----- | ----- | ----- | ----- |
| MtACT6 | ---T----- | ----- | ----- | ----- | ----- |
| | | | | | |
| MtACT1 | LSTFQQMWIS | KGEYDESGPS | IVHRKCF | | |
| MtACT2 | ----- | -----A | ----- | | |
| MtACT3 | -----A | -A----- | ----- | | |
| MtACT4 | -----A | -A----- | ----- | | |
| MtACT5 | -----A | -A----- | ----- | | |
| MtACT6 | -----A | -A----- | ----- | | |

Figure 1. Alignments of the 6 MtACT proteins. Hyphens (-) mark identical bases in sequences.

Table II. *MtACT* gene expression analyzed by Virtual Northern blot

| Origin of banks | No. of banks | No. of ESTs | <i>MtACT1</i> | <i>MtACT2</i> | <i>MtACT3</i> | <i>MtACT4</i> | <i>MtACT5</i> |
|--------------------|--------------|-------------|---------------|---------------|---------------|---------------|---------------|
| Roots various | 4 | 17902 | 0.11 (2) | 0.17 (3) | 0.45 (8) | 0.05 (1) | 0.06 (1) |
| Roots Mycorrhiza | 3 | 16881 | 0.18 (3) | 0.30 (5) | 0.06 (1) | 0.06 (1) | 0 |
| Roots Rhizobium | 3 | 11600 | 0 | 0.09 (1) | 0.17 (2) | 0 | 0 |
| Roots Nematodes | 1 | 3154 | 0 | 0.32 (1) | 0.32 (1) | 0 | 0 |
| Roots Phytophthora | 2 | 4967 | 0 | 0.40 (2) | 0.20 (1) | 0 | 0 |
| Roots Elicitors | 1 | 5789 | 0 | 0.17 (1) | 0.17 (1) | 0.17 (1) | 0 |
| Root hairs/tips | 1 | 882 | 4.5 (4) | 0 | 1.1 (1) | 0 | 0 |
| Nodules | 5 | 20525 | 0.05 (1) | 0.24 (5) | 0.05 (1) | 0.1 (2) | 0.05 (1) |
| Stems | 1 | 10336 | 0 | 0 | 0.39 (4) | 0.48 (5) | 0.1 (1) |
| Leaves various | 3 | 19121 | 0 | 0.10 (2) | 0.10 (2) | 0 | 0 |
| Leaves fungal | 1 | 5987 | 0.17 (1) | 0 | 0 | 0 | 0 |
| Leaves Phoma inf. | 1 | 3166 | 0.63 (2) | 0.32 (1) | 0.32 (1) | 0.63 (2) | 0 |
| Leaves insect | 1 | 9892 | 0.10 (1) | 0 | 0 | 0 | 0 |
| Plantlets | 2 | 13438 | 0.07 (1) | 0.30 (4) | 0 | 0 | 0 |
| Flowers | 2 | 7813 | 0.13 (1) | 0.38 (3) | 0.38 (3) | 0.13 (1) | 0.13 (1) |
| Seeds/Pods | 5 | 15183 | 0.07 (1) | 0.20 (3) | 0.07 (1) | 0.20 (3) | 0 |
| Cell cultures | 1 | 9065 | 0 | 0 | 0 | 0 | 0 |
| Total | 37 | 175701 | 0.10 (18) | 0.18 (31) | 0.15 (27) | 0.10 (17) | 0.02 (4) |

Table II. *MtACT* gene sequences were used for a blast search of the TIGR EST database. The resulting ESTs were classified, based on the sequence, in 5 classes from *MtACT1* to *MtACT5*. No ESTs for *MtACT6* were present in the database. For each actin gene the number of ESTs present in each library group is expressed for 1000 ESTs of the total number of ESTs in that library group. The absolute number of ESTs is also indicated between brackets. The EST clusters for each *MtACT* gene were:

MtACT1: TC 86577; *MtACT2*: TC 85698; *MtACT3*: TC 85697; *MtACT4*: TC 86486; *MtACT5*: TC 89940.

For more details on library groups see Material and Methods.

The Medicago truncatula actin gene family

The identification of five different actin genes indicates that *M. truncatula* actin proteins are encoded by a gene family, as previously reported for other plants (Hightower and Meagher, 1985; Baird and Meagher, 1990; McElroy et al., 1990; McLean et al., 1990a; McLean et al., 1990b; McDowell et al., 1996a). To determine whether, in addition to the five above described genes, *M. truncatula* has additional actin genes, genomic DNA blots were hybridized, at low stringency (see Materials and Methods), with a 580 bp PCR fragment from the *MtACT2* cDNA, containing a region more than 80% conserved among the 5 identified *M. truncatula* actin genes. This fragment does not contain a *HindIII* site in any of the identified *M. truncatula* actin genes. Five restriction fragments appeared to hybridize to the *MtACT2* probe when the genomic DNA was digested with *HindIII* (Fig. 2). However, the intensity of the lower band was higher than that of the others, probably due to the presence of fragments from more than one actin gene within this band (Fig. 2). This was confirmed by the presence of 6 hybridizing fragments using different restriction enzymes (data not shown), indicating that *M. truncatula* has more than five actin genes. To isolate this additional actin gene we screened a *M. truncatula* bacterial artificial chromosome (BAC; Nam et al., 1999) library, using the same probe and the same hybridization conditions as above. Fifteen hybridizing BAC clones were isolated. To assign each BAC clone to a specific actin isoform, gene specific primers were designed in the highly divergent 3' UTR region of each actin gene (see materials and methods; Table V). Using these gene specific primer pairs it was shown that all the BAC clones, except one, namely MtH1-25G05, contained one of the five already identified actin genes (Table III). DNA sequence analysis of MtH1-25G05 revealed that it indeed contained an additional actin gene, named *MtACTIN6* (*MtACT6*).

Analysis of the *M. truncatula* EST database (TIGR dbEST), containing 175701 ESTs (January, 2004) from 34 different libraries, revealed the presence of 95 actin clones (Table II), corresponding to *MtACT1* (TC86577), *MtACT2* (TC85698), *MtACT3* (TC85697), *MtACT4* (TC86486) and *MtACT5* (TC89940). No sequences corresponding to *MtACT6* or to actin genes other than the five already isolated were present in the EST database.

To confirm that we isolated all the *M. truncatula* actin genes, one BAC clone was selected for each actin gene (Table III). These BAC clones as well as genomic DNA were digested with *HindIII* and, subsequently, hybridized with the *MtACT2* probe. The resulting hybridization pattern showed that each actin genomic fragment corresponded to a fragment of the same size in one of the BAC clones (Fig. 2). Therefore *M. truncatula* has 6 actin genes, of which at least 5 are expressed. An alignment of the 6 *M. truncatula* actin proteins is shown in Fig. 1. *M. truncatula* actins have 93%-97% amino acid identity and so are highly conserved as is the case in other species.

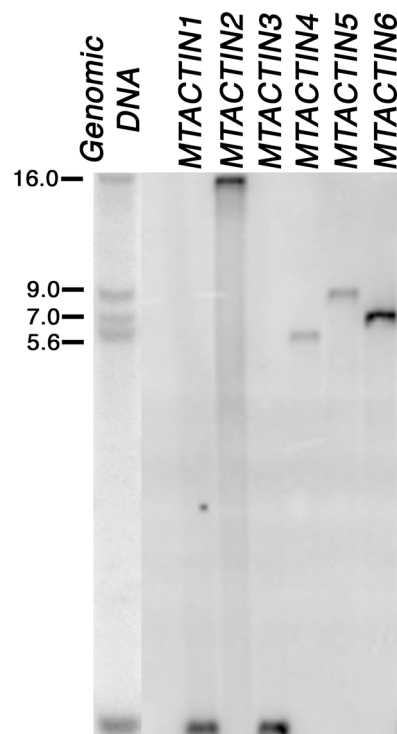


Figure 2. Southern blot of the actin gene family in *M. truncatula*. Medicago genomic DNA and one BAC DNA, for each *MtACT* gene, were digested with *Hind*III, separated on a 0.8% agarose gel, blotted onto a nylon membrane and hybridized with a 580 bp PCR fragment from the *MtACT2* cDNA, containing a highly conserved region among the *MtACT* genes. The position of the molecular size marker is indicated on the left of the autoradiogram.

Table III. BAC containing *MtACT* genes

| <i>MtACT</i> gene | MtH1-BAC |
|-------------------|---|
| <i>MtACT1</i> | 47 K 18, 21 O 22, 24 M 07, 48 K 16, 28 P 15, 80 L 24 |
| <i>MtACT2</i> | 01 N 01 |
| <i>MtACT3</i> | 69 I 01 , 61 D 01 |
| <i>MtACT4</i> | 48 I 22 |
| <i>MtACT5</i> | 21 M 04, 37 A 18 , 31 P 13, 44 I 11, |
| <i>MtACT6</i> | 25 G 05 |

Table III. A *M. truncatula* BAC library was screened using as probe a fragment of the *MtACT2* gene. Fifteen hybridising BAC clones were identified and assigned to each *MtACT* gene using gene specific PCR primers. One BAC for each *MtACT* gene was selected for further analysis (indicated in bold).

Virtual Northern Blot

To determine whether some *MtACT* genes were preferentially expressed in root hairs we analyzed their expression pattern. First, we determined the frequency of each of the 5 expressed *M. truncatula* actin genes in the TIGR database (db). As mentioned above, this db contains 95 actin EST clones. The number of clones for each actin gene in the ESTdb

and the tissues from which they originate are indicated in Table II. In contrast to their low frequencies in the root hair/tip library, *MtACT2* and *MtACT3* clones were most abundant, with 31 and 27 ESTs, respectively, representing in total about 63% of the actin sequences in the db. These two actin genes seem to be expressed in most tissues, but a relatively high number of *MtACT3* ESTs (8) came from the root libraries. Interestingly, 5 of these ESTs were isolated from libraries of plants starved for nitrogen or phosphate. *MtACT1* is not highly represented in the ESTdb, although it is the most frequent occurring actin clone in the root hair/tip library, suggesting that this actin gene might be preferentially expressed in root hairs or root tips. Moreover, within the different leave libraries, *MtACT1* ESTs originated only from leaves infected with various pathogens, suggesting that this actin gene might be induced in leaves upon infection. *MtACT4* was present at the highest level in the stem libraries, with 5 ESTs (Table II), whereas *MtACT5* occurred at a low frequency in the different libraries with only 4 ESTs in the EST db (Table II).

Expression of the M. truncatula actin genes during root hair development

To determine the expression pattern of the different *M. truncatula* actin genes during root hair development we used promoter reporter fusions. Since the actin genes are highly conserved promoter reporter studies *in planta* are the best way to address this question. We cloned, from the corresponding BACs, the 5' regions of the four actin genes that, according to the analysis of the EST db, were highest expressed in roots (*MtACT1*, *MtACT2*, *MtACT3* and *MtACT4*). These 5' regions include the promoter regions, the intron and the exon in the leader region and part of the first exon encoding the first 19 amino acids. These elements have been shown to be important for the correct regulation of actin gene expression in *Arabidopsis* (Huang et al., 1996; An et al., 1996a; An et al., 1996b; McDowell et al., 1996b; Huang et al., 1997).

Root hair development is a relatively fast process. Therefore, most of the commonly used reporters, such as GUS, GFP or DsRED, would not have been useful to reveal changes in gene expression in root hairs of different ages due to their relatively high stability. We used the fluorescent marker DsRED-E5. DsRED-E5 is a DsRED variant, that changes its fluorescence from green to red over time in a concentration independent manner (Tersikh et al., 2000; Mirabella et al., 2004). The green to red fluorescence ratio (G/R) reflects the age of the DsRED-E5 molecules and provides additional information about the timing of gene expression (Mirabella et al., 2004). Previously, we have shown that the green as well as the red fluorescence of DsRED-E5 can be distinguished efficiently from autofluorescence of the root epidermis. Moreover, when DsRED-E5 is produced constitutively a steady-state value of the G/R will be reached that is independent of the promoter strength. We showed that deviations of this steady-state G/R value indicate changes in promoter activity and can be successfully used to study dynamics of genes expression (Mirabella et al., 2004).

The above described 5' regions of the actin genes were fused to the coding region of DsRED-E5. The *MtACTp::DsRED-E5* fusions were introduced into *M. truncatula* roots by *Agrobacterium rhizogenes* mediated root transformation. Transformed roots were selected by DsRED-E5 fluorescence using a stereo fluorescence macroscope and were further analyzed by confocal laser scanning microscopy (CLSM). For each *MtACTp::DsRED-E5* transgene 4-5 independently transformed roots were analyzed.

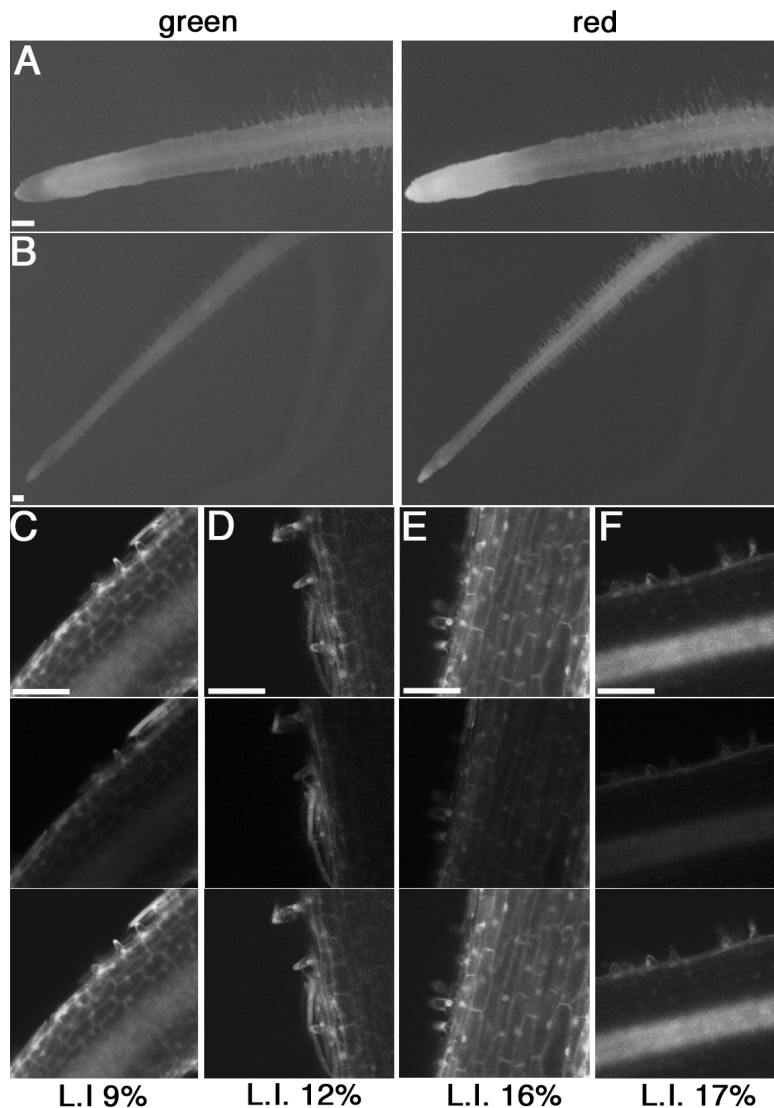


Figure 3. Expression pattern of the *MtACT* promoters in roots transformed with the different *MtACTp::DsRED-E5* fusions. A) Stereo fluorescence macroscope image of a root transformed with the *MtACT1p::DsRED-E5* fusion showing higher expression of *MtACT1* in root tip. B) Stereo fluorescence macroscope image of a root transformed with the *MtACT2p::DsRED-E5* fusion showing constitutive expression of the *MtACT2* promoter. C) to F) Confocal fluorescence image of the root region in which root hair development starts in roots expressing the different *MtACTp::DsRED-E5* transgenes. C) higher expression of *MtACT1* in the root epidermis compared to cortical cells and vascular tissue. D) and E) constitutive expression of *MtACT2* and *MtACT3*, respectively, in the root tissues. F) *MtACT4* expression in the root epidermis and in the vascular

tissue. Note higher expression in the latter tissue. Bars = 50 μ m. L.I. = Laser intensity. (Color figure, see appendix).

Previously, we had shown that *MtACT2* is constitutively expressed in all the root tissues (Mirabella et al., 2004). Since a steady-state value of G/R is needed to analyze the expression of the actin genes during root hair formation, we first determined the G/R value in the epidermal cells transformed with the *MtACT2p::DsRED-E5* transgene. Roots transformed with this transgene showed an equal level of fluorescence in all its cells consistent with the constitutive mode of expression of this actin gene in all the root tissues

(Fig. 3B and D) including epidermis and root hairs (Fig. 4A to C). We determined G/R values in these roots in bulges and growing, growth terminating and mature root hairs. The latter were located in a region of about 0.5 mm just above the growth terminating hairs. The different developmental stages of root hairs were identified considering both (1) their position along the root and (2) their cytoarchitecture, as described in the introduction. The G/R values were 2.8 ± 0.32 ($n = 45$), 2.8 ± 0.18 ($n = 28$) and 2.7 ± 0.28 ($n = 21$), respectively, in bulges/growing, growth terminating and mature root hairs (Table IV). These data confirm that the *MtACT2* gene is constitutively expressed during root hair development and indicates a steady-state G/R value in root hairs of ~ 2.8 . Therefore, this value was used to analyze the expression pattern of the other 3 actin genes.

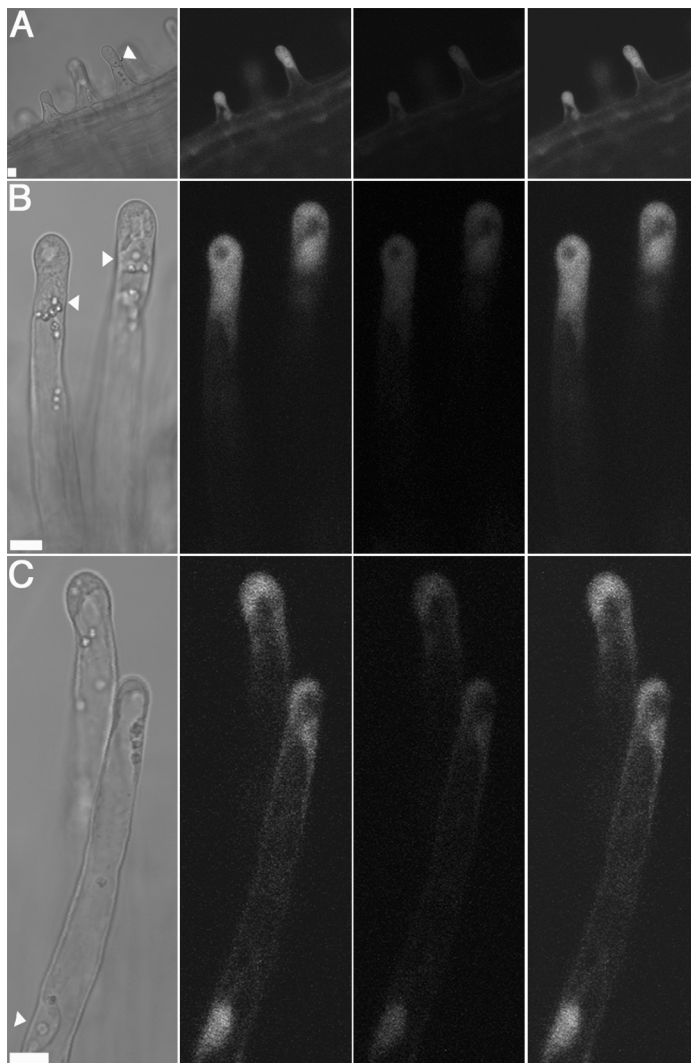


Figure 4. Expression pattern of the *MtACT2* promoter in *M. truncatula* root hairs transformed with the *MtACT2p::DsRED-E5* fusion. Confocal fluorescence images of growing (A), growth terminating (B) and “young mature” (C) root hairs. Nucleus is indicated by the arrowhead. Bars = 10 μm . (Color figure, see appendix).

Table IV. G/R in root hairs expressing different *MtACTp::DsRED-E5* transgenes

| Root | Bulges\Growing root hairs | Growth terminating root hairs | “Young mature” root hairs |
|------------------|------------------------------|----------------------------------|------------------------------|
| transgene | | <i>MtACT1p::DsRED-E5</i> | |
| Root 1 | 2.6 ± 0.2 (n = 10) | 2.1 ± 0.33 (n = 3) | 0.96 ± 0.26 (n = 8) |
| Root 2 | 2.6 ± 0.25 (n = 12) | 2.15 ± 0.28 (n = 11) | 1.18 ± 0.15 (n = 11) |
| Root 3 | 3.0 ± 0.3 (n = 11) | 2.0 ± 0.20 (n = 7) | 1.05 ± 0.05 (n = 5) |
| Root 4 | 3.1 ± 0.4 (n = 13) | 2.4 ± 0.25 (n = 4) | 0.85 ± 0.07 (n = 5) |
| Root 5 | 2.6 ± 0.3 (n = 7) | 1.7 ± 0.17 (n = 5) | 0.8 ± 0.13 (n = 4) |
| Total | 2.8 ± 0.4 (n = 53) | 2.1 ± 0.3 (n = 30) | 1 ± 0.2 (n = 33) |
| transgene | | <i>MtACT2p::DsRED-E5</i> | |
| Root 1 | 2.77 ± 0.21 (n = 12) | 2.66 ± 0.17 (n = 6) | 2.45 ± 0.23 (n = 4) |
| Root 2 | 2.79 ± 0.37 (n = 8) | 2.6 ± 0.25 (n = 4) | 2.45 ± 0.2 (n = 5) |
| Root 3 | 2.86 ± 0.39 (n = 9) | 2.9 ± 0.07 (n = 6) | 2.9 ± 0.24 (n = 6) |
| Root 4 | 2.91 ± 0.13 (n = 10) | 2.88 ± 0 (n = 6) | 2.8 ± 0.13 (n = 3) |
| Root 5 | 2.88 ± 0.56 (n = 6) | 2.86 ± 0.18 (n = 6) | 2.8 ± 0.14 (n = 3) |
| Total | 2.8 ± 0.32 (n = 45) | 2.8 ± 0.18 (n = 28) | 2.7 ± 0.28 (n = 21) |
| transgene | | <i>MtACT3p::DsRED-E5</i> | |
| Root 1 | 3.2 ± 0.5 (n = 8) | 2.6 ± 0.26 (n = 4) | 2.5 ± 0.27 (n = 7) |
| Root 2 | 3.1 ± 0.4 (n = 10) | 2.5 ± 0.20 (n = 3) | 2.5 ± 0.33 (n = 3) |
| Root 3 | 3.35 ± 0.6 (n = 5) | 2.9 ± 0.28 (n = 6) | 2.5 ± 0.17 (n = 5) |
| Root 4 | 2.6 ± 0.4 (n = 9) | 2.25 ± 0.14 (n = 5) | 1.8 ± 0.1 (n = 3) |
| Total | 3.03 ± 0.5 (n = 32) | 2.6 ± 0.35 (n = 18) | 2.4 ± 0.34 (n = 18) |
| transgene | | <i>MtACT4p::DsRED-E5</i> | |
| Root 1 | 9.45 ± 2.5 (n = 10) | 9.4 ± 1.45 (n = 8) | 3.0 ± 0.60 (n = 4) |
| Root 2 | 10.5 ± 2.3 (n = 5) | 9.9 ± 2.25 (n = 4) | 2.9 ± 0.40 (n = 3) |
| Root 3 | 8.5 ± 1.5 (n = 7) | 8.04 ± 1.4 (n = 6) | 2.9 ± 0.40 (n = 4) |
| Root 4 | 13.1 ± 4.1 (n = 4) | 12.6 ± 3.7 (n = 5) | 3.0 ± 0.55 (n = 4) |
| Total | 10.0 ± 3.0 (n = 26) | 10.0 ± 2.7 (n = 23) | 3.0 ± 0.48 (n = 15) |

Table IV. G/R measured in bulges, growing, growth terminating and young mature *M. truncatula* root hairs transformed with different *MtACTp::DsRED-E5* fusions. The data presented for each fusion were obtained from 4-5 independently transformed roots. G/R are indicated as mean value ± standard deviation. The number of root hairs analyzed per root for each stage of development is indicated between brackets.

Roots expressing the *MtACT1p::DsRED-E5* transgene had the strongest fluorescence intensity (Fig. 3 A and C), indicating that this is the actin gene expressed at the highest level in roots. In these roots the promoter activity was highest in a region of about 1 cm just above the root tip, encompassing the apical meristem as well as the elongation zone (Fig. 3A).

These data are consistent with the results obtained from the root hair/tip library screening in which *MtACT1* clones were shown to occur most frequently. To analyze the *MtACT1* expression in root hairs, the region of the root where root hair development occurs was analyzed in more detail by CLSM (Fig. 3C). The *MtACT1* promoter was strongest expressed in the epidermis but was also active in the other root tissues, including the vascular bundle and the cortex (Fig. 3C). Next, we compared the expression level of the *MtACT1* gene with that of other actin genes and analyzed its expression during different stages of root hair development (Fig. 5).

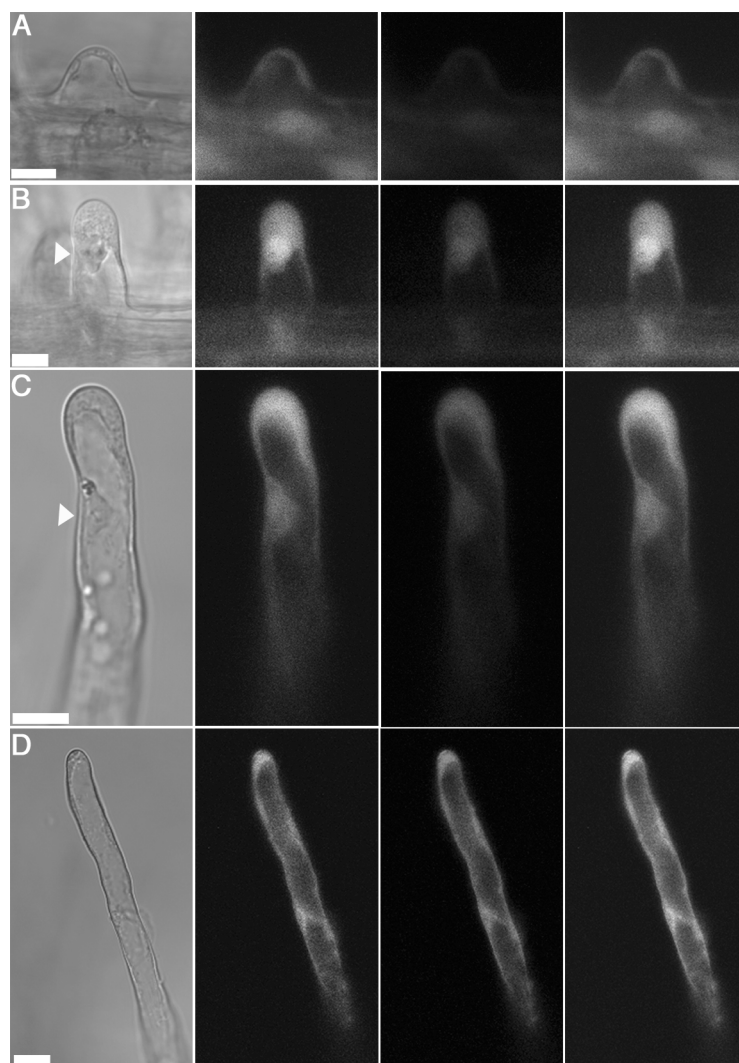


Figure 5. Expression pattern of the *MtACT1* promoter during *M. truncatula* root hair development in roots transformed with the *MtACT1p::DsRED-E5* fusion. Confocal fluorescence images of bulges (A), growing (B), growth terminating (C) and “young mature” (D) root hairs. Note the fluorescence color change moving from growing to “young mature” hairs. Nucleus is indicated by the arrowhead. Bars = 10 μ m. (Color figure, see appendix).

Growing root hairs expressed the *MtACT1p::DsRed-E5* transgene at a higher level than the other *MtACT* promoter fusions (Fig. 5B), indicating that *MtACT1* is the highest expressed actin gene in growing hairs. Moreover, the intensity of the green fluorescence, that indicates promoter activity, was equal in epidermal cells before root hairs are formed and in growing root hairs. However, the intensity was markedly lower in full-grown root hairs (Fig. 5), suggesting that the activity of the promoter was down-regulated during root hair development. Concomitantly with the decrease in green fluorescence intensity the overall

fluorescence color changed from green to orange as root hair development proceeds (Fig. 5). To analyze the timing of the decrease of the *MtACT1* promoter activity more accurately, we determined the G/R values in root hairs of different ages. This analysis was done in the region of the root spanning from bulges to “young mature” root hairs. In bulges and growing hairs (Fig. 5C and D) G/R was at a steady-state level, having a value of 2.8 ± 0.4 ($n = 53$; Table IV). In contrast, in growth terminating (Fig. 5E) and “young mature” hairs (Fig. 5F) we measured a value of G/R of 2.1 ± 0.3 ($n = 30$) and 1.0 ± 0.2 ($n = 33$; Table IV), respectively. This shows that the activity of the *MtACT1* promoter is down regulated in growth terminating hairs, as the G/R value was lower than the steady-state G/R.

The *MtACT3p::DsRED-E5* fusion showed the lowest expression level of the studied Medicago actin promoters (Fig. 3E) and fluorescence could only be observed when roots were analyzed by CLSM. This analysis showed that the *MtACT3* promoter was constitutively active in roots (Fig. 3E), although the fluorescence intensity was higher in the cap cells (data not shown). This promoter appeared to be constitutively active also during root hair development, as the intensity of the green fluorescence remained constant and the overall fluorescence color did not change (Fig. 6C and D).

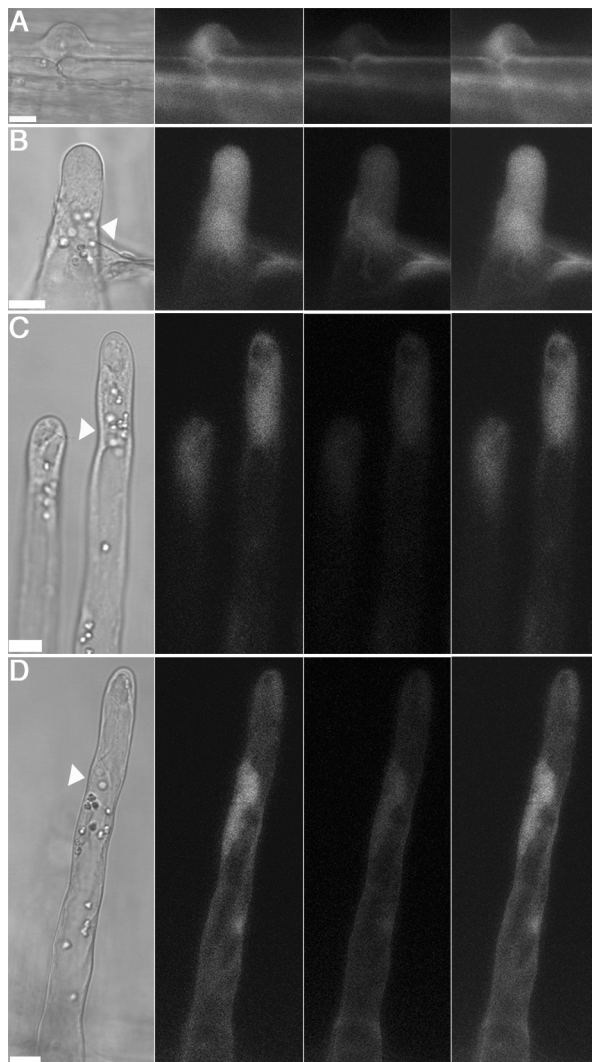


Figure 6. Expression pattern of the *MtACT3* promoter during *M. truncatula* root hair development in roots transformed with the *MtACT3p::DsRED-E5* fusion. Confocal fluorescence images of bulges (A), growing (B), growth terminating (C) and “young mature” (D) root hairs. Nucleus is indicated by the arrowhead. Bars = 10 μ m.

The G/R values confirmed the constitutive nature of this actin gene as they were close to the steady-state level in root hairs at all developmental stages (Table IV).

Finally, we analyzed the *MtACT4p::DsRED-E5* fluorescence pattern (Fig. 3F). Expression of this promoter could be detected only in the younger part of the root (about 1/3 of the total root length) after which the fluorescence intensity gradually decreased (data not shown). The highest level of expression was observed in the root vascular bundles (Fig. 3F). Expression could also be detected in the cap cells (data not shown) and in the epidermal cells (Fig. 3F), although at a lower level. Moreover, in the epidermis the fluorescence could be detected only in cells with root hairs (Fig. 7), suggesting that this promoter is induced when root hairs are formed. To test this, a more detailed analysis of the *MtACT4* gene expression pattern during root hair development was performed (Fig. 7).

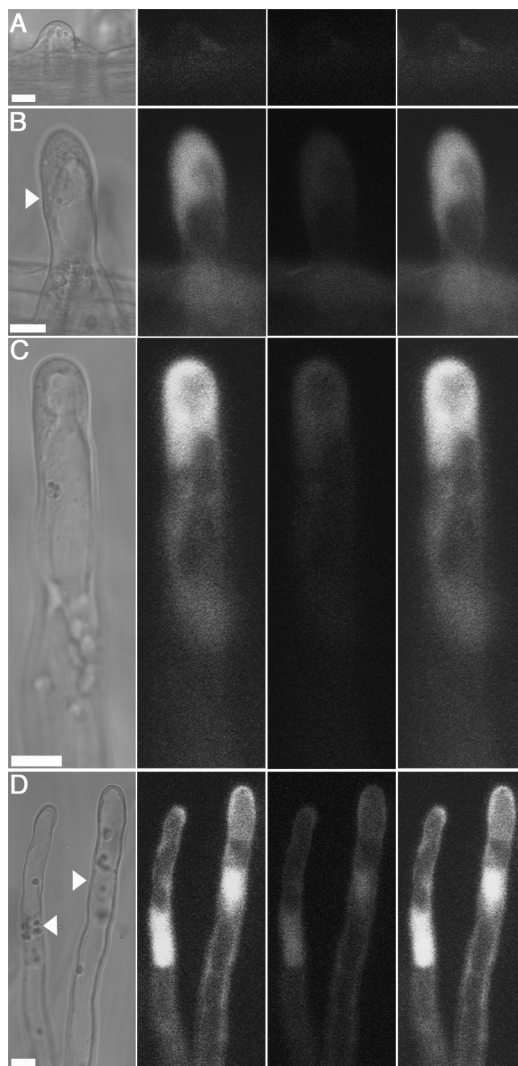


Figure 7. Expression pattern of the *MtACT4* promoter during *M. truncatula* root hair development in roots transformed with the *MtACT4p::DsRED-E5* fusion. Confocal fluorescence images of bulges (A) growing (B), growth terminating (C) and “young mature” (D) root hairs. Note absence of fluorescence in bulges. Nucleus is indicated by the arrow head. Bars = 10 μ m. (Color figure, see appendix).

In bulges the fluorescence signal was too low to be detected (Fig. 7A). Fluorescence could first be detected in the region where bulges become tip growing root hairs (Fig. 7B), after which the intensity of the green fluorescence remained at a constant level during root hair development (Fig. 7C and D). These data indicate that the *MtACT4p* is induced in root hairs

and its activity is maintained throughout root hair development. This was confirmed by the measured G/R values that, in growing and growth terminating root hairs, were markedly higher than the steady-state value (Table IV), whereas in “young mature” hairs they were close to the steady-state value.

RT-PCR analysis of the *M. truncatula* actin genes in roots

The analysis of the *MtACTp::DsRED-E5* fusion expression pattern in roots indicate that the *M. truncatula* actin genes are differentially expressed in roots and during root hair development. To confirm the expression pattern revealed by the *MtACTp::DsRED-E5* fusions, we performed a semi-quantitative RT-PCR analysis on RNA isolated from total root, root tip (excised ~ 3 mm behind the tip) and root hairs (Fig. 8), respectively, using the gene specific primers described above (Table V). Control reactions, in which total actin cDNA (Fig. 8) or ubiquitin cDNA (data not shown) was amplified, were included. The PCR products were separated by agarose gel electrophoresis and quantified after hybridization with a gene specific probe (Fig. 8 and 9). The results presented in Fig. 8 are representative of two independent experiments. The quantification data shown in Fig. 9 are the average of the data obtained in the two experiments.

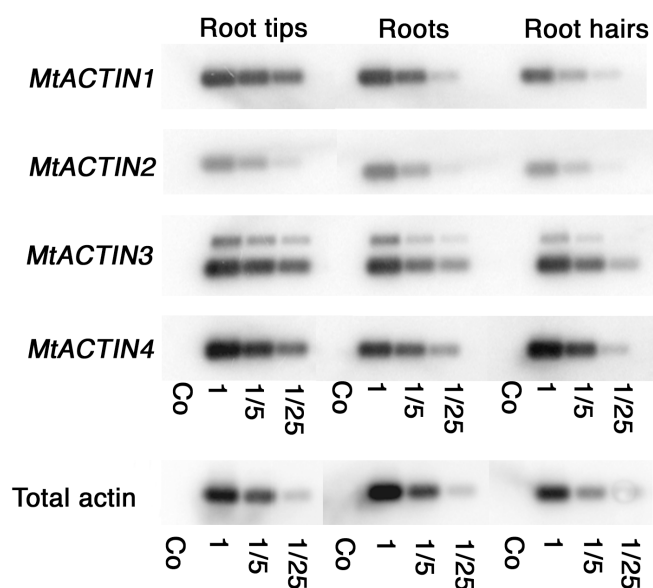


Figure 8. RT-PCR analysis of the expression of the *M. truncatula* actin genes in various tissues. Twenty-two cycles of PCR were performed using actin gene specific primers (Table V) on cDNA made from root tips, total roots and root hairs. The PCR products were resolved on a 1% agarose gel, blotted to a nylon membrane and hybridized with gene specific probes. To quantify the intensity of each hybridization signal PCR reactions were included using as template the same amount of plasmid DNA carrying each of the actin cDNA. For the latter amplifications the same primers and PCR conditions as for the cDNA amplifications were used (see text and material and methods). As control total actin cDNA was amplified (20 cycles) using PCR

primers that anneal to all the 6 *M. truncatula* actin cDNAs (Table V). The same result was obtained when ubiquitin was used as control (data not shown). Co, control in which no reverse transcriptase was added to the cDNA synthesis reaction, to verify absence of genomic DNA contamination.

These data show that the amount of *MtACT1* mRNA was about 4 times higher in root tips than in total roots (Fig. 8 and 9A), confirming the expression pattern revealed by the *MtACT1p::DsRED-E5* transgene. Further, the amount of *MtACT1* messenger was also low in the root hair RNA preparation. Since the root hair isolation leads to an enrichment of mature root hairs this is also consistent with the observed down-regulation of the *MtACT1p::DsRED-*

E5 transgene in mature root hairs. Moreover, the RT-PCR experiment showed that *MtACT4* is expressed at a considerable higher level in root hairs than in root tips and roots (Fig. 8 and 9A). This is in agreement with the induction of the *MtACT4* gene activity in root hairs and the maintenance of expression of *MtACT4p::DsRED-E5* in mature hairs. *MtACT2* mRNA levels appeared to be similar level in the different tissues, being consistent with the observed constitutive expression of the *MtACT2p::DsRED-E5* transgene (Fig. 8 and 9A). *MtACT3* mRNA was present at a markedly higher level in the root tip sample, reflecting the higher expression in cap cells observed in the *MtACT3p::DsRED-E5* expressing roots (Fig. 8 and 9A).

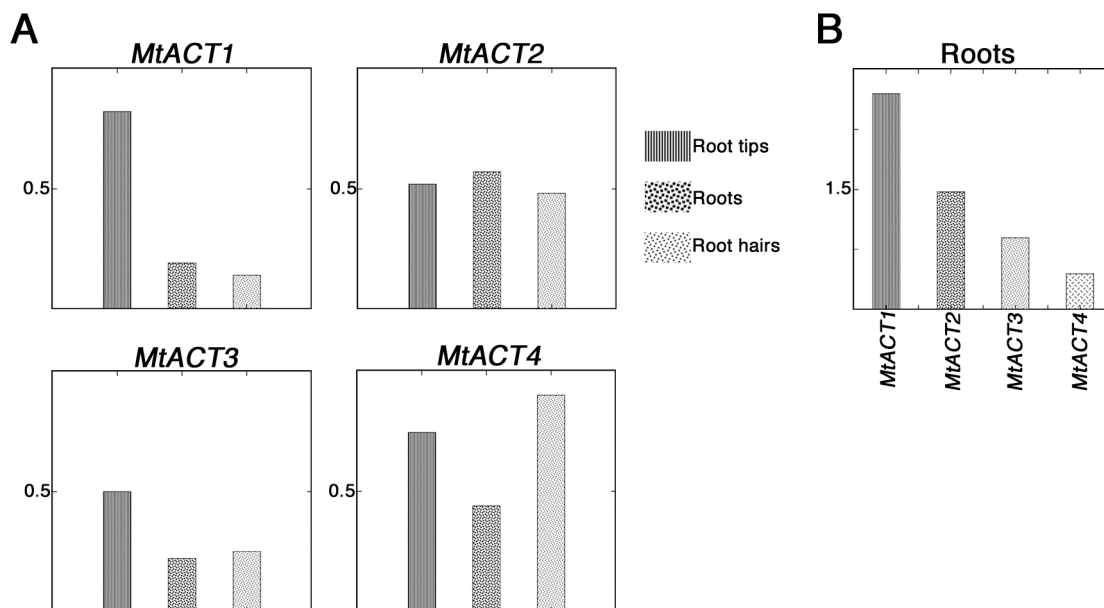


Figure 9. Quantification of the expression level of the *MtACT* genes from the RT-PCR analysis in Fig. 8. **A)** The expression level of each actin gene was compared in root tips, roots and root hairs. For the quantification of *MtACT1* and *MtACT3* mRNA level, the intensity of the 1/25 cDNA amplification dilution was used; for the quantification of *MtACT2* and *MtACT4* expression levels the intensities of the 1/5 cDNA amplification dilutions were used. **B)** Quantification of the expression levels of the actin genes in roots. For the quantification of the expression levels the intensities of all the dilutions were used. The signal intensities in the control reactions, in which total actin or ubiquitin were amplified, were also quantified to normalize for differences in the cDNA amount present in the different tissue samples. Values on the Y-axis are arbitrary units

To determine which of the actin gene was highest expressed in roots, we included control PCR reactions, in which we used the same primers for the cDNA amplifications but as template 4 plasmids carrying each one of the *MtACT* sequences. In this way we could normalize for the different efficiencies in the PCR amplifications and in the hybridization reactions. We quantified the signal intensities (see materials and methods) and this analysis confirmed that *MtACT1* and *MtACT2* were the highest expressed actin genes in roots (Fig. 9B).

In conclusion, these data indicate that the expression pattern of the actin promoters is in agreement with the expression pattern of the endogenous actin genes as revealed by the RT-PCR analysis.

Discussion

In this study we characterized the expression pattern of the *M. truncatula* actin genes during root hair development. *M. truncatula* has six different actin genes, of which four are expressed at a relatively high level in root hairs. By promoter fusion with the reporter DsRED-E5, we showed that two of these genes, *MtACT2* and *MtACT3*, are constitutively expressed during root hair development whereas *MtACT4* expression is induced in root hairs and *MtACT1* expression is down regulated when root hairs mature. Further, *MtACT1* is the highest expressed actin gene in growing root hairs.

Spatio-temporal regulation of actin gene expression is well known in e.g. *Arabidopsis* and soybean (Hightower and Meagher, 1985; McLean et al., 1990b; Meagher et al., 1999). However, this is the first report showing regulation of actin gene expression during root hair development. Our studies show that the decrease of *MtACT1* promoter activity during root hair development coincides with a major configuration change in the actin cytoskeleton. FB-actin is present only in growing root hairs and it disappears simultaneously with the *MtACT1* down regulation when root hairs stop growing (Miller et al., 1999). This suggests that FB-actin might be enriched for the *MtACT1* isovariant. The use of isovariant-specific antibodies or GFP fusions would be required to test this hypothesis.

The interaction of rhizobial bacteria and legumes results in nitrogen fixing root nodules. Several steps of the developmental program leading to the formation of nodules most likely require a functional actin skeleton. For example, this could involve the root hair curling and infection thread growth because both appear to involve tip growth. Further the configuration of the actin skeleton in root hairs rapidly changes as response to the application of rhizobial Nod factors (de Ruijter et al., 1999; Miller et al., 1999). Therefore, it seems probable that actin genes will be differentially regulated during the steps leading to nodule formation. Stable transformed Medicago lines expressing the *MtACTp::DsRED-E5* transgenes will be useful tools to study the dynamics of actin genes expression during this symbiotic interaction.

Materials and Methods

Isolation of cDNA clones and sequences

Actin cDNA clones were isolated from a root hair/root tip library (Covitz et al., 1998). Plaque lifts and phage work were carried out according to standard procedures (Sambrook and Russel, 2001), using Hybond N⁺ nylon membranes (Amersham). The library was screened using as probe a 550 bp fragment from a *Pisum sativa* actin cDNA (Hadri and Bisseling, unpublished data). The hybridization conditions were: 0.5% SDS, 5X Denhart

solution, 5X SSPE and 100µg/ml salmon sperm at 60°C and the washes were done, at the same temperature, 30 min. in 0.1% SDS and 2X SSPE, 30 min. in 0.1% SDS and 1X SSPE and 15 min. in 0.1% SDS and 0.5X SSPE. cDNA clones in the positive plaques were amplified by PCR using M13 primers and the PCR fragments were sequenced. Sequencing was done by the dideoxy chain termination method (BigDye; Perkin-Elmer, Foster City, CA) and was analyzed on an ABI 377 DNA sequencer (Applied Biosystems, Foster City, CA). The derived sequences were manually aligned and the pBK-CMV phagemid, containing each of the five *MtACT* genes, were excised from the Zap Express vector and transformed into XL0LR cells according to manufacturers descriptions (Stratagene, La Jolla, CA), generating the pBK-CMV*MtACT* vectors.

Genomic and BAC DNA isolation and blots

M. truncatula genomic DNA and Bacterial Artificial Chromosome (BAC) DNA were isolated according to Gualtieri (Gualtieri et al., 2002) and Nam (Nam et al., 1999), respectively. The DNA was digested, separated on a 0.8% agarose gel and transferred to a Hybond N⁺ nylon membrane (Amersham) according to the manufacturers instructions. DNA probes for southern blot were labeled with ³²PdATP using the random priming method (Feinberg and Vogelstein, 1983). Hybridization and washing conditions were as described above for the cDNA library screening. Primers used to obtain the *MtACT2* probe, previously mentioned are indicated in Table V. To assign each BAC to a specific *MtACT* gene, isovariant specific primers were designed in the 3' UTR of each *M. truncatula* actin gene. To confirm the specificity of these actin primer pairs, each pair was used in PCR reactions using as template each cDNAs of the six *M. truncatula* actin genes. Only amplification in the presence of the specific template was observed (data not shown). The isovariant specific primer pairs are listed in Table V.

Table V. Primers used for RT-PCR and BAC analysis

| <i>MtACT</i> gene | Forward primer | Reverse primer |
|---------------------|-------------------------|------------------------|
| <i>MtACT1</i> | CAAAATGATGCGATAATGG | AGCATCACAACTCACTCCT |
| <i>MtACT2</i> | TGTGCCATATTTCAAGTCAAG | CTACAAAGTTCAATACCATCC |
| <i>MtACT3</i> | GAGAAAGAGGGAAAGACT | TACGCAGAATGAACCAGT |
| <i>MtACT4</i> | GATGAGAGCTGGATTAAG | GAGGGAAAATTGAATCTTAC |
| <i>MtACT5</i> | TCTCATCAAAATCCAAACC | TAAGAAATACCATAAAACTG |
| <i>MtACT6</i> | AGCGACTTGCGACGATG | GGTAAAACAAAATAAATGAAAG |
| <i>MtACT-all</i> | AGTAGCATGAAGATCAAGG | CCTTGGCAATCCACATCTG |
| <i>MtACT2</i> probe | ACAATGGAAGTGAATGG | GAGGTACTGAAGGAGTATCC |
| ubiquitin | ATGCAGAT(CT)TTTGTGAAGAC | ACCACCACG(AG)AGACGGAG |

Table V (page 67). Primer pairs from *MtACT1* to *MtACT6* were designed in the 3'UTR and are gene specific. *MtACT-all* primers anneal to all the *M. truncatula* actin genes. *MtACT2* probe primers have been used to obtain the PCR fragment for the BAC library screening.

Comparison to *M. truncatula* ESTs and electronic Northern

The full-length cDNAs of each *MtAct* gene were used for Blast analysis of the *M. truncatula* database at TIGR (<http://www.tigr.org/tdb/tgi/mtgi>). Ninety-five ESTs were identified, manually aligned and grouped into 5 different clusters. ESTs from the same gene and derived from the same cDNA library that started at the same nucleotide were not used for further analysis, since they could have arose from the same cloning event. To obtain data on the expression pattern of the 5 genes (electronic northern), the 37 cDNA libraries were grouped into 17 classes of similar origin and the frequency of each gene in each bank group was calculated by dividing the number of specific and of total ESTs in the library class, expressed for 1000 ESTs. The cDNA libraries were grouped in the 17 classes as follow: Roots various (MtBA, KV0, MHRP and NR-RT); Root hair/tip (MtRHE); Roots-mycorrhiza (MtBC, MTGIM and MHAM); Roots-Rhizobium (KV1, KV2 and KV3); Roots nematodes (BNIR); Roots Phytophthora (DSIR, MGHG); Roots elicitors (HOGA); Nodules (GVN, MtBB, GVSN, R108 and NF-NR); Stems

(NF-ST); Leaves-various (DSLCL, NF-LF and NF-PL); Leaves fungal (DSLIL); Leaves Phoma infected (NF-PH); Leaves-insects (NF-IN); Plantlets (NF-DT and NF-IR); Flowers (NF-FL, MTFLOW); Seeds/pods (GPOD, GESD, NF-GS, MTPOSE and GLSD); Cell cultures (NF-EC).

RT-PCR expression analysis

Total RNA was isolated according to Pawlowski (Pawlowski et al., 1994) from 1 week old seedlings. Root hairs were collected as described in Gloudemans (Gloudemans et al., 1989). For the RT-PCR analysis, after DNAase I treatment, cDNA was made from 1 µg total RNA in a volume of 20 µl containing 50mM Tris-HCl pH=8.8, 75 mM KCl, 3 mM MgCl₂, 10 mM DTT, 1 mM dNTPs, 1µg oligodT17T/A/G/C mix, 20 U RNase OUT (Invitrogen) and 20 U M-MLV reverse transcriptase for 1hour at 37°C, followed by 5 min. at 95°C. To be sure that no genomic DNA was present in the c-DNA samples also a reaction was performed in the same conditions described above but in absence of the reverse transcriptase. The RT samples were then diluted to 50 µl. The PCR reactions were carried out, according to standard procedures (Sambrook and Russel, 2001), with 2 µl of the cDNA solution and three serial dilutions of 1/5 each. For the control PCR reactions, pBK-CMV vectors carrying each of the *MtAct* cDNA were used as template. For all the vectors described above equal amounts of DNA was used (3×10^{-6} and 3×10^{-7} picomoles). cDNA and plasmid amplifications were performed in the same conditions and within the same PCR reaction. The primers used for the PCR reactions are listed in Table V.

The PCR thermocycle profile was: 95°C, 52°C and 72°C, 30 sec. each step and 22 cycles when each actin gene was independently amplified and 20 cycles when the total actin genes or ubiquitin were amplified. PCR products were separated on 1% agarose gel, transferred onto a Hybond N⁺ nylon membrane using alkali denaturation and hybridized to ³²P-labeled PCR fragments of the respective transcripts, under the same conditions for the different PCR products. For probe labeling with ³²P-dATP equal amount of DNA template were used for each actin gene. Hybridizations were carried out using about 7×10^6 cpm. Hybridizations and washings were performed as described for the library screenings but at 65°C and in the same conditions for all the different blots. Autoradiograms were obtained using a Molecular Dynamics Phosphorimager (Sunnyvale, CA) and the quantification of the signal intensities was performed using the QUANT IMAGE TL software (Amersham). The expression level of each actin gene was quantified from the ratio between the intensity of the cDNA and the relative plasmid amplification signal, respectively. For each quantification the intensity of the amplification of the second plasmid dilution was used.

To quantify the expression level of the same actin gene in the different tissues the intensity of the amplification of the last cDNA dilution with a signal intensity above background was used. More in detail the quantification of *MtACT1* and *MtACT3* expression was done based on the intensity of the 1/25 dilution whereas the 1/5 dilution was used for *MtACT2* and *MtACT4*. To quantify the expression level of the different actin genes in the same tissue the intensity of the amplification of all the dilutions was used. Finally, the signal intensities in the reactions in which total actin or ubiquitin were amplified were also quantified to normalize for differences in the cDNA amount present in the different tissue samples.

DNA Manipulation and Plasmid Construction

Molecular biology protocols were conducted according to standard procedures (Sambrook and Russel, 2001) and all fragments generated by PCR were sequenced. The isolation of the *MtACT2* and *MtACT4* promoters has already been described (Mirabella et al., 2004). To isolate the 5' flanking region of *MtACT1* a 3.190 Kb fragment was amplified from the BAC Mth1-80L24, in combination with the following primers: 5' MtACT1p-B CGGGATCCAAATGGTAAGTTTGTTTAAATATG (underlined *Bam*HI site) and 3' MtACT1p-K GGGGTACCTTACCATTCAGTTCC (underlined *Kpn*I site). To isolate the 5' flanking region of *MtACT3* a 3.310 Kb fragment was amplified using the BAC Mth1-69I01 as template and the following primers: 5' MtACT3p-B CGGGATCCTGTTTTTGTCCCTTTTG (underlined *Bam*HI site) and 3' MtACT3p-K GGGGTACCTTAACCATTCCAGTTCC (underlined *Kpn*I site). The amplified fragments (*MtACT1p* and *MtACT3p*) were fused in-frame to the DsRED-E5 in the pTimer vector, using the *Bam*HI-*Kpn*I sites. Next, the

MtACT1::DsRED-E5 and the *MtACT3::DsRED-E5* fusions were excised *Bam*HI-*Eco*RI fragments and sub-cloned in the same sites of the pBinplus vector (van Engelen et al., 1995), containing the NOS terminator (*T-NOS*) between the *Eco*RI and the *Pac*I sites.

All the vectors used for plant transformation were transformed into the *Agrobacterium rhizogenes* strain MSU440, containing the helper plasmid pRiA4 (Sonti et al., 1995).

Plant Material, Growth Condition and Transformation

Medicago truncatula (Jemalong A17) root transformation was performed as previously reported (Stiller et al., 1997), with few modifications. Seeds, sterilized for 10 min with H₂SO₄ followed by 10 min with commercial bleach and extensively washed with sterile water, were germinated on a wet filter paper in a petri dish containing Fåhræus (Fåhræus, 1957) agar medium (0.9% agar; Daishin, Brunswick), supplemented with 0.75 mM Ca(NO₃)₂ and 0.7 mM CaCl₂. Subsequently, seeds were incubated in the dark at 4°C overnight and germinated upside down at 24°C for one more day. After removing the seed coat, seedlings were transferred to new Fåhræus agar (Fåhræus, 1957) plates and sealed for 2/3 with parafilm. The plates were incubated in a growth chamber in a vertical position with 16-h daylight period at 21°C and 70-80% relative humidity. Five days later the plantlets, having unfolded cotyledons and the first leaf, were inoculated with *A. rhizogenes*. The bacteria, grown for 2 d on agar plates, were streaked on the top of the hypocotyls area with a sterile curled glass pipette. Subsequently, the root was removed by cutting the hypocotyls region where the *A. rhizogenes* was streaked. In this way the freshly cut surface was inoculated. Plants were cultivated under the same conditions and, after five days, transferred to emergence medium containing: 1x SH-A salt (g liter⁻¹): KNO₃ (2.5), MgSO₄·7H₂O (0.4), NH₄H₂PO₄ (0.3), CaCl₂·2H₂O (0.2), MnSO₄·4H₂O (0.01), H₃BO₃ (5 × 10⁻³), ZnSO₄·7H₂O (1 × 10⁻³), KI (1 × 10⁻³), CuSO₄·5H₂O (2 × 10⁻⁴), NaMoO₄·2H₂O (1 × 10⁻⁴), CoCl₂·6H₂O (1 × 10⁻⁴), FeSO₄·7H₂O (0.015) and Na₂EDTA (0.02) ; 1x UM-C vitamins (Diaz, 1989; mg liter⁻¹) myoinositol (100), nicotinic acid (5), pyridoxine-HCl (10), thiamine-HCl (10), glycine (2); 1% sucrose, 3mM MES pH 5.8, 0.9% Daishin agar and 300 µg/ml cefotaxime. After 2-3 weeks the newly formed roots could be analyzed. Using this method we obtain a transformation efficiency of ~ 50%.

Transformed roots were selected scoring for green or red fluorescence, using a Leica (Wetzlar, Germany) MZFLIII stereo fluorescence microscope and further analyzed by Confocal Laser Scanning Microscopy (CLSM). For this purpose roots were mounted in liquid emergence medium under a glass coverslip.

Microscopy and G/R quantification

DsRED-E5 can be excited using the 488 nm and the 543 nm laser for the green and the red emitting form, respectively, or alternatively, due to the overlap of their excitation spectra, the single 488 wavelength can be used to excite both emitting forms. However, at this wavelength, the absorbance of the red form of DsRED-E5 is ~ 40% of the absorbance at 558 nm. We chose to excite DsRED-E5 with the single argon laser (488 nm) for two different reasons: first, using two different wavelengths to excite dsRED-E5 (488 nm and 543 nm) we observed a pronounced photobleaching (Mirabella et al., 2004), especially at the high laser power required to excite DsRED-E5 in root hairs. This photobleaching would have affected the fluorescence intensities measured after excitation with the second laser, by which the data would be unreliable. Second, the use of two lasers to excite DsRED-E5 could lead to variations in the fluorescence intensities due to laser instability over time. Therefore, we decided to use the single 488 nm wavelength to excite both the green and the red emitting form of DsRED-E5. The reduced red fluorescence intensity, due to the non optimal excitation of the red emitting form of DsRED-E5 will not invalidate our data, since G/R will be affected similarly in all stages. Using the single 488 nm laser for DsRED-E5 excitation, the broad emission spectrum of its green emitting form, that extends from 475 to 625 nm, causes a bleed-through in the red channel (emission: band pass 565-595 nm; Mirabella et al., 2004). Previously, we quantified this bleed-through as being the 15% of the fluorescence intensity measured in the green channel (Mirabella et al., 2004). Therefore, when G/R was calculated the intensity of the red channel was reduced by 15% of the intensity detected in the green channel. Moreover, also the background fluorescence, detected in untransformed roots, was subtracted from the signal detected in both the green and red channel.

Fluorescence microscopy was performed using a Zeiss LSM 510 CLSM implemented on an inverted microscope (Axiovert 100). Excitation was provided by the 488 nm Ar laser line, controlled by an acousto optical tuneable filter (AOTF). To separate excitation from emission and to divide the fluorescence emission into the green and red channels, two dichroic beam splitters were used. The HFT 488 dichroic beam splitter was used to reflect excitation and transmit fluorescence emission. A mirror was used to reflect the emitted fluorescence to the NFT 545 secondary beam splitter. Fluorescence reflected by the NFT 545 splitter was filtered through a 505-530 nm band pass filter, resulting in the green channel, whereas fluorescence transmitted by the NFT 545 splitter was filtered through a 565-590 nm band pass filter, resulting in the red channel. A Zeiss plan-neofluar 40× (N.A. 1.3) oil immersion objective lens was used for scanning. For detection of green and red fluorescence equal detection settings were used. For imaging root hairs the pinhole was fully open. To determine G/R, time series images were acquired. To quantify the fluorescence intensities, equally sized regions of interest were drawn in cytoplasmic rich regions of root hairs and the pixel intensities in these regions were determined using the Zeiss LSM 510 software

Acknowledgments

We would like to thank Dr. C. Albrecht for valuable comments concerning the RT-PCR analysis. R.M. was supported by a grant from the European Community TMR program FMRX CT 98-0239.

References

- An Y-Q, Huang S, McDowell JM, McKinney EC, Meagher RB (1996b) Conserved expression of the *Arabidopsis* ACT1 and ACT3 actin subclass in organ primordia and mature pollen. *Plant Cell* **8**: 15-30
- An Y-Q, McDowell JM, Huang S, McKinney EC, Meagher RB (1996a) Strong, constitutive expression of the *Arabidopsis* ACT2/ACT8 actin subclass in vegetative tissues. *Plant Journal* **10**: 107-121
- Baird WV, Meagher RB (1990) A complex gene superfamily encodes actin in petunia. *Embo Journal* **11**: 3223-3231
- Covitz PA, Smith LS, Long SR (1998) Expressed sequence tags from a root-hair-enriched *Medicago truncatula* cDNA library. *Plant Physiol* **117**: 1325-1332
- de Ruijter NCA, Bisseling T, Emons AMC (1999) Rhizobium Nod factors induce an increase in sub-apical fine bundles of actin in *Vicia sativa* root hairs within minutes. *Molecular Plant-Microbe Interact* **12**: 829-832
- Fåhræus G (1957) The infection of clover root hairs by nodule bacteria studied by a simple glass slide technique. *Journal of Genetic Microbiology* **16**: 374-381
- Feinberg A, Vogelstein B (1983) A technique for radiolabeling DNA restriction endonuclease fragments to high specific activity. *Anal. Biochem.* **132**: 6-13
- Fowler JE, Quatrano RS (1997) Plant cell morphogenesis: plasma membrane interaction with the cytoskeleton and cell wall. *Annu. Rev. Cell Dev. Bio.* **13**
- Gilliland LU, Kandasamy MK, Pawloski LC, Meagher RB (2002) Both vegetative and reproductive actin isoforms complement the stunted root hair phenotype of the *Arabidopsis* act2-1 mutation. *Plant Physiol.* **130**: 2199-2209
- Gloudemans T, Bhuvaneswari TV, Moerman M, Van Brussels AAN, Van Kammen A, Bisseling T (1989) Involvement of *Rhizobium leguminosarum* nodulation genes in gene expression in pea root hairs. *Plant Mol Biol* **12**: 157-167
- Gualtieri G, Kulikova O, Limpens E, Kim DJ, Cook DR, Bisseling T, Geurts R (2002) Microsynteny between Pea and *Medicago truncatula* in the SYM-2 region. *Plant Mol Biol* **50**: 225-235
- Hightower RC, Meagher RB (1985) Divergence and differential expression of soybean actin genes. *Embo Journal* **4**: 1-8
- Huang S, An Y-Q, McDowell JM, McKinney EC, Meagher RB (1996) The *Arabidopsis* ACT4/ACT12 actin gene subclass is strongly expressed in post-mitotic pollen. *Plant Journal* **10**
- Huang S, An Y-Q, McDowell JM, McKinney EC, Meagher RB (1997) The *Arabidopsis* ACT11 gene is strongly expressed in tissues of the emerging inflorescence, pollen and developing ovules. *Plant Mol. Biol.* **33**: 125-139
- Kandasamy MK, McKinney EC, Meagher RB (1999) The late pollen-specific actins in angiosperms. *Plant Journal* **18**: 681-691
- Kandasamy MK, McKinney EC, Meagher RB (2002) Functional Nonequivalency of Actin Isoforms in *Arabidopsis*. *Molecular Biology of the Cell* **13**: 251-261

- Mascarenhas JP** (1993) Molecular mechanism of pollen tube growth and differentiation. *Plant Cell* **5**: 1313-1314
- McDowell JM, An Y-Q, McKinney EC, Huang S, Meagher RB** (1996b) The Arabidopsis *ACT7* gene is expressed in rapidly developing tissues and responds to several external stimuli. *Plant Physiol.* **111**: 699-711
- McDowell JM, Huang S, McKinney EC, An Y-Q, Meagher RB** (1996a) Structure and evolution of the actin gene family in *Arabidopsis thaliana*. *Genetics* **142**: 587-602
- McElroy D, Rothenberg M, Reece KS, Wu R** (1990) Characterization of the rice (*Oryza sativa*) actin gene family. *Plant Mol Biol* **15**: 257-268
- McLean M, Eubanks S, Meagher RB** (1990b) Tissue specific expression of divergent actins in soybean root. *Plant Cell* **2**: 335-344
- McLean M, Gerats AGM, Baird WV, Meagher RB** (1990a) Six Actin Gene Subfamily Map to Five Chromosome of *Petunia hybrida*. *Journal of Heredity* **81**: 341-346
- Meagher RB, McKinney EC, Kandasamy MK** (1999) Isovariant dynamics expands and buffers the responses of complex systems: The diverse plant actin gene family. *Plant Cell* **11**: 1-12
- Miller DD, de Ruijter NCA, Bisseling T, Emons AMC** (1999) The role of actin in root hair morphogenesis: studies with lipochito-oligosaccharide as a growth stimulator and cytochalasin as an acting perturbing drug. *The Plant Journal* **17**: 141-154
- Mirabella R, Franken C, van der Krogt GNM, Bisseling T, Geurts R** (2004) Use of the "Fluorescent Timer" DsRED-E5 as Reporter to Monitor Dynamics of Gene Activity in Plants. *Plant Physiol* **in press**
- Nam YW, Penmetsa RV, Endre G, Uribe P, Kim D, Cook DR** (1999) Construction of a bacterial artificial chromosome library of *Medicago truncatula* and identification of clones containing ethylene - response genes. *Theor. Appl. Genet.* **98**: 638-646
- Nick P** (1999) Signals, Motors, morphogenesis-the cytoskeleton in plant development. *Plant Biol* **1**: 169-179
- Pawlowski K, Kunze R, De Vries S, Bisseling T** (1994) Isolation of total, poly(A) and polysomal RNA from plant tissue. In SB Gelvin, RA Schilperoort, eds, In *Plant Molecular Biology manual*, Ed 2nd. Kluwer Academic Publishers, Dordrecht, The Netherlands, pp 1-13
- Ringli C, Baumberger N, Diet A, Frey B, Keller B** (2002) ACTIN2 Is Essential for Bulge Site Selection and Tip Growth during Root Hair Development of Arabidopsis. *Plant Physiology* **129**: 1464-1472
- Sambrook, Russel** (2001) *Molecular cloning: a laboratory manual*. Cold spring harbor, NY
- Schmidt A, Hall MN** (1998) Signaling to the actin cytoskeleton. *Annu. Rev. Cell Dev. Bio.* **15**: 305-334
- Sieberer B, Emons AMC** (2000) Cytoarchitecture and pattern of cytoplasmic streaming in root hairs of *Medicago truncatula* during development and deformation by nodulation factors. *Protoplasma* **214**: 118-127
- Sonti RV, Chiurazzi M, Wong D, Davies CS, Harlow GR, Mount DW, Singer ER** (1995) Arabidopsis mutant deficient in T-DNA integration. *Proc Natl Acad Sci U S A* **92**: 11786-11790
- Staehelein LA, Hepler PK** (1996) Cytokinesis in higher plants. *Cell* **84**
- Staiger CJ** (2000) Signaling to the actin cytoskeleton in plants. *Annu. Rev. Plant Physiol. Plant Mol. Biol.* **51**: 257-278
- Stiller J, Martirani L, Tupple S, Chian R, Chiurazzi M, Gresshoff PM** (1997) High frequency transformation and regeneration of transgenic plants in the model legume *Lotus Japonicus*. *Journal Experimental Botany* **48**: 1357-1365
- Tersikh A, Fradkov A, Ermakova G, Zaisky A, Tan P, Kajava AV, Zhao X, Lukyanov S, Matz M, Kim S, Weissman I, Siebert P** (2000) "Fluorescent Timer": Protein That Changes Color with Time. *Science* **290**: 1585-1588
- van Engelen FA, Molthoff JW, Conner AJ, Nap J-P, Pereira A, Stiekema WJ** (1995) pBINPLUS: an improved plant transformation vector based on pBIN19. *Transgenic Research* **4**: 288-290
- Williamson RE** (1993) Organelle movements. *Annu. Rev. Plant Physiol. Plant Mol. Biol.* **44**: 181-202

CHAPTER 4

Tight Regulation of ROP GTPase Expression is Required to Maintain Symbiosomes in *Medicago truncatula* Root Nodules

Abstract

Several processes occurring during nodule development in legumes may be controlled by ROP GTPases, such as tip growth of infection threads, endocytosis of bacteria in the plant cells and symbiosome development, considering the proposed vacuolar nature of these compartments. Here we analyzed the role of ROPs during nodule development.

In wild-type *M. truncatula* nodules *ROP* genes are expressed in the apical region of the nodule (encompassing the nodule meristem and few cell layers below it), whereas in Fix⁻ nodules, characterized by early senescence, *ROP*s are expressed through all the nodule cells. To determine the role of ROPs during nodule development, we overexpressed a *M. truncatula ROP* (*MtROP1*) in nodules under the control of a *Rhizobium* inducible promoter (*MtENOD12*) by *Agrobacterium rhizogenes*-mediated root transformation. *MtROP1* overexpression did not influence the infection process (i.e. infection thread formation/growth and bacterial release) but impaired symbiosome development. Nodules overexpressing *MtROP1* showed fewer non-elongated bacteroids per cell, persistence of the central vacuole and lack of fully infected cells. In more severe cases complete degradation of the nodule central tissue was observed. Electron microscopy analysis of these nodules showed that symbiosomes, arrested in early stages of development, fused giving rise to vacuole like structures in which bacteroids were degraded. This degradation ultimately involved all the infected nodule cells. These data, together with the *ROP* expression pattern in nodules, support the vacuolar nature of symbiosomes and suggest that the loss of the ability to down-regulate *ROP* expression is causative for the premature senescence that occurs in Fix⁻ nodules.

Rossana Mirabella, Elena Fedorova, Andrea Jahraus, Carolien Franken, René Geurts and Ton Bisseling

Introduction

The endosymbiosis of rhizobia and legumes results in the formation of root nodules. These are newly formed organs in which the bacteria are hosted in an intracellular manner (Brewin, 1991; Hirsch, 1992; Mylona et al., 1995; Brewin, 1996; Cohn et al., 1998). In such nodules the bacteria differentiate into, so-called bacteroids, that are able to fix nitrogen. At the start of nodule formation the rhizobia enter the plant by a newly formed tube-like structure, which is named infection thread. Infection threads are surrounded by a plant membrane and inside the thread the bacteria are imbedded in a matrix that is composed of plant and bacterial derived molecules. Infection threads are formed in root hairs and, subsequently, they grow towards the nodule primordia that have concomitantly been formed in the root cortex. When the infection threads reach the nodule primordia the bacteria are released into the plant cells (Brewin, 1991; Hirsch, 1992; Mylona et al., 1995; Brewin, 1996; Cohn et al., 1998). Although the mechanism of rhizobial uptake is poorly understood, it is assumed that it is related to endocytosis (Brewin, 1991). In herbaceous legumes, so-called infection droplets bud off from the infection thread and are surrounded by a single plant membrane, derived from the infection thread. The rhizobia enclosed by the plant membrane are named symbiosomes and this plant membrane is named symbiosomal or peribacteroid membrane (Roth and Stacey, 1989a). The symbiosomes divide and ultimately several thousand symbiosomes are present in an infected nodule cell. This proliferation requires a strict coordination of bacterial division and peribacteroid membrane synthesis by the plant. Small GTP binding proteins belonging to the Rab family and a membrane associated phosphatidylinositol-3-kinase are probably controlling the flow of vesicles to the growing symbiosomes (Cheon et al., 1993; Verma et al., 1994; Son et al., 2003). Further, it is possible that actin is involved in the targeting of these vesicles as networks of actin filaments surround each symbiosome (Davidson and Newcomb, 2001).

At the time of bacterial release into the plant cells, the peribacteroid membrane originates from the infection thread membrane, which is plasma membrane-like. Subsequently, as the symbiosomes divide the peribacteroid membrane extends by insertion of vesicles coming from the ER and the Golgi apparatus (Roth and Stacey, 1989b). However, when the symbiosomes mature, the symbiosome membrane obtains characteristics of the vacuolar membrane (Mellor, 1989; Verma and Hong, 1996). This is exemplified by the presence of nodulins in the peribacteroid membrane, that are nodule specific forms of tonoplast proteins (e.g. nodulin26; Miao and Verma, 1993). Moreover, the symbiosomal fluid contains many host derived vacuolar proteins, such as α -mannosidase (Kinnback et al., 1987), cysteine protease (Kardailsky and Brewin, 1996; Vincent and Brewin, 2000; Vincent et al., 2000), acid trehalase (Mellor, 1988) and protease inhibitors (Garbers et al., 1988; Manen et al., 1991). Thus, symbiosomes may be related to vacuolar structures but they remain small separate units that do not fuse to a large lytic compartment (Marty, 1999).

Although nodule formation is a unique process, it is also clear that most steps are derived from mechanisms that are more ancient in evolution and are also used in non-symbiotic processes. Therefore, it is probable that molecular mechanisms controlling symbiotic developmental steps will use regulatory elements that are also used in non-symbiotic development (Gualtieri and Bisseling, 2000). Recent studies on plant Rho-like GTPases show that these molecular switches are involved in the control of processes that share similarity with several steps occurring during nodule formation (see below).

Rho GTPases are ubiquitous GTP binding proteins of the Ras superfamily of monomeric G-proteins. They act as molecular switches, cycling between GTP-bound (on) and GDP-bound (off) states. In animals, plants, fungi and yeast, they have emerged as central components in signaling pathways. Once activated by extracellular stimuli, Rho GTPases control a variety of key cellular processes, including actin cytoskeleton and microtubules rearrangements, exocytosis and endocytosis, organelle biogenesis, cell wall synthesis, cell cycle progression, establishment of cell polarity and activation of the machinery required for reactive oxygen production (Ridley, 1995; Hall, 1998; Arellano et al., 1999; Ridley, 2000; Erickson and Cerione, 2001; Settleman, 2001; Wittmann and Waterman-Storer, 2001). In animal and yeast, the Rho GTPases family includes three subgroups termed RAC, CDC42 and RHO, each of them having multiple distinct roles in controlling different cellular functions.

Plants have evolved a unique subfamily of Rho GTPases named ROPs (for Rho related GTPases from plants) by some researchers (Zheng and Yang, 2000) or RACs by others (Winge et al., 1997). Plant ROPs share the highest similarity with mammalian Rac GTPases and are members of rather large gene families in plants like *Arabidopsis*, pea, cotton and rice (Valster et al., 2000; Zheng and Yang, 2000). The *Arabidopsis* ROP family, for example, consists of 11 members. Based on phylogenetic analysis, plant ROPs can be placed into four distinct groups (Zheng and Yang, 2000). These 4 groups seem to be functionally different (Yang, 2002). Group IV contains the majority of the *Arabidopsis* ROP genes. Three of the ROP genes of this group (*AtROP1*, *AtROP3* and *AtROP5*) are expressed in pollen tubes and, at least 2 of them (*AtROP1* and *AtROP5*), are required for pollen tube tip growth (Kost et al., 1999; Li et al., 1999). The other three members (*AtROP2*, *AtROP4* and *AtROP6*) are expressed in vegetative cells and are shown to be involved in tip growth of root hair (Molendijk et al., 2001; Fu et al., 2002; Jones et al., 2002) as well as expansion of cells in various tissues (*AtROP2*; Fu and Yang, 2001; Li et al., 2001; Fu et al., 2002). Group II ROPs seem to be involved in stress responses as overexpression of ROP genes belonging to this class leads to altered ABA responses (*AtROP9/10*) or H₂O₂ production (*OsRAC1*); (Kawasaki et al., 1999; Yang, 2002; Zheng et al., 2002). Group I contains only one member (*AtROP8*), whose function is not known; group III ROPs from cotton (*GhRAC9/GhRAC13*) are involved in H₂O₂ production (Potikha et al., 1999).

Further, ROP proteins, although unclear to which group they belong, have been shown to be located at the tonoplast of developing vacuoles but are absent from the central vacuole. This

suggests that ROPs may participate in the signaling pathway that regulates vacuole development or functioning (Lin et al., 2001).

Several processes that occur during nodulation are candidate to be regulated by ROP proteins. Examples are the rapid change in the actin configuration that is induced in root hairs (de Ruijter et al., 1999; Miller et al., 1999), the putative tip growth of infection threads (Dart, 1974), the formation of infection droplets by endocytosis, the formation and functioning of an actin skeleton around the symbiosomes and the formation or maintenance of symbiosomes, considering their putative vacuolar nature.

We tested whether ROPs can regulate steps in nodulation by overexpressing *ROPs* in the model legume *Medicago truncatula*, focusing on the role of ROP during nodule development. For these studies we selected a *M. truncatula* ROP (*MtROP1*) that is related to the *Arabidopsis* group IV ROPs. This *MtROP1* is the most abundantly expressed member of this group in vegetative organs and is also expressed in nodules. We overexpressed *MtROP1* under the control of a *Rhizobium* inducible promoter (*MtENOD12* promoter) and analysed the nodule structure by light and electron microscopy. We show that *MtROP1* overexpression in nodules induces symbiosome fusion and degradation, followed by lysis of the host cells.

Results

Medicago truncatula ROPs

To isolate cDNA clones encoding *M. truncatula* ROP GTPases, we screened a *M. truncatula* root hair/root tip cDNA library (Covitz et al., 1998), using as a probe the *Pisum sativum* *PsRHO1* gene (Yang and Watson, 1993). Twelve positive colonies were randomly selected and the corresponding cDNAs were sequenced. These clones appeared to be cDNAs corresponding to 2 different *ROP* genes, designated as *MtROP1* and *MtROP2*. Full size cDNA clones of both ROPs had a single open reading frame of 197 amino acid residues, a 5' and 3' untranslated region (UTR) of about 180 bp and 200-300 bp, respectively, and a long polyA tail (data not shown).

Multiple alignment of various plant ROP proteins (Fig.1A) showed that *MtROP1* and *MtROP2* contain all the conserved regions that are critical for nucleotide binding and GTPase activity. These regions are underlined in Fig. 1A. Also all the residues or motifs that are unique of ROP proteins are present (arrows in Fig.1A). These include the effector domain (residues 29-49, including the ROP specific amino acid residues T30, T33, F43 and V48) and the asparagine residues N42, representing the site for specific ADP-ribosylation by the *Clostridium botulinum* C3 toxin ADP-ribosyl transferase. Moreover, a prenylation motif with the consensus sequence CaaX (where C is Cys, a is usually an aliphatic residue and X one of several residues; two-headed arrow in Fig.1A) and a polybasic region were present at the C-terminus of both *MtROP1* and *MtROP2* (Fig. 1A). *MtROP1* and *MtROP2* also have a

10 amino acid long region (128-137), which is the so-called “insert region” typical of ROP GTPases (boxed in Fig.1A). MtROP1 and MtROP2 differ only by 5 amino acids and are 97% identical (Fig. 1A).

A

| | | | | | |
|--------|---------------------|----------------------|------------------------------------|-----------------------------|----------------------------|
| MtROP1 | MSASRFIKCV | TVGDGAVGKT | CLLISYTSNT | FPTDYVPTVF | DNFSANVVV |
| MtROP2 | MSASRFIKCV | TVGDGAVGKT | CLLISYTSNT | FPTDYVPTVF | DNFSANVVVN |
| PsRH01 | MSASRFIKCV | TVGDGAVGKT | CLLISYTSNT | FPTDYVPTVF | DNFSANVVVN |
| AtROP1 | MSASRFV K CV | TVGDGAVGKT | CLLISYTSNT | FPTDYVPTVF | DNFSANVVVN |
| | | | | | |
| MtROP1 | GSTVNLGLWD | TAGQEDYNRL | RPLSYRGADV | FILAFSLISK | ASYENVSKK |
| MtROP2 | GS I VNLGLWD | TAGQEDYNRL | RPLSYRGADV | FILAFSLISK | ASYENVSKKW |
| PsRH01 | GSTVNLGLWD | TAGQEDYNRL | RPLSYRGADV | FILAFSLISK | ASYENVSKKW |
| AtROP1 | GSTVNLGLWD | TAGQEDYNRL | RPLSYRGADV | FILAFSLISK | ASYENVSKKW |
| | | | | | |
| MtROP1 | IPELKHYAPG | VPIILVGTKL | DLRDDKQFFV | DHPGAVPITT | AQGEELRKLI |
| MtROP2 | IPELKHYAPG | VPIILVGTKL | DLRDDKQ F C I | DHPGAVPITT | AQGEELRKLI |
| PsRH01 | IPELKHYAPG | VPIILVGTKL | DLRDDKQFFV | DHPGAVPITT | AQGEELRKLI |
| AtROP1 | IPELKHYAPG | VPI V LVGTKL | DLRDDKQ F I | DHPGAVPITT | AQGEELRK Q I |
| | | | | | |
| MtROP1 | NAPAYIECSS | KSQQNVKAVF | DAAIRVVLQP | PKQKKKKSKA | QKACSIL |
| MtROP2 | NAPAYIECSS | KSQ E ENVKAVF | DAAIRVVLQP | PKQKKKK N K A | QKACSIL |
| PsRH01 | NAPAYIECSS | KSQQNVKAVF | DAAIRVVLQP | PKQKKKKSKA | QKACSIL |
| AtROP1 | G APTYIECSS | K TQENVKAVF | DAAIRVVLQP | PKQKKKKSKA | QKACSIL |

B

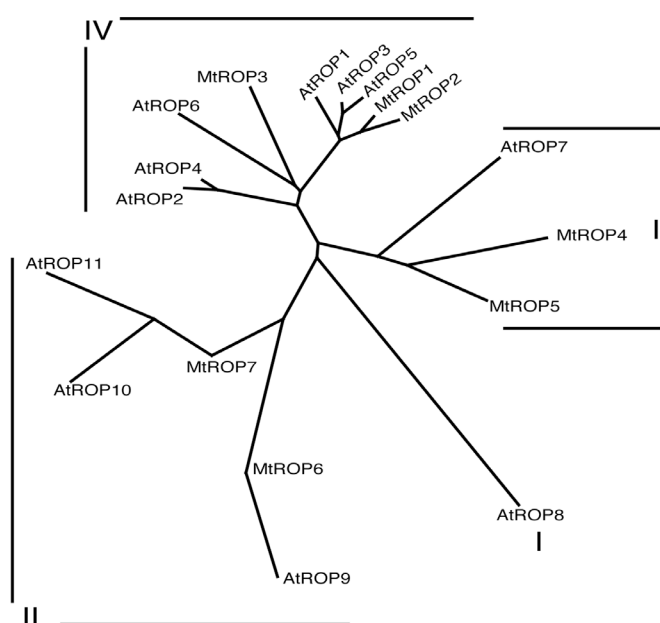


Figure 1. A) Alignment of the deduced amino acid sequence of the *M. truncatula* MtROP1 and MtROP2 with homologous ROPs from other species. Highly conserved regions of the GTPase superfamily are indicated with lines above the sequence alignment and the ROP specific residues are indicated by arrow heads. The “effector region” is boxed and the isoprenylation motif (CAAX) is indicated by two-headed arrow. Mt, *Medicago truncatula*; Ps, *Pisum sativum*; At, *Arabidopsis thaliana*. The sequences used for this analysis are from the Gene Bank data base. **B)** Phylogenetic analysis and classification of *M. truncatula* and *Arabidopsis* ROPs. MtROP6 and MtROP7 are partial sequences. ROP groups I to IV are indicated.

To search for other *M. truncatula* ROPs, we used the *MtROP1* and *MtROP2* sequences to screen the *M. truncatula* database, containing 175701 ESTs (January, 2004) from 34 different libraries. Sixty-one ESTs had a high homology to *MtROP1/2* and corresponded to 8 different *MtROP* genes. The result of the blast search is summarized in Table 1, in which also the occurrence, in each library group, of the cDNAs corresponding to the 8 different *MtROP* genes is indicated. From this analysis, it appeared that *MtROP1* occurred most frequently in the ESTdb, encompassing almost 40% of all the ROPs present in the libraries (Table 1), whereas *MtROP6*, *MtROP8* and *MtROP7* only occurred with 2, 2 and 1 ESTs, respectively (Table 1). *MtROP1*, as well as *MtROP3*, was expressed in all the vegetative tissues analyzed, including nodules. Moreover, *MtROP1* seemed to be slightly down regulated in nodules compared to roots, since the *MtROP1* clones represented 0.18‰ and 0.10 % of all the ESTs isolated from roots and nodules, respectively. Interestingly, the 2 nodule *MtROP1* ESTs arose from 1 month old nodules. Besides *MtROP1* and *MtROP3*, three other *ROP* genes (*MtROP5* and *MtROP6* and *MtROP8*) were also expressed in nodules (Table 1). Most of the *MtROP6* clones were isolated from nodule libraries (2 out of 3) whereas *MtROP8* appeared to be nodule specific.

We were interested in group IV ROPs, since ROPs belonging to this class control processes that also occurs during nodulation. To identify which of the *M. truncatula* ROPs belonged to the group IV, we compared their sequences with those of the 11 AtROPs (Fig. 1B). MtROP8 was not included in this analysis since only a small part of the deduced protein sequence was available. MtROPs could be arranged in clusters that corresponded to the AtROP groups II, III and IV. MtROP6 and MtROP7 had the highest homology with group II AtROP GTPases, MtROP4 and MtROP5 were most similar to group III AtROPs, whereas MtROP1, MtROP2 and MtROP3 had the highest homology with the group IV AtROPs (Fig. 1B). These AtROPs are involved both in the control of tip growth, in root hairs and pollen tubes, and cell expansion, suggesting a role for MtROP1, MtROP2 and MtROP3 in similar processes. MtROP1 and MtROP2 shared the highest homology with AtROP1 and AtROP5 (96% and 95% respectively), whereas MtROP3 had the highest homology with AtROP6 (89%). Arabidopsis group IV ROPs can be divided in “reproductive” and “vegetative” GTPases: *AtROP1*, *AtROP3* and *AtROP5* are expressed in pollen tubes, whereas *AtROP2*, *AtROP4* and *AtROP6*, are expressed in all vegetative tissues. It is not clear whether the 3 class IV *MtROPs* are expressed in pollen tubes or whether pollen specific MtROPs exist that have not yet been identified, since the database does not contain libraries from Medicago pollen. Although MtROP1 shares the highest homology with reproductive group IV AtROPs, it is the most abundantly expressed MtROP in vegetative tissues. Furthermore, it is expressed in nodules and therefore we decided to focus on the role of MtROP1 during nodule development.

Table 1. *MtROP* gene expression analyzed by Virtual Northern blot

| Origin of banks | No. of banks | No. of ESTs | <i>ROP1</i> | <i>ROP2</i> | <i>ROP3</i> | <i>ROP4</i> | <i>ROP5</i> | <i>ROP6</i> | <i>ROP7</i> | <i>ROP8</i> |
|-----------------|--------------|-------------|--------------|--------------|--------------|-------------|-------------|-------------|--------------|-------------|
| Roots various | 9 | 32694 | 0.18 (6) | 0.12 (4) | 0.09 (3) | 0 | 0.06 (2) | 0 | 0 | 0 |
| Roots Mycor. | 3 | 17601 | 0.28 (5) | 0 | 0 | 0 | 0 | 0 | 0 | 0 |
| Roots rhizobium | 3 | 11600 | 0 | 0 | 0 | 0 | 0 | 0 | 0 | 0 |
| Nodules | 5 | 20525 | 0.10 (2) | 0 | 0.10 (2) | 0 | 0.10 (2) | 0.10 (2) | 0 | 0.10 (2) |
| Stems | 1 | 10336 | 0 | 0 | 0 | 0.19 (2) | 0.19 (2) | 0 | 0 | 0 |
| Leaves various | 4 | 22287 | 0.04 (1) | 0.13 (3) | 0.13 (3) | 0 | 0.04 (1) | 0 | 0 | 0 |
| Leaves fungal | 1 | 5987 | 0.17 (1) | 0 | 0 | 0.17 (1) | 0 | 0 | 0 | 0 |
| Leaves insect | 1 | 9892 | 0 | 0.10 (1) | 0 | 0 | 0 | 0 | 0 | 0 |
| Plantlets | 2 | 13438 | 0.22 (3) | 0 | 0 | 0 | 0 | 0 | 0 | 0 |
| Flowers | 2 | 7813 | 0.13 (1) | 0 | 0.13 (1) | 0.13 (1) | 0 | 0.13 (1) | 0 | 0 |
| Seeds/Pods | 5 | 15183 | 0.13 (2) | 0.20 (3) | 0.07 (1) | 0.07 (1) | 0 | 0 | 0 | 0 |
| Cell cultures | 1 | 9065 | 0.11 (1) | 0 | 0 | 0 | 0 | 0 | 0.11 (1) | 0 |
| Total | 37 | 176421 | 0.12 (22) | 0.06 (11) | 0.06 (10) | 0.03 (5) | 0.04 (7) | 0.02 (3) | 0.006 (1) | 0.01 (2) |

Table 1. *MtROP1* and *MtROP2* sequences were used for a blast search of the TIGR EST database. The resulting ESTs encoding for *ROP* genes were classified, based on the sequence, in 8 classes from *MtROP1* to *MtROP8*. For each class the number of ESTs present in each library group is indicated as expressed for 1000 ESTs of the total number of ESTs in that library group. The absolute number of ESTs is also indicated between brackets. The EST clusters for each *MtROP* gene were: *MtROP1*: TC 86339; *MtROP2*: TC 87204; *MtROP3*: TC 78546; *MtROP4*: TC 79983; *MtROP5*: TC 88346; *MtROP6*: TC 90907; *MtROP7*: BF 647926; *MtROP8*: TC93339. For more details on the library groups see Material and Methods.

MtROP expression in nodules

To confirm that *MtROP1* is expressed in nodules we compared the expression of this gene in roots and nodules by RT-PCR. mRNA isolated from *M. truncatula* total roots and nodules 14 days after inoculation (d.p.i.) with *Sinorhizobium meliloti* (2011), was reverse transcribed and the cDNA was used as template for PCR. Specific *MtROP1* primers were designed in the 3' UTR of the gene and the ubiquitously expressed *ACTIN* genes were chosen as control. Amplified fragments were hybridized with an *MtROP1* specific probe at high stringency. As shown in Fig. 2A, *MtROP1* transcript was present, at about the same level, in roots as well as in nodules. We could not detect a down-regulation of *MtROP1* expression in nodules, as suggested by the analysis of the database. This could be due to the fact that RT-PCR is not suited to detect a two-fold difference in expression levels.

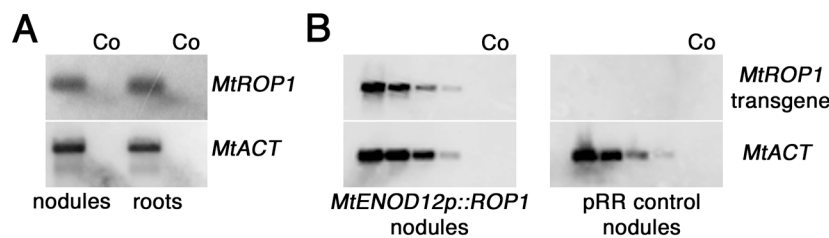


Figure 2. A) RT-PCR analysis of *MtROP1* mRNA in *M. truncatula* roots and nodules 14 d.p.i.. B) RT-PCR analysis of mRNA from nodules (12-14 d.p.i.) transformed with the pRR vector and the *MtENOD12p::MtROP1* fusion, respectively. Primers specifically amplified the transgene. Actin RT-PCR was included as control. N, nodules; R, roots; Co, control in which no reverse transcriptase was added to the cDNA synthesis reaction, to verify absence of genomic DNA contamination

To determine in which nodule cells *MtROPs* were expressed we performed *in situ* hybridization on longitudinal section of 14 days old *M. truncatula* nodules. These are indeterminate nodules and, therefore, the tissues are of graded age with the youngest cells near the apical meristem and the oldest cells close to the root attachment point. The central tissue has been divided into the following zones: the meristem (I), located at the nodule apex, is followed by the infection zone (zone II), in which bacteria are released from the infection threads and division and differentiation occurs. The infection zone is followed by the fixation zone (zone III). The transition of infection zone into fixation zone can be easily identified since the start of the fixation zone is marked by the appearance of amyloplasts (arrowhead in Fig. 3A). A more detailed description of nodule cytology will be given in the next paragraph. Nodule sections were hybridized with a probe corresponding to the *MtROP1* coding region. This region is highly conserved and, therefore, not specific for *MtROP1*. Nodules showed the most intense hybridization signal in the meristem and in a few cell layers below it (distal part of zone II; Fig. 3A and 3B). In the proximal part of zone II and in zone III *MtROP* expression is not above the background (Fig. 3A and 3B). Due to the highly conserved coding region of the different *MtROP* genes, this pattern is most likely caused by

hybridization to mRNAs of the different *MtROP* genes expressed in nodules, including *MtROP1*.

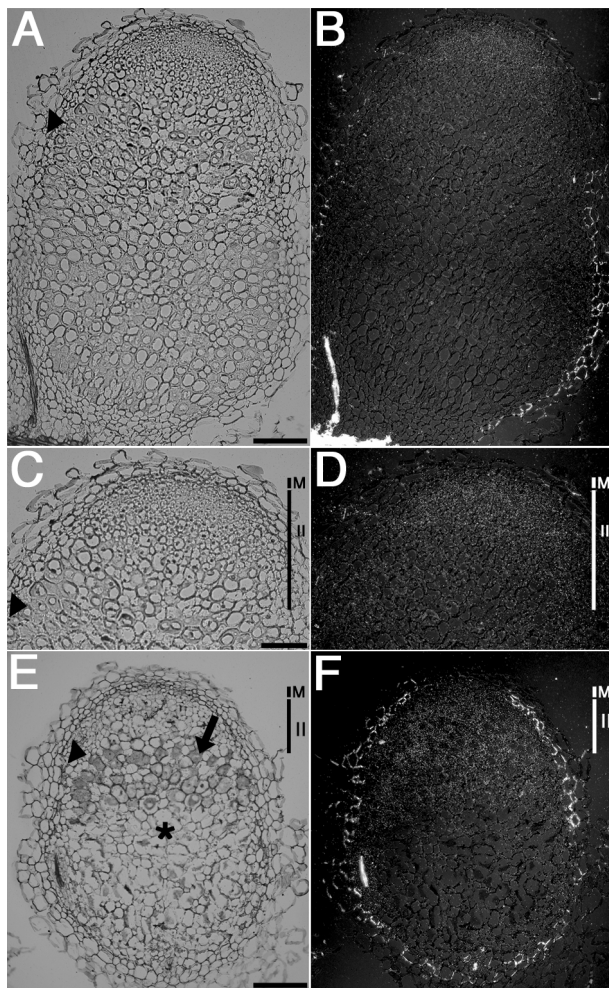


Figure 3. Expression of *MtROP* genes in *M. truncatula* wild-type and *Fix⁻* nodules by *in situ* hybridization; A) and C) bright field B) and D) epipolarisation images of wild-type nodules (14 d.p.i.) hybridized with ³⁵S-UTP labeled *MtROP1* probes. A and B are a composite of two images. D) and E) bright field and epipolarisation images, respectively, of *Fix⁻* nodules (10 d.p.i.) hybridized with ³⁵S-UTP labeled *MtROP1* probes. Silver grains appear as green dots. In D, arrow, fully infected cells; *, degraded cells. Arrowhead indicates the cell layer in which starch accumulation starts. M; meristem; II; zone II region.

Bar = 200 µm. (Color figure, see appendix).

Effect of MtROP1 overexpression on nodule development

To determine the function of *MtROP1* during nodule formation, we generated transgenic roots that overexpressed the wild-type *MtROP1*. In addition, constitutively active (CA) and dominant negative (DN) forms of *MtROP1* were also introduced (*Mtrop1* G15V and *Mtrop1* T20N, respectively). We decided to express *MtROP1* in a broader region than the region where the endogenous gene is expressed. For this purpose we selected the promoter of the early nodulin gene *MtENOD12* as it is known to be expressed in a major part of zone II (Pichon et al., 1992). To compare the expression patterns of *MtENOD12* and *MtROPs* we performed *in situ* hybridizations on nodule longitudinal sections, using a *MtENOD12* sense probe (Fig. 4). *MtENOD12* was expressed in zone II till 3-4 cell layers above the start of zone III (Fig. 4A) and was absent in the nodule meristem (asterisk in Fig. 4A). This expression pattern is similar to that reported by Pichon et al., (1992) and is markedly larger than the region where *MtROP* genes are expressed (compare Fig. 3C and D with Fig. 4A

and B). This indicates that overexpression of *MtROP1* under the control of the *MtENOD12* promoter will lead to expression of *MtROP1* in the proximal cell layers of zone II in which normally the gene is not expressed. *MtENOD12p::GUS* expression was shown to be similar to that of the endogenous *MtENOD12* gene. The GUS activity in nodules (10-14 d.p.i.) formed on *Agrobacterium rhizogenes* (MSU 440) transformed roots was restricted to zone II (data not shown). In general the *ENOD12* promoter is not active in non symbiotic-tissues, but in roots in which the transgene is expressed at a high level in nodules the GUS activity could also be detected in root tips and at the site of lateral root emergence (data not shown). In other experiments we used constitutively active promoters to overexpress *MtROP* genes. However, we failed to generate transgenic roots (data not shown). Therefore, the use of a *S. meliloti* inducible promoter also bypassed this problem.

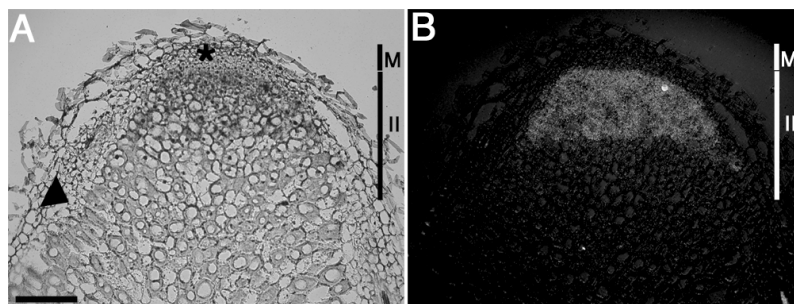


Figure 4. Expression of the *ENOD12* gene in *M. truncatula* nodules (14 d.p.i.) by *in situ* hybridization. A) bright field and B) epipolarisation images of wild-type nodules (14 d.p.i.) hybridized with ^{35}S -UTP labeled *MtENOD12* probe. Silver grains appear as black or green dots, respectively. M; meristem; II; zone II region. *, shows absence of expression in the nodule meristem; Arrowhead, indicates the cell layer in which starch accumulation starts. Bar = 200 μm . (Color figure, see appendix).

Transformed roots were induced on *M. truncatula* by *A. rhizogenes*, containing pRedRoot (pRR) in which one of the three ROP constructs, *MtENOD12p::MtROP1/CA/DN*, was cloned or the empty pRR vector, respectively. This pRR vector contained *AtQ10p::DsRED* that is constitutively active and can be used as vital fluorescent reporter to select transgenic roots (Limpens et al., 2003). Under our conditions 10-60% of the roots that are formed express *DsRED* and almost all the *DsRED* expressing roots are co-transformed with the transgene of interest (data not shown).

First we determined whether the *MtROP1* transgene was expressed in the nodules transformed with the *ENOD12p::MtROP1* fusion. For this purpose, transformed roots were inoculated with *S. meliloti* and nodules, from *DsRED* expressing control and *MtENOD12p::MtROP1* roots were harvested 12-14 d.p.i. RNA was extracted and used for a semi-quantitative RT-PCR analysis, using transgene specific primers. As shown in Fig. 2B transgene expression could be detected only in the *MtENOD12p::MtROP1* nodules.

Nodules on *DsRED* expressing control roots and *MtENOD12p::MtROP1* transformed roots from 50 different plants, for each construct, were compared. Control and *MtENOD12p::MtROP1* expressing roots had the same number of nodules, suggesting that

the early stages of nodule development were not affected by expression of *MtENOD12p::MtROP1*. Moreover, nodules on *MtENOD12p::MtROP1* transformed roots microscopically could not be distinguished from control nodules nor by their size, shape or position at the root. To further investigate the possible effect of overexpression of *MtROP1*, nodules were examined by light microscopy. Twenty nodules, from various DsRED expressing roots, were harvested from control and *MtENOD12p::MtROP1* plants. The results described were reproducibly obtained in three independent experiments. Control nodules showed the zonation that is typical of indeterminate nodules (Fig. 5A). At the apex the meristematic zone (I) is found which contains small cytoplasmic rich cells that do not contain infection threads nor released bacteria (Fig. 5B). This zone is followed by the infection zone (II). In the distal part of this zone bacteria are released from the infection threads in the host cells (Fig. 5B). Subsequently, the symbiosomes divide and the rhizobia start to elongate. The latter is visible at the LM level as elongated bacteroids can be distinguished from the rhizobia shortly after the release from the infection thread that are short rods and resemble free living bacteria (Fig. 5C). Therefore, short rod-like bacteroids can be observed only in two to three cell layers of control nodules. Finally, in the nitrogen-fixing zone (III), located at the proximal part of the nodule, the vacuoles have almost completely disappeared and the infected cells are fully packed with elongated bacteroids (Fig. 5D). In older nodules (4-6 weeks p.i.) a fourth region occurs, at the base of the nodule, in which senescence takes place (data not shown). This is characterized by bacteroid degradation and lysis of the host cells.

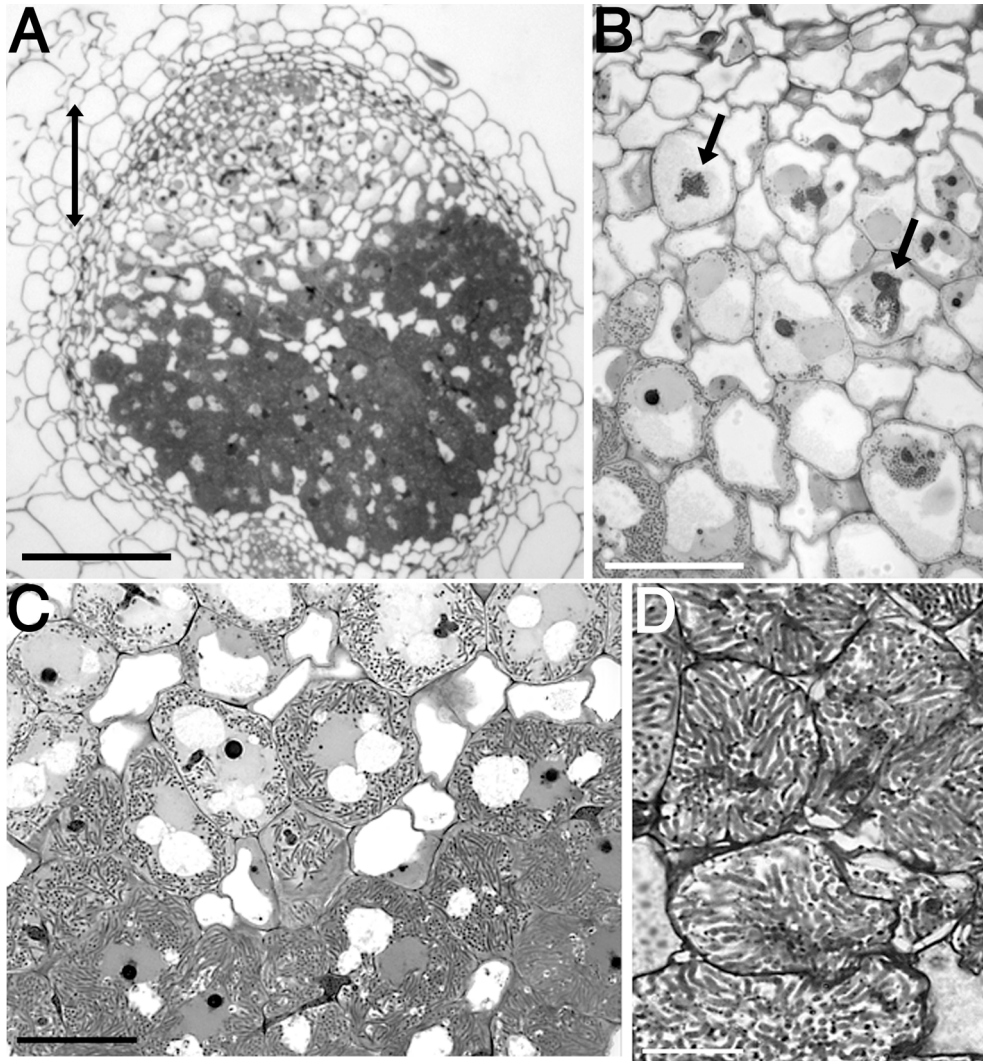


Figure 5. Light micrographs of *M. truncatula* nodules containing the pRR vector (control).

A) longitudinal section of a nodule 12 d.p.i.; Two-headed arrow indicates the cell layers in which the number of infection threads was determined; **B)** part of the meristem and distal zone II with infection threads (arrow) releasing bacteria; **C)** proximal zone II with appearance of elongated bacteroids; **D)** zone III cells. The bar corresponds in panel A to 500 µm, in panel B and D to 50 µm, in panel C to 100 µm.

In contrast to control nodules, about 50% of the *MtENOD12p::MtROP1* nodules showed an aberrant zonation of the central tissue. Based on the severity of the phenotype these nodules could be divided in three different groups. First a detailed description of the nodules with the weaker phenotype will be given, followed by the analysis of the other two groups.

In the least disturbed nodules (type 1) the zones from the apex of the nodule to the root attachment point seem to represent subsequent stages of development and the nodule cells are alive. In these nodules the meristem had already disappeared and the most distal zone of the central tissue resembles somehow zone II (Fig. 6A). The efficiency of the infection process in control and *MtROP1* overexpressing nodules was studied by counting the number of infection threads. The analysis was done in the cell layers representing the proximal zone

II in control nodules (about 5 cell layers; arrow in Fig. 5A) and in cell layers at a similar position in *MtENOD12p::MtROP1* nodules (arrow in Fig. 6A, Fig. 7A and C), using three median longitudinal sections from 5 control as well as 5 *MtENOD12p::MtROP1* nodules.

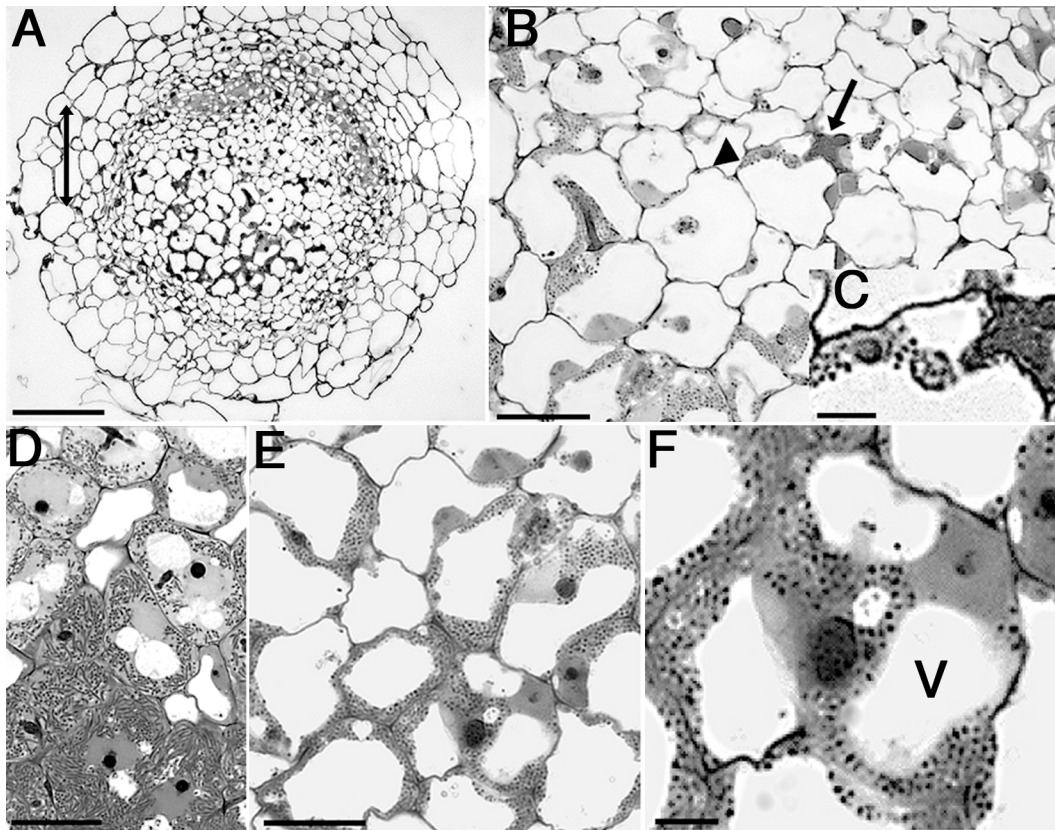


Figure 6. Light micrographs of *M.truncatula* nodules containing the *MtENOD12::MtROP1* fusion (type 1). **A)** longitudinal section of a nodule 12 d.p.i.; Two-headed arrow indicates the cell layers in which the number of infection threads was determined; **B)** magnification of the distal part of the nodule. Arrow; infection threads and arrowhead; bacteria released from the infection thread; **C)** magnification of the region indicated by arrow in 6B; **D)** see Fig. 5C; **E)** magnification of the proximal part of the nodule. Note the absence of elongated bacteroids; **F)** magnification of 6E. V = vacuole. The bar corresponds in panel A to 500 μm , in panel B, D and E to 100 μm , in panel C and F to 10 μm .

The average number of infection threads per section was higher in *MtENOD12p::MtROP1* than in control nodules (17.6 ± 5.5 ($n = 22$) versus 11 ± 3 , ($n = 18$) $p < 0.001$, per section, respectively). Moreover, these infection threads were releasing bacteria into the host cells in wild-type as well as in *MtROP1* overexpressing nodules (arrowhead in Fig. 6C). Therefore these data showed that the infection process, *i.e.* infection thread formation and bacterial release, was not impaired in *MtENOD12p::MtROP1* nodules. Nevertheless, in type 1 *MtROP1* overexpressing nodules, infected cells throughout the central tissue, both in the proximal and in the distal part of the nodule, contained only a few short rod-shaped bacteroids (Fig. 6B and D). Bacteroids with a similar morphology were found only in two cell layers of the distal part of zone II in control nodules (compare Fig. 6D and 6A, E). Further, the bacteroids only occurred at the periphery of the cells and a large central vacuole

remained present (Fig. 6E). No zone III comparable to that present in control nodules, with cells fully packed with elongated bacteroids (Fig. 5D), was observed in type 1 *MtENOD12p::MtROP1* nodules. Therefore, these data suggested that *MtROP1* overexpression could impair bacteroid division and development into elongated forms.

In the most disturbed nodules (type 2) successive stage of development can still be distinguished but, in contrast to the type 1 nodule, only few cells in the apical part of the nodule retained their integrity and the rest of the infected cells appeared to have lost their cytoplasm (Fig. 7A). These cells in fact were dead and filled with membranes most likely of plant and bacterial origin (Fig. 7B). In addition, several bacteria were present in these, having a similar size as free living rhizobia (Fig. 7B) and most likely representing a saprophytic colonization of the nodule empty cells, as already described for senescent cells in *M. truncatula* wild-type nodules (Timmers et al., 2000). Considering the presence of dead cells, type 2 nodules most likely represents a later stage of development than type 1 nodules.

In addition to the above described nodules occasionally “chimeric” nodules are formed (type 3) of which an example is shown in Fig. 7C. The apical part of these nodules, just below the meristem (more distal region of zone II), contains zones which are similar to type 2 nodules, including dead cells filled with remnants of bacteroids and membranes (arrows in Fig. 7D). However, in these nodules the proximal cells are similar to those of control nodules and are fully packed with elongated bacteroids, although they still retained a rather large central vacuole (Fig. 7C). To better understand the phenotype observed in these nodules, it should be kept in mind that the *MtENOD12* promoter is only active in zone II. Although we did not determine the stability of *MtROP1*, it seems probable that in some cases nodule cells can be rescued when they develop into zone III cells and the *MtENOD12p::MtROP1* transgene is no longer active.

The phenotypes described above for *MtENOD12p::MtROP1* nodules were also observed in about 50% of the nodules overexpressing *CA-Mtrop1* (data not shown), whereas no phenotype was observed in nodules that overexpress *DN-Mtrop1* (data not shown), confirming that the phenotypic alteration observed in the *MtENOD12p::MtROP1* nodules are caused by *MtROP1* overexpression.

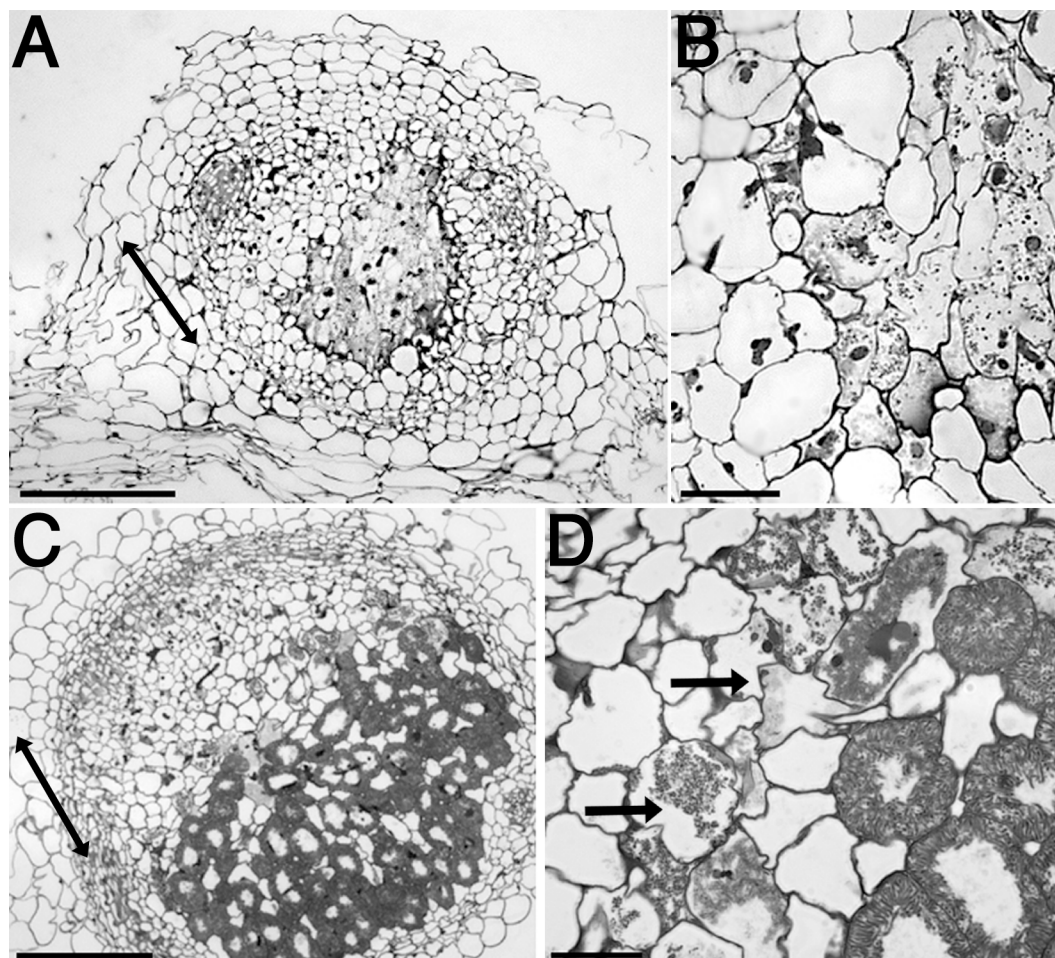


Figure 7. Light micrographs of *M. truncatula* nodules containing the *MtENOD12::MtROP1* fusion. **A** and **B**, type 2 nodule; **C** and **D**, type 3 nodule. **A**) longitudinal section of a nodule 12 d.p.i. (type 2); Two-headed arrow indicates the cell layers in which the number of infection threads was determined; **B**) magnification of the region of the nodule, with cells colonized by rhizobia having a similar size as free living bacteria; **C**) longitudinal section of a nodule 12 d.p.i. (type 3); Two-headed arrow indicates the cell layers in which the number of infection threads was determined; **D**) magnification of the zone II region of the same nodule. Arrow, cells filled with remnants of bacteroids and membranes. The bar corresponds in panel A and C to 500 μm , in panel B and D to 100 μm .

Ultrastructural analysis of MtROP1 overexpressing nodules

The light microscopic analyses of the *MtROP1* overexpressing nodules indicated that symbiosome division and development was highly impaired. Therefore we decided to characterize bacteroid development in *MtROP1* overexpressing nodules by electron microscopy. The same nodules that were used for the light microscopic analyses were also used for these studies. As reference, first a short description of symbiosome development in control nodules will be given.

In the most distal region of zone II in control nodules, released bacteroids were short rods and the symbiosome contained a single bacterium (data not shown). In the proximal region of zone II elongate bacteroids as well as short rods occurred (Fig. 8A). These bacteroids were characterized by a cytoplasm with a homogenous appearance (Fig. 8A) and the space

between the peribacteroid membrane and the bacteroids, the so-called peribacteroid space (symbiosome space), was small (Fig. 8A). In zone III cells of control nodules, bacteroids were elongated structures, filling almost completely the cytosolic volume of the host cell, and symbiosomes contained a single bacteroid (data not shown). A more detailed description of the ultra structural characterization of bacteroids at different developmental stages will be published elsewhere (Fedorova et al., in preparation).

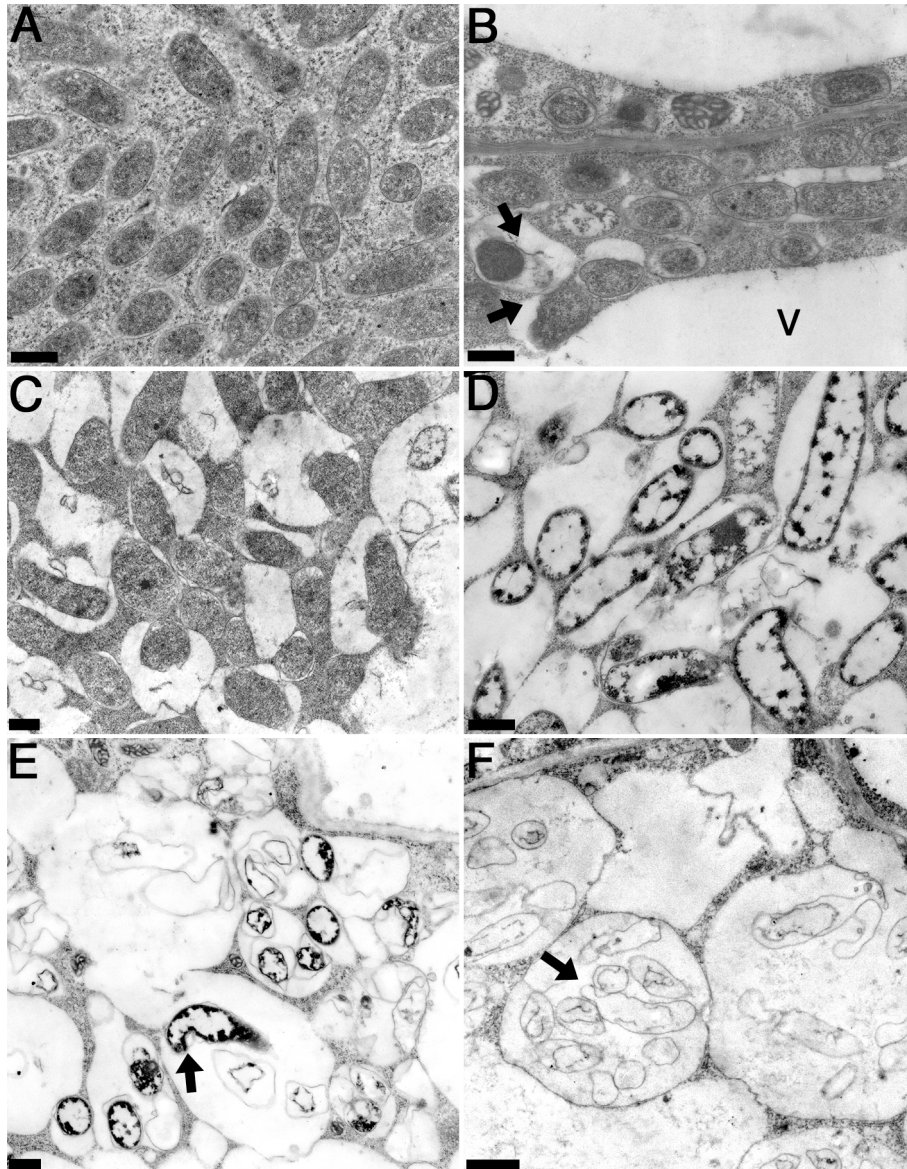


Figure 8. Ultrastructure of control (**A**) and the *MtENOD12::MtROP1* overexpressing nodules (**B-F**). **A**) zone II cells in control nodules containing elongating bacteroids as well as short rods; **B**) distal zone II cells in type 1 nodules. Arrow; fusing symbiosomes with enlarged peribacteroid space; **C**) type 1 nodule cells older than B. Note fusing symbiosomes with enlarged peribacteroid space; **D**) proximal cells in type 1 nodules, with senescent bacteroids with marbled cytoplasm; **E**) and **F**) infected cells in type 2 nodules and degraded cells in type 3 nodules. **E**) part of infected cells with several symbiosomes, each containing 2-5 bacteroids and membrane remnants, separated by a thin layer of host cell cytoplasm; **F**) empty cells with vacuole-like structures containing membrane remnants. Arrow in **E**; degraded bacteroids and in **F**; ghost membranes. The bar corresponds in panels A, B, C, D to 200 nm, in panel E and F to 1 μ m. V = vacuole.

Electron microscopic analyses of *MtENOD12p::MtROP1* nodules revealed that symbiosome development in these nodules was highly disturbed. Examples of different aberrant symbiosome structures that were observed are shown in Fig. 8. These structures most likely represent successive stages of a process that leads to fusion of peribacteroid membranes and subsequent lysis of the bacteroids. In all the cells analyzed the majority of the bacteroids were small rods and only few were elongated (Fig. 8B-8F). Exceptions were the infected cells at the proximal region of type 3 nodules that contained elongate bacteroids (data not shown). In the least disturbed cells (distal part of zone II in type 1 nodules) the majority of the symbiosomes contained a single bacteroid, but in some cells the peribacteroid space was larger than in control nodules (arrows in Fig. 8B). In a few cases fusion of symbiosomes could be detected (arrows in Fig. 8B). In slightly older cells (type I nodules) the peribacteroid space was enlarged and the majority of the symbiosomes had fused giving rise to electron-translucent compartments, resembling vacuoles (Fig. 8C). In more proximal cells (type 1 nodules), the bacteroids in these vacuole-like structures were characterized by a cytoplasm with a pronounced contrast between electron-dense and electron-translucent material (Fig. 8D), representing most likely highly degraded cytoplasm. In the most disturbed regions of *MtROP1* overexpressing nodules (degraded cells in type 2 and type 3 nodules) cells were found with large symbiosomes containing, in addition to degenerated bacteroids (arrow in Fig. 8E), many “ghost” membranes which probably represent the remnants of bacteroids (arrow in Fig. 8F). In plant cells that are dead and only contained some remnants of cytoplasm and organelles, bacteria occurred that are not surrounded by a peribacteroid membrane (Fig. 9A). These bacteria most likely escaped from the infection threads (arrow in Fig. 9B) and had saprophytically colonized the dead nodule cells.

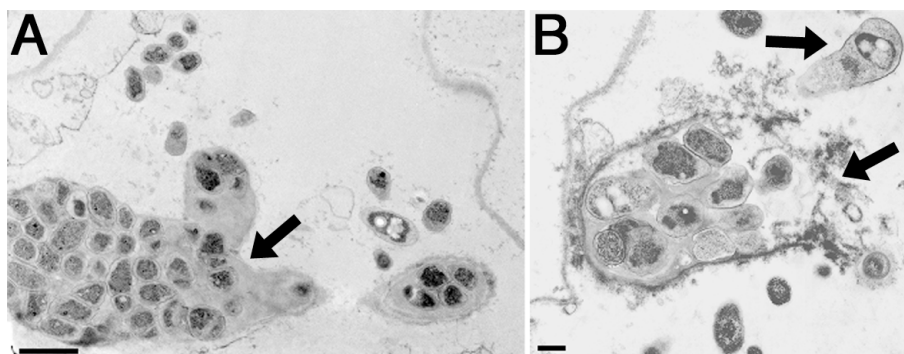


Figure 9. Ultrastructure of cells in Fig. 7B. **A)** dead cell with an infection thread (arrow) and bacteria; **B)** bacteria escaped from the infection thread into a dead cell (arrow). The bar corresponds in panel A to 500 nm and in panel B to 200 nm.

Expression pattern of MtROPs in Fix⁻ nodules

The *MtENOD12p::MtROP1* nodules showed that *MtROP1* overexpression induces fusion of symbiosomes in vacuole like structures in which, subsequently, bacteroids are degraded. Fusion of symbiosomes also occurs in nodules formed by certain ineffective (Fix⁻) bacterial mutants (Vasse et al., 1990). These bacteria do infect nodule cells but the symbiosomes fuse at an early stage of nodule development. This results in nodules in which infected cells are formed, containing many rhizobia (arrow in Fig. 3E). However these are rapidly degraded and also the host cells die by which the cells of the central tissue of the proximal half of the nodule have an empty appearance (asterisk in Fig. 3E).

Since ROPs seem to be involved in the process of symbiosome fusion and bacteroid degradation, we determine, by *in situ* hybridization, whether *MtROPs* are expressed in the cells in which the symbiosome fusion occurs in the Fix⁻ nodules. Sections from nodules (10 d.p.i.) were hybridized with the *MtROP1* probes. This showed that *MtROP* mRNA is present in the nodule at an equal level from meristem up to the fully infected cells (Fig. 3E and F). In the proximal half of the nodule *MtROP* mRNA is not detectable because the cells are dead and do not contain any cytoplasm (Fig. 3E and F).

MtROP expression pattern in nodules formed by wild-type and Fix⁻ bacteria is markedly different. In wild-type nodules *MtROP* mRNA occurs in the meristem and in a few cell layers adjacent to this meristem. However, it is not detectable in the cells where symbiosomes propagate and differentiate, whereas in the Fix⁻ nodules *MtROP* expression is maintained at high levels up to the stage where rhizobia have proliferated and differentiate (Fig. 3). At this stage symbiosomes have fused (data not shown) which might have been caused by a high ROP activity in these cells and which, subsequently, triggers degradation of rhizobia.

Discussion

In this study we show that the expression of *ROP* genes during nodule development in *M. truncatula* is down regulated in the cell layers where symbiosomes proliferate and differentiate. Ectopic expression/overexpression of wild-type *MtROP1* as well as its constitutive active (CA) form in these cell layers, causes degradation of bacteroids. This degradation is most likely initiated by ROP induced fusion of symbiosomes and leads ultimately to complete lyses of the nodule cells. We hypothesize that ROP activity has to be tightly controlled to allow symbiosomes to be maintained as separate units.

Down regulation of MtROP expression is essential for proper nodule development

M. truncatula *ROP* genes are expressed in the nodule meristem as well as in the most distal part of the infection zone. Their expression is markedly reduced in the proximal region of the infection zone II where symbiosomes proliferate and differentiate. The down regulation of

MtROP expression at this stage of nodule development appears to be essential for proper nodule development since ectopic expression of *MtROP1* or its CA form in the proximal part of zone II causes rapid senescence of both bacteroids and plant cells.

Fusion of symbiosomes is an initial step in the premature senescence

In the *MtROP1* overexpressing nodules, the symbiosome fusion starts already in young zone II cells and precedes the first morphological changes in the cytoplasm of the bacteria which is a hall mark of the start of senescence. Therefore, it is possible that fusion of symbiosomes causes the observed degradation of bacteroids.

Communication between rhizobia and host is involved in down regulation of MtROP expression

Cytological analysis has previously shown that in certain Fix^- nodules symbiosome fusion occurs in the proximal cell layers of zone II, in a similar way as we observed in our *MtROP1* overexpressing nodules (Vasse et al., 1990). We used one of these Fix^- mutants, namely *S. meliloti* Fix^- mutant strain GMI351. This strain carries a transpon Tn5 insertion in the *fixI* gene, encoding a putative cation pump (Kahn et al., 1989). We show that, in these Fix^- nodules, the expression of *MtROP* genes is not down regulated, as observed in wild-type nodules, but remains at a high level until the stage where rhizobia have proliferated and differentiate. Our studies in which we express an *MtROP* transgene ectopically proved that this is sufficient to cause premature symbiosome fusion. Therefore, we conclude that in the Fix^- nodules symbiosome fusion is caused by the loss of the ability to down regulate *MtROP* expression.

Since this down regulation is impaired by a bacterial mutation it is very likely that communication between bacteria and host is part of the mechanism by which *MtROP* expression is down regulated in the proximal cell layers of zone II. Since several Fix^- bacterial strains cause premature symbiosome fusion, we suppose that they all are disturbed in this communication and they will all have the same aberrant *ROP* expression pattern that we observed in the nodules induced by the *fixI* *Rhizobium* mutant. Which bacterial molecules are involved in this communication remains to be elucidated.

Symbiosome-Vacuole model to explain the mode of action of ROP activity in symbiosome fusion

Our studies demonstrated that ectopic expression of *MtROP1* causes premature senescence and our cytological studies strongly suggest that this senescence is induced by the fusion of symbiosomes.

Several studies have revealed similarities between symbiosomes and vacuoles (Mellor, 1989). For example, the peribacteroid space (*i.e.* the matrix between the symbiosome membrane and the bacteroids) contains several lysosomal activities, such as cysteine

proteases (Kardailsky and Brewin, 1996; Vincent and Brewin, 2000; Vincent et al., 2000), acid trehalase (Mellor, 1988), α -mannosidase II (Kinnback et al., 1987) and protease inhibitors (Garbers et al., 1988; Manen et al., 1991), all of which are typically found in vacuoles. Moreover, some proteins in the peribacteroid space seem to have a very rapid turnover, as result of proteolytic activity (Campos et al., 1995; Dahiya et al., 1997; Balestrini et al., 1999). Further, the symbiosome membrane possesses tonoplast properties (Mellor, 1989; Verma and Hong, 1996), as exemplify by the presence in this membrane of nodulin-26, a nodule specific form of a vacuolar protein (Miao and Verma, 1993). Therefore, it has been proposed that symbiosomes are small vacuolar structures and their coalescence to form a large vacuolar compartment or fusion to the main lytic vacuole is blocked till nodule senescence (Mellor, 1989). Nodule senescence takes place at a late stage of development (Kijne, 1975; Vasse et al., 1990) and is characterized by symbiosome fusion and subsequent degradation of bacteroids and lysis of the host cell, in a similar way as observed in the *MtROP1* overexpressing nodules.

In Pea tapetal cells it has been shown, by immunocytology, that ROP proteins localize at the membrane of developing vacuoles when they fuse to form larger mature vacuoles whereas ROPs do not occur on prevacuolar structures or on the tonoplast of mature vacuoles (Lin et al., 2001). This localization suggests that ROPs might participate in the signaling pathway controlling the fusion of early vacuoles to form the central mature vacuole (Lin et al., 2001).

Therefore, we propose that symbiosomes share properties with vacuolar structures, as suggested previously and by a mechanism similar to that involved in vacuole formation, ectopic ROP activity in the zone where symbiosomes proliferate and differentiate causes fusion of these symbiosomes.

An involvement of ROPs in vacuole formation in nodules is consistent with the disappearance of vacuoles in infected cells when symbiosomes proliferate/differentiate. However, no alteration in vacuole formation was observed in nodules overexpressing the dominant negative (DN) form of *MtROP1*. This would suggest that ROPs are not required for vacuole formation in the nodule cells. Alternatively, the transgene expression level in these nodules might be too low to affect vacuole development. Roots/nodules expressing the *MtENOD12p::Mtrop1DN* fusion were obtained with lower frequency compared to roots expressing the other transgenes (data not shown), suggesting the presence of a negative selection against roots expressing high level of *Mtrop1DN*. Further, in other cases, overexpression of DN forms of ROPs led to no or weaker phenotypes compare to *ROP* (or CA) overexpression (Li et al., 2001; Molendijk et al., 2001).

To find further support to the vacuole-symbiosome hypothesis, we tried to determine whether in the *MtROP1* overexpressing nodules ROP proteins are located at the membranes of fusing symbiosomes. Unfortunately, an anti-ROP1Ps polyclonal antibody (Lin et al., 2001) did not sufficiently cross react with *M. truncatula* ROPs and, therefore, did not allow immuno localization of ROP proteins in nodules.

RAB and ROP activity in symbiosome development

Previously, it has been shown that other small GTP-binding proteins, the so called RABs, are required for symbiosome membrane synthesis. Genes encoding plant homologues of RAB1p and RAB7p (*sRAB1*, *sRAB7* and *vRAB7*) are induced during nodulation (Cheon et al., 1993; Son et al., 2003). Nodules expressing antisense constructs of these genes, under the control of a nodule specific promoter, showed lack of expansion of infected cells, fewer bacteroids per cell, persistence of central vacuole (Cheon et al., 1993). Therefore, it was concluded that RAB1p and RAB7p control the flow of vesicles from the Golgi to the developing symbiosome membrane and are, therefore, essential for the formation of the symbiosome compartment. Here we showed that overexpression of the DN form of *MtROP1* has no effect on symbiosome formation, whereas overexpression of *MtROP1* or of its CA form causes symbiosome fusion. Therefore, this strongly indicates that ROPs, contrary to RAB GTPases, are not required for symbiosome formation.

Material and Methods

Bacterial strain and medium

Sinorhizobium meliloti strain 1021, containing the plasmid pGHMC60 (Limpens et al., 2003) or strain GMI351 (Fix⁻; Vasse et al., 1990), was grown at 30°C in YEM medium containing (g liter⁻¹): mannitol (5), sodium gluconate (5), yeast extract (0.5), MgSO₄·7H₂O (0.2), NaCl (0.1), K₂HPO₄ (0.5) and supplemented with CaCl₂ (ml liter⁻¹): 16.6% (1).

Agrobacterium rhizogenes strain MSU440, containing the helper plasmid pRiA4, (Sonti et al., 1995) was grown in TY medium containing (g liter⁻¹): NaCl (8), trypton (10), yeast extract (5).

Plant material, growth condition, transformation and nodulation

Medicago truncatula (Jemalong A17) root transformation was performed as previously reported (Stiller et al., 1997), with few modifications. Seeds, sterilized for 10 min with H₂SO₄ followed by 10 min with commercial bleach and extensively washed with sterile water, were germinated on a wet filter paper in a petri dish containing Fåhræus (Fåhræus, 1957) agar medium (0.9% agar; Daishin, Brunswick), supplemented with 0.75 mM Ca(NO₃)₂ and 0.7 mM CaCl₂. Subsequently, seeds were incubated in the dark at 4°C overnight and germinated upside down at 24°C for one more day. After removing the seed coat, seedlings were transferred to new Fåhræus agar plates and sealed for 2/3 with parafilm. The plates were incubated in a growth chamber in a vertical position with 16-h daylight period at 21°C and 70 to 80% relative humidity. Five days later the plantlets, having unfolded cotyledons and the first leaf, were inoculated with *A. rhizogenes*. The bacteria, grown for 2 d on agar plates, were streaked on the top of the hypocotyl area with a sterile curled glass pipette. Subsequently, the root was removed by cutting the hypocotyl region where the *A. rhizogenes* was streaked. In this way the freshly cut surface was inoculated. Plants were cultivated under the same conditions and, after five days, transferred to emergence medium containing: 1x SH-A salt (g liter⁻¹): KNO₃ (2.5), MgSO₄·7H₂O (0.4), NH₄H₂PO₄ (0.3), CaCl₂·2H₂O (0.2), MnSO₄·4H₂O (0.01), H₃BO₃ (5 × 10⁻³), ZnSO₄·7H₂O (1 × 10⁻³), KI (1 × 10⁻³), CuSO₄·5H₂O (2 × 10⁻⁴), NaMoO₄·2H₂O (1 × 10⁻⁴), CoCl₂·6H₂O (1 × 10⁻⁴), FeSO₄·7H₂O (0.015) and Na₂EDTA (0.02); 1x UM-C vitamins (Diaz, 1989; mg liter⁻¹) myoinositol (100), nicotinic acid (5), pyridoxine-HCl (10), thiamine-HCl (10), glycine (2); 1% sucrose, 3mM MES pH 5.8, 0.9% Daishin agar and 300 mg/ml cefotaxime. After 2-3 weeks the newly formed roots could be analyzed.

Transgenic roots were selected scoring for red fluorescence, using a Leica (Wetzlar, Germany) MZFLIII stereomicroscope. Plants containing transformed roots were starved for nitrogen for three days prior inoculation with *Sinorhizobium meliloti* or (O.D.₆₀₀= 0.1). Inoculated plants were grown in gravel and watered with Fahraus medium without NO₃.

Isolation of cDNA clones and sequences

cDNA clones were isolated from a root hair/root tip library (Covitz et al., 1998). Plaque lifts and phage work were carried out according to standard procedures (Sambrook and Russel, 2001), using Hybond N⁺ membranes (Amersham). The library was screened using as probe the full-length clone of the *PsRHO1* gene (Yang and Watson, 1993). The hybridization conditions were: 0.5% SDS, 5X Denhart solution, 5X SSPE and 100µg/ml salmon sperm at 60°C and the washes were done, at the same temperature, 30 min. in 0.1% SDS and 2X SSPE, 30 min. in 0.1% SDS and 1X SSPE and 15 min. in 0.1% SDS and 0.5X SSPE. cDNAs cloned in the positive plaques were amplified by PCR using M13 primers and the PCR fragments were sequenced. Sequencing was done by the dideoxy chain termination method (BigDye; Perkin-Elmer, Foster City, CA) and was analyzed on an ABI 377 DNA sequencer (Applied Biosystems, Foster City, CA). The sequences were manually aligned and the pBK-CMV phagemid, containing the longest c-DNA insert, were excised from the Zap Express vector and transformed into XL0LR cells according to manufacturers descriptions (Stratagene, La Jolla, CA), generating the pBK-CMVMtROP1 vector.

Medicago truncatula ESTs

The full-length cDNAs of *MtROP1* and *MtROP2* were used for Blast analysis on the *M. truncatula* database at TIGR (<http://www.tigr.org/tdb/tgi/mtgi>). Sixty-five ESTs were identified, manually aligned and grouped into 8 different clusters. ESTs from the same gene and derived from the same cDNA library that started at the same nucleotide were not used for further analysis, since they could have arose from the same cloning event. To obtain data on the expression pattern of the 8 genes (electronic northern), the 37 cDNA banks were grouped into 12 classes of similar origin and the frequency of each gene in each bank group was calculated dividing the number of specific and of total ESTs in the bank class. expressed for 1000 ESTs. The cDNA banks were grouped in the 12 classes as follow: Roots various (MtBA, KV0, MHRP, DSIR, MGHG, BNIR, MtRHE, HOGA and NR-RT); Roots-Rhizobium (KV1, KV2 and KV3); Roots-mycorrhiza (MtBC, MTGIM and MHAM); Nodules (GVN, MtBB, GVSN, R108 and NF-NR); Stems (NF-ST); Leaves-various (DSLCL, NF-PH, NF-LF and NF-PL); leaves-fungi (DSLIL); Leaves-insects (NF-IN); Plantlets (NF-DT and NF-IR); Flowers (NF-FL, MTFLOW); Seeds/pods (GPOD, GESD, NF-GS, MTPOSE and GLSD); Cell cultures (NF-EC).

Sequence comparison and phylogenetic analysis

Sequence data were analyzed using computer software from DNASTAR, Inc. (Madison, WI) and derived protein sequences were aligned using the MegAlign program (DNASTAR, Inc., Madison, WI). Phylogenetic analyses were performed using the GCG PileUP program (Genetic Computer Group, Madison, WI).

RT-PCR expression analysis

Total RNA was isolated according to Pawlowski (Pawlowski et al., 1994) followed by DNAase I treatment. cDNA was made from 1 µg total RNA in a volume of 20 µl containing 50mM Tris\Cl pH=8.8, 75 mM KCl, 3 mM MgCl₂, 10 mM DTT, 1 mM dNTPs, 1µg oligodT17T/A/G/C mix, 20 U RNAse OUT (Invitrogen) and 20 U M-MLV reverse transcriptase for 1hour at 37°C, followed by 5 min. at 95°C. To certify for the absence of genomic DNA in the cDNA samples, also a reaction was performed under the same conditions described above but in the absence of reverse transcriptase. The RT samples were then diluted to 50 µl. The PCR reaction was carried out with 2 µl of the cDNA solution according to standard procedures (Sambrook and Russel, 2001). The primers 5'MtACTIN (ACAATGGAAGTGAATGG) and 3'MtACTIN (CCTCCAATCCAGAACT) were designed in such a way to amplify a 1.1 Kb fragment from all the *M. truncatula* ACTIN genes (Mirabella et al., in preparation). The primers

MtROP1 3Uf (TCCTATTATGCTGAAGAAG) and MtROP1 3Ur (ATGTTAAGAAAAAGGTGGG) were designed in the 3'UTR region of *MtROP1* to amplify a 180 bp fragment. The primers MtROP1/700 (TGCAGCCATAAGAGTTGTC) and 3' T-NOS (GGACTCTAATCATAAAAACCC) were designed to amplify a 600 bp fragment within the *MtROP1/T-NOS* transgene. The PCR thermocycle profile was: 95°C, 52°C and 72°C, 1 min. each step and 24 cycles for the *ACTIN* genes and 95°C, 52°C and 72°C, 20 sec. each step and 28 cycles for MtROP1/(T-NOS). PCR products were separated on 1% agarose gel, transferred onto a Hybond N⁺ membrane using alkali denaturation and transfer and hybridized to ³²P-labeled *MtACTIN* or *MtROP1/(T-NOS)* probe.

DNA manipulation and plasmid constructs

All the cloning work was carried out according to standard procedure (Sambrook and Russel, 2001) and all DNA fragments amplified by PCR were sequenced.

To obtain the *MtENOD12p::GUS* fusion, 836 bp region of the *MtENOD12* promoter was amplified by PCR, using as template the pbluescript *MtENOD12::GUS* plasmid in combination with the following primers: 5' *ENOD12pH* CCCAAGCITGAAGGGTAAAATAGAAAAG (underlined 5' *Hind*III site) and 3' *ENOD12pX* GCTCTAGATTTTAATGTTAGTGCATATAAC (underlined 3' *Xba*I site). The amplified fragment was cloned into the *Hind*III-*Xba*I sites of the pBI101.3 vector (Clontech, Palo Alto, CA). To generate *MtENOD12p::MtROP1* fusion the same *MtENOD12* promoter fragment, described above, was cloned in the *Hind*III-*Xba*I sites of the pGem4 vector (Promega), generating the pGem4MtENOD12p vector. The 5'UTR and the coding region of *MtROP1* were amplified from the pBK-CMVtROP1 vector using the primers 5' MtROP1UX GCTCTAGACTCGTGCCGAACGAACG (underlined 5' *Xba*I site) and 3' MtROP1K GGTACCTCACAATATCGAACAAGCC (underlined the 3' *Kpn*I site). The PCR fragment was subsequently cloned into the *Xba*I-*Kpn*I sites of pGem4MtENOD12p and the resulting vector was named pGem4MtENOD12p::MtROP1 vector. The *ENOD12::MtROP1* fragment was subcloned in the *Hind*III-*Kpn*I sites of the pRR vector (Limpens et al., 2003), containing the *T-NOS* between the *Eco*RI and the *Pac*I sites.

CA-MtROP1 and DN-MtROP1 were generated using the QuickchangeTM site-direct mutagenesis kit (Stratagene, La Jolla, CA) and the primers: G15V GGGTTTGTGGGACACTGCAGGACTAGAGGATTATAACAGATTAAGACC and T20N GGGGATGGAGCTGTTGGTAAAAATTGTTTGTTAATTTTCATACACCAGC, respectively and subsequently subcloned in the pRR vector, as described above.

Histochemical GUS analysis and sectioning

At various time-points post inoculation, plants were harvested and stained. GUS staining was performed according to (Jefferson et al., 1987), with few modifications. Plant material was incubated in 0.05% (w/v) X-Gluc (Duchefa) in 0.1M sodium phosphate buffer (pH 7) with 3% sucrose, 5μM potassium-ferrocyanide and 5μM potassium-ferricyanide. Vacuum was applied for 1 h and the samples were incubated at 37°C. Nodules were embedded in Technovit 7100 as described in the protocol (Kulzer, Heraeus). Sections (10μm) were made using a Leica microtome, dried into glass slides at 43°C and mounted with Euparal (Agar Scientific LTD.). For imaging a Nikon (Tokyo, Japan) SMZ-U stereomicroscope and a Nikon optiphot-2 bright field microscope were used and photographs were made using a Nikon coolpix990 digital camera.

In situ hybridization

Nodules were harvested 14 or 10 days post inoculation (d.p.i.), respectively, and fixed in 4% paraformaldehyde supplemented with 0.25% glutaraldehyde in 10 mM sodium phosphate buffer (pH=7.4) for 3 h (Van de Wiel et al., 1990). Fixed nodules were dehydrated, by passing through a series of grade ethanol, and embedded into paraffin (Paraclean; Klinipath, Duiven, The Netherlands) by routine methods (Van de Wiel et al., 1990). Sections (7 μm) were dried on polylysine-coated slides at 37° C overnight, deparaffinized with xylene and rehydrated via a graded ethanol series. Hybridization pre-treatment, hybridization and washing were performed as described by Cox (Cox and Goldberg, 1988) and adapted by Van de Wiel (Van de Wiel et al., 1990).

For preparing antisense *MtROP1* RNA probes the fragments 22-236 bp, 218-423 bp and 381-586 bp, within the *MtROP1* coding region, were subcloned in the *HindIII*-*EcoRI* sites of the pGem4 vector. Subsequently, the fragments were amplified by PCR using the M13 reverse primer and 5' end primers specific for the *MtROP1* fragments (AGTGTGTTACTGTTGGG, TGAGTTATCGTGGTGCCG and TCTTGCTGCACCATCCAG for the fragment 22-236 bp, 218-423 bp and 381-586 bp, respectively). The amplified fragments were used as substrate to synthesise antisense RNA probes with T7 RNA polymerase (Promega), in the presence of [³⁵S]-UTP (1000-1500 Ci mmol⁻¹, Amersham). For the hybridisation a mixture containing 2 × 10⁶ cpm of each probe was used.

For preparing an antisense *MtENOD12* RNA probe, a 280 bp fragment of the *MtENOD12* coding region was amplified using as template nodule cDNA in the presence of the following primers: 5' *MtENOD12* GAAAGGAATCACCGACGCATAGG and 3'*MtENOD12* CACATAGCACGATTTTACACTCA. The amplified fragment was cloned in the pGemT vector and, subsequently, was amplified by PCR using M13 reverse and 5' *MtENOD12* primers. The amplified fragment was used as template to synthesize antisense RNA probes, as described above. For the hybridization 6 × 10⁶ cpm of the probe were used.

After washing, the slides were coated with microautoradiography emulsion LM-1 (Amersham) and exposed for 3 weeks at 4° C. They were developed for 5 min in Kodak D-19 developer (East-man Kodak, Rochester, NY) and fixed in Kodak fixative. Sections were counterstained with toluidine blue. For imaging a Nikon (Tokyo, Japan) optiphot-2 bright field microscope with epipolarization optics was used. Photographs were made using a Nikon coolpix990 digital camera and processed using Adobe photoshop (Adobe, systems, Inc.).

Optical and electron microscopy

About 12-14 d.p.i. after inoculation individual transgenic nodules, scored for the presence of red fluorescence, were excised from the roots and fixed immediately in 50mM potassium phosphate buffer (pH=7.4) containing 4% paraformaldehyde, 3% glutaraldehyde and 4% sucrose for 3 h. Subsequently, the nodules were rinsed in the same buffer, post fixed for 1 hour in 50mM potassium phosphate buffer (pH=7.4) containing 1% osmium tetroxide, rinsed three times in the same buffer and dehydrated, by passing through a series of grade ethanol, and embedded in LR white resin (Sigma). Ultrathin sections were cut with a Reichter Omu2 microtome equipped with a diamond knife (Diatome), stained with uranyl acetate and lead citrate and observed in a Philips EM208 electron microscope. Semi-thin section (2-3 µm) of the same samples, counterstained with methylene blue (0.04%), were used for light microscopical studies.

Acknowledgments

We are grateful to Dr. D. Barker for providing the pBluescript *MtENOD12::GUS* plasmid. R. M. was supported by a grant from the European Community TMR program FMRX CT 98-0239.

References

- Arellano M, Coll PM and Perez P** (1999) RHO GTPases in the control of cell morphology, cell polarity, and actin localization in fission yeast. *Microsc Res Tech* **47**: 51-60
- Balestrini B, Perotto N, Gasverde E, Dahiya P, Guldmann L-LG, Brewin NJ and Bonfante P** (1999) Transcription of a gene encoding a lectin-like glycoprotein is induced in root cells harbouring arbuscular mycorrhizal fungi in *Pisum*. *Molecular Plant-Microbe Interact* **12**: 785-791
- Brewin NJ** (1991) Development of the legume root nodule. *Ann Rev Cell Biol* **7**: 191-226
- Brewin NJ** (1996) Tissue and Cell Invasion by *Rhizobium*: The Structure and Development of Infection Threads and Symbiosomes. In HP Spaink, A Kondorosi, PGG Hooykaas, eds, *The Rhizobiaceae: molecular biology of model plant-associated bacteria*. Kluwer Academic Publisher, New York, pp 417-428
- Campos F, Carsolio C, Kuin H, Bisseling T, Rocha-Sosa M and Sanchez F** (1995) *Plant Physiol* **109**: 363-370
- Cheon CI, Lee NG, Siddique AB, Bal AK and Verma DP** (1993) Roles of plant homologs of Rab1p and Rab7p in the biogenesis of the peribacteroid membrane, a subcellular compartment formed de novo during root nodule symbiosis. *Embo J* **12**: 4125-4135
- Cohn J, Day B and Stacey G** (1998) Legume nodule organogenesis. *Trends in Plant Science* **3**: 105-109

- Covitz PA, Smith LS and Long SR** (1998) Expressed sequence tags from a root-hair-enriched *Medicago truncatula* cDNA library. *Plant Physiol* **117**: 1325-1332
- Cox KH and Goldberg RB** (1988) Analysis of plant gene expression. In CH Shaw, ed, *Plant Molecular Biology: A practical approach*. IRL press, Oxford, pp 1-34
- Dahiya P, Kardailsky IV and Brewin NJ** (1997) Immunolocalization of PsNLEC-1, a lectin like glycoprotein expressed in developing pea nodules. *Plant Physiol* **115**: 1431-1442
- Dart PJ** (1974) The Infection Process. In A Quispel, ed, *The Biology of Nitrogen Fixation*. North-Holland publishing company, pp 381-429
- Davidson AL and Newcomb W** (2001) Changes in actin microfilaments arrays in developing pea root nodule cells. *Can. J. Bot.* **79**: 767-776
- de Ruijter NCA, Bisseling T and Emons AMC** (1999) *Rhizobium* Nod factors induce an increase in sub-apical fine bundles of actin in *Vicia sativa* root hairs within minutes. *Molecular Plant-Microbe Interact* **12**: 829-832
- Erickson JW and Cerione RA** (2001) Multiple roles for Cdc42 in cell regulation. *Curr Opin Cell Biol* **13**: 153-157
- Fåhræus G** (1957) The infection of clover root hairs by nodule bacteria studied by a simple glass slide technique. *Journal of Genetic Microbiology* **16**: 374-381
- Fu Y, Li H and Yang Z** (2002) The ROP2 GTPase controls the formation of cortical fine F-actin and the early phase of directional cell expansion during Arabidopsis organogenesis. *Plant Cell* **14**: 777-794
- Fu Y and Yang Z** (2001) The Rop GTPase: A master switch of cell polarity development in plant cells. *Trends Plant Sci* **6**: 545-547
- Garbers C, Menkbach R, Mellor RB and Werner D** (1988) Protease (thermolysin) inhibition activity in the peribacteroid space of *Glycine max* root nodules. *Journal of Plant Physiology* **132**: 442-445
- Gualtieri G and Bisseling T** (2000) The evolution of nodulation. *Plant Mol Biol* **42**: 181-194
- Hall A** (1998) Rho GTPases and the actin cytoskeleton. *Science* **279**: 509-514
- Hirsch AM** (1992) Developmental biology of legume nodulation. *New Phytol.* **122**: 211-237
- Jefferson AR, Kavanagh TA and Bevan MW** (1987) Gus fusions: *b-glucuronidase* as a sensitive and versatile gene fusion marker in higher plants. *The EMBO Journal* **6**: 3901-3907
- Jones MA, Shen JJ, Fu Y, Li H, Yang Z and Grierson CS** (2002) The Arabidopsis ROP2 GTPase is a positive regulator of both root hair initiation and tip growth. *Plant Cell* **14**: 763-776
- Kahn D, David M, Domergue O, Daveran M-L, Ghai J, Hirsch PR and Batut J** (1989) *Rhizobium meliloti fixGHI* Sequence Predicts Involvement of a Specific Cation Pump in Symbiotic Nitrogen Fixation. *J Bacteriol* **171**: 929-939
- Kardailsky IV and Brewin NJ** (1996) Expression of cysteine protease genes in pea nodule development and senescence. *Molecular Plant-Microbe Interact* **9**: 689-695
- Kawasaki T, Henmil K, Ono E, Hatakeyama S, Iwano M, Satoh H and Shimamoto K** (1999) The small GTP-binding protein Rac is a regulator of cell death in plants. *Proc. Natl. Acad. Sci. USA* **99**: 10922-10926
- Kijne JW** (1975) The fine structure of pea root nodule. Senescence and disintegration of the bacteroid tissue. *Physiol. Plant Pathol.* **7**: 17-21
- Kinnback ARB, Mellor B and Werner D** (1987) Alpha-mannosidase II isoenzyme in the peribacteroid space of *Glycin max* root nodules. *J. Exp. Bot.* **38**: 1373-1377
- Kost B, Lemichez E, Spielhofer P, Hong Y, Tolias K, Carpenter C and Chua NH** (1999) Rac homologues and compartmentalized phosphatidylinositol 4, 5-bisphosphate act in a common pathway to regulate polar pollen tube growth. *J Cell Biol* **145**: 317-330
- Li H, Lin Y, Heath RM, Zhu MX and Yang Z** (1999) Control of pollen tube tip growth by a Rop GTPase-dependent pathway that leads to tip-localized calcium influx. *Plant Cell* **11**: 1731-1742
- Li H, Shen JJ, Zheng ZL, Lin Y and Yang Z** (2001) The Rop GTPase switch controls multiple developmental processes in Arabidopsis. *Plant Physiol* **126**: 670-684
- Limpens E, Franken C, Smit P, Willemse J, Bisseling T and Geurts R** (2003) LysM domain receptor kinases regulating rhizobial Nod factor-induced infection. *Science* **302**: 630-633
- Lin Y, Seals DF, Randall SK and Yang Z** (2001) Dynamic localization of Rop GTPases to the tonoplast during vacuole development. *Plant Physiol* **125**: 241-251
- Manen JF, Simon P, Van Slooten JC, Osteras M, Frutiger S and Hughes GJ** (1991) A nodulin specifically expressed in senescent nodules of winged bean is a protease inhibitor. *Plant Cell* **3**: 259-270
- Marty F** (1999) Plant Vacuoles. *Plant Cell* **11**: 587-599
- Mellor B** (1988) Distribution of trehalase in soybean root nodule cells: Implication for trehalose metabolism. *Journal of Plant Physiology* **133**: 173-177
- Mellor RB** (1989) Bacteroids in the *Rhizobium*-legume symbiosis inhabit a plant internal lytic compartment: implications for other microbial endosymbiosome. *J Exp Bot* **40**: 831-839
- Miao GH and Verma DP** (1993) Soybean nodulin-26 gene encoding a channel protein is expressed only in the infected cells of nodules and is regulated differently in roots of homologous and heterologous plants. *Plant Cell* **5**: 781-794
- Miller DD, de Ruijter NCA, Bisseling T and Emons AMC** (1999) The role of actin in root hair morphogenesis: studies with lipochito-oligosaccharide as a growth stimulator and cytochalasin as an acting perturbing drug. *The Plant Journal* **17**: 141-154
- Molendijk AJ, Bischoff F, Rajendrakumar CS, Friml J, Braun M, Gilroy S and Palme K** (2001) Arabidopsis thaliana Rop GTPases are localized to tips of root hairs and control polar growth. *Embo J* **20**: 2779-2788

- Mylona P, Pawlowski K and Bisseling T** (1995) Symbiotic Nitrogen Fixation. *Plant Cell* **7**: 869-885
- Pawlowski K, Kunze R, De Vries S and Bisseling T** (1994) Isolation of total, poly(A) and polysomal RNA from plant tissue. In SB Gelvin, RA Schilperoort, eds, In *Plant Molecular Biology manual*, Ed 2nd. Kluwer Academic Publishers, Dordrecht, The Netherlands, pp 1-13
- Pichon M, Journet EP, Dedieu A, de Billy F, Truchet G and Barker DG** (1992) *Rhizobium meliloti* elicits transient expression of the early nodulin gene ENOD12 in the differentiating root epidermis of transgenic alfalfa. *Plant Cell* **4**: 1199-1211
- Potikha TS, Collins CC, Johnson DI, Delmer DP and Levine A** (1999) The involvement of hydrogen peroxide in the differentiation of secondary walls in cotton fibers. *Plant Physiol* **119**: 849-858
- Ridley A** (2000) Rho. In A Hall, ed, *GTPases*. Oxford University Press, Oxford, pp 89-136
- Ridley AJ** (1995) Intracellular regulation. RAC and BCR regulate phagocytic phoxes. *Curr Biol* **5**: 710-712
- Roth LE and Stacey G** (1989a) Bacterium release into host cells of nitrogen-fixing soybean nodules: the symbiosome membrane comes from three sources. *Eur J Cell Biol* **49**: 13-23
- Roth LE and Stacey G** (1989b) Cytoplasmic membrane systems involved in bacterium release into soybean nodule cells as studied with two *Bradyrhizobium japonicum* mutant strains. *Eur J Cell Biol* **49**: 24-32
- Sambrook and Russel** (2001) Molecular cloning: a laboratory manual. In. Cold spring harbor laboratory press, Cold spring harbor, NY
- Settleman J** (2001) Rac 'n Rho: the music that shapes a developing embryo. *Dev Cell* **1**: 321-331
- Son O, Yang H-S, Lee H-J, Lee M-Y, Shin K-H, Jeon S-L, Lee M-S, Choi S-Y, Chun J-Y, Kim H, An C-S, Hong S-K, Kim N-S, Koh S-K, Cho MJ, Kim S, Verma DPS and Cheon C-I** (2003) Expression of *srab7* and *SCaM* genes required for endocytosis of *Rhizobium* in root nodules. *Plant Science* **165**: 1239-1244
- Sonti RV, Chiurazzi M, Wong D, Davies CS, Harlow GR, Mount DW and Signer ER** (1995) Arabidopsis mutants deficient in T-DNA integration. *Proc Natl Acad Sci U S A* **92**: 11786-11790
- Stiller J, Martirani L, Tupple S, Chian R, Chiurazzi M and Gresshoff PM** (1997) High frequency transformation and regeneration of transgenic plants in the model legume *Lotus Japonicus*. *Journal Experimental Botany* **48**: 1357-1365
- Timmers AC, Soupene E, Auriac MC, de Billy F, Vasse J, Boistard P and Truchet G** (2000) Saprophytic intracellular rhizobia in alfalfa nodules. *Mol Plant Microbe Interact* **13**: 1204-1213
- Valster AH, Hepler PK and Chernoff J** (2000) Plant GTPases: the Rhos in bloom. *Trends Cell Biol* **10**: 141-146
- Van de Wiel C, Scheres B, Franssen H, Van Lierop MJ, Van Lammeren A, Van Kammen A and Bisseling T** (1990) The early nodulin transcript ENOD2 is located in the nodule perenchima (inner cortex) of pea and soybean root nodules. *Embo J* **9**: 1-7
- Vasse J, de Billy F, Camut S and Truchet G** (1990) Correlation between ultrastructural differentiation of bacteroids and nitrogen fixation in alfalfa nodules. *J Bacteriol* **172**: 4295-4306
- Verma D, Cheon C and Hong Z** (1994) Small GTP-Binding Proteins and Membrane Biogenesis in Plants. *Plant Physiol* **106**: 1-6
- Verma DPS and Hong Z** (1996) Biogenesis of peribacteroid membrane in root nodules. *Trends in Microbiology* **4**: 364-368
- Vincent JL and Brewin NJ** (2000) Immunolocalization of a cysteine protease in vacuoles, vesicles, and symbiosomes of pea nodule cells. *Plant Physiol* **123**: 521-530
- Vincent JL, Knox MR, Ellis NTH, Kalò P, Kiss GB and Brewin NJ** (2000) Nodule-Expressed *Cyp15a* Cysteine Protease Genes Map to Syntenic Genome Regions in *Pisum* and *Medicago* spp. *Molecular Plant-Microbe Interact* **7**: 715-723
- Winge P, Brembu T and Bones AM** (1997) Cloning and characterization of Rac-like cDNAs from Arabidopsis thaliana. *Plant Mol Biol* **35**: 483-495
- Wittmann T and Waterman-Storer CM** (2001) Cell motility: can Rho GTPases and microtubules point the way? *J Cell Sci* **114**: 3795-3803
- Yang Z** (2002) Small GTPases: Versatile Signaling Switches in Plants. *Plant Cell* **14**: S375-S388
- Yang Z and Watson JC** (1993) Molecular cloning and characterization of Rho, a Ras-related small GTP-binding protein from the garden pea. *Proc. Natl. Acad. Sci. USA* **90**: 6636-6640
- Zheng Z-L, Nafisi M, Tam A, Li H, Crowell DN, Chary SN, Schroeder JI, Shen J and Yang Z** (2002) Plasma Membrane-Associated ROP10 Small GTPase Is a Specific Negative Regulator of Abscissic Acid Responses in Arabidopsis. *Plant Cell* **14**
- Zheng ZL and Yang Z** (2000) The Rop GTPase: an emerging signaling switch in plants. *Plant Mol Biol* **44**: 1-9

CHAPTER 5

NODULATION RECEPTOR KINASE Controls the Switch from Infection Thread Growth to Release of Bacteria in Nodule Cells

Abstract

The formation of nitrogen-fixing root nodules is triggered by the perception of rhizobial signaling molecules, named Nod factors, in the epidermis of the root. The key-players of the Nod factor-signaling pathway have been identified and are characterized by the fact that mutations in these genes block nodulation at an initial stage of the interaction. One of the key-players is the *Medicago truncatula* *NODULATION RECEPTOR KINASE* (*NORK*). Here we show that the expression pattern of *NORK* in the nodule coincides with the region where rhizobial *nod* genes are active in the nodule. This corresponds to the place where the bacteria are released in the plant host cells. By mimicking allelic series of *NORK* by RNA interference and by ectopic expression of *NORK* in the mutant background we show that *NORK* controls the switch from infection thread growth to release of bacteria in the nodule. This suggests a role for the Nod factor perception and signaling machinery in this process in the nodule.

Erik Limpens, Rossana Mirabella, Carolien Franken, Elena Federova, Ton Bisseling and René Geurts

Introduction

Rhizobial signaling molecules, called Nod factors, play a pivotal role in the establishment of a successful nitrogen-fixing root nodule through the activation of a conserved Nod factor-signaling pathway (1,2). Genetic analysis in model legumes formed the basis to identify and clone the key-players of this Nod factor-signaling pathway. Based on these studies it is hypothesized that Nod factors are recognized by LysM domain containing receptor kinases (3-5). In the model legume *Medicago truncatula* (Medicago), these include *LYK3* and *LYK4* (3) and *NFP*, which is the putative ortholog of the *Lotus japonicus* *NFR5* gene (4; Gough and Geurts, unpublished). Other essential components of the Nod factor signal transduction pathway include the *DOES NOT MAKE INFECTIONS 1* gene (*DMI1*), *DMI3* and *NODULATION RECEPTOR-LIKE KINASE (NORK)*, which encode, respectively, a putative cation channel, a calcium/calmodulin-dependent kinase and a leucine-rich repeat (LRR) containing receptor kinase (6-10). Upon perception of Nod factors these components are all involved in the formation of infection threads in the root hairs, by which the bacteria gain entry into the root, as well as in the induction of responses in the inner cell layers leading to the formation of the nodule organ.

The Nod factor-signaling components have been identified in genetic screens that were based on a search for loss of nodulation, and as a result all the characterized mutant alleles cause a block of nodulation at the initial steps. For example, the only morphological response that is observed after inoculation with rhizobia in the 4 different mutant alleles of *NORK* that are characterized to date, is the induction of root hair swellings (6,11). Similar phenotypes have been reported for mutants of *SYMRK* in *Lotus japonicus*, *NORK* in alfalfa and *SYM19* in pea, which represent orthologs of Medicago *NORK* (7,12). Although it is obvious that Nod factor signaling is essential at initial stages of the interaction, several observations indicate that the Nod factor perception and signaling machinery also plays a role in the nodule. By fusions of the *nod* genes with the *gusA* reporter gene it has been shown that the rhizobial *nod* genes -involved in Nod factor biosynthesis- are expressed by rhizobia throughout the infection zone of the nodule (13). Highest GUS activity was observed in the distal part of the infection zone and GUS activity diminished towards the proximal regions. *In situ* hybridizations detected *nod* gene expression more specifically in the distal region of the infection zone, and led to the conclusion that rhizobial *nod* genes are switched off as soon as bacteria are released into the nodule cells (14). The involvement of Nod factor perception and signaling in the nodule is further supported by the fact that several of the Nod factor perception and signaling genes (e.g. *LYK3* and *DMI3* in Medicago and *SYM10* in pea) are transcribed in the nodule, although their expression pattern is unknown (3,4,9). If the Nod factor signaling genes would play a role in Nod factor perception and transduction in the nodule we hypothesized that their expression pattern would coincide with that of *nod* genes. Therefore we determined the expression pattern of *NORK* in the nodule. We show that

NORK is highly expressed in the distal part of the infection zone of the nodule, which coincides with the region where the rhizobial *nod* genes are expressed. This is the region where bacteria are released from the infection threads into the plant host cells and start to divide (15). These bacteria remain surrounded by a plant-derived membrane and are called symbiosomes (16). By mimicking allelic series of *NORK* using RNA interference and by expression of *NORK* in the mutant background we show that high expression levels of *NORK* are required to restrict growth of infection threads in the nodule and to facilitate the release of bacteria in the plant host cells. This suggests a role for the Nod factor perception and transduction machinery in these processes in the nodule.

Results

NORK expression is highly upregulated in the distal region of the infection zone

To determine whether Nod factor signaling could occur in nodules we examined whether the expression pattern of the Nod factor signaling component, *NORK*, coincides with the region where the rhizobial *nod* genes are expressed. The rhizobial *nod* genes are most strongly expressed in the distal part of the infection zone of the nodule (13,14). Quantitative RT-PCR (qPCR) showed that *NORK* expression was mainly detected in roots and in nodules (Fig. 1).

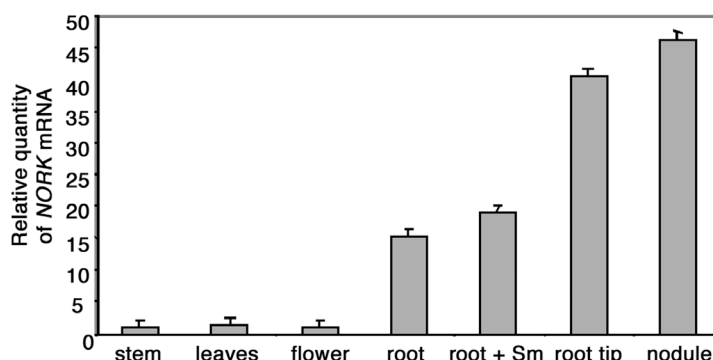


Figure 1. Quantification of *NORK* mRNA levels in stem, leaves, flowers, roots, roots 48 h post-inoculation with *S. meliloti*, root tips and 2-week-old nodules. Relative transcript levels were determined by qRT-PCR, and normalized using *MtACTIN2* that is constitutively expressed in all tissues tested.

Very low *NORK* expression levels were detected in the aerial parts of the plant (e.g. stem, leaves and flowers), which suggests that *NORK* has a specific role in the root system. Up-regulation of *NORK* expression was observed in roots upon inoculation with *Sinorhizobium meliloti* and in root nodules, when compared to un-inoculated roots. To determine in which nodule cell types *NORK* is expressed we conducted *in situ* hybridizations on 2-week old nodules using *NORK* anti-sense RNA as probe. These studies showed that *NORK* is highly expressed in the distal region of the infection zone, in the 2 - 3 cell layers adjacent to the meristem (Fig. 2A). *NORK* expression levels rapidly diminished towards to proximal region of the infection zone. This indicates that regions where *nod* genes are active and *NORK* is expressed coincide (13,14). The distal part of the infection zone is the place where bacteria

are released from the infection threads into the plant host cells and division of symbiosomes starts (15).

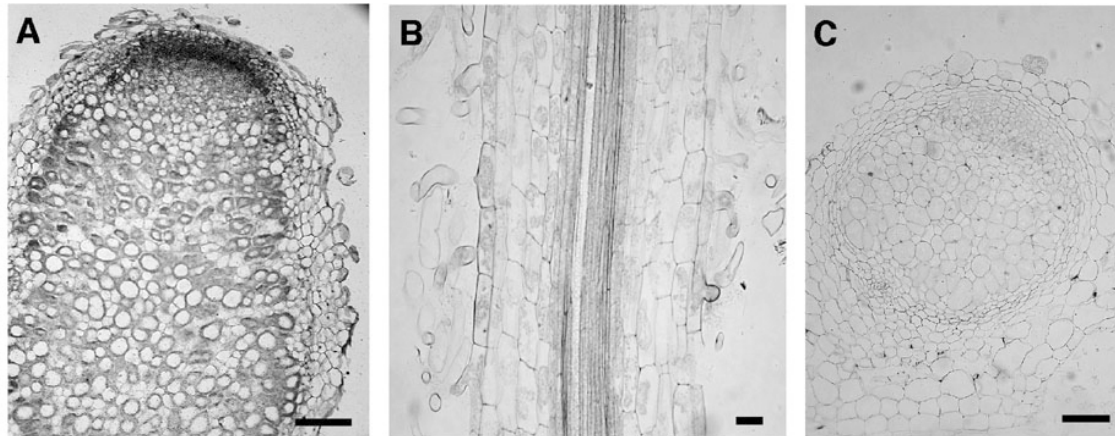


Figure 2. *NORK* expression profiling. (A) *In situ* hybridization of a longitudinal section hybridized with ^{35}S -UTP labeled anti-sense *NORK* probes; signal appears as silver grains. Section is counterstained with toluidine blue. Strong hybridization is observed in the distal part of the infection zone adjacent to the meristem and rapidly declines towards more proximal regions. (B) Histochemical localization of GUS activity in semi-thin (5 μm) longitudinal section of *NORKp::GUS* transformed roots. (C) Localization of *NORKp::GUS* expression in a longitudinal section (5 μm) of a 2-week-old nodule. GUS activity is observed in the infection zone (zone II) of the nodule. Sections in (B) and (C) are stained with 0.1% ruthenium red. Bars in (A) and (C) = 200 μm ; Bar in (B) = 25 μm . (Color figure, see appendix).

NORK controls the switch from infection thread growth to release of bacteria in the nodule

To gain insight into the function of *NORK* and probably Nod factor signaling in the infection zone of the nodule we used two strategies. First we mimicked allelic series of *NORK* by using RNA interference (RNAi) and second, the gene was over-expressed using the *CaMV* 35S promoter.

RNAi is a powerful tool to knock-down the expression of genes in order to study their function and it has been shown that RNAi can result in phenotypes that mimic allelic series due to partial knock-down of the target mRNA (17,18). Previously, we have shown that gene knock-down by RNAi via *A. rhizogenes* mediated root transformation in *Medicago* is very effective (3,18). In the case of *NORK*, 75% of the RNAi roots displayed a phenotype identical to the described knock-out mutants (3). So only in 25% of the cases some nodules were formed on roots where the silencing construct was introduced. We decided to examine such nodules to determine whether a weak knock-down phenotype could reveal a function of *NORK* in the nodule. In total 57 roots, homogeneously transformed with a *NORK* hairpin construct, were inoculated with *S. meliloti* 2011-pHC60 expressing *GFP*. Fourteen days after inoculation 25 nodules were observed on 9 homogeneously transformed roots. Histological examination by analyzing sections of 12 of these nodules with light microscopy revealed in 6 of the nodules the presence of numerous wide infection threads in the central tissue of the nodule with no, or very few bacteria in the nodule cells (Fig. 3A). The remaining 6 nodules showed infected cells filled with released bacteria similar to control nodules (data not

shown). Control nodules, transformed with an empty binary vector, all showed a normal histology, typical for indeterminate nodules, with infected host cells containing bacteroids (Fig. 3B) (15). This suggests that partial knock down of *NORK* expression causes extensive infection thread growth in the nodule with no, or very inefficient, release of bacteria from the infection threads.

In addition to knock-down of *NORK* expression, we over-expressed *NORK* by introducing the *NORK* coding sequence into wild-type roots under the control of the *CaMV* 35S promoter (*35S::NORK*) via *A. rhizogenes* mediated root transformation. To check whether the construct was functional we introduced the *NORK* coding sequence under the control of the *CaMV* 35S promoter into the *nork* mutant TR25 and under the control of a 2200 bp *NORK*-upstream putative promoter region (*NORKp::NORK*) (6). To determine whether this *NORK* upstream region truly represents the endogenous *NORK* promoter we cloned the 2200 bp *NORK* upstream-region also into a binary vector containing the *uidA* reporter gene encoding β -glucuronidase (GUS). The resulting plasmid was introduced into the plant by *Agrobacterium rhizogenes* mediated root transformation.

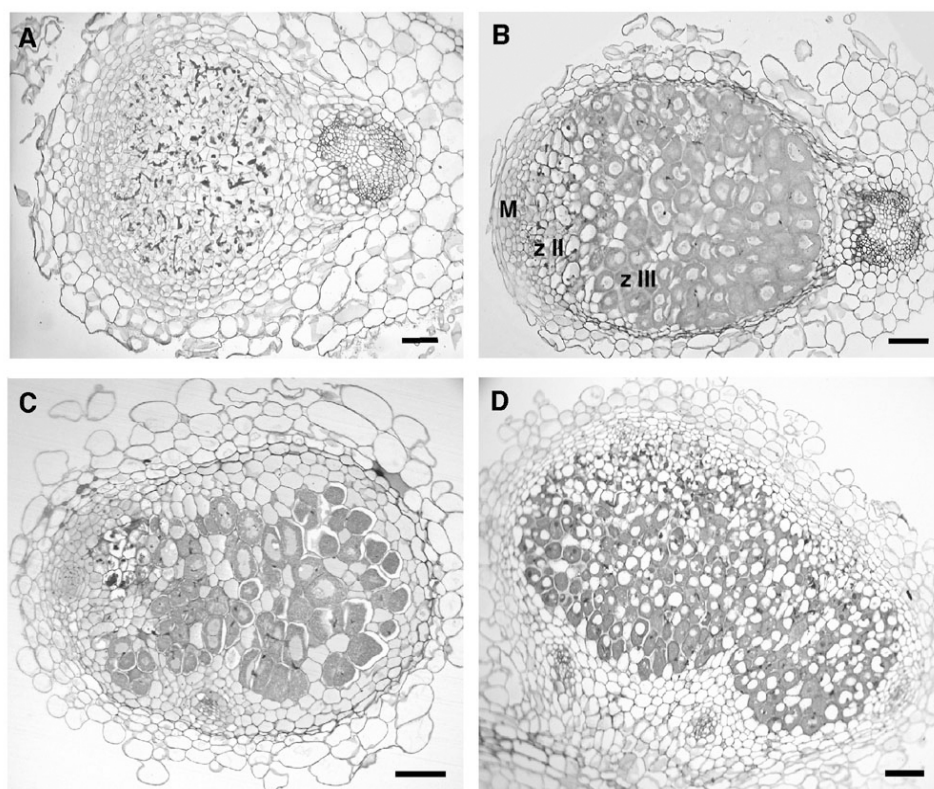


Figure 3. Histochemical analysis of nodules by light microscopy. Longitudinal sections (5 μ m) of 2-week-old nodules formed on (A) *NORK* knock-down (RNAi) roots, (B) wild type (A17) roots transformed with an empty binary vector, (C) *35S::NORK* transformed wild type roots and (D) *NORKp::NORK* transformed TR25 roots. Sections are stained with toluidine blue. M = meristem; z II = zone II or infection zone; z III = zone III or fixation zone with infected cells containing bacteroids. Bars in (A) to (D) = 100 μ m.

Histological GUS staining revealed that under non-symbiotic conditions the *NORK* promoter was active in all tissues of the root (Fig. 2B). Stronger GUS activity was detected in the root

apex containing dividing cells and in lateral root primordia. Quantitative RT-PCR on RNA isolated from root tips (excised ~3mm behind the tip) confirmed the strong expression of *NORK* in the root apex (Fig. 1). Upon inoculation with rhizobia *NORK* promoter activity was up-regulated in nodule primordia and root nodules. In 2-week-old nodules GUS activity was especially observed in the infection zone of the nodule, which is consistent with the expression pattern of *NORK* observed by the *in situ* hybridizations and indicates that the 2200 bp *NORK* upstream-region indeed represents the endogenous *NORK* promoter (Fig 2C).

Inoculation of *NORKp::NORK* transformed TR25 roots resulted in on average 7 nodules / transformed root (n=22), that showed a wild type histology including fully infected cells (Fig. 3D). This shows that the *NORK* cDNA construct was functional and could complement the TR25 mutant. Introduction of *35S::NORK* into wild type roots did not affect nodule development. Fourteen days after inoculation with *S. meliloti* 2011-pHC60 on average 8 nodules were formed per transformed root (n=8) and these nodules showed a normal histology (Fig. 3C). This shows that over-expression of *NORK* does not negatively affect nodulation. Introduction of *35S::NORK* into the TR25 mutant effectively complemented early Nod factor induced responses (data not shown), however, the nodulation efficiency was reduced. On average 2 nodules formed on a transformed TR25 root (n=43). Strikingly, histological examination of these nodules revealed a similar phenotype as observed in the *NORK* knock-down nodules; extensive infection thread growth in the central tissue of the nodule with no, or very few bacteria in the nodule cells.

Cytology of 35S::NORK transformed TR25 nodules

Introduction of *NORK* under the control of the 35S promoter into the *nork* mutant resulted in nodules with a similar histology as that of nodules obtained by RNAi. Because of higher nodule numbers and consistency of the phenotypes in the *35S::NORK* transformed TR25 roots, we studied the cytology of *35S::NORK* transformed TR25 nodules in more detail. Based on light microscopic analysis of semi-thin sections of the 2-week-old *35S::NORK* transformed TR25 nodules we divided the nodules into two groups. Group I consisted of small nodules (12-18 cell layers in longitudinal sections) showing very wide infection threads in many cells of the central tissue of the nodule as well as big intercellular bacterial colonies. The infection threads penetrated and traversed the cells and no release of bacteria into the nodule cells was observed (Fig. 4A to C). In sections of wild type nodules only a few infection threads are typically seen in cells of the central tissue (Fig 4D). Since the thickness (0.6-1 μ m) of semi-thin sections represents less than 1/20 -1/50 of the diameter of nodule cells, the occurrence of infection threads in almost every cell in a thin section of the *35S::NORK* TR25 nodules, indicates that the infection threads almost completely fill these cells.

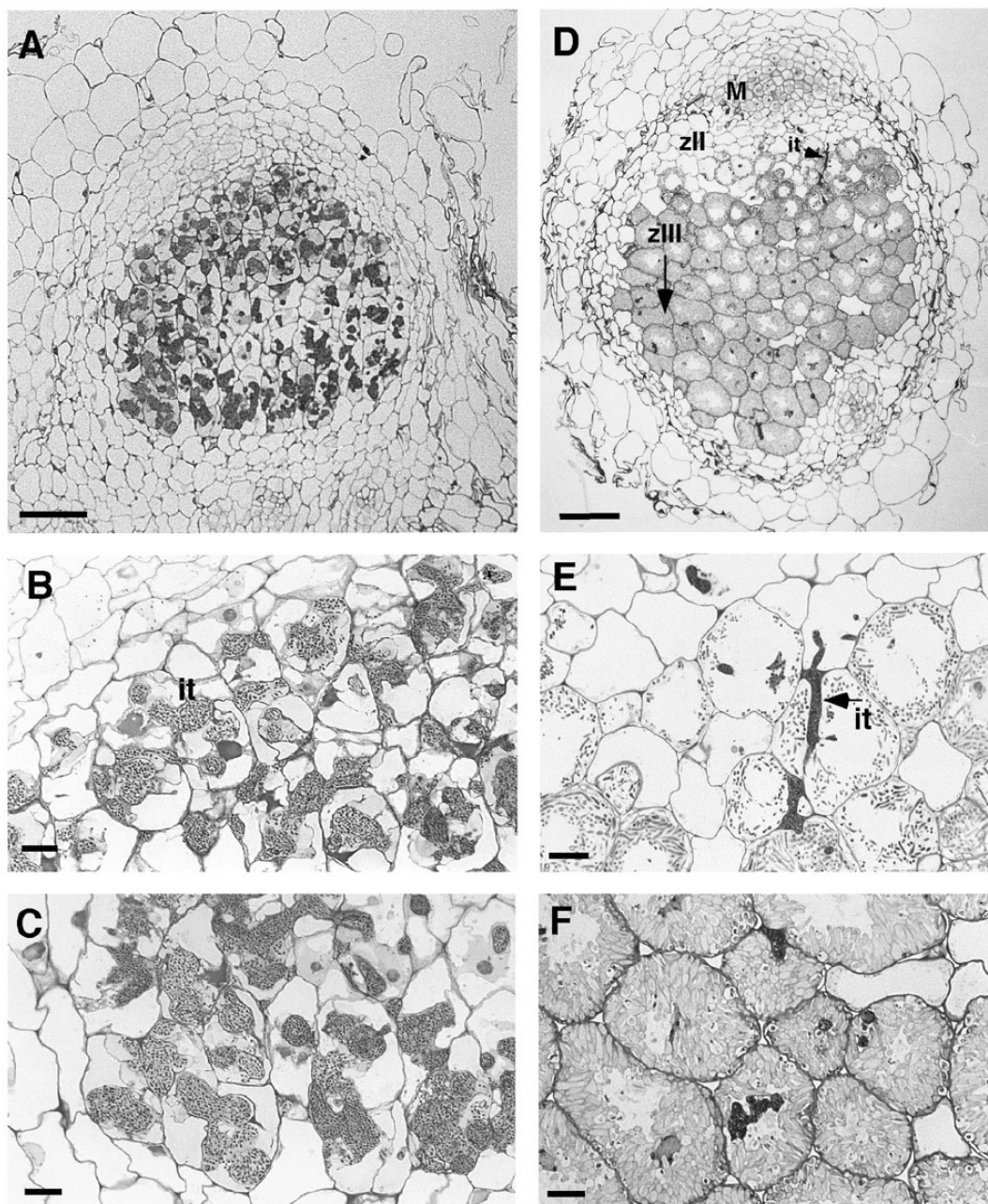


Figure 4. Histology of 2-week-old *35S::NORK* transformed TR25 group I nodules compared to control nodules. (A) Longitudinal section of a small *35S::NORK* transformed TR25 group I nodule shows that most cells of the central tissue contain an infection thread. These threads are very wide. (B,C) Magnification of (A) in the apical part and basal part of the nodule, respectively. No release of bacteria is observed. (D) Longitudinal section of a control nodule (transformed with an empty binary vector). A typical zonation of indeterminate nodules can be seen, with M = meristem; z II = infection zone and z III = zone III or fixation zone with infected cells containing elongated bacteroids. (D,E) Magnification of (D) in the infection zone and basal part of the nodule, respectively. Sections (0.6-1 μm) are stained with 0,5% toluidine, 0,5% methylene blue. It = infection thread. Bars in (A,D) = 100 μm , Bars in (B,C,E,F) = 20 μm .

Further, infected cells are interspersed by small groups of uninfected cells that have a function in the nitrogen assimilation process. These uninfected cells often form small

clusters in wild type nodules. Since several small groups of cells without infection threads could be observed in thin sections of the *35S::NORK* TR25 nodules, this suggests that the uninfected cell type can still be formed and are not penetrated by infection threads. Transmission electron microscopy showed that infection threads had a similar morphology as wild type infection threads with the bacteria embedded in a matrix with a low electron density surrounded by a fibrillar wall and a membrane (Fig. 6A). The only difference with wild-type infection threads was their length and diameter, with some threads accommodating up to 100 bacteria compared to 10-15 bacteria observed in cross-sections of infection threads in *35S::NORK* TR25 nodules and wild type nodules, respectively. The second group showed nodules that were bigger in size (22-30 cell layer long central tissue), and these also contained numerous (wide) infection threads and large intercellular bacterial colonies in the central tissue (Fig 5A). However, in these nodules intracellular bacteria were occasionally observed in the proximal cell layers (Fig. 5B).

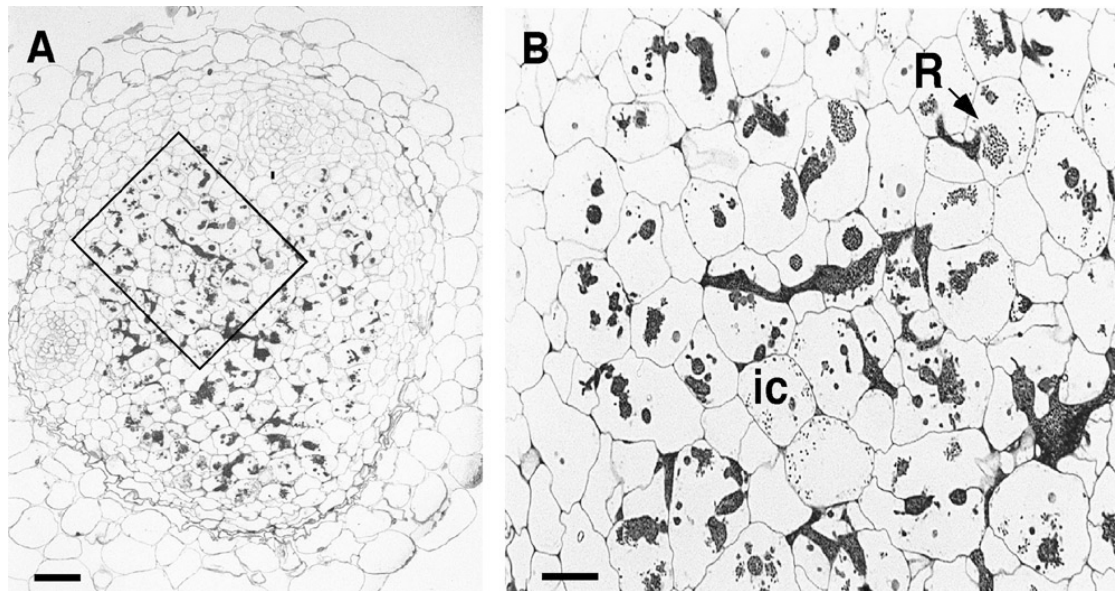


Figure 5. Light microscopic analysis of 2-week-old *35S::NORK* transformed TR25 group II nodules. (A) Longitudinal section of a *35S::NORK* transformed group II TR25 nodule. (B) Magnification of boxed area in (A) showing release of bacteria from the infection threads (R and arrow) and several infected cells (ic) containing few bacteroids in the cytoplasm. Bar in (A) = 100 μ m, Bar in (B) = 30 μ m

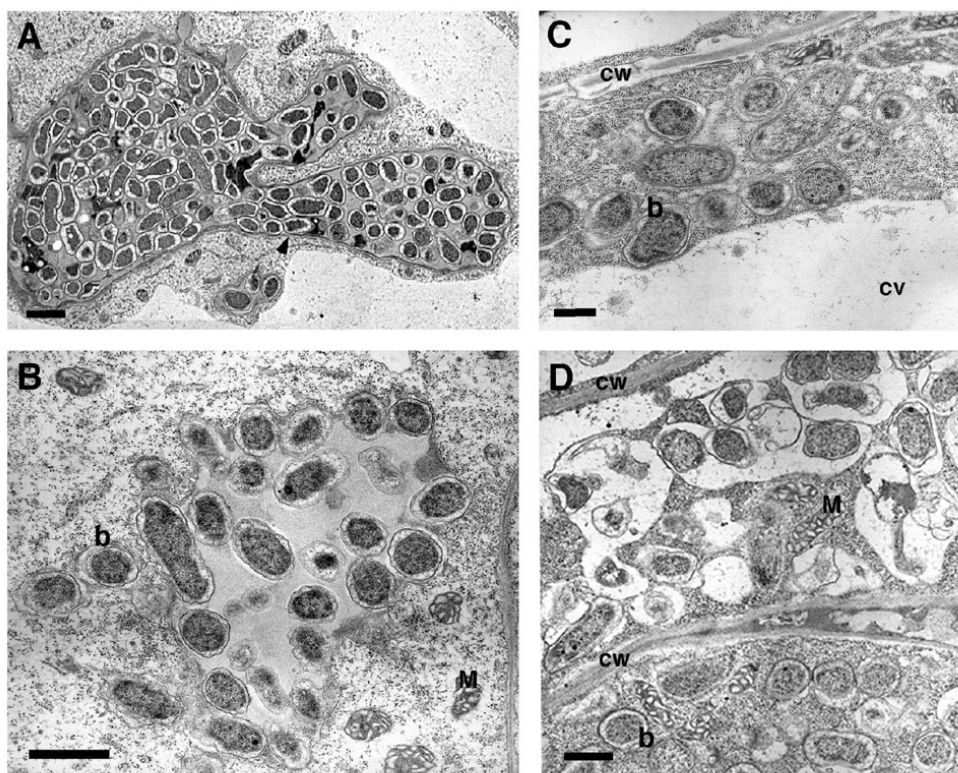


Figure 6. Transmission electron microscopy of 35S::NORK transformed TR25 nodules. (A) Section showing a nodule cell with an infection thread without releasing bacteria. The infection thread has a fibrillar wall and is surrounded by a membrane (arrow). (B) Release of bacteria from an unwalled infection droplet. Note that the released bacteria (b) are surrounded by a membrane. (C) Released bacteria do not elongate and are located in a thin layer of cytoplasm surrounding the big central vacuole. (D) Two cells containing bacteria at different stages of senescence. Some symbiosomes have a big peribacteroid space and symbiosome membranes have fused to form vacuole-like structures, some ghost membranes probably of lysed bacteria are present. CW = cell wall, M = mitochondria, b = bacteroid, cv = central vacuole. Bars in (A to C) = 1 μ m, Bar in (D) = 0.5 μ m.

In wild type nodules infection thread growth is directed towards the meristem and bacteria are normally released in the first 2 – 3 cell layers adjacent to the meristem after which they start to multiply (Fig. 4D to F). In most of the 2-week old 35S::NORK transformed TR25 nodules no meristem was observed, and release of bacteria, as judged by the presence of unwalled infection droplets, appeared to occur in the more proximal cell layers. Such events are rare and most infection threads invaded and traversed the cells without release of bacteria. In the cases where bacterial release was observed division of the bacteria was limited as only a few symbiosomes were observed in the cytoplasm of the infected cells and these infected cells did not show an increase in cell size, which is typically observed (3 - 4x) in wild type infected cells (Fig. 4D). Transmission electron microscopy revealed that bacteria were released inside the living cells from unwalled infection droplets. From these unwalled droplets single bacteria emerged that were surrounded by a plant-derived membrane, the symbiosome membrane (Fig. 6B) (16,19). However, the released bacteria did not elongate as observed in wild type infected cells (15) (Fig. 6C). Some of the

symbiosomes revealed typical features of premature senescence, having an electron dense cytoplasm, abnormal morphologies and some symbiosomes seemed to fuse, forming vacuole-like structures causing lysis of bacteroids entrapped inside (Fig. 6D). In several *35S::NORK* transformed TR25 nodules, especially older nodules, the host cells in the central and basal part of the nodule also showed premature senescence with loss of cytoplasm and without visible nuclei. These cells appeared to be repopulated by saprophytic bacteria (data not shown).

Discussion

The *NORK* gene was shown to be required for the induction of many Nod factor induced epidermal responses, such as the induction of early nodulin genes, infection thread formation and also the induction of cortical cell divisions (6). Here we show that a high *NORK* expression level in the distal part of the infection zone of the nodule is required to restrict infection thread growth in the nodule and to facilitate the release of bacteria into the plant host cells. Since *NORK* is an essential component of the Nod factor perception and signaling machinery this suggests a role for Nod factor signaling in these processes in the nodule.

In situ hybridisation revealed high *NORK* expression levels in 2 – 3 cell layers of the infection zone adjacent to the meristem. Previously, it has been shown that rhizobial *nod* genes are active in these cell layers (13,14). This suggests that Nod factor signaling takes place in this zone. Whether the zone where Nod factor signaling takes place is larger than the first 3 cell layers of the infection zone will depend on the stability of the Nod factor signaling proteins. The *in situ* hybridization studies of Schlaman *et al.*, (14) indicate that *nod* gene expression coincides with the region where *NORK* is expressed. The studies of Sharma and Signer (13) suggest that the *nod*-expressing zone might be broader. However it seems probable that this is due to the stability of the GUS protein that has been used as reporter. Infection threads grow in the direction of and penetrate new cells that originate from dividing meristem cells. Bacteria are released from the infection threads in the 2-3 cell layers adjacent to the meristem after which the symbiosomes start to multiply (15,20). Thus the region where *NORK* is expressed in the nodule coincides with the place where the rhizobial *nod* genes are active and corresponds to the region where infection thread growth and release of bacteria from the infection threads and subsequent division take place. This suggests a role for Nod factor signaling via *NORK* in these processes.

Partial knock down of *NORK* expression via RNAi affected infection thread growth and release of bacteria in the nodule cells. In most roots knock-down of *NORK* expression by RNAi blocked nodulation at an initial step, since nodules are not formed. Therefore we expect that in RNAi knock down roots, which still allow nodules to be formed, that *NORK* mRNA levels are less reduced. This indicates that the observed nodule phenotypes are the

result of partial knock down of *NORK* expression. As other Nod factor responses appeared to be induced in these partial knock down roots this suggests that the switch from infection thread growth to release of bacteria (and possibly division of symbiosomes) requires a higher threshold level of *NORK* than do other Nod factor responses. Fifty percent of the *NORK* RNAi nodules did not show an aberrant nodulation phenotype, indicating that *NORK* expression levels in these nodules still reached the threshold level. In line with the hypothesis that relatively high expression levels of *NORK* need to be reached to facilitate bacterial release is the observation that over-expression of *NORK* in wild type roots under the control of the 35S promoter did not negatively affect nodulation. It further indicates that expression of *NORK* in the proximal cell layers does not affect nodulation. Introduction of 35S::*NORK* into the mutant background resulted in similar nodule phenotypes as observed in the knock-down nodules. This suggests that the phenotypes observed in the 35S::*NORK* transformed TR25 nodules are also the result of *NORK* mRNA levels that are below the threshold value needed to induce bacterial release.

The most markedly affected processes in these “*NORK* mutant” nodules was the release of bacteria from the infection threads and the sustained growth of infection threads that continually invaded and traversed cells without releasing bacteria. The observation of clusters of cells that are not invaded by infection threads in the semi-thin sections suggests that, although the infection threads appear to be numerous, still uninfected cells are present. This indicates that in the RNAi and 35S::*NORK* TR25 nodules not more cells are infected by rhizobia, but rather that in the infected cells the switch from infection thread growth to bacterial release is disturbed by which infection threads occupy large parts of these cells. Occasionally, release of bacteria was observed in the more proximal cell layers of the 35S::*NORK* transformed TR25 nodules. However, only a few bacteria occur in these nodule cells, which indicates that the symbiosomes do not efficiently divide. As a result no increase in cell size of the infected cells was observed, which is typical for wild type infected cells (15,20). The fact that release occurs in older cells that are in a different developmental stage could be a reason for the impaired division of the bacteria in the proximal cell layers of the 35S::*NORK* TR25 nodules. However, it cannot be excluded that Nod factor signaling plays a role in this process as well.

The release of bacteria from an infection thread coincides with the stop of growth of this thread. Infection thread growth involves the deposition of plant cell wall material to the growing thread, while release of bacteria from the infection thread involves the formation of unwallied infection droplets that extrude from the infection threads (16,19,21). From such unwallied infection droplets single bacteria are released into the cytoplasm that stay surrounded by a plant derived symbiosome membrane (16,22). Although the molecular basis of bacterial release is unknown, it is thought to be related to the process of endocytosis (16,23). It is clear that the symbiosomal membrane and the membrane surrounding the infection droplets have no associated plant cell wall (16,23). Thus the

release of bacteria from the infection thread seems to involve a change in the kind of vesicles, and their cargo, that fuse with the tip of the infection thread by which infection thread growth is not sustained, but instead unwallated droplets are formed. Nod factor signaling via NORK appears to be involved in inducing this switch in infection thread growth. The continued growth of infection threads and large intercellular bacterial colonies, as observed in the “NORK mutant” nodules, could both be a consequence of continued secretion of infection thread matrix to the tip of the infection thread and into the intercellular spaces allowing the bacteria to proliferate there. It can thus be hypothesized that sustained infection thread growth and suppressed release of bacteria are interlinked processes. Further, Nod factor signaling involving high threshold levels of NORK is essential in the switch from infection thread growth to release of bacteria in the nodule.

Infection thread growth and “endocytosis” of the bacteria both require continuous and extensive membrane proliferation, cytoskeletal rearrangements as well as targeted vesicle transport (23,24). The underlying molecular mechanism of a switch from infection thread growth to release of bacteria is therefore expected to involve regulation of cytoskeletal organization (microtubuli and/or actin) and targeting of vesicle insertions to the tip of infection threads. The observation that redirecting and sustaining polar growth of root hairs in response to Nod factors is impaired in the *NORK* knock-out mutants supports the idea that NORK facilitates cytoskeletal re-organization and vesicle transport (6). Examination of the actin cytoskeleton and microtubule structure in response to Nod factor treatment in root hairs of the *NORK* knock-out mutants and in nodule cells of the knock-down mutants, should give insight into Nod factor signaling to the cytoskeleton. As small GTPases (e.g. ROPs) are known to be key regulators of the cytoskeletal organization and vesicular transport (25), these might represent likely downstream targets of Nod factor signaling via NORK.

Release of bacteria into the nodule cells appears to require higher *NORK* mRNA levels than Nod factor induced epidermal responses and induction of cortical cell divisions. This could indicate that NORK associates in different (Nod factor perception) complexes in the nodule cells. As infection thread growth, which depends on Nod factor signaling in the epidermis, still occurs in “*NORK* mutant” nodules it shows that infection thread growth and release of bacteria in the nodule require different threshold levels of NORK. Therefore, it cannot be excluded that Nod factor signaling plays additional roles in the nodule, e.g. in infection thread growth. However, since the rhizobial *nod* genes appear to be switched off as soon as bacteria are released into the cells it is unlikely that Nod factor signaling plays a role in the subsequent cell layers of the nodule.

Materials and Methods

Plasmids and vectors

To isolate the *NORK* promoter a 2200 bp region upstream from the ATG startcodon was PCR amplified from Medicago A17 genomic DNA using primers that introduce *Hind*III and *Bam*HI restriction sites and cloned into pGEM-t (Promega): 5' AAGCTTCAAATTTGGACCGAACTG 3' and 5' GGATCCAACTTGAATCCATGCTAACTAACT 3'. This fragment was cloned *Hind*III-*Bam*HI into the pCambia1304 binary vector from which all *CaMV* 35S sequences were deleted, resulting in the *NORKp::GUS* fusion construct. The full length *NORK* coding sequence was PCR amplified from Medicago root cDNA using primers containing *Nhe*I and *Sac*I restriction-sites: 5' CTAGCTAGCATGATGGAGTTACAAGTTATTAAG 3' and 5' TCCGAGCTCTATAGCTCTGTTGAAGTGTC 3'. The 3103 bp fragment was subsequently cloned into pGEM-t (Promega). After sequence analysis, the full length *NORK* cDNA was cloned *Nhe*I-*Sac*I into a modified pBluescriptII SK+ vector, which contains the *CaMV* 35S promoter from pMON999 (Monsanto) or the *NORK* promoter and a *NOS*-terminator sequence with an introduced *Pac*I restriction-site and subsequently cloned *Hind*III-*Pac*I into the binary vector pRedRoot (18), resulting in *d35S::NORK* and *NORKp::NORK*.

Plant material and rhizobial strain

Medicago accession Jemalong A17 and *nork* mutant TR25 containing *MtENOD11::GUS* (6) were used for transformations. The Medicago A17 line containing *ENOD11::GUS* was kindly provided by David Barker/Annemie Emons. *Sinorhizobium meliloti* 2011.pHC60 (3) was used to inoculate plants.

A. rhizogenes mediated transformation and RNAi

Agrobacterium strain MSU440 containing the pRi plasmid pRiA4 (26) was used to transform Medicago. The binary vectors were introduced into MSU440 by electrotransformation and grown for two days at 28°C under kanamycin selection (50 µg/ml). *A. rhizogenes* mediated root transformation of 5 day old Medicago seedlings was performed according to Limpens *et al.* (3). *A. rhizogenes* mediated RNAi of *NORK* was performed as described in Limpens *et al.* (3).

Plant assays

Medicago seeds were surface sterilized by incubating for 10 min. in concentrated Sulfuric acid, 6x washing in sterile water, 10 min incubation in 4% hyper chlorite (commercial bleach) and 7x washing in sterile water and subsequently plated on Färhaeus medium (3). Seeds were vernalized for 1 day at 4°C and germinated at 25°C for 24 hours in darkness. For mass-inoculation with *S. meliloti* 2011.pHC60 composite Medicago plants were starved for nitrate for 3 days (22°C; 16h light-8h darkness) on agra-perlite (Maasmond-Westland, The Netherlands) saturated with Färhaeus medium (without Ca(NO₃)₂). Plants were inoculated with 1 ml culture of *S. meliloti* 2011.pHC60 (OD600: 0.1) per plant and grown for two weeks (22°C; 16h light-8h darkness). Root hair deformation studies were performed with 10⁻⁹ M *S. meliloti* Nod factors added directly to transformed plants growing on BNM medium (27) with 1.2% agar and 0.1 µM AVG. 6 hours after treatment with 10⁻⁹ M *S. meliloti* Nod factors *A. rhizogenes* transformed roots were stained for *ENOD11::GUS* activity. Root hair deformations were checked 16h post inoculation after staining with 0.002% methylene blue. To examine cortical cell divisions *A. rhizogenes* transformed roots were grown on BNM medium and spot inoculated with ~0.3 µl *S. meliloti* 2011.pHC60 (OD600: 0.1).

Histochemical analysis and microscopy

Histochemical GUS staining was performed according to Jefferson *et al.* (28), with few modifications. Plant material was incubated in 0.05% (w/v) X-Gluc (Duchefa) in 0.1M sodium phosphate buffer (pH 7) with 3%

sucrose, 5µM potassium-ferrocyanide and 5µM potassium. Roots were infiltrated for 30 min. under vacuum and further incubated at 37°C.

For sectioning, roots or nodules (Fig. 2 and 3) were fixed for 1h in 2.5% glutaraldehyde buffered in 0.1M sodium phosphate buffer (pH 7), dehydrated in an alcohol series and embedded in Technovit 7100 (Heraeus Kulzer). 5 µm-thick sections were made using a Leica microtome, stained with 0.04% toluidine blue or 0.1% ruthenium red and mounted on glass slides with Euparal (Agar Scientific LTD.).

For electron microscopy, nodules were fixed for 3,5h in a mixture of 4% paraformaldehyde and 3% glutaraldehyde in 50 mM potassium phosphate buffer, pH 7.4. The nodules were postfixed for 3h with 1% osmium tetroxide, dehydrated through an ethanol series and embedded in London Resin White. Ultrathin sections (60 nm) were obtained with a Reichert Ultracuts Leica ultratome, stained with 2% of uranyl acetate and Reynolds lead citrate solution, and observed with a Philips EM208 electron microscope (Eindhoven, the Netherlands). For light microscopy semithin sections (1-0,6 mm; Fig. 4 and 5) were stained with 1:1 mix of 1% toluidine blue and 1% methylene blue solution and embedded in Paraplast (EMS). Sections were viewed with a Nikon Optiphot-2 microscope. Images were processed electronically using Adobe Photoshop 6.0. Imaging of DsRED1 or GFP fluorescence was done using the Leica MZIII fluorescence stereomicroscope and a Nikon Optiphot-2 coupled to a mercury-lamp.

RNA extraction and qPCR

Total RNA was extracted from un-inoculated roots, roots inoculated with *S. meliloti* 2011 48h dpi, root tips (excised ~3mm behind the tip), leaves, stem, flowers and 2-week-old nodules according to Pawlowski *et al.*, (29) followed by DNaseI (Promega) treatment. cDNA was made from 1 µg total RNA using the Taqman Gold RT-PCR kit (Perkin-Elmer Applied Biosystems) in a total volume of 50 µl using the supplied hexamer primers. qPCR reactions were performed in triplo on 6,5 µl cDNA using the SYBR-GreenR PCR Master kit (Perkin-Elmer Applied Biosystems; 40 cycles of 95°C for 10 s, 60°C for 1 min) and real-time detection was performed on the ABI 7700 and analyzed using the GeneAmp 5700 SDS software (Perkin-Elmer Applied Biosystems). The specificity of the PCR amplification procedures was checked with a heat dissociation step (from 60°C-95°C) at the end of the run and by agarose gel electrophoresis. Results were standardized to the *MtACTIN2* expression levels. Primers used: *MtACTIN2*: 5' TGGCATCACTCAGTACCTTTCAACAG 3' and 5' ACCCAAAGCATCAAATAATAAGTCAACC 3' *MtDMI-2*: 5' TGGACCCCTTTTGAATGCCTATG 3' and 5' TCCACTCCAACCTCTCCAATGCTTC 3'

In situ hybridization

Nodules were harvested 14 days post-inoculation and fixed in 4% paraformaldehyde supplemented with 0.25% glutaraldehyde in 10 mM sodium phosphate buffer (pH 7.4) for 3 h (30). Fixed nodules were dehydrated, by passing through a series of grade ethanol, and embedded into paraffin (Paraclean; Klinipath, Duiven, The Netherlands) by routine methods (30). Sections (7 µm) were dried on polylysine-coated slides at 37° C overnight, deparaffinized with xylene and rehydrated via a graded ethanol series. Hybridisation pre-treatment, hybridisation and washing were performed as described by Cox (31) and adapted by Van de Wiel (30). For preparing antisense *NORK* RNA probes the fragments 373-617 bp, 784-1039 bp, 1200-1453 bp, 1610-1864 bp and 1964-2219 bp within the *NORK* coding region, were PCR amplified and subcloned into a pGEM-t vector (Promega). An Apal restriction site in the 3' end primer (see below) allowed the removal of polylinker sequences from the vector. Subsequently, the fragments were amplified by PCR using M13-forward and 5' end primers specific for the *NORK* fragments. The amplified fragments were used as substrate to synthesise antisense RNA probes with T7 RNA polymerase (Promega), in the presence of [³⁵S]-UTP (1000-1500 Ci mmol⁻¹, Amersham). For the hybridisation a mixture containing 1 × 10⁶ cpm of each probe was used. After washing, the slides were coated with microautoradiography emulsion LM-1 (Amersham) and exposed for 3 weeks at 4° C. They were developed for 5 min in Kodak D-19 developer (East-man Kodak, Rochester, NY) and fixed in Kodak fixative. Sections were

counterstained with toluidine blue and subsequently mounted. For imaging a Nikon (Tokyo, Japan) optiphot-2 bright field microscope was used. Primers used for *NORK* fragments (*Apal* restriction-site underlined):

373-617bp: 5' TCATGATGGAGTTACAAGTTATTA 3' and 5' GGGCCCTTTTTATTGCTTCTGTGG 3'
 784-1039bp: 5' GAGGACTTGGAAATTGAGGGAG 3' and 5' GGGCCCATGTTGGAGTTGAAGTT 3'
 1200-1453bp: 5' CTTTCTTGAATAAATGGCACTGT 3' and 5' GGGCCCTTTTGGTTGGTCTCTTCA 3'
 1610-1864bp: 5' ATCTTTCTCCAATAATCTCAAGGG 3' and 5' GGGCCCTTGTTGTATCTTCGTCCTC 3'
 1964-2219bp: 5' CACTTTTGATTACTTTGGCTGTTG 3' and 5' GGGCCCTCTAGAGTGCCCTGTAAAC 3'

References

- 1 Oldroyd GED: **Dissecting symbiosis: Development in Nod factor signal transduction.** *Ann Bot* 2001, **87**: 709-718.
- 2 Limpens E, Bisseling T: **Signaling in Symbiosis.** *Curr Opin Plant Biol* 2003, **6**: 343-350.
- 3 Limpens E, Franken C, Smit P, Willemse J, Bisseling T, Geurts R: **LysM domain receptor kinases regulating rhizobial Nod factor-induced infection.** *Science* 2003, **302**: 630-633.
- 4 Madsen EB, Madsen LH, Radutoiu S, Olbryt M, Rakwalska M, Szczyglowski K, Sato S, Kaneko T, Tabata S, Sandal N, Stougaard J: **A receptor kinase gene of the LysM type is involved in legume perception of rhizobial signals.** *Nature* 2003, **425**: 637-640.
- 5 Radutoiu S, Madsen LH, Madsen EB, Felle HH, Umehara Y, Gronlund M, Sato S, Nakamura Y, Tabata S, Sandal N, Stougaard J: **Plant recognition of symbiotic bacteria requires two LysM receptor-like kinases.** *Nature* 2003, **425**: 585-592.
- 6 Catoira R, Galera C, De Billy F, Penmetsa RV, Journet EP, Maillat F, Rosenberg C, Cook D, Gough C, Dénarié J: **Four genes of *Medicago truncatula* controlling components of a Nod factor transduction pathway.** *Plant Cell* 2000, **12**: 1647-1666.
- 7 Endre G, Kereszt A, Kevei Z, Mihacea S, Kaló P, Kiss GB: **Cloning of a receptor kinase gene regulating symbiotic nodule development.** *Nature* 2002, **417**: 962-966.
- 8 Ané JM, Kiss GB, Riely BK, Penmetsa RV, Oldroyd GE, Ayax C, Levy J, Debelle F, Baek JM, Kaló P, Rosenberg C, Roe BA, Long SR, Dénarié J, Cook DR: ***Medicago truncatula* DMI1 required for bacterial and fungal symbioses in legumes.** *Science* 2004, **303**: 1364-1367.
- 9 Levy J, Bres C, Geurts R, Chalhoub B, Kulikova O, Duc G, Journet EP, Ané JM, Lauber E, Bisseling T, Dénarié J, Rosenberg C, Debelle F: **A putative Ca²⁺ and calmodulin-dependent protein kinase required for bacterial and fungal symbioses.** *Science* 2004, **303**: 1361-1364.
- 10 Mitra RM, Gleason CA, Edwards A, Hadfield J, Downie JA, Oldroyd GE, Long SR: **A Ca²⁺/calmodulin-dependent protein kinase required for symbiotic nodule development: Gene identification by transcript-based cloning.** *Proc Natl Acad Sci USA* 2004, **0**: 40059510-0.
- 11 Wais RJ, Galera C, Oldroyd G, Catoira R, Penmetsa RV, Cook D, Gough C, Dénarié J, Long SR: **Genetic analysis of calcium spiking responses in nodulation mutants of *Medicago truncatula*.** *Proc Natl Acad Sci USA* 2000, **97**: 13407-13412.
- 12 Stracke S, Kistner C, Yoshida S, Mulder L, Sato S, Kaneko T, Tabata S, Sandal N, Stougaard J, Szczyglowski K, Parniske M: **A plant receptor-like kinase required for both bacterial and fungal symbiosis.** *Nature* 2002, **417**: 959-962.
- 13 Sharma SB, Signer ER: **Temporal and spatial regulation of the symbiotic genes of *Rhizobium meliloti* in planta revealed by transposon *Tn5-gusA*.** *Genes Dev* 1990, **4**: 344-356.
- 14 Schlaman HR, Horvath B, Vijgenboom E, Okker RJ, Lugtenberg BJ: **Suppression of nodulation gene expression in bacteroids of *Rhizobium leguminosarum* biovar *viciae*.** *J Bacteriol* 1991, **173**: 4277-4287.
- 15 Vasse J, de Billy F, Camut S, Truchet G: **Correlation between ultrastructural differentiation of bacteroids and nitrogen fixation in alfalfa nodules.** *J Bacteriol* 1990, **172**: 4295-4306.
- 16 Brewin NJ: **Development of the legume root nodule.** *Annu Rev Cell Biol* 1991, **7**: 191-226.
- 17 Chuang C, Meyerowitz M: **Specific and heritable genetic interference by double-stranded RNA in *Arabidopsis thaliana*.** *Proc Natl Acad Sci USA* 2000, **97**: 4985-4990.
- 18 Limpens E, Ramos J, Franken C, Raz V, Compaan B, Franssen H, Bisseling T, Geurts R: **RNA interference in *Agrobacterium rhizogenes* transformed roots of *Arabidopsis* and *Medicago truncatula*** *Journal of Experimental Botany* 2004, **55**: in press.
- 19 Roth LE, Stacey G: **Bacterium release into host cells of nitrogen-fixing soybean nodules: the symbiosome membrane comes from three sources.** *Eur J Cell Biol* 1989, **49**: 13-23.
- 20 Kijne JW: **The *Rhizobium* infection process.** In: Stacey G, Burris RH, Evans HJ, eds. *Biological Nitrogen Fixation*. New York: Chapman and Hall, 1992: 349-398.

- 21 Callaham DA, Torrey JG: **The structural basis for infection of root hairs of *Trifolium repens* by *Rhizobium*.** *Can J Bot* 1981, **59**:1647-1664.
- 22 Rae AL, Bonfante-Fasolo P, Brewin NJ: **Structure and growth of infection threads in the legume symbiosis with *Rhizobium leguminosarum*.** *Plant J* 1992, **2**: 385-395.
- 23 Brewin NJ: **Tissue and cell invasion by *Rhizobium*: The structure and development of infection threads and symbiosomes.** In: Spaink HP, Kondorosi A, Hooykaas PJJ, eds. *The Rhizobiaceae*. Dordrecht: Kluwer Academic Publishers, 1998: 417-429.
- 24 Verma DP, Hong Z: **Biogenesis of the peribacteroid membrane in root nodules.** *Trends Microbiol* 1996, **4**: 364-368.
- 25 Yang Z: **Small GTPases: versatile signaling switches in plants.** *Plant Cell* 2002, **14** Suppl: S375-S388.
- 26 Sonti RV, Chiurazzi M, Wong D, Davies CS, Harlow GR, Mount DW, Signer ER: ***Arabidopsis* mutants deficient in T-DNA integration.** *Proc Natl Acad Sci USA* 1995, **92**: 11786-11790.
- 27 Ehrhardt DW, Atkinson EM, Long SR: **Depolarization of alfalfa root hair membrane potential by *Rhizobium meliloti* Nod factors.** *Science* 1992, **256**: 998-1000.
- 28 Jefferson AR, Kavanagh TA, Bevan MW: **Gus fusions: β -glucuronidase as a sensitive and versatile gene fusion marker in higher plants.** *EMBO J.* 1987, **6**: 3901-3907.
- 29 Pawlowski K, Kunze R, de Vries S, Bisseling T: **Isolation of total, poly(A) and polysomal RNA from plant tissues.** In: Gelvin, SB Schilperoort RA (eds) *Plant Molecular Biology Manual*. Kluwer Academic Publishers. Dordrecht 1994, pp D5 1-13.
- 30 Van De Wiel C, Norris JH, Bochenek B, Dickstein R, Bisseling T: **Nodulin gene expression and *ENOD2* localization in effective, nitrogen-fixing and ineffective, bacteria-free nodules of alfalfa.** *Plant Cell* 1990, **2**: 1009-1017.
- 31 Cox KH, Goldberg RB: **Analysis of plant gene expression.** In: *Plant Molecular Biology: A practical approach*, C.H. Shaw, ed. Oxford: IRL Press 1988, pp 1-34.

CHAPTER 6

The Expression Pattern of Nod Factor Signaling Genes Reveals a role for Nod Factor Signaling in Nodule Infection

Abstract

The perception of *Rhizobium* nodulation factors (Nod factors) by the root epidermis of legumes triggers the formation of nitrogen-fixing root nodules. Recently several components involved in the Nod factor perception and transduction have been cloned. In *Medicago truncatula* these include *LYK3* and *NFP*, supposed to function as Nod factor receptors, and downstream components such as *NORK*, *DMI1* and *DMI3*. Since the bacterial *nod* genes, involved in the Nod factor biosynthesis, are expressed in nodules a role for the Nod factor signaling can be proposed in this organ. To test this hypothesis we analyzed the expression pattern of the different Nod factor signaling genes in nodules by *in situ* hybridization. We showed that all the above mentioned genes are highly induced in the first 3 cell layers of the nodule infection zone, the same region in which the *nod* genes are expressed. This region corresponds to the place where infection threads branch, invade the host cells and bacteria release occurs. Therefore, this suggests a role for the Nod factor signaling machinery in these processes.

Rossana Mirabella, Marijke Hartog, Carolien Franken, Ton Bisseling and René Geurts

Introduction

The formation of nitrogen fixing nodules on the roots of legumes starts with a molecular dialogue between the host and its microsymbiont, *Rhizobium* (Mylona et al., 1995; Cohn et al., 1998; Geurts and Bisseling, 2002). Flavonoids, excreted by the roots of the host, are recognized by the rhizobia and this leads to the induction of the bacterial nodulation (*nod*) genes. The proteins encoded by these genes are involved in the biosynthesis and secretion of specific lipo-chito-oligosaccharides, the so-called Nod factors, which are required and in most cases sufficient to establish the early steps of this bacterium-plant interaction (Spaink et al., 1991; Cullimore et al., 2001).

The interaction starts at the epidermis where root hairs deform and some form curls in which the rhizobia become entrapped. Subsequently, the bacteria invade the host by a newly formed infection thread that grows towards the base of the root hair. Concomitantly, cortical cells divide in a local manner to form a nodule primordium. The infection thread traverses the root cortical cells and grows towards the nodule primordium, where bacteria are released from the infection threads into the cytoplasm of the host cells. Subsequently, the primordium develops into a nodule, in which the bacteria reduce nitrogen into ammonia that can be utilized by the plant.

Genetic analysis in pea and in the model legumes *Medicago truncatula* (Medicago) and *Lotus japonicus* (Lotus) have identified sets of symbiosis specific genes that are essential for Nod factor perception and transduction. Recently, most of these Nod factor signaling (NFS) genes have been cloned and they appear to be orthologous in the 3 above mentioned legumes. Nod factor perception most likely involves transmembrane LysM domain containing receptor kinases that are proposed to form heterodimeric Nod factor receptors (Limpens et al., 2003; Madsen et al., 2003; Radutoiu et al., 2003). In Medicago these include LYK3 and LYK4 (Limpens et al., 2003) and NFP (Amor et al., 2003; C. Gough and R. Geurts, unpublished). Downstream components of the Nod factor signaling pathway in Medicago are the DOES NOT MAKE INFECTION1 (*DMI1*; Ane et al., 2004), the *DMI3* (Levy et al., 2004; Mitra et al., 2004) and the NODULATION RECEPTOR KINASE (*NORK*; Endre et al., 2002), encoding for a putative cation channel, a calcium/calmodulin-dependent protein kinase and a leucine-rich repeat receptor-like protein kinase, respectively. The Lotus orthologue of NORK has also been cloned (Stracke et al., 2002). Plants carrying mutations in these genes are blocked at the stage of root hair deformation (Catoira et al., 2000; Wais et al., 2000; Stracke et al., 2002). Beside these Nod factor signaling genes, a putative transcription factor, named NODULE INCEPTION (*NIN*), essential for infection thread formation and nodule primordium initiation has been characterized (Schauser et al., 1999; Borisov et al., 2003). This gene has been cloned in Lotus and pea (Schauser et al., 1999; Borisov et al., 2003) and here we describe the cloning of the Medicago *NIN* gene.

Temperate legumes, such as *Medicago*, form indeterminate nodules (Crespi and Galvez, 2000). These nodules contain a persistent meristem, also designated as zone I, located at the nodule apex and characterized by small cells rich in cytoplasm that do not contain any bacteria or infection threads. The meristem continuously divides by which it is maintained and also adds new cells to the different nodule tissues. As a consequence the nodule central tissue can be divided into several zones representing successive developmental stages, from the apex (distal region) to the root attachment point (proximal region). The cell layers adjacent to the meristem form the infection zone, also indicated as zone II. In the distal region of zone II infection threads branch and penetrate host cells, in which bacteria are released. The released bacteria, enclosed in a membrane envelop and now called symbiosomes, proliferate and start to differentiate into the nitrogen-fixing forms. In the nitrogen fixing zone (zone III), at the base of the nodule, the plant cells are completely filled with thousands of nitrogen-fixing bacteroids.

Nod factors induce several responses in the epidermis and are also sufficient to induce the formation of nodule primordia (Cullimore et al., 2001; Geurts and Bisseling, 2002). However, their involvement in later stages of nodule development is less clear. The best indication that Nod factors play a role at such later stages comes from studies showing that rhizobial *nod* genes are expressed in the distal part of the nodule infection zone (Sharma and Signer, 1990; Schlaman et al., 1991). This suggests that the Nod factors are produced in the nodule in the zone where infection threads grow and bacteria are released. In case Nod factors induce responses in the nodule this probably requires the presence of a Nod factor perception and transduction machinery. To obtain insight in this we studied whether and where the above described NFS genes and *MtNIN* are active in *Medicago* nodules. We used a combination of real time RT-PCR and *in situ* hybridization and due to the indeterminate growth behavior of *Medicago* nodules an accurate correlation between Nod factor signaling gene expression and developmental stage has been obtained.

Results

Zonation of the central tissue of Medicago nodules

We first determined whether in *Medicago* nodules sharp boundaries could be identified between meristem and infection zone, and infection and fixation zone, respectively, as already described for Pea and alfalfa nodules (Scheres et al., 1990; Vasse et al., 1990; Yang and Bisselin, 1993). For this purpose we analyzed the expression pattern of the same set of marker genes that were used in these species on longitudinal sections from nodules 14 days after inoculation (d.p.i); namely the early nodulin gene *MtENOD12*, *LEGHEMOGLOBIN (LB)* and the bacterial gene *nifH*, encoding Nitrogenase component II.

MtENOD12 mRNA is present at its maximal level in the distal cell layers of the infection zone II adjacent to the meristem but it is not active in this meristem (Fig. 1A and B). Therefore, we

conclude that also in *Medicago* a sharp boundary exists between the meristem and the infection zone.

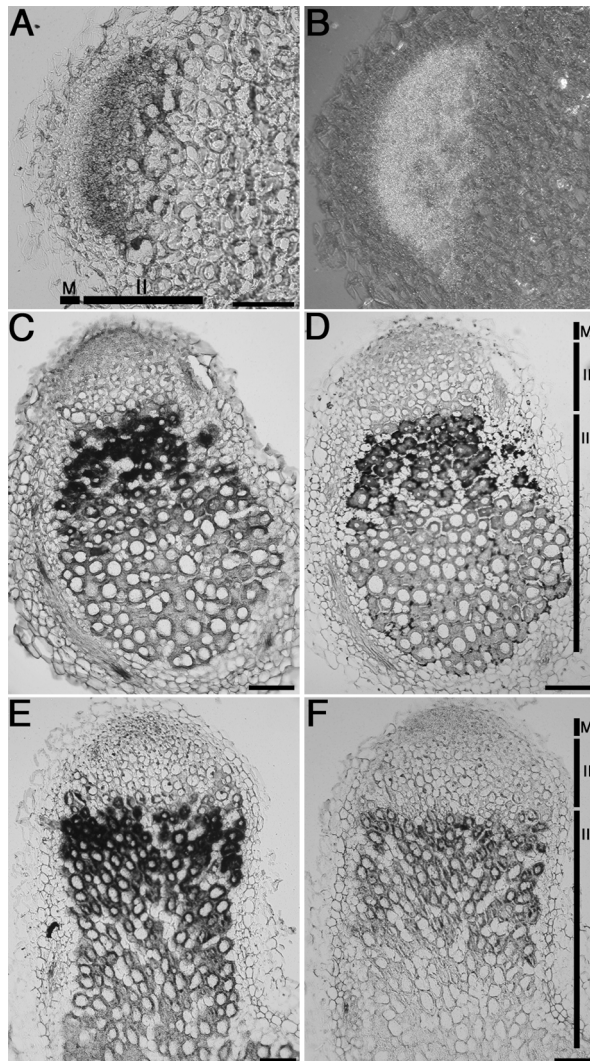


Figure 1. *In situ* localization of *MtENOD12*, *LB* and *nifH* mRNA in longitudinal section of 14-day-old *M. truncatula* nodules. A) Bright field image of the apical part of a longitudinal nodule section hybridized with a ^{35}S -labeled antisense *MtENOD12* probe. Cells containing high concentration of silver grains are black. Note absence of silver grains in the meristem. B) Epipolarisation image of A. Green dots are the signal. C) Bright field image of a nodule section hybridized with a ^{35}S -labeled antisense *LB* probe. D) Bright field image of an adjacent section of C showing amyloplast accumulation. E) Bright field image of a nodule section hybridized with a ^{35}S -labeled antisense *LB* probe. F) Bright field image of an adjacent section of E hybridized with a ^{35}S -labeled antisense *nifH* probe. M, Meristem; II, Infection zone (zone II); III, Nitrogen fixing zone (zone III). Bar = 200µm. (Color figure, see appendix).

As shown in Fig. 1C the presence of *LB* mRNA at maximal level in the first cell layers of the fixation zone (previously named interzone; Vasse et al., 1990) as well as the appearance of amyloplasts in the same cell layers (Fig. 1D) reveals that a sharp boundary is also present between infection and fixation zone. Also the bacterial *nifH* gene is induced at the transition between these 2 zones (Fig. 1E and F). However, the intensity of the signal is rather low, probably due to poor permeability of the bacteroids. Therefore, the plant encoded *LB* is a better molecular marker than the bacterial *nifH* to visualize the molecular switch from zone II to zone III. In conclusion, these data show that, like in pea and alfalfa, the nodule central tissue is characterized by 2 rapid developmental switches. This results in sharp boundaries between the 3 successive zones: meristem, infection zone and fixation zone. Further, within the infection and fixation zone, respectively, a gradual progression of differentiation occurs.

Isolation of MtNIN

We aimed to determine where and when during Medicago nodule development the NFS genes as well as the *MtNIN* gene are expressed. Since the Medicago *NIN* gene has not yet been cloned we first isolated a cDNA corresponding to this gene. For this purpose we searched the EST collection of Medicago (<http://tigrblast.tigr.org/tgi/>) and identified a single EST clone (BG581784), originating from a nodule cDNA library that is homologous (77% identity) to the 3' end of *PsNIN*, including the 3' untranslated region. To clone this Medicago *NIN* homolog RT-PCR on nodule RNA was conducted using oligos that were designed on *PsNIN* for the 5' end and on the EST clone BG581784 for the 3' end. The resulting 2,974 bp fragment was cloned and its nucleotide sequence was determined. This clone has 75% homology with *PsNIN* and the encoded putative protein of 933 amino acids has a similarity of 77% to *PsNIN*. The putative protein contains all 7 conserved domains (domain I-VI and L) as well as short amino acid repeats that are characteristics of NIN-like proteins (Fig. 2); (Schauser et al., 1999; Borisov et al., 2003). Furthermore, characterization of the genomic sequence revealed a similar intron/exon organization as described for *PsNIN* and *LjNIN* (data not shown). Genetic mapping in Medicago showed that the isolated *NIN* homolog is located at linkage group 5 to the telomeric site of marker DK355-L. This region is highly syntenic to a region of pea linkage group 1 and *PsNIN* is located in this area (Gualtieri et al., 2002; Borisov et al., 2003). Further, Southern blot analysis suggests that there is only a single copy of this gene present in the Medicago genome (data not shown). Taken together, it seems very probable that the identified gene is the true ortholog of *LjNIN* and *PsNIN* and we named this gene *MtNIN*.

In situ localization of MtNIN, NORK, DMI3, LYK3/4 and NFP mRNA in nodules

Next we determined in which nodule cells the genes involved in the Nod factor perception and transduction are expressed. In longitudinal nodule sections *MtNIN* transcript was detected in the apical part of the nodule (Fig. 3A to D). A comparison with the *MtENOD12* expression pattern shows that the region in which *MtNIN* is expressed is broader and comprises the nodule meristem and all the cell layers of zone II (compare Fig. 3D and 3H). At the transition from the infection zone to the fixation zone its concentration markedly decreased (Fig. 3E and F). In general the *MtNIN* mRNA level is rather similar throughout the region where it is expressed. However, in sections exposed for a shorter time the accumulation of the *MtNIN* mRNA was higher in the 2 most proximal cell layers of zone II (data not shown).

MtNIN **MEYGGGIVADGGVFGPMVGGGGDQADIIEELLGEGCWIEASENSLMAMQQTTPQSQYMS**
PsNIN **MEYGGGIVDDGGVFGTMVGG---DQGDIIIEELLGEGCWIEASENNMMAMQQTASPPQQHY**
LjNIN **MEYGSLLVQQQQQDCNSAYG-----SLSNLSDDCGSVTTAEADHHIIIEELLVQGCWVE**

I

MtNIN **NNNNIPMGMEGDHFNHHHHHHPPHHQMECTAPAAHDDQO-ESGFVVGKRWIGPRAN**
PsNIN **IGNNIPIGMGEGDHFNNH-----QVDQ-ESGFVVGKRWIGPRGS**
LjNIN **VSG---VGVREGEL-----QLQQDESSFFVVGKRWIGPAAA**

MtNIN **PGP--TTSVKERLVVAVGYLKEYTKNSSNNVLIQIWVPMRRRSALIHQNH--YLOQESS**
PsNIN **QGP--STSVKERLVVAVGYLKEYTKNSSNNVLIQIWVPALRRRSALIH-----YLOQDSS**
LjNIN **VAGSCNSSVKERLVIAGVYLDYTRNS--NVLIQIWVP-LRRGILHDHDYHTNYLLSNPN**

II

MtNIN **S-----APVSVNPN---MNVHVRFFRSHDYPRHQOQOQO- YGSLLALPVF**
PsNIN **SS-----VPVSVNPN---MNVHVRFFRSHEYPRHQOQOQOQYGSLLALPVF**
LjNIN **PPQPEAAADHESVSLGFPMPAAPNSNLYSNVHVRFFRSHEYPRVQAQO--YGSLLALPVF**

MtNIN **ERGSCTCLGVIEFVISNQTILINYPQLDHLNLSAL-EAVDFRSSHNMNIPQAVK-VFEELY**
PsNIN **ERGSCTCLGVIEFVIANQNLINYPQLDHLNLSAL-EAVDFRSSHNMNIQPAVKVFEELY**
LjNIN **ERGTCTCLGVLEIVITNQTINYN-----VSNALDQAVDFRSSQSF-IPPAIK-VYDELY**

III

MtNIN **EAAVNEIMEVLASVCKTHNLPLALTWPACLOOQOQGGGKGSSGASGCGVST-----**
PsNIN **EAAVNEIVEVLASVCKTHNLPLALTWPACIOOQO-GGGKGTTGGGCGSVSVTVPTDQMNIN**
LjNIN **QAAVNEIEVMTSVCKTHNLPLALTWPACIOO-----GKCGCGVSS-----**

IV

MtNIN **---MSCCISTVDSACYVGDMVLGFQEQACSEYHLFNGQGIVGTAFTTTKPCFAIDITAFS**
PsNIN **NHMMMSCISTVDSACYVGDMVLGFQEQACSEYHLFNGQGIVGTAFTTTKPCFAIDITAFS**
LjNIN **-ENYMWCVSTVDSACFVGDLDFLGFQEQACSEYHLFNGQGIVGTAFTTSKPCFAIDITAFS**

MtNIN **KSEYPLAHHANMFGLHAAVAIPLRSVYTGSAADFVLEFFLPKDCRDTEQQKQMLNLSLV**
PsNIN **KAHEYPLAHHADMFGLHAAVAIPLRSVYTGSAADFVLEFFLPKDCRDTEQQKQMLNLSLV**
LjNIN **KAHEYPLAHHANMFGLHAAVAIPLRSVYTGSAADFVLEFFLPKDCHDSEEQQLNLSLSMV**

MtNIN **VQOACRSLHLHVMDNNNNNMNDNNSADHDHDQFTFP-TTNSYMPSSASEP-----L**
PsNIN **VQOACRSLHLHVMDNANHHED-----QDQFTFP-TTNYMPSSASDAATTAS-L**
LjNIN **VQOACRSLHVVLV-ED-----EYTLPMPSHTSKEELEEEITITNNH**

L

MtNIN **SQVDAVSGCSTKDT-SSSCSWIAHMMEAQNGKGVSVSLEYLQEPKEEFKVTTTCNWDRER**
PsNIN **SQVDAASGCSTKDTSSSCSWIAHMMEAQNGKGVSVSLEYLQEPKEEFKVTTTCNWEREG**
LjNIN **EQKLFVSPSSHESECSKESSWIAHMMEAQQKGVSVSLEYLQEPKEEFKVTT-NWDSST**

MtNIN **EDNVFSEFGQVLQOQOQHDQSSNSRASVVSVEAGEESPGACGRRSSSSSSGRKSGDKRRTK**
PsNIN **-NSVFSEFGQVIQ---HDQSSNSRASVEAGEESGGGGTGGGRRSSSSSSGRKSGDKRRTK**
LjNIN **---DHDQQAQVFSSDFGQMSSGFKASTVEGGDQESSYTF-GSRRSSS-GGRKSQEKRRTK**

V

MtNIN **AEKTISLPVLRQYFAGSLKDAAKSIGVCPTTLKRICRQHGITRWPSRKIKKVGHSLKKLO**
PsNIN **AEKTISLPVLRQYFAGSLKDAAKSIG-GPTTLKRICRQHGITRWPSRKIKKVGHSLKKLO**
LjNIN **AEKTISLQVLRQYFAGSLKDAAKSIGVCPTTLKRICRQHGITRWPSRKIKKVGHSLKKLO**

MtNIN **LVIDSVQGAEGAIQIGSFYASFPELSNATANGGDGNDN-----SNNSFYNNHGDG**
PsNIN **LVIDSVQGAEGAIQIGSFYASFPELSTAAAHGGGGGGGDH-----INNNSFYNN-SHGD-**
LjNIN **LVIDSVQGAEGAIQIGSFYASFPELSSSDFASACRSDDSKKMHNYPDQNN'TLYGHGDHGG**

MtNIN **IVTSLKSPPSACSQTHAGNKLPMTT---TTAINHHHVMTENPTGAPLGVDHAFMHASNI**
PsNIN **LVTNLKSPPSACSQTHAGNKSIIINGDHHHHHHHQLVMTEN-LAAPSVDALMQHASTI**
LjNIN **VVTSLKSPPSACSQTFAGNQP-----CTIINNGDVLMTES-PPVPEALLSRRDHCEEA**

MtNIN **NIQDYHQLOEDLDTKQLLLHFNNNN-----QILPPRPTVWNNNNSSSTLLERGAFRV**
PsNIN **NIQDYQQLQEDHDTKQLLLHFNNNNNNNNNNNNTLPPRPTVTWNNNNSSSGLLERGAFRV**
LjNIN **ELLNNASIQEDTKR-----FSRPK-----SQTLP-----LSDSSGWNSETGAFRV**

VI

MtNIN **KATFADEKIRFSLQAMWGFRLQLEIARRFNLDMNNLVLYLDDEGEWVVLSCDADLEE**
PsNIN **KATFADEKIRFSLQAVWCFRDLQLEIARRFNLDMNNLVLYLDDEGEWVVLACDSDLEE**
LjNIN **KATFADEKIRFSLQPIWGFSDQLQLEIARRFNLNDVTNILLKYLDDEGEWVVLACDGDLEE**

MtNIN **CKDLHTSSHTRTIRLSLFQASPLN-LPNTFRNSSSSSPSS**
PsNIN **CKDLHTSSHTRTIRLSLFQASPLNLANFRNNSSS-PS**
LjNIN **CKDIHRSSQSRRTIRLSLFQASPLN-LANTFRNSS---PS-**

Subsequently, *in situ* hybridization was carried out on adjacent longitudinal nodule sections using *NORK* and *DMI-3* antisense probes. This showed that *NORK* and *DMI-3* expression patterns coincided (Fig. 4). The two genes appeared to be highly expressed in the most distal 2-3 cell layers of zone II, just adjacent to the meristem (Fig. 4A to F). This region is markedly smaller than the region where *MtENOD12* is expressed (compare Fig. 4G with 4H). Moreover, a weaker signal was also observed in the nodule meristem. As mentioned above, *MtENOD12* is not expressed in the nodule meristem. A comparison of the signal present in the meristem in sections hybridized with *NORK* or *MtENOD12* antisense probes and showing similar signal intensity is shown in Fig. 4G and H. The signal intensity in the meristem was markedly higher in the sections hybridized with the *NORK* probe, suggesting that this signal is due to expression of *NORK* in the meristem and not to background. Finally, moving to more proximal cell layers of zone II the expression rapidly decreased to the basal level (Fig. 4A and B). In a second set of experiments we determined the expression patterns of *LYK3* and *NFP* (Fig. 5). Strikingly *LYK3* (Fig. 5A to D) and *NFP* (Fig. 5 E to H) showed the same expression as *NORK* and *DMI-3*. However a longer exposure time was required to detect the mRNA of both receptors.

Expression levels of Nod factor signaling genes in root and nodules

Knock out mutants of NFS genes have a similar phenotype, being blocked in most of the early Nod factor induced responses. Therefore, it has been postulated that some of the encoded proteins could function together in a complex (Cullimore and Denarie, 2003; Parniske and Downie, 2003). This is further supported by the *in situ* expression analyses described above, which showed that NFS genes are expressed at a relatively high level in about 3 cell layers of the infection zone. However, if two or more of the encoded proteins indeed form a complex, we postulate that the expression of those genes is regulated in similar way in root and nodules, respectively. To test whether this is the case we performed quantitative RT-PCR (qPCR) analysis of *NFP*, *LYK3*, *NORK*, *DMI1* and *DMI3*. Therefore, mRNA of the apical parts of nodules was isolated. This nodule material is enriched for cells of the meristem and the infection zone. cDNA was synthesized from this nodule RNA as well as from RNA of uninoculated nitrogen-starved roots. qPCR, performed on these samples, confirmed that *NFP*, *LYK3*, *NORK*, *DMI1* and *DMI3* are expressed in both tissues (Table 1).

Figure 2. Alignment of MtNIN to PsNIN and LjNIN. MtNIN contains all 7 conserved domains (domain I-VI and L marked by gray boxes) that are present in NIN proteins (Borisov et al., 2003). Domain V is a putative RWP-RK motive, whereas Domain VI is a putative PB1 motive as present in many eukaryotic cytoplasmic signaling proteins. Short repeats of particular amino acids (Q, H, N or S) are underlined. Such stretched are a typical characteristic of NIN proteins. In bold conserved amino acids are given. The DNA sequence encoding the first 8 amino acids was derived from the 5' primer used for the isolation of *MtNIN* and was not confirmed by other methods.

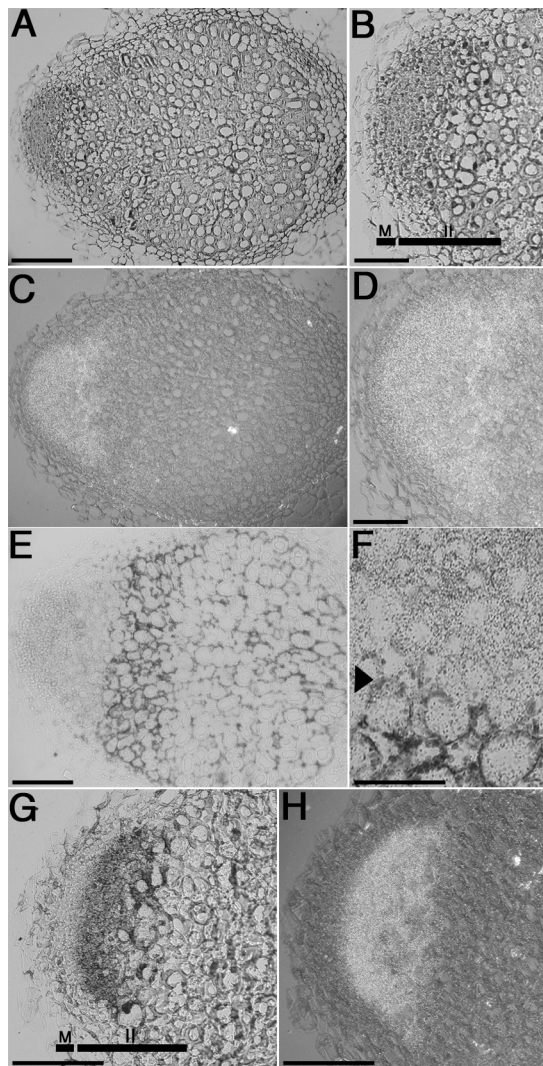


Figure 3. *In situ* localization of *MtNIN* and *MtENOD12* mRNA in longitudinal section of 14-day-old *M. truncatula* nodules. A) Bright field image of a nodule section hybridized with a ^{35}S -labeled antisense *MtNIN* probe. B) Magnification of A. C) and D) Epipolarisation images of A and B. E) Bright field image of an adjacent section of A showing amyloplast accumulation used to mark the transition between zone II and zone III. F) Magnification of E. Note the decrease in the number of silver grains in cells in which amyloplasts are present. Arrowhead points to cells in which starch accumulation starts. G) Bright field image of an adjacent section of A hybridized with a ^{35}S -labeled antisense *MtENOD12* probe. H) Epipolarisation image of G. Note absence of silver grains in the meristem. M, Meristem; II, Zone II. Bar = 200 μm in A), C), E) and 100 μm in B), D), F), G) and H). (Color figure, see appendix).

However, the ratio of the expression levels of the Nod factor signaling genes in nodules versus roots (N/R) differs markedly. For example *DMI1*, *DMI3* and *NORK* are upregulated in the nodule apex compared to roots since the N/R rates are 8.7, 3.2 and 1.9 fold, respectively, whereas both putative Nod factor receptors, *NFP* and *LYK3*, are downregulated (N/R of 0.1 and 0.24, respectively). Assuming that there is a rather strict correlation between mRNA and protein levels, these data indicate that the ratios of protein concentrations between Nod factor signaling proteins differ in uninoculated roots and in the nodule apex. For example, the ratio between *NFP* and *NORK* changes over hundred fold in the two tissues. Therefore, it is unlikely that these proteins form a rather static complex during subsequent steps in Nod factor signaling.

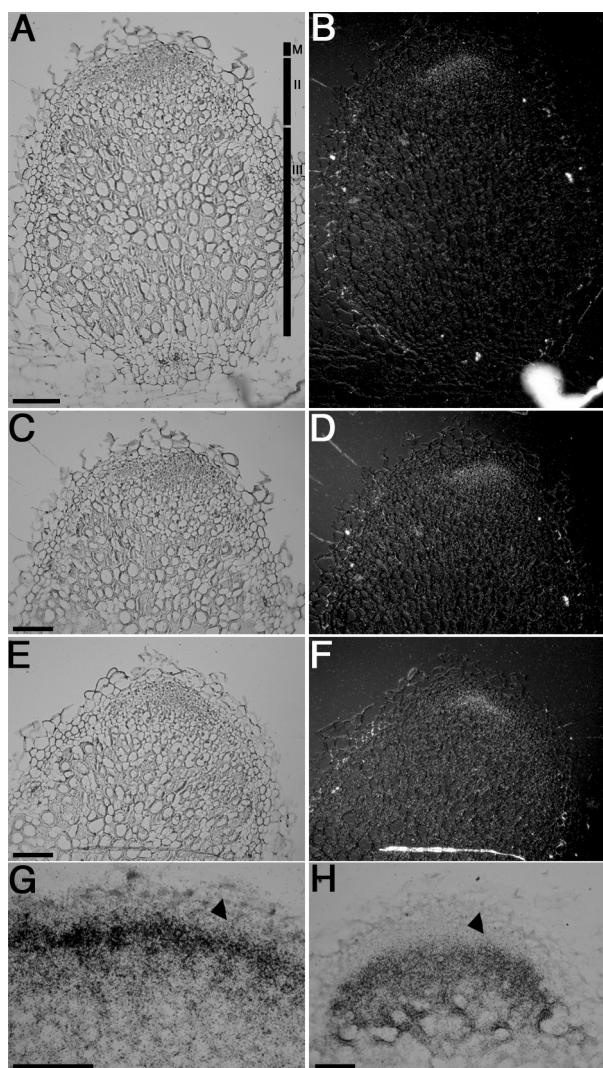


Figure 4. *In situ* localization of *NORK* and *DMI3* mRNA in longitudinal section of 14-day-old *Medicago* nodules. A) Bright field image of a nodule section hybridized with a ^{35}S -labeled antisense *DMI3* probe. C) Magnification of A. B) and D) Epipolarisation images of A and C. E) and F) Bright field and epipolarisation images, respectively, of an adjacent section of A) hybridized with a ^{35}S -labeled antisense *NORK* probe. G) Apical part of a nodule longitudinal section hybridized with a ^{35}S -labeled antisense *NORK* probe. H) Apical part of a nodule longitudinal section hybridized with a ^{35}S -labeled antisense *MtENOD12* probe. M, Meristem; II, Zone II; III, Zone III. Arrow head, Meristem. Bar = 200µm in A), C) and E) and 100µm in G) and H). (Color figure, see appendix).

Table 1. pPCR analysis of the Nod factor signaling genes

| | <i>ROOT</i> | <i>NODULE apex</i> | <i>NODULE/ROOT</i> <i>ratio</i> |
|--------------|--------------|--------------------|------------------------------------|
| <i>NFP</i> | 49.8 ± 2.3 | 4.9 ± 0.51 | 0.1 |
| <i>LYK3</i> | 105.0 ± 21.6 | 24.8 ± 1.1 | 0.24 |
| <i>NORK</i> | 399.7 ± 58.9 | 750.7 ± 43.6 | 1.9 |
| <i>DMI1</i> | 9.30 ± 0.80 | 81.2 ± 5.0 | 8.7 |
| <i>DMI3</i> | 64.5 ± 15.9 | 209.4 ± 8.8 | 3.2 |
| <i>MtNIN</i> | 4.3 ± 0.17 | 773.3 ± 77.1 | 178 |

Table1. Quantification of *NFP*, *LYK3*, *NORK*, *DMI1*, *DMI3* and *MtNIN* mRNA in roots and in the nodule apical region by qPCR.

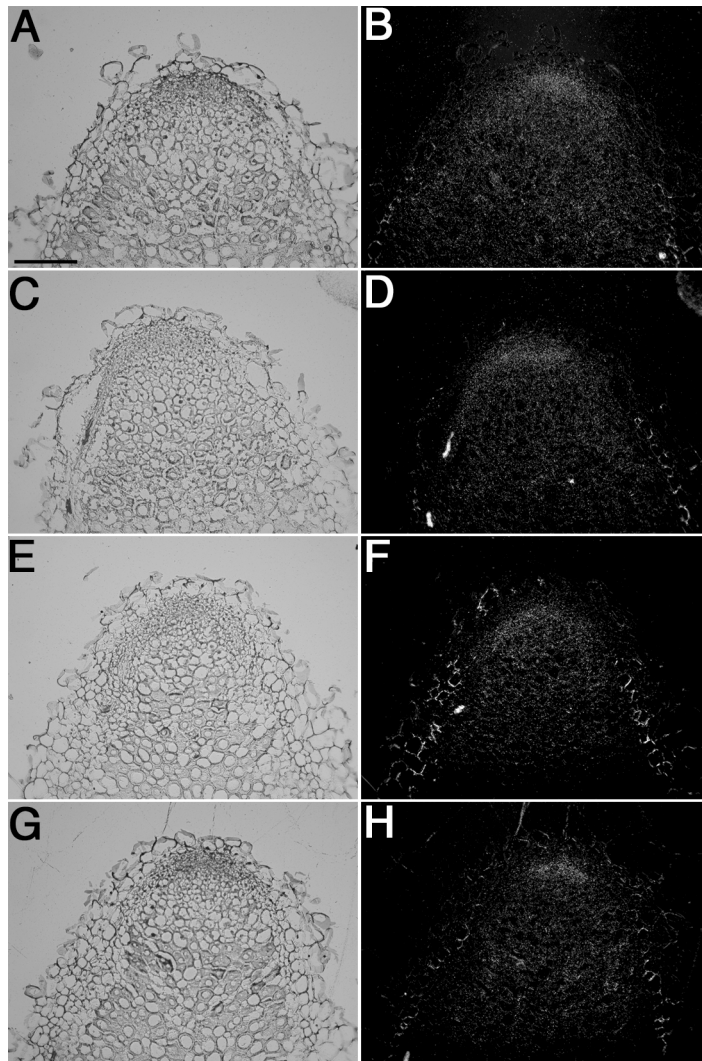


Figure 5. *In situ* localization of *NORK/LYK3* (A to D) and *NFP/LYK3* (E to H) mRNA in longitudinal section of 14-day-old *Medicago* nodules. A) and B) Bright field and epipolarisation images, respectively, of a nodule section hybridized with a ^{35}S -labeled antisense *NORK* probe. C) and D) Bright field and epipolarisation images, respectively, of a nodule section adjacent of A hybridized with a ^{35}S -labeled antisense *LYK3* probe.

E) and F) Bright field and epipolarisation images, respectively, of a nodule section hybridized with a ^{35}S -labeled antisense *NFP* probe. G) and H) Bright field and epipolarisation images, respectively, of a nodule section adjacent of E hybridized with a ^{35}S -labeled antisense *LYK3* probe. Bar = 200 μm . (Color figure, see appendix).

Discussion

We analyzed the expression pattern in nodules of *MtNIN* and the NFS genes by *in situ* hybridization and due to the indeterminate growth behavior of *Medicago* nodules a correlation between developmental stage and gene expression could be obtained.

Sharp boundaries exist between zones of the central tissue

First we analyzed the zonation of *Medicago* nodules in more detail. We showed that a sharp boundary exists between meristem and infection zone and this is well visualized by the *MtENOD12* mRNA distribution. This RNA is absent in meristematic cells and present immediately at a maximal level in the cell layer of the infection zone adjacent to the meristem. A similar sharp boundary occurs between infection and fixation zone, as visualized by the expression of the *Medicago LB* and the *Synorhizobium meliloti nifH* genes as well as from the pattern of starch accumulation. Therefore, *nifH* and *LB* expression and starch accumulation can be used as markers for this transition. Previously, the fixation zone

was defined as the zone where nitrogen fixation takes place. This was determined in an indirect manner as nitrogen fixation activity was measured on intact nodules by the acetylene reduction assay (Vasse et al., 1990). In this way nitrogenase activity was detected only in nodules in which several layers of infected cells were present after the region where amyloplasts accumulate. Therefore, it was proposed to name the zone marked by the start of starch accumulation interzone, whereas the fixation zone was proposed to start a couple (3-4) of cell layers proximally. For the following 2 reasons we propose not to distinguish an interzone and fixation zone but to call both together fixation zone. First, the interzone is characterized by the induction of *nif* genes (including *nifH*) and the delay in detecting acetylene reduction is probably caused by the sensitivity of the method. Second to our knowledge no molecular marker has been identified that marks the proposed transition from interzone into fixation zone.

Nod factors are produced at the site where NFS genes are expressed at the highest level

The highest expression of the NFS genes was detected in the first 3 cell layers of zone II. Previously, it has been shown that *Rhizobium nod* genes are active in this region. This has been reported by Sharma and Signer (1990) using reporter constructs based on the *uidA* gene. Further, Schlaman et al., (1991) showed by *in situ* hybridization that expression of various *nod* genes specifically occurs in the more distal cell layers of zone II. Therefore it is probable that Nod factors are produced by the rhizobia in the cell layers where the NFS genes are expressed at the highest level. It is possible that Nod factors are also produced by rhizobia in more proximal layers of the infection zone but this will depend on the stability of the rhizobial Nod proteins.

Function of Nod factor signaling in the nodule

In the most distal layers of zone II, in which the expression of the NFS genes is relatively high, infection threads branch, penetrate plant cells and bacteria are released into the host cells. The correlation between infection thread growth/bacteria release and up regulation of the NFS genes suggests a role for the Nod factor signaling in these processes. This hypothesis is supported by knock down studies on *NORK*. Partial knock down of *NORK* does not cause a block of nodulation, but in the nodules that are formed the release of bacteria into nodule cells is blocked (chapter 5).

Regulation of gene expression by Nod factor signaling

In addition to a role of Nod factor signaling in bacterial release it seems probable that Nod factor signaling plays a role in the regulation of gene expression. The gene expression analysis as conducted in this study is summarized in Fig. 6 and supports this hypothesis. *MtENOD12* can be used as example of a gene induced by Nod factors. Its expression can be induced e.g. in the root epidermis by Nod factor application (Scheres et al., 1990; Pichon

et al., 1992). In the nodule, *MtENOD12* expression starts in the distal cell layers of the infection zone where both NFS genes and the rhizobial *nod* genes are active. Since the NFS genes are already expressed in the nodule meristem whereas *MtENOD12* expression is not, synthesis of the NFS components appears to precede that of *MtENOD12* activation. This is well in line with a role of Nod factor signaling in the induction of *MtENOD12* expression.

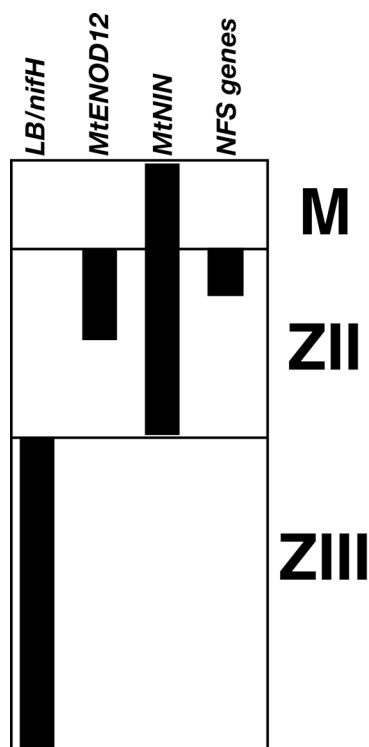


Figure 6. Schematic representation of an indeterminate nodule. The expression pattern of *LBnifH*, *MtENOD12*, *MtNIN* and the NFS genes is indicated.

A basal expression of the NFS genes was observed in the nodule meristem, whereas in the zone where Nod factors might be produced the expression level of these genes is markedly upregulated. This suggests that Nod factor signaling causes a positive feedback and leads to enhanced NFS gene expression. In case the enhanced expression level of the NFS genes and the induction of *MtENOD12* are both induced by Nod factors it is remarkable that the decrease of their expression levels occurs at a different time point in development. Considering that Nod factor production might be restricted to the most distal layers of zone II the observed patterns could be explained by assuming that the upregulation of NFS gene expression requires continuous Nod factor signaling, whereas maintenance of *MtENOD12* expression does not.

In Lotus, it has been shown that *MtNIN* expression is induced in the root epidermis by Nod factor application (Radutoiu et al., 2003), similar to the regulation of *MtENOD12* in pea and Medicago. Therefore, it is remarkable that the expression patterns of *MtENOD12* and *MtNIN* in Medicago nodules are markedly different. Moreover, the expression of *MtNIN* in the meristem and in the complete infection zone, at the same level, does not suggest that Nod factor signaling plays an important role in the expression of *MtNIN* in nodules. This might be

a characteristic unique for the *Medicago NIN* gene. In fact in pea the *NIN* gene is expressed in the meristem, as well as the *Medicago* orthologue, but within the infection zone the expression of *PsNIN* is limited to the distal cell layers (Borisov et al., 2003) and does not extend to the complete zone II as observed for *MtNIN*. This suggests that *NIN* genes might be regulated in different ways in different legumes. Moreover, the rapid decrease of *MtNIN* mRNA levels at the transition from infection zone to fixation zone supports the notion that a developmental switch occurs at this transition.

Mode of action of Nod factor signaling proteins

It has been proposed that the different NFS proteins act together in the initial Nod factor signaling. This is underlined by their similar expression patterns in root nodule. All the NFS genes that we studied are expressed at that highest level in a few cell layers in the most distal part of the infection zone. *NIN* is generally considered to be a more downstream component of Nod factor signal transduction and this is consistent with its expression pattern that is clearly different from that of the NFS genes.

The transmembrane receptor kinases *NFP*, *LYK3* and *NORK* as well as *DMI1* - as a putative subunit of a cation channel - are likely to localize in the plasmamembrane. Since all these proteins are involved in Nod factor perception and/or signaling it is hypothesized that some of them could be present together in a larger complex (Cullimore and Denarie, 2003; Parniske and Downie, 2003). The quantitative expression analyses presented here showed that the absolute amount of mRNAs molecules, and therefore probably of the encoded proteins, varies markedly for the different NFS proteins. For example, both in root and nodule the number of *NORK* and *DMI1* mRNA molecules differs substantially, being *NORK* mRNA 40 and 10 more abundant than *DMI1* mRNA in nodules and roots, respectively. It has been proposed, based on their similar mutant phenotype, that *NORK* and *DMI1* might form a complex. If this is the case such a complex cannot be a static complex. Further, quantitative qPCR analysis showed that the relative amounts of the NFS mRNAs in nodules and roots is markedly different. For example, in roots *NORK* mRNA is about 8 times more abundant than *NFP* mRNA. In nodules this ratio increases to about 150. Taken together these quantitative data do not provide a support for the idea that NFS components are only active in a complex. Further, these data indicate that Nod factor signaling in the root and the distal region of the infection zone is different.

Material and Methods

Cloning of MtNIN

MtNIN was PCR amplified on root nodule cDNA as well as genomic DNA of *Medicago* line A17 using the the oligos 5'-TTAGGATGGAATATGGTGGTGGGATAGTGG-3' and 5'-AAAGCCGCAGAATCTAACTTAACGAG-3' and subsequently cloned in pGEM-t (Promega) and sequenced. Genetic mapping was conducted by RFLP analysis on *HindIII* digested genomic DNA of a F2 segregating population of 40 individuals of the cross A17 x

DZA315.16 using the first 1,500 bp of *MtNIN* as probe. Other markers of linkage group 5 (DK003-R, MtEIL2-1 and DK355-L) were used as described in Gualtieri *et al.* (2002).

In situ hybridization

Nodules were harvested 14 days post inoculation (d.p.i.) and fixed in 4% paraformaldehyde supplemented with 0.25% glutaraldehyde in 10 mM sodium phosphate buffer (pH=7.4) for 3 h (Van de Wiel *et al.*, 1990). Fixed nodules were dehydrated, by passing through a series of grade ethanol, and embedded into paraffin (Paraclean; Klinipath, Duiven, The Netherlands) as described previously (Van de Wiel *et al.*, 1990). Sections (7 μ m) were dried on polylysine-coated slides at 37° C overnight, deparaffinized with xylene and rehydrated via a graded ethanol series. Hybridisation pre-treatment, hybridisation and washing were performed as described by Cox (Cox and Goldberg, 1988) and adapted by Van de Wiel (Van de Wiel *et al.*, 1990).

For preparing antisense RNA probes fragments of 170-260 bp of the coding region or 3' UTR region of the different genes were used (*MtNFR5* (ORF = 1,788 bp): 28-260 bp, 425-654 bp, 661-905 bp, 976-1218 bp and 1239-1464 bp; *LYK3* (ORF = 1,863 bp): 113-342 bp, 483-694 bp, 866-1079 bp, 1258-1486 bp and 1705-1947 bp; *NORK* (ORF = 2,778 bp): 373-617 bp, 784-1039 bp, 1200-1453 bp, 1610-1864 bp and 1964-2219 bp); *DMI3* (ORF = 1,569 bp): 12-229 bp, 221-467 bp, 472-712 bp and 1198-1388 bp, *MtNIN* (ORF = 2,802 bp): 117-335 bp, 391-628 bp, 1,934-2,119 and 2,418-2,663 and *MtENOD12* (ORF = 383 bp) 36-236 bp. For *MtLB* the 146-383 bp region of the ORF of TC76546 (441 bp; TIGR *Medicago truncatula* Gene index) was used and for *NifH* of *S. meliloti* 178-454 bp region of the ORF (939 bp) was used. These fragments were PCR-amplified including a T7 promoter at the 3'-end. Amplified fragments were used as substrate to synthesize antisense RNA with T7 RNA polymerase in the presence of [³⁵S]-UTP (1000-1500 Ci mmol⁻¹). For the hybridization 6 x 10⁶ cpm were used in mixture containing equal amounts of each probe. After washing, the slides were coated with microautoradiography emulsion LM-1 (Amersham) and exposed for 1-3 weeks at 4°C. Next, slides were developed for 5 min in Kodak D-19 developer and fixed in Kodak fixative. Sections were counterstained with toluidine blue and subsequently mounted. Lugol was used to stain amyloplasts. For imaging a Nikon Optiphot-2 bright field microscope with epipolarization optics was used.

RNA extraction and qPCR

Total RNA was extracted from un-inoculated roots and from the apex (2-3 mm) of 2-week-old nodules according to Pawlowski *et al.*, (Pawlowski *et al.*, 1994) followed by DNaseI treatment. cDNA was made from 1 μ g total RNA using the Taqman Gold RT-PCR kit (Perkin-Elmer Applied Biosystems) in a total volume of 50 μ l using the supplied hexamer primers. qPCR reactions were performed in triplo on 6,5 μ l cDNA using the SYBR-GreenR PCR Master kit (Perkin-Elmer Applied Biosystems; 40 cycles of 95°C for 10 s, 60°C for 1 min) and real-time detection was performed on the ABI 7700 and analysed using the GeneAmp 5700 SDS software (Perkin-Elmer Applied Biosystems). The specificity of the PCR amplification procedures was checked with a heat dissociation step (from 60°C-95°C) at the end of the run and by agarose gel electrophoresis. Results were standardized to the *MtACTIN2* expression levels. Primers used:

MtACTIN2: 5'-TGGCATCACTCAGTACCTTTCAACAG-3' and 5'-ACCCAAAGCATCAAATAATAAGTCAACC-3'

MtNFR5: 5'-ATGGATGTTGCAATCGGTCTGC-3' and 5'-CACCCCAAAGCGAAAACATCA-3'

NORK: 5'-TGGACCCCTTTGAATGCCTATG-3' and 5'-TCCACTCCAACCTCTCCAATGCTTC-3'

DMI1: 5'-GTTGCTGCAGATGGAGGGAAGAT-3' and 5'-GCGCCAGCCACAAAACAGTAT-3'

DMI3: 5'-TCATTGATCCCTTTTGCTTCTCGT-3' and 5'-GATGCTACTTCCTCTTTGCTGATGC-3'

MtNIN: 5'-ATTGCAAGGCGATTAACTAACCA-3' and 5'-GAGAGGGGAAGCTTGAAAAAGAGA-3'

References

- Amor BB, Shaw SL, Oldroyd GE, Maillet F, Penmetsa RV, Cook D, Long SR, Denarie J, Gough C (2003) The NFP locus of *Medicago truncatula* controls an early step of Nod factor signal transduction upstream of a rapid calcium flux and root hair deformation. *Plant J* **34**: 495-506
- Ane JM, Kiss GB, Riely BK, Penmetsa RV, Oldroyd GE, Ajax C, Levy J, Debelle F, Baek JM, Kalo P, Rosenberg C, Roe BA, Long SR, Denarie J, Cook DR (2004) *Medicago truncatula* DMI1 required for bacterial and fungal symbioses in legumes. *Science* **303**: 1364-1367
- Borisov AY, Madsen LH, Tsyganov VE, Umehara Y, Voroshilova VA, Batagov AO, Sandal N, Mortensen A, Schauser L, Ellis N, Tikhonovich IA, Stougaard J (2003) The SYM35 gene required for root nodule development in pea is an ortholog of Nin from *Lotus japonicus*. *Plant Physiol* **131**: 1009-1017
- Catoira R, Galera C, de Billy F, Penmetsa RV, Journet EP, Maillet F, Rosenberg C, Cook D, Gough C, Denarie J (2000) Four genes of *Medicago truncatula* controlling components of a nod factor transduction pathway. *Plant Cell* **12**: 1647-1666
- Cohn J, Day B, Stacey G (1998) Legume nodule organogenesis. *Trends in Plant Science* **3**: 105-109
- Cox KH, Goldberg RB (1988) Analysis of plant gene expression. In CH Shaw, ed, *Plant Molecular Biology: A practical approach*. IRL press, Oxford, pp 1-34
- Crespi M, Galvez S (2000) Molecular Mechanisms in Root Nodule Development. *Journal of Plant Growth Regulation* **19**: 155-166
- Cullimore J, Denarie J (2003) Plant sciences. How legumes select their sweet talking symbionts. *Science* **302**: 575-578
- Cullimore JV, Ranjeva R, Bono JJ (2001) Perception of lipo-chitooligosaccharidic Nod factors in legumes. *Trends Plant Sci* **6**: 24-30
- Endre G, Kereszt A, Kevei Z, Mihacea S, Kalo P, Kiss GB (2002) A receptor kinase gene regulating symbiotic nodule development. *Nature* **417**: 962-966
- Geurts R, Bisseling T (2002) *Rhizobium* nod factor perception and signalling. *Plant Cell* **14 Suppl**: S239-249
- Gualtieri G, Kulikova O, Limpens E, Kim DJ, Cook DR, Bisseling T, Geurts R (2002) Microsynteny between pea and *Medicago truncatula* in the SYM2 region. *Plant Mol Biol* **50**: 225-235
- Levy J, Bres C, Geurts R, Chalhoub B, Kulikova O, Duc G, Journet EP, Ane JM, Lauber E, Bisseling T, Denarie J, Rosenberg C, Debelle F (2004) A putative Ca²⁺ and calmodulin-dependent protein kinase required for bacterial and fungal symbioses. *Science* **303**: 1361-1364
- Limpens E, Franken C, Smit P, Willemse J, Bisseling T, Geurts R (2003) LysM domain receptor kinases regulating rhizobial Nod factor-induced infection. *Science* **302**: 630-633
- Madsen EB, Madsen LH, Radutoiu S, Olbryt M, Rakwalska M, Szczyglowski K, Sato S, Kaneko T, Tabata S, Sandal N, Stougaard J (2003) A receptor kinase gene of the LysM type is involved in legume perception of rhizobial signals. *Nature* **425**: 637-640
- Mitra RM, Gleason CA, Edwards A, Hadfield J, Downie JA, Oldroyd GE, Long SR (2004) A Ca²⁺/calmodulin-dependent protein kinase required for symbiotic nodule development: Gene identification by transcript-based cloning. *Proc Natl Acad Sci U S A*
- Mylona P, Pawlowski K, Bisseling T (1995) Symbiotic Nitrogen Fixation. *Plant Cell* **7**: 869-885
- Parniske M, Downie JA (2003) Plant biology: locks, keys and symbioses. *Nature* **425**: 569-570
- Pawlowski K, Kunze R, De Vries S, Bisseling T (1994) Isolation of total, poly(A) and polisomal RNA from plant tissue. In SB Gelvin, RA Schilperoort, eds, *In Plant Molecular Biology manual*, Ed 2nd. Kluwer Academic Publishers, Dordrecht, The Netherlands, pp 1-13
- Pichon M, Journet EP, Dedieu A, de Billy F, Truchet G, Barker DG (1992) *Rhizobium meliloti* elicits transient expression of the early nodulin gene *ENOD12* in the differentiating root epidermis of transgenic alfalfa. *Plant Cell* **4**: 1199-1211
- Radutoiu S, Madsen LH, Madsen EB, Felle HH, Umehara Y, Gronlund M, Sato S, Nakamura Y, Tabata S, Sandal N, Stougaard J (2003) Plant recognition of symbiotic bacteria requires two LysM receptor-like kinases. *Nature* **425**: 585-592
- Schauser L, Roussis A, Stiller J, Stougaard J (1999) A plant regulator controlling development of symbiotic root nodules. *Nature* **402**: 191-195
- Scheres B, Van De Wiel C, Zalensky A, Horvath B, Spaink H, Van Eck H, Zwartkruis F, Wolters AM, Gloudemans T, Van Kammen A, et al. (1990) The *ENOD12* gene product is involved in the infection process during the pea-Rhizobium interaction. *Cell* **60**: 281-294
- Scheres B, van Engelen F, van der Knaap E, van de Wiel C, van Kammen A, Bisseling T (1990) Sequential induction of nodulin gene expression in the developing pea nodule. *Plant Cell* **2**: 687-700
- Schlaman HR, Horvath B, Vijgenboom E, Okker RJ, Lugtenberg BJ (1991) Suppression of nodulation gene expression in bacteroids of *Rhizobium leguminosarum biovar viciae*. *J Bacteriol* **173**: 4277-4287
- Sharma SB, Signer ER (1990) Temporal and spatial regulation of the symbiotic genes of *Rhizobium meliloti* in planta revealed by transposon Tn5-gusA. *Genes Dev* **4**: 344-356
- Spaink HP, Sheeley DM, van Brussel AA, Glushka J, York WS, Tak T, Geiger O, Kennedy EP, Reinhold VN, Lugtenberg BJ (1991) A novel highly unsaturated fatty acid moiety of lipo-oligosaccharide signals determines host specificity of *Rhizobium*. *Nature* **354**: 125-130

- Stracke S, Kistner C, Yoshida S, Mulder L, Sato S, Kaneko T, Tabata S, Sandal N, Stougaard J, Szczyglowski K, Parniske M** (2002) A plant receptor-like kinase required for both bacterial and fungal symbiosis. *Nature* **417**: 959-962
- Van de Wiel C, Scheres B, Franssen H, Van Lierop MJ, Van Lammeren A, Van Kammen A, Bisseling T** (1990) The early nodulin transcript *ENOD2* is located in the nodule perenchima (inner cortex) of pea and soybean root nodules. *Embo J* **9**: 1-7
- Vasse J, de Billy F, Camut S, Truchet G** (1990) Correlation between ultrastructural differentiation of bacteroids and nitrogen fixation in alfalfa nodules. *J Bacteriol* **172**: 4295-4306
- Wais RJ, Galera C, Oldroyd G, Catoira R, Penmetsa RV, Cook D, Gough C, Denarie J, Long SR** (2000) Genetic analysis of calcium spiking responses in nodulation mutants of *Medicago truncatula*. *Proc Natl Acad Sci U S A* **97**: 13407-13412
- Yang WC, Bisseling T** (1993) Nodulin gene expression during pea nodule development. *In* X Dou, ed, *Current Developments in Soybean-Rhizobium Symbiotic Nitrogen Fixation*. Heilongjiang Science and Technology Publishing House, Harbin, pp 55-62

CHAPTER 7

Concluding Remarks

A key process in the *Rhizobium*-legume interaction is the infection of plant cells by the micro-symbiont. The aim of the research described in this thesis was to study the mechanism regulating this infection process and I focused on the role of Nod factor signaling and small G proteins. The infection takes place at two different sites: in the root epidermis, where infection thread formation is initiated, and in nodules. In indeterminate growing nodules newly formed cells are continuously infected and this infection process can be divided in four subsequent steps: (1) infection thread growth, (2) bacterial release into the host cells, (3) symbiosome proliferation and (4) symbiosome maintenance (Brewin, 1996)

We choose as experimental system the model legume *Medicago truncatula*, which forms indeterminate nodules. In these nodules a persistent meristem is present at the distal end that continuously divides by which it maintains itself and adds new cells to the different nodule tissues. Therefore, these tissues are of graded age (chapter 6) and the above mentioned infection steps occur in subsequent cell layers, by which the effect of different genes on each step can be studied. In the indeterminate nodules infection thread growth and bacterial release occur in the distal region of the infection zone II. Upon release from the infection thread, the bacteria, with a rod-like shape, become enclosed by a host derived membrane and are now called symbiosomes. Symbiosomes divide and differentiate into the elongated nitrogen-fixing bacteroids. This differentiation process terminates at the transition from zone II to zone III. A critical step in the differentiation of symbiosomes is the maintenance of symbiosomes. This involves an active mechanism since fusion and degradation of symbiosomes occurs in nodules elicited by several Fix^- *Rhizobium* mutants (Vasse et al., 1990).

Role of Nod factor signaling in infection of nodule cells

Recently, most of the *Medicago* genes involved in the Nod factor signaling (NFS) have been cloned. These are the LysM domain containing receptor kinases, *LYK3/4* (Limpen et al., 2003) and *NFP* (*NOD FACTOR PERCEPTION*; Amor et al., 2003). The latter is supposed to be the ortholog of the Pea *SYM10* gene and of the Lotus *NFR5* (Madsen et al., 2003; Radutoiu et al., 2003), both encoding LysM domain containing receptor kinases (Gough and Geurts, unpublished). Other NFS genes are *DOES NOT MAKE INFECTION 1*, *DMI1*, encoding a putative cation channel; *NODULATION RECEPTOR KINASE*, *NORK*, encoding a leucine repeat receptor kinase and, finally, *DMI3*, that was shown to encode a calcium calmodulin dependent protein kinase. Knock out mutations of these genes are blocked in the early Nod factor responses that occur in the epidermis (Catoira et al., 2000; Wais et al., 2000) and as a consequence nodules cannot form. To study the role of Nod factor signaling in nodules we made use of partial knock-down of a NFS gene, namely *NORK*, in combination with *in situ* hybridization. The *in situ* hybridization analysis showed that all the NFS genes that we studied, namely *LYK3*, *NFP*, *NORK* and *DMI3*, are expressed in nodules. Further, they all have the same expression pattern, being markedly higher

expressed in the first 2-3 cell layers of the infection zone II (chapter 6). In these cell layers infection threads branch and penetrate the host cells in which bacteria are subsequently released. Since the expression of NFS genes coincides with that of the bacterial *nod* genes (Sharma and Signer, 1990; Schlaman et al., 1991), it is very likely that Nod factor signaling takes place in the nodule. Moreover, based on the expression pattern of the NFS genes, the Nod factor signaling could be involved in infection thread growth and/or bacteria released in the nodule cells. To study the function of the NFS genes in the nodule we made use of RNAi induced partial knock-down of *NORK*. In nodules, in which *NORK* was silenced by RNAi under the control of the *CaMV 35S* promoter, persistent infection thread growth was observed in almost all the cells of the nodule central tissue, whereas release of bacteria from the infection threads was impaired (chapter 5). Although infection thread growth is not blocked in the *NORK* silenced nodules, it is still very likely that Nod factor signaling is essential for this process. Since nodules are formed on the *NORK* silenced roots, a residual level of *NORK* expression is still present. This residual level is apparently sufficient to allow infection thread formation and growth in the epidermis, the cortex and the nodule cells. Moreover, the involvement of the Nod factor signaling in infection thread development is supported by the observation that knock-down of *LYK3/4* impaired both infection thread formation and growth (Limpens et al., 2003). Infection thread growth requires delivery of vesicles, containing matrix, plasma membrane and cell wall material, at their site of growth (Brewin, 1991; Rea et al., 1992), a process mediated by the cytoskeleton. This suggests that a low level of *NORK* is sufficient to facilitate cytoskeletal re-organization and vesicle transport to the infection thread tip. This hypothesis is further supported by the observation that polar growth of root hairs after Nod factor application is impaired in the *NORK* knock-down mutants (Catoira et al., 2000).

The occurrence of sustained infection thread growth and the absence of bacteria release in the *NORK* silenced nodules indicates that these two processes are tightly linked. Moreover, it indicates that high levels of *NORK* expression in the most distal cell layers of zone II are required to stop infection thread growth and to induce the release of bacteria from the infection threads. This release is thought to occur by endocytosis (Brewin, 1991), a process that, similarly to infection thread growth, requires targeted vesicle transport (Brewin, 1991; Rea et al., 1992). The release of bacteria starts with the formation of infection droplets that protrude from the infection thread (Callaham and Torrey, 1981; Roth and Stacey, 1989a; Brewin, 1991). At this stage the infection droplets are surrounded by a membrane that forms a continuum with the infection thread plasma membrane but it is not associated with cell wall components (Brewin, 1991; Rea et al., 1992). It has been observed that at the site where infection droplets are formed deposition of plasma membrane and matrix material continues whereas deposition of cell wall components ceases or become disorganized (Roth and Stacey, 1989a, 1989b), allowing the unwallled droplet to expand. Thus, in the partial knock down roots the sustained growth of the infection threads might be due to the inability to

uncouple the delivery and/or the fusion of the three different components at the infection thread tip. This hypothesis is in agreement with a role of *NORK* in regulating cytoskeleton reorganization and vesicle delivery.

As other Nod factor responses, such as infection thread growth, are induced in the partial *NORK* knock-down roots it seems that the switch from infection thread growth to release of bacteria requires a higher level of *NORK* expression than do other Nod factor responses. The mechanisms by which different levels of *NORK* regulate the different Nod factor responses remain to be elucidated.

Role of small GTPases in the nodule infection

Upon release from the infection droplets, bacteria, surrounded by the symbiosome membrane, start dividing and differentiate. As these processes proceed, new membrane vesicles are synthesized and delivered to the developing symbiosome compartments. Cheon and coworkers (Cheon et al., 1993) showed that the small GTPases of the RAB family are involved in the biosynthesis of the symbiosome membranes. In eukaryotic cells RAB proteins are involved in the regulation of membrane trafficking. Several RABs have been identified in nodules (Borg et al., 1997) and, among these, expression of RAB1p and RAB7p homologues (*sRAB1*, *sRAB7* and *vRAB*) is highly up-regulated in soybean nodules at the time of bacterial release and symbiosome proliferation (Cheon et al., 1993). Expression in soybean nodules of antisense constructs of *sRAB1* or *sRAB7*, under the control of a Leghemoglobin promoter, blocked the flow of vesicles to the symbiosomes and as a result the nodules showed lack of expansion of infected cells, fewer bacteroids per cell and persistence of the central vacuole (Cheon et al., 1993). Therefore, it was concluded that RAB1p and RAB7p regulate the flow of vesicles from the ER/Golgi to the developing symbiosome membranes and are essential for the formation of the symbiosome compartment and for symbiosome division (Cheon et al., 1993).

In contrast to RAB GTPases that are induced in nodules at the stage of symbiosome proliferation, expression of ROP GTPases is down regulated in the cell layers in which symbiosome division and differentiation occurs. By *in situ* hybridization, we showed that in Medicago nodules *ROP* genes are expressed in the meristem and in the distal cell layers of zone II (chapter 4). This expression pattern suggested that the role of ROPs during nodule formation was different from that of RABs. The function of ROPs in nodule development became clear from the expression pattern of *MtROPs* in nodules elicited by a *Fix⁻ Rhizobium* strain. In these nodules symbiosome development is arrested at an early stage and symbiosomes fuse to form vacuolar like compartments in which bacteroids are degraded (Vasse et al., 1990). In these *Fix⁻* nodules no down-regulation of *MtROP* expression was observed, instead *MtROPs* were expressed at the same level in the complete infection zone (chapter 4). This suggested that the symbiosome fusion observed in the *Fix⁻* nodules is directly correlated to the sustained *MtROP* expression in the infected cells of these nodules.

Based on the protein composition of the symbiosome membrane and fluids (e.g. the matrix between the symbiosome membrane and the bacteroid), symbiosomes have been compared to small vacuolar structures that do not fuse to a main lytic compartment but stay separate units (Mellor, 1989), a process that we can refer to as symbiosome maintenance. In pea tapetal cells, ROP GTPases localize to the tonoplast during vacuole development (Lin et al., 2001), suggesting an involvement of these GTPases in vacuole biogenesis. Considering the vacuolar nature of symbiosomes and the putative role of ROPs in vacuole formation, it could be hypothesized that down regulation of *MtROP* expression in the proximal cell layers of zone II is essential to avoid symbiosome fusion and bacteroid degradation and, therefore, for symbiosome maintenance. To test this hypothesis we determined whether ectopic expression of *MtROPs* in the proximal cell layers of zone II was sufficient to induce symbiosome fusion as observed in the Fix^- nodules. For this purpose, we expressed a Medicago *ROP*, *MtROP1*, in nodules under the control of the *MtENOD12* promoter. This promoter is expressed in zone II in a broader region than *MtROPs*. Therefore, overexpression of *MtROP1* under the control of the *MtENOD12* promoter leads to *ROP* expression in more proximal cell layers of zone II, compared to the cell layers in which endogenous *MtROP* genes are expressed. Ectopic expression of *MtROP1* in these cell layers led to a premature senescence of the nodule infected cells, due to symbiosome fusion and consequent bacteroid degradation (chapter 4). This shows that ectopic expression of *MtROP1* in the proximal cell layers of zone II is sufficient to induce symbiosome fusion and showed that down regulation of *MtROP* expression is essential for symbiosome maintenance. Nodule senescence is not only observed upon inoculation with Fix^- *Rhizobium* strain, but it also occurs as nodule age and when plants are grown under stress condition (for example darkness). We suppose that in all these cases senescence of the nodule tissue is initiated by a ROP mediated symbiosome fusions.

The phenotype observed in the *MtENOD12p::MtROP1* expressing nodules strongly supports the hypotheses that symbiosomes have a vacuolar nature and that ROPs have a role in vacuole biogenesis. This is further supported by the observation that in mammalian cells several small G proteins, belonging to the same family of ROPs (Rho GTPases), localize to endosomes and are supposed to play a direct role in endosome formation (Ridley, 2001).

The role of ROPs in regulating symbiosome fusion has implications for other organ specific forms of vacuoles. For example, the protein reserves in seed are contained in vacuole-like organelles called protein bodies. As seed germination proceeds the protein bodies fuse and their content is degraded in a similar way as observed for the symbiosome fusion during nodule senescence (Matile and Wiemken, 1976). Our data strongly suggest a role of ROP GTPases in this process.

An intriguing question is how *MtROP* expression is down regulated at the early stages of nodule development. As discussed in chapter 6, expression of nodulin genes, such as *MtENOD12*, as well as expression of the NFS genes is most likely regulated by Nod factor

signaling. At the moment we have no data indicating a similar role of Nod factor signaling in regulating *MtROP* expression. However, albeit at low level, NFS genes are expressed in the proximal cell layers of zone II, where the down regulation of *MtROP* expression occurs. Therefore, it cannot be excluded that Nod factor signaling plays a role in the down regulation of *MtROP* expression. However, it is clear that Nod factor signaling cannot be the only factor down regulating *MtROP* expression, since in the Fix^- nodules Nod factor signaling is most likely not disturbed whereas *MtROP* expression is not down regulated. This indicates that other *Rhizobium* signals play a role in down regulating *MtROP* expression in nodules. Premature symbiosome fusion does not occur in nodules induced by *Rhizobium* strains mutated in genes encoding components of Nitrogenase. This indicates that the down-regulation of *MtROP* expression is not under the control of the nitrogen fixation, a process that anyway starts in more proximal cells (zone III cells) of the ones where down regulation of *MtROP* expression is observed. Further study to determine the mechanisms by which *MtROP* expression is regulated could make use of plant mutants that show premature nodule senescence. Such mutants have been described in Pea (Morzhina et al., 2000) but so far not in the legume models *Medicago* or *Lotus*. The cloning of such host genes will give insight in the mechanisms regulating *MtROP* expression in nodules.

Role of actin in the infection process

Rhizobium infection, both in the epidermis and in the nodule cells, most likely involves the actin cytoskeleton. Moreover, since infection threads are supposed to be tip growing structures (Dart, 1974) it is probable that the actin cytoskeleton plays a key role in infection thread growth. In nodule cells the actin cytoskeleton reorganizes upon rhizobia release and complex arrays of actin filaments are formed around the symbiosomes (Whitehead et al., 1998; Davidson and Newcomb, 2001), suggesting a role of the actin cytoskeleton in bacteria release and proliferation.

We decided to study the role of the actin cytoskeleton in the infection process starting with the root epidermis, since root hairs are easily accessible for microscopy analysis. The actin cytoskeleton in root hairs consists of two different configurations: thick actin cables that run longitudinally along the hair length and that flare out into thinner bundles at the hair tip. The latter are referred to as FB-actin. FB-actin is specific for growing root hairs and disappears when root hairs stop growing (Miller et al., 1999). As a first step in studying the role of the actin cytoskeleton during infection thread formation/growth in root hairs we characterized the expression of the *Medicago* actin gene family during root hair development (chapter 3). For this purpose, we used promoter fusions with the fluorescent marker DsRED-E5. We showed that this marker allows an accurate analysis of regulation of gene expression, also during a relatively fast process such as root hair development (chapter 2). With this approach we showed that two actin genes, *MtACT2* and *MtACT3* are constitutively expressed in root hairs, *MtACT4* is induced in root hairs whereas expression of *MtACT1* is clearly regulated

during root hair development (chapter 3). This gene is in fact highly expressed in growing root hairs and is down regulated when root hairs stop growing. Therefore, the expression pattern of *MtACT1* perfectly correlates with the disappearance of the FB-actin when root hairs stop growing. Based on this observation one can speculate that the FB-actin is enriched in the *MtACT1* isovariant. Application of Nod factor induces root hair deformation that involves root hair swelling and subsequent reinitiation of tip growth. In deforming root hairs the FB-actin reappears (Miller et al., 1999). Since *MtACT1* expression in root hairs correlates with the presence of FB-actin, an intriguing question is whether Nod factor application also induces *MtACT1* expression in deforming root hairs or whether, considering the putative tip growth of infection threads, *MtACT1* expression is induced in root/nodule cells in which infection threads grow. The analysis of *MtACT1* expression upon Nod factor application or infection with *Rhizobium* was not yet studied mainly due to technical difficulties in working with *Agrobacterium rhizogenes* transformed roots. Analysis of actin gene expression during infection with *Rhizobium* will require stable transformed Medicago lines.

Are ROP GTPases involved in early steps of the infection process?

As discussed above both infection thread growth and endocytosis of bacteria require localized insertion of vesicles, a process that is regulated by the actin cytoskeleton. ROP GTPases are well known to control processes such as tip growth and endocytosis by regulating the actin cytoskeleton (Yang, 2002). Therefore, it seems probable that ROP GTPases play a role also in the early steps of the infection process both in root hairs and in nodules. The expression of *MtROPs* in the nodule infection zone supports this hypothesis. However, in roots in which *MtROP1* or its Constitutive Active (CA) or Dominant Negative (DN) forms were introduced under the control of the *MtENOD12* promoter no effect of the transgene was observed on infection thread growth, neither in root hairs or nodule cells. Further, no effect was seen on bacterial release. This suggests that *MtROP1* is not involved in infection thread growth and release of bacteria. A possible explanation is that other Medicago ROPs regulate these processes. However, this seems unlikely, since *MtROP1* is most homologous to the Arabidopsis ROPs belonging to group IV and shown to be involved in tip growth (chapter 4). Further, *MtROP1* is the highest expressed group IV Medicago ROP and it is also expressed in root hairs and nodules (chapter 4). Therefore, it would be improbable that, if group IV *MtROPs* are involved in infection thread growth/bacterial release, *MtROP1* would not affect these processes. This observation leads to the hypothesis that the lack of effect of *MtROP1*/CA/DN overexpression on the early steps of epidermis/nodule infection is due to the fact that roots transformed with these transgenes did not express *MtROP1*/CA/DN at a high enough level to interfere with these processes.

In addition to the *Rhizobium* induced *MtENOD12* promoter we performed several studies using a constitutive promoter (*CaMV 35S*), as well as root hair specific promoters, to drive *MtROP1* expression. In such studies we never observed an effect of *MtROP1* on root hair

development. Although we did not analyze the expression level of *MtROP1* in these transgenic roots, it seems probable that the transgene was expressed at too low levels to affect root hair growth. This might be due to the fact that too high levels of *MtROP1* expression are toxic for the plant and therefore, roots expressing this transgene at high levels are subject to negative selection. Especially the latter results indicate that the data obtained on the role of *MtROP1* on infection thread growth and bacterial release cannot be considered definitive and new experiments need to be performed.

References

- Borg S, Brandstrup B, Jensen BJ, Poulsen C** (1997) Identification of new protein species among 33 different small GTP-binding proteins encoded by cDNAs of *Lotus japonicus*, and expression of corresponding mRNAs in developing root nodules. *Plant Journal* **11**: 237-250
- Brewin NJ** (1991) Development of the legume root nodule. *Ann Rev Cell Biol* **7**: 191-226
- Brewin NJ** (1996) Tissue and Cell Invasion by *Rhizobium*: The Structure and Development of Infection Threads and Symbiosomes. In HP Spaik, A Kondorosi, PGG Hooykaas, eds, *The Rhizobiaceae: molecular biology of model plant-associated bacteria*. Kluwer Academic Publisher, New York, pp 417-428
- Callahan DA, Torrey JG** (1981) The structural basis for infection of root hairs of *Trifolium repens* by *Rhizobium*. *Can. J. Bot.* **59**: 1647-1664
- Catoira R, Galera C, de Billy F, Penmetsa RV, Journet EP, Maillet F, Rosenberg C, Cook D, Gough C, Denarie J** (2000) Four genes of *Medicago truncatula* controlling components of a Nod factor transduction pathway. *Plant Cell* **12**: 1647-1666
- Cheon CI, Lee NG, Siddique AB, Bal AK, Verma DP** (1993) Roles of plant homologs of Rab1p and Rab7p in the biogenesis of the peribacteroid membrane, a subcellular compartment formed de novo during root nodule symbiosis. *Embo J* **12**: 4125-4135
- Dart PJ** (1974) The Infection Process. In A Quispel, ed, *The Biology of Nitrogen Fixation*. North-Holland publishing company, pp 381-429
- Davidson AL, Newcomb W** (2001) Changes in actin microfilaments arrays in developing pea root nodule cells. *Can. J. Bot.* **79**: 767-776
- Limpens E, Franken C, Smit P, Willemse J, Bisseling T, Geurts R** (2003) LysM domain receptor kinases regulating rhizobial Nod factor-induced infection. *Science* **302**: 630-633
- Lin Y, Seals DF, Randall SK, Yang Z** (2001) Dynamic localization of ROP GTPases to the tonoplast during vacuole development. *Plant Physiol* **125**: 241-251
- Madsen EB, Madsen LH, Radutoiu S, Olbryt M, Rakwalska M, Szczyglowski K, Sato S, Kaneko T, Tabata S, Sandal N, Stougaard J** (2003) A receptor kinase gene of the LysM type is involved in legume perception of rhizobial signals. *Nature* **425**: 637-640
- Matile P, Wiemken A** (1976) Interactions between cytoplasm and vacuole. In CR Stocking, U Heber, eds, *Encyclopaedia of plant physiology*, Vol 3. Springer, Heidelberg, pp 255-287
- Mellor RB** (1989) Bacteroids in the *Rhizobium*-legume symbiosis inhabit a plant internal lytic compartment: implications for other microbial endosymbioses. *J Exp Bot* **40**: 831-839
- Miller DD, de Ruijter NCA, Bisseling T, Emons AMC** (1999) The role of actin in root hair morphogenesis: studies with lipochito-oligosaccharide as a growth stimulator and cytochalasin as an acting perturbing drug. *The Plant Journal* **17**: 141-154
- Morzhina EV, Tsyganov VE, Borisov AY, Lebsky VK, Tikhonovich IA** (2000) Four developmental stages identified by genetic dissection of pea (*Pisum sativum* L.) root nodule morphogenesis. *Plant Science* **155**: 75-83
- Radutoiu S, Madsen LH, Madsen EB, Felle HH, Umehara Y, Gronlund M, Sato S, Nakamura Y, Tabata S, Sandal N, Stougaard J** (2003) Plant recognition of symbiotic bacteria requires two LysM receptor-like kinases. *Nature* **425**: 585-592
- Rea AL, Bonfanto-Fasolo P, Brewin NJ** (1992) Structure and growth of infection threads in the legume symbiosis with *Rhizobium leguminosarum*. *Plant Journal* **2**: 385-395
- Ridley A** (2001) Rho Proteins: Linking Signaling With Membrane Trafficking. *Traffic* **2**: 303-310
- Roth LE, Stacey G** (1989a) Bacterium release into host cells of nitrogen-fixing soybean nodules: the symbiosome membrane comes from three sources. *Eur J Cell Biol* **49**: 13-23
- Roth LE, Stacey G** (1989b) Cytoplasmic membrane systems involved in bacterium release into soybean nodule cells as studied with two *Bradyrhizobium japonicum* mutant strains. *Eur J Cell Biol* **49**: 24-32
- Schlaman HR, Horvath B, Vijgenboom E, Okker RJ, Lugtenberg BJ** (1991) Suppression of nodulation gene expression in bacteroids of *Rhizobium leguminosarum biovar viciae*. *J Bacteriol* **173**: 4277-4287

- Sharma SB, Signer ER** (1990) Temporal and spatial regulation of the symbiotic genes of *Rhizobium meliloti* in *planta* revealed by transposon Tn5-gusA. *Genes Dev* **4**: 344-356
- Vasse J, de Billy F, Camut S, Truchet G** (1990) Correlation between ultrastructural differentiation of bacteroids and nitrogen fixation in alfalfa nodules. *J Bacteriol* **172**: 4295-4306
- Wais RJ, Galera C, Oldroyd G, Catoira R, Penmetsa RV, Cook D, Gough C, Denarie J, Long SR** (2000) Genetic analysis of calcium spiking responses in nodulation mutants of *Medicago truncatula*. *Proc Natl Acad Sci U S A* **97**: 13407-13412
- Whitehead LF, Day AD, Hardham AR** (1998) Cytoskeletal arrays in the cells of soybean root nodules: the role of actin microfilaments in the organisation of symbiosomes. *Protoplasma* **203**: 194-205
- Yang Z** (2002) Small GTPases: Versatile Signaling Switches in Plants. *Plant Cell* **14**: S375-S388

Nederlandse samenvatting

De symbiotische interactie van *Rhizobium* bacteriën en vlinderbloemige planten leidt tot de vorming van wortelknollen. De rhizobia worden gehuisvest in speciale cellen van deze knollen waar ze stikstof uit de lucht kunnen omzetten in ammoniak. Dit is een bron van stikstof voor de gastheer en indirect voor alle levende organismen. De bacteriën die in de knolcellen aanwezig zijn, zijn omringd door een membraan afkomstig van de plant. Een door een plantenmembraan omringde bacterie wordt een symbiosoom genoemd en is zo eigenlijk een stikstofbindend organel geworden, dat door de plant aan de buitenkant niet als celvreemd herkend kan worden.

De vorming van stikstofbindende wortelknollen vereist enerzijds dat de plant bestaande wortelcellen herprogrammeert om een wortelknolprimordium te vormen, anderzijds moet de bacterie op een door de plant gecontroleerde wijze de wortel en uiteindelijk wortelknol cellen kunnen binnenkomen. Mechanismen die dit infectieproces controleren zijn in dit proefschrift bestudeerd.

Nod factoren zijn moleculen die de rhizobia maken als zij in contact komen met hun gastheer. Deze Nod factoren zijn essentieel voor de vorming van de knolprimordia en ook voor het infectieproces. In dit proefschrift is o.a. bestudeerd hoe door Nod factoren geactiveerde signaaltransductie een rol speelt bij het infectieproces in de wortelknol.

Het infectieproces start in de wortelharen. Daar wordt in sommige gevallen de krulling van wortelharen geïnduceerd. De krul vormt een afgesloten ruimte waarin de bacterie wordt gevangen. In deze krul wordt vervolgens een infectiedraad gevormd. Dit is een buisachtige structuur waardoor de rhizobia de knolprimordia bereiken.

In wortelknollen zoals die b.v. door erwten en *Medicago* gevormd worden is een meristeem aanwezig. Meristeemcellen delen en op deze wijze wordt enerzijds het meristeem in stand gehouden en anderzijds worden er cellen aan de knolweefsels toegevoegd. Op de grens van het meristeem en het centrale weefsel groeien de infectiedraden en deze infecteren cellen die afkomstig zijn van het delende meristeem. Dit in de knol plaatsvindende infectieproces is in het bijzonder bestudeerd.

Het was bekend bij de start van dit project dat als epidermiscellen een Nod factor herkennen dit tot snelle veranderingen in de configuratie van het actineskelet leidt. Verder was het zeer waarschijnlijk dat het actineskelet een cruciale rol speelt bij de groei van infectiedraden. Daarom zijn alle actinegenen van de modelplant geïsoleerd en is m.b.v. promotor reporter fusies bestudeerd waar deze genen tot expressie komen. Op deze wijze zijn de actinegenen geïdentificeerd die tot expressie komen tijdens wortelhaarontwikkeling. Om te bepalen wanneer tijdens de wortelhaarontwikkeling deze actine genen aan of uitgezet worden, is gebruik gemaakt van een reporter gen dat codeert voor een rood-fluorescent eiwit. Dit eiwit heet *timer* want voordat het rijpe rood-fluorescente eiwit gevormd wordt ontstaat eerst een

groen-fluorescente intermediair. De kleur van het eiwit geeft dus informatie over de leeftijd van het molecuul. Dit is de reden dat het eiwit *timer* wordt genoemd en gebruikt kan worden om nauwkeuriger vast te stellen wanneer een gen wordt aan- of uitgeschakeld.

Omdat de configuratie van het actineskelet snel verandert na herkenning van Nod factoren werd gepostuleerd dat kleine G proteïnes (ROP eiwitten) een belangrijke rol spelen in de Nod factor signaaltransductie die betrokken is bij infectiedraadvorming. Daartoe is eerst de familie van ROP genen van *Medicago* gekarakteriseerd en een van deze genen is geselecteerd om de functies van ROPs in het infectieproces te bestuderen. Hiervoor is gebruik gemaakt van dominant-negatieve- en dominant-positieve vormen van ROP. Deze werden tot expressie gebracht met een promotor die wordt aangeschakeld tijdens het infectieproces. Op deze wijze werd een negatief effect op andere plantprocessen geminimaliseerd. Zo werd zichtbaar gemaakt dat ROP-genexpressie uitgeschakeld moet worden in cellen waarin de symbiosomen zich vermenigvuldigen. Sommige *Rhizobium* mutanten zijn niet in staat ROP-genexpressie uit te schakelen en dit leidt tot knollen waarin geen stikstofbinding plaats vindt.

Recent is een aantal *Medicago* genen geïsoleerd die een unieke functie hebben in Nod factor herkenning en de hierdoor geactiveerde signaaltransductie. Mutaties in deze genen blokkeren de interactie van rhizobia en de gastheer in de wortelhaar en een wortelknol wordt niet gevormd. Echter het actieve infectieproces in de knol suggereert dat ook in de knol Nod factor signalering plaats vindt. M.b.v. in situ hybridisatie werd aangetoond dat alle geanalyseerde Nod factor signalering genen tot expressie komen in de knol. Deze genen komen alleen tot expressie in een paar cellagen en dit zijn precies de cellen waarin het infectieproces plaats vindt. Ten slotte werd getoetst met een RNAi strategie of Nod factor signalering essentieel is voor het infectieproces. Door de expressie van een van de Nod factor signalering genen sterk te verlagen, werden knollen verkregen waarin veel infectiedraden voorkomen maar geen symbiosomen gevormd worden. Dit betekent dat in de knol Nod factor signalering tenminste essentieel is voor het vrijkomen van de bacteriën uit de infectiedraad.

Riassunto

L'azoto è un elemento essenziale per la crescita delle piante e di tutti gli organismi viventi. Sebbene l'atmosfera è ricca di azoto questo non può essere usato dalle piante. L'interazione tra i batteri del genere *Rhizobium* e le piante leguminose induce la formazione, sulle radici della pianta, di nuovi organi, i noduli radicali, nei quali i batteri riducono l'azoto atmosferico ad ammonio che viene utilizzato dalla pianta. Affinché i noduli si formino è necessario l'ingresso dei batteri nella pianta. L'infezione delle cellule vegetali avviene in due diversi tessuti: l'epidermide della radice, dove l'interazione inizia, e le cellule dei noduli. L'interazione ha inizio con lo scambio di segnali molecolari tra i due simbionti. I "segnali molecolari" secreti da *Rhizobium* sono chiamati Fattori Nod. I Fattori Nod sono essenziali per l'infezione dei peli radicali. I batteri entrano nei peli radicali attraverso la formazione di una nuova struttura tubulare chiamata canale d'infezione. I canali d'infezione attraversano i peli radicali e raggiungono le cellule del nodulo, dove rilasciano i batteri. Nelle cellule del nodulo i batteri sono circondati da una membrana di origine vegetale chiamata membrana del simbiosoma. La struttura formata dai batteri e dalla membrana che li circonda è chiamata simbiosoma.

Medicago truncatula forma noduli di tipo indeterminato, in cui un meristema è presente all'apice del nodulo. Questo meristema si divide aggiungendo continuamente nuove cellule al nodulo. In questa maniera si forma un gradiente di sviluppo spostandosi dall'apice (regione distale) alla base (regione prossimale) del nodulo. La regione del nodulo immediatamente al di sotto del meristema viene chiamata zona d'infezione. In questa zona le nuove cellule formatesi dalla divisione del meristema vengono infettate. I canali d'infezione entrano nelle cellule distali della zona d'infezione dove rilasciano i batteri. Nella cellule della zona d'infezione più prossimali i simbiosomi si dividono e si differenziano nella forma matura capace di ridurre l'azoto. Alla fine le cellule alla base del nodulo sono occupate da migliaia di simbiosomi che fissano l'azoto.

L'organizzazione del citoscheletro di actina cambia rapidamente nei peli radicali dopo l'aggiunta dei fattori Nod. Inoltre, diverse evidenze suggeriscono che lo stesso citoscheletro ha un ruolo fondamentale nella crescita dei canali d'infezione. Come primo passo nello studio del ruolo dell'actina durante l'infezione dei peli radicali, abbiamo analizzato l'espressione dei geni dell'actina durante lo sviluppo dei peli radicali in *Medicago*. Nelle angiosperme l'actina è codificata da famiglie di geni; in *Medicago* sono presenti 6 differenti geni dell'actina, di cui 4 sono espressi nella radice. Per studiarne l'espressione durante lo sviluppo dei peli radicali, abbiamo fuso i promotori di questi 4 geni al reporter fluorescente DsRED-E5 (capitolo 3), la cui fluorescenza è verde appena la proteina è sintetizzata e cambia in rosso con il tempo. Di conseguenza il colore della fluorescenza indica l'età della proteina e fornisce informazioni dettagliate sul momento in cui un'espressione di un

promotore è attivata o spenta. Usando questo approccio, abbiamo dimostrato che 2 dei 4 geni dell'actina (*MtACT2* and *MtACT3*) sono espressi costitutivamente durante lo sviluppo dei peli radicali, l'espressione del gene *MtACT4* è indotta nei peli mentre l'espressione del gene *MtACT1* è regolata durante lo sviluppo dei peli radicali. Questo gene è, infatti, attivo solo nei peli radicali che crescono e non quando i peli smettono di crescere. Diverse evidenze suggeriscono che i canali d'infezione crescono in maniera simile ai peli radicali, per cui è possibile che l'espressione di questo gene sia regolata anche nelle cellule in cui i canali d'infezione crescono.

All'inizio di questo lavoro è diventato chiaro che le proteine della famiglia delle ROP (piccole proteine G) regolano l'organizzazione del citoscheletro di actina. Poiché la struttura del citoscheletro di actina cambia nelle cellule che sono infettate da *Rhizobium* abbiamo deciso di studiare il ruolo delle ROP nell'infezione dei noduli. Usando l'ibridazione *in situ* abbiamo dimostrato che nei noduli wild-type di *Medicago* le ROP sono espresse nella regione apicale che comprende il meristema e la parte più distale della zona d'infezione, dove i canali d'infezione entrano nelle cellule del nodulo e rilasciano i batteri. Spostandosi verso le cellule più prossime al nodulo, dove i simbiosomi si dividono e si differenziano, l'espressione dei geni delle ROP diminuisce. I noduli formati da mutanti di *Rhizobium* (*Fix⁻*), il cui sviluppo si arresta ad uno stadio precoce, sono caratterizzati da fusione e successiva degradazione dei simbiosomi e non sono in grado di ridurre l'azoto. In questi noduli, a differenza dei noduli wild-type, l'espressione delle ROP rimane costante in tutta la zona d'infezione, incluso la parte più prossimale. Questo suggerisce che la fusione e la successiva degradazione dei simbiosomi nei noduli *Fix⁻* sia direttamente correlata alla espressione costante delle ROP in tutte le cellule della zona d'infezione. Per verificare questa ipotesi abbiamo determinato se l'espressione ectopica delle ROP nelle cellule più prossime della regione d'infezione, dove i simbiosomi si dividono e si differenziano e dove normalmente queste proteine G non sono espresse, è sufficiente ad indurre fusione e degradazione dei simbiosomi. A questo scopo abbiamo espresso nei noduli una delle ROP di *Medicago*, MtROP1, sotto il controllo di un promotore indotto da *Rhizobium* (*MtENOD12*). In questo modo abbiamo evitato che l'over espressione delle ROP potesse interferire con lo sviluppo di altri organi vegetali. L'analisi dei noduli trasformati, come descritto sopra, attraverso una combinazione di microscopia ottica ed elettronica, ha dimostrato che l'espressione ectopica di MtROP1 nella parte prossimale della regione d'infezione induce la fusione dei simbiosomi a formare delle strutture simili a vacuoli in cui i batteri sono degradati. Questi dati indicano che l'abbassamento dell'espressione delle ROP nelle cellule in cui i simbiosomi si dividono e si differenziano è essenziale per permettere il normale sviluppo dei noduli.

Recentemente diversi geni coinvolti nella percezione e trasduzione dei Fattori Nod sono stati clonati. Questi geni sono essenziali per la formazione dei canali d'infezione nell'epidermide e i relativi mutanti non sono infettati da *Rhizobium* e non formano noduli. I canali d'infezione

crescono anche nelle cellule del nodulo. In più i geni *nod* –che sono coinvolti nella biosintesi e secrezione dei Fattori Nod- sono anche espressi nel nodulo. Questo suggerisce che il segnale mediato dai Fattori Nod è attivo anche nei noduli. Attraverso l'ibridazione *in situ*, abbiamo dimostrato che tutti i geni menzionati sopra sono espressi nel nodulo nei 2-3 strati cellulari al di sotto del meristema. In questi strati cellulari, gli stessi in cui i geni *nod* sono espressi, i canali d'infezione entrano nelle cellule del nodulo e vi rilasciano i batteri, suggerendo che il segnale mediato dai Fattori Nod regoli questi processi. Abbiamo verificato questa ipotesi riducendo drasticamente il livello d'espressione di uno dei geni coinvolti nella percezione dei Fattori Nod, *NORK*, nei noduli tramite RNAi. Noduli in cui solo un residuo livello di *NORK* è presente sono caratterizzati dalla presenza di molti canali d'infezione ma il rilascio dei batteri dai canali d'infezione è bloccato, indicando che il segnale mediato dai Fattori Nod è essenziale per quest'ultimo processo.

Curriculum Vitae

Rossana Mirabella was born in Naples, Italy, on the 18th of May 1973. In 1991 she obtained the diploma at the scientific lyceum. From September 1991 she studied Biology, in the Faculty of Mathematical, Chemical and Physical Sciences, of the Federico II University in Naples. In September 1995 she started a research project in the laboratory of Dr. Maurizio Iaccarino, in the International Institute of Genetics and Biophysics, CNR, Naples, under the supervision of Dr. Maurizio Chiurazzi. In March 1997 she obtained the Laurea degree in Molecular Biology, *summa cum laude*, with a thesis entitled “Analysis of the expression pattern of the nodulin *ENOD40* of Soja in the model system *Arabidopsis thaliana*”. From May 1997 till October 1998 she worked with a fellowship in the same group on the establishment of gene-tagging lines in *Lotus japonicus*. During this time she visited Prof. Dr. Ton Bisseling’s laboratory at the department of Molecular Biology, Wageningen University, Wageningen, The Netherlands, for 5 months. In November 1998 she started her PhD in the same laboratory, under the supervision of Prof. Dr. Ton Bisseling and Dr. René Geurts. She finished her PhD research in February 2004. From March 2004 she is working as post-doc at the department of Plant Physiology, University of Amsterdam, in the group of Dr. Robert Schuurink.

List of publications

Mirabella R, Martirani L, Lamberti A, Iaccarino M, Chiurazzi M (1999) The Soybean ENOD40(2) promoter is active in *Arabidopsis thaliana* and is temporally and spatially regulated. *Plant Mol Biol.* **39** 177-181

Martirani L, Stiller J, Mirabella R, Alfano F, Lamberti A, Radutoiu S E, Iaccarino M, Gresshoff P M, and Chiurazzi, M (1999) T-DNA Tagging of Nodulation- and Root-Related Genes in *Lotus japonicus*: Expression Patterns and Potential for Promoter Trapping and Insertional Mutagenesis. *MPMI* **12** 275-284

Ercolano E, Mirabella R, Merrick M, Chiurazzi M (2001) The *Rhizobium leguminosarum* glnB gene is down-regulated during symbiosis. *Mol Gen Genet.* **264** 555-564

Mirabella R, Franken, C, van der Krogt G N M, Bisseling T and Geurts, R (2004) Use of the “Fluorescent Timer” DsRed-E5 as a Reporter to Monitor Dynamics of Gene Activity in Plants. *Plant Physiol* **in press**

In preparation

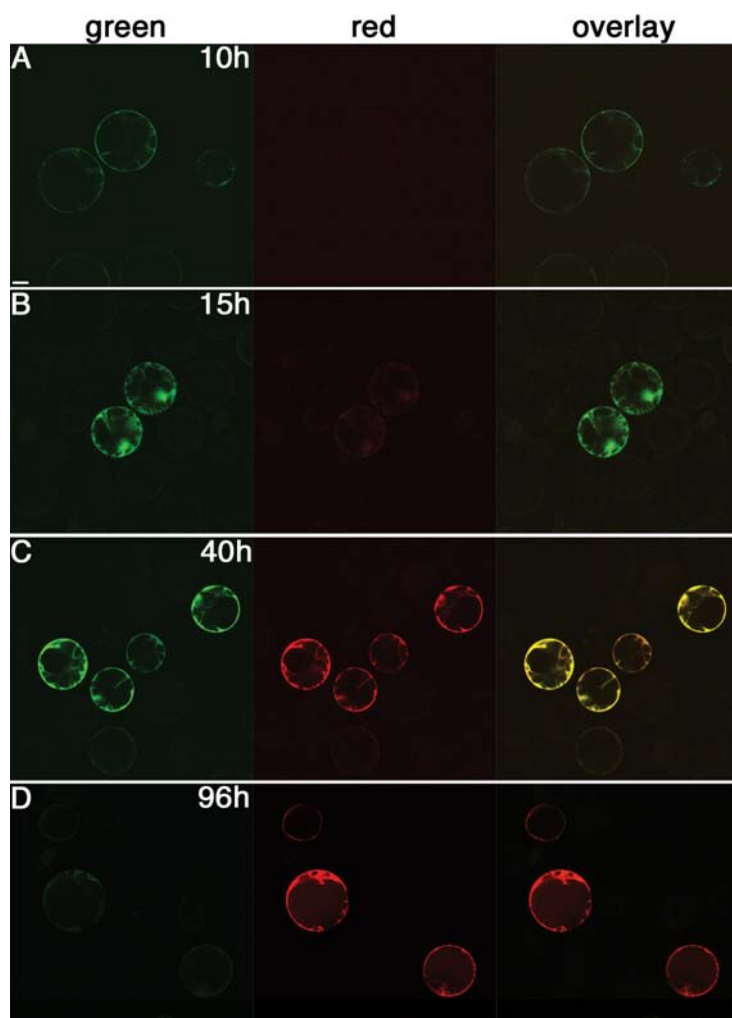
Mirabella R, Franken C, Geurts R and Bisseling T Regulation of Actin Gene Expression during *Medicago truncatula* Root Hair Development

Mirabella R, Federova E, Jahraus A, Franken C, Geurts R and Bisseling T Tight Regulation of ROP GTPases Expression is Required to Maintain Symbiosomes in *Medicago truncatula* Root Nodules

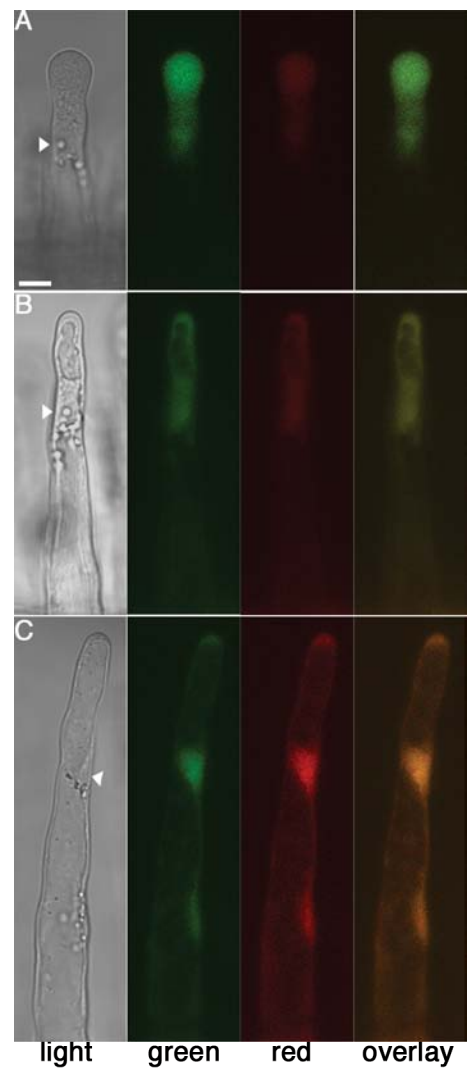
Appendix

Color Figures Chapter 2 and 3

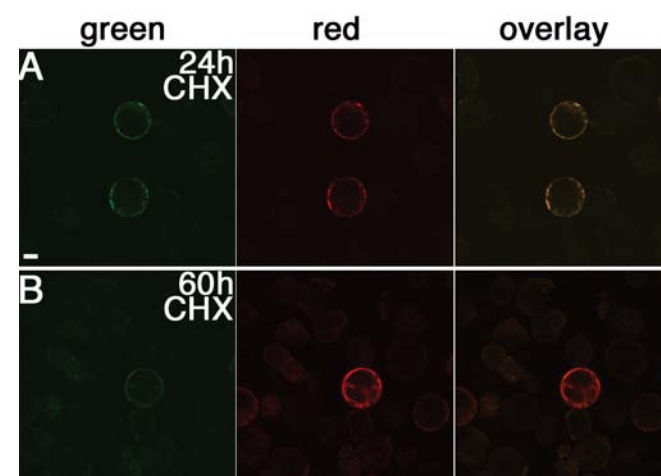
Chapter 2, Figure 1



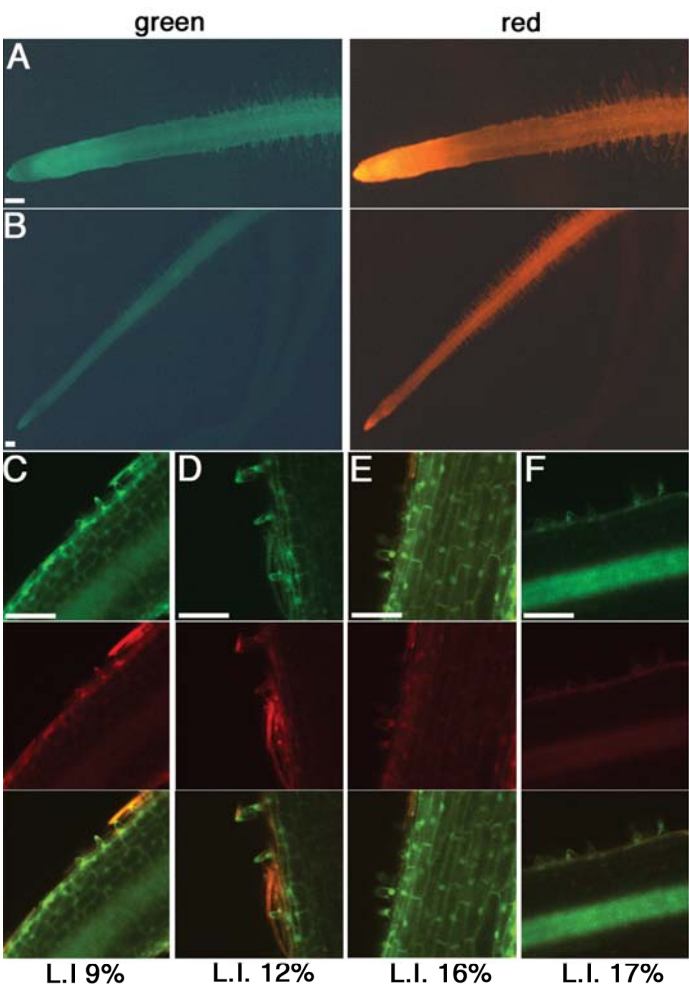
Chapter 2, Figure 6



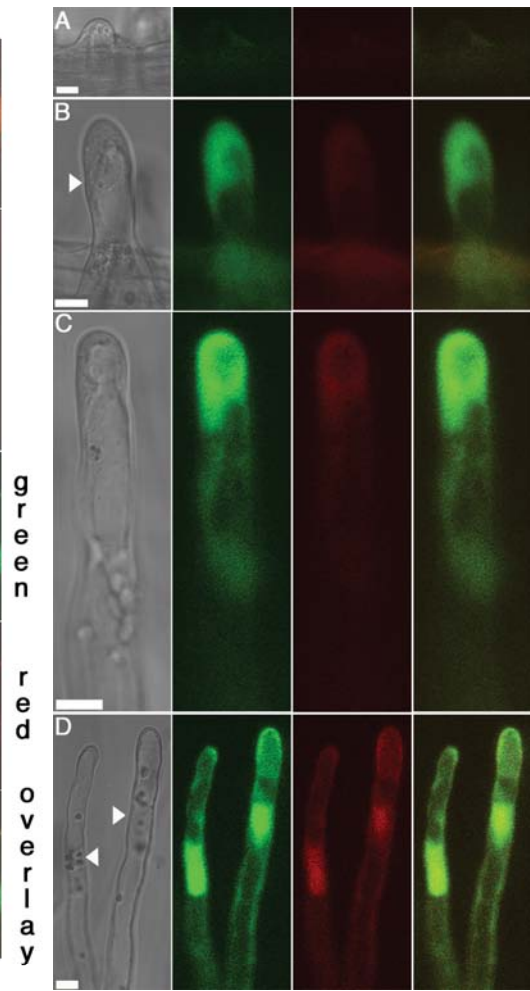
Chapter 2, Figure 2



Chapter 3, Figure 3



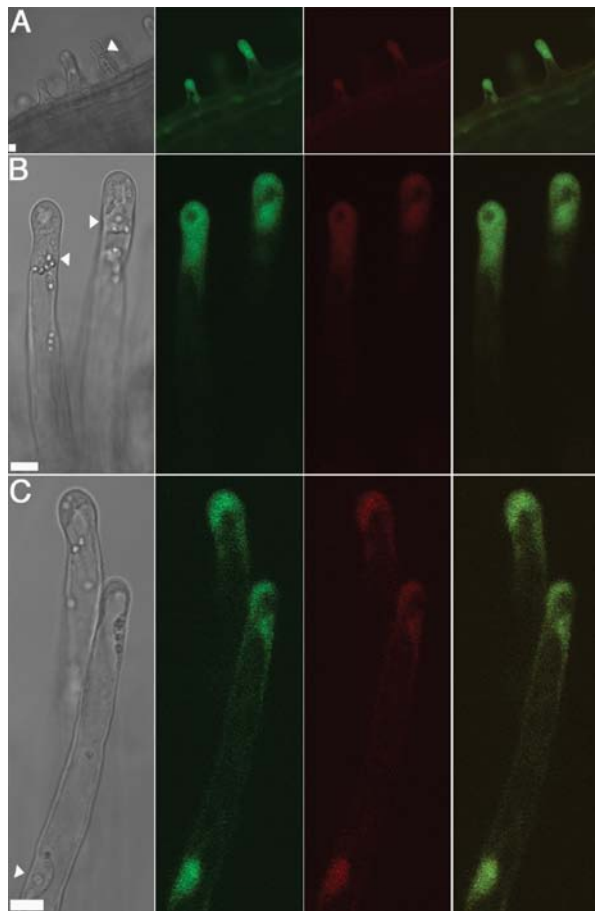
Chapter 3, Figure 7



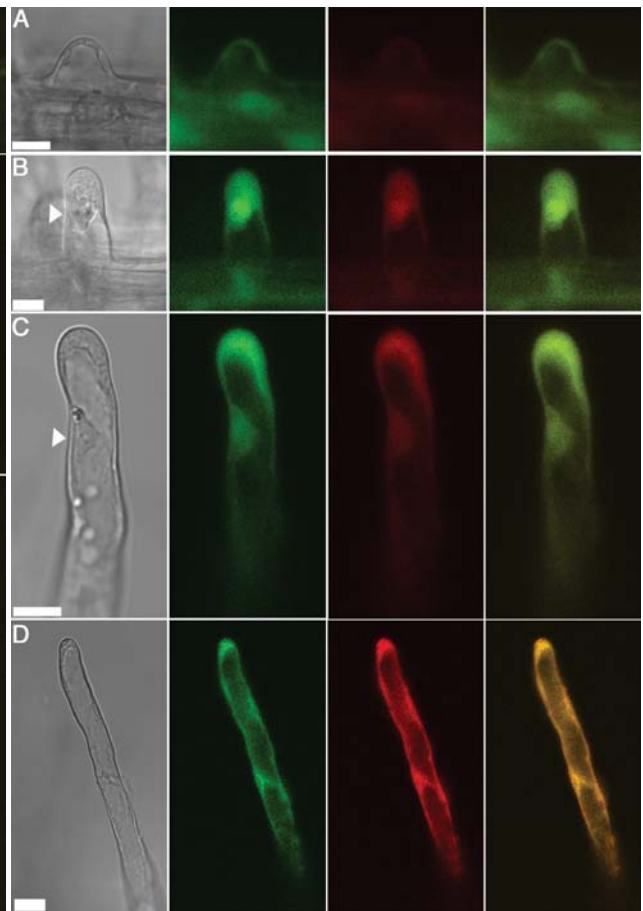
Appendix

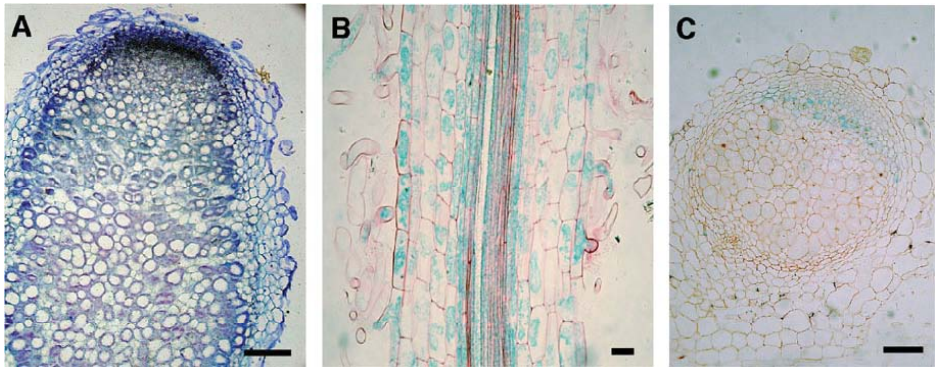
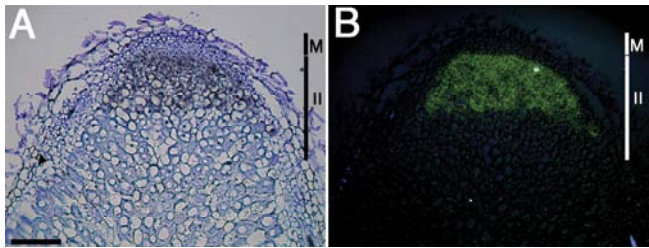
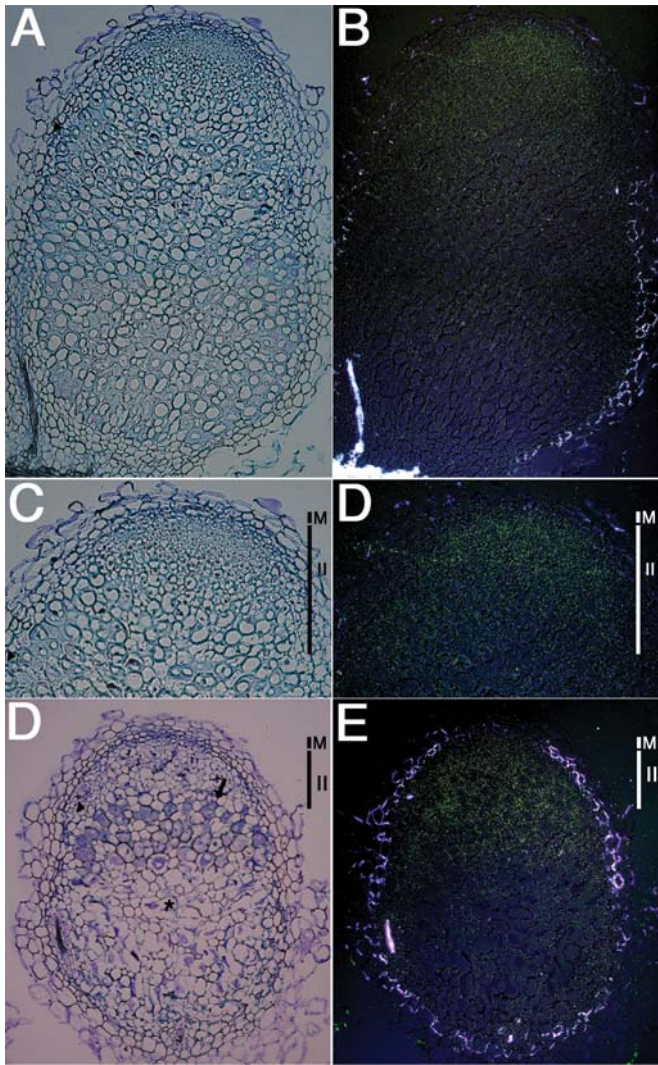
**Color figures
Chapter 3, 4 and 5**

Chapter 3, Figure 4



Chapter 3, Figure 5



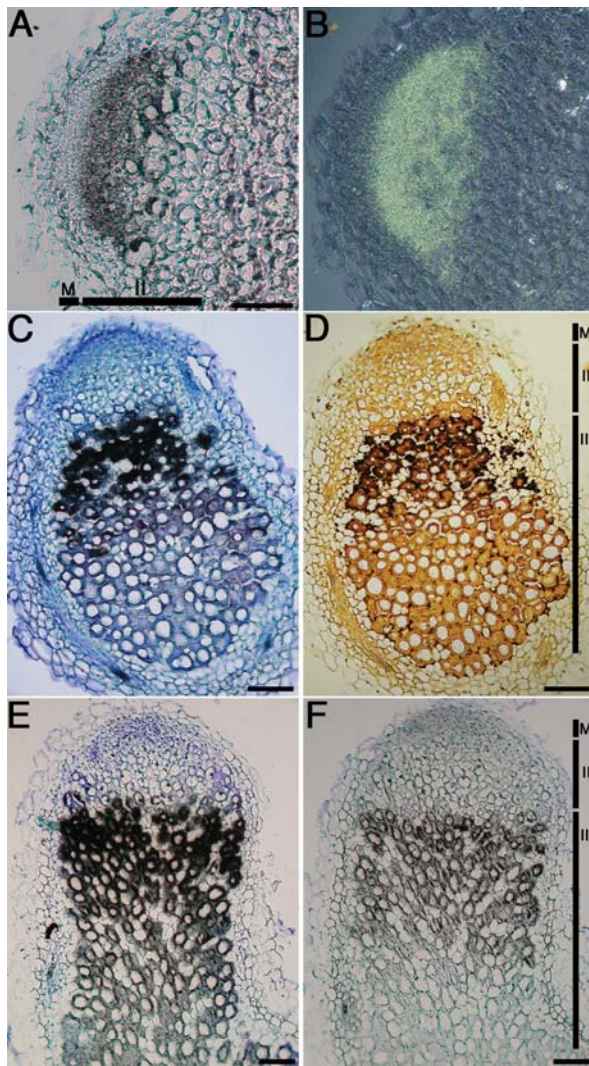


Appendix

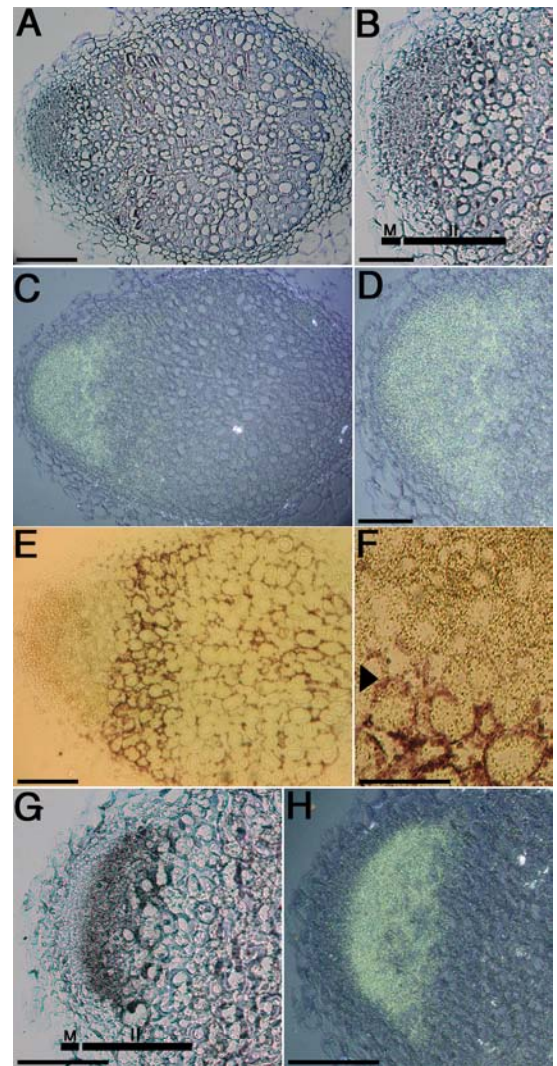
Color figures

Chapter 6

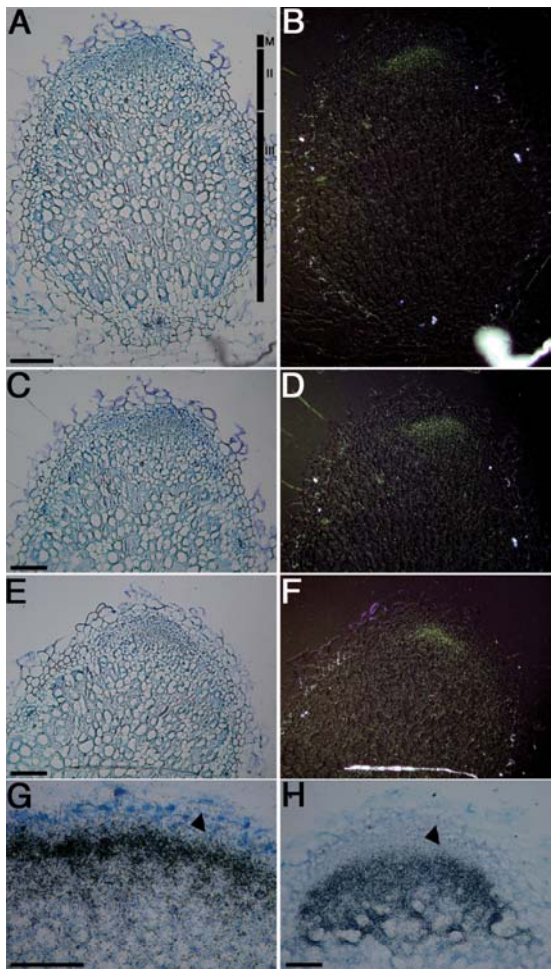
Chapter 6, Figure 1



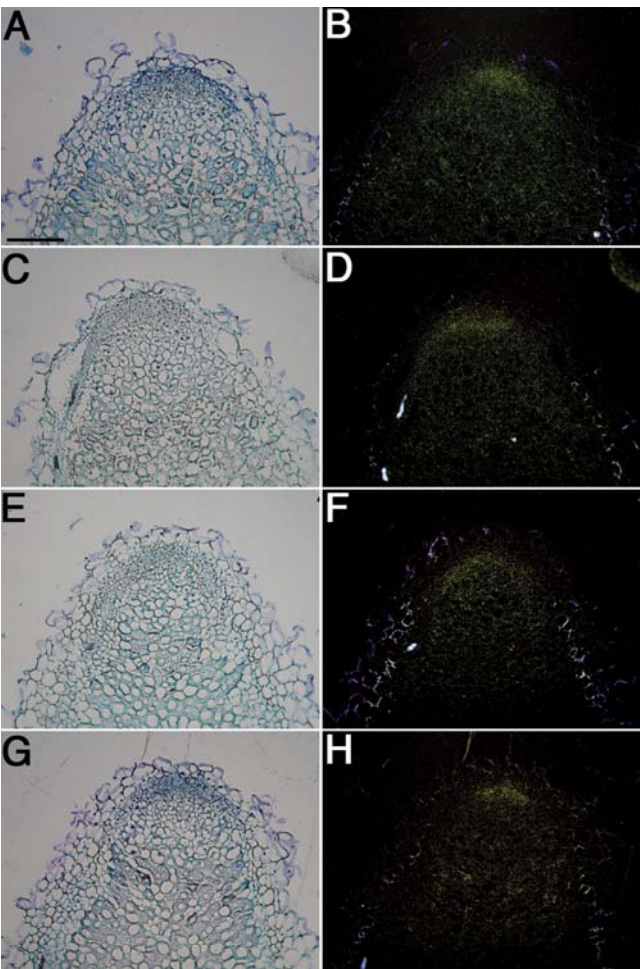
Chapter 6, Figure 3



Chapter 5, Figure 4



Chapter 5, Figure 5



Acknowledgments

The work described in this thesis represents 5 years of work in the molbi department. It is time to sit and think back about all the people who helped and supported me inside and outside the lab.

First, I would like to thank Ton Bisseling, who has been my supervisor, for giving me the opportunity to do my PhD in his lab. I specially appreciate the help in putting my thoughts in the right order and the “droplets of wisdom” that I received from him every now and then. Special thanks to René who followed my work in the last years and found the means to extend my stay in the molbi. Without your help the accomplishment of my thesis would have been a bit more difficult.

In these 5 years I met many people at the molbi and some of them became good friends. First of all I want to express my gratitude to the other member of the “actin group”: Gerard. We shared the up and down moments, in and outside the lab, and I really appreciate his support. Gerard, I could not wish for a better paranymph! My special thanks also to Jenny, Ingrid and Tommy for their friendship and all the good times outside the lab. Finally, I want to thank all the people in the molbi department for making the atmosphere so alive and pleasant to work and especially Carolien for all the help with the plant work.

All my gratitude to the people who, outside the lab, helped me to enjoy my stay in Wageningen, which was not an easy task! I deeply thank Evie, Ambra, Vassos, Delphin and Mohamed.

Ik wil graag Bert, Lucia en de rest van de familie Vermeer bedanken. Jullie hebben me een warm welkom gegeven, en het gevoel gegeven dat ik nu ook een 2e familie heb. Infine vorrei ringraziare la mia famiglia, mamma, papà, Paola e Toby per essermi stati vicino in tutti questi anni e per il sostegno incondizionato....soprattutto grazie mamma per essere venuta in Olanda tutte le volte che potevi! L'ultimo pensiero è per Joop, che ha sempre creduto in me anche quando niente funzionava e mi ha sempre spinto a continuare.....Joop grazie per la tua presenza costante e per il tuo aiuto.

Rossana